

ABSTRACT

Yoon-Seok Chang for the degree of Doctor of Philosophy
in Chemistry presented on September 10, 1990

Title: THE SYNTHESIS AND ELECTRON CAPTURE NEGATIVE ION MASS
SPECTROMETRY OF POLYCHLORINATED DIPHENYL ETHERS
AND DIBENZOFURANS

Abstract approved: _____

Redacted for privacy

Max L. Deinzer

The reductive dechlorination mechanism of polychlorinated dibenzofurans (PCDBFs) and diphenyl ethers (PCDPEs) has been studied under electron capture negative ion (ECNI) mass spectrometry conditions. For this study a series of chlorine-37 regiospecifically labeled PCDPEs and PCDBFs were synthesized. A photochemical synthetic method for the preparation of these compounds by conversion of aromatic hydroxyl groups to chlorine in chlorine saturated carbon tetrachloride solution has been developed. The strategy for introducing chlorine-37 label regiospecifically involved reduction of the nitro derivative, conversion of the corresponding amine to the diazonium salt with t-butyl nitrite, and displacement of nitrogen via the Sandmeyer reaction with chlorine-37 labeled copper chloride.

Relationships were found between experimentally measured molecular radical anion abundances under ECNI mass spectrometry conditions and calculated lowest unoccupied

molecular orbital energies. PCDBFs with CNDO calculated $\epsilon_{LUMO} > 2.0$ eV showed 0 % molecular radical anion and those with $\epsilon_{LUMO} < 1.4$ eV showed > 80 % molecular radical anion abundance. B/E linked scan analysis provided evidence for the presence of negative metastable ions.

Observations were made for the regiospecific chloride ion loss from chlorine-37 labeled PCDBFs under ECNI mass spectrometry conditions. Attempts have been made to explain the regiochemistry of chloride ion loss on the basis of the molecular properties of the molecules. These properties which include electron affinity, electron density and various orbital energies can be estimated from molecular orbital calculations. The calculated energy dependence of the C-Cl bond lengths of PCDBF isomers showed qualitative correlations with C-Cl bonds that are reductively cleaved. Lower activation energies and smoother $\pi^*-\sigma^*$ electron transitions were related with higher reactivities in the bonds that are cleaved. A model proposed for this cleavage involves a "bent" bond in the transition state in which the chlorine rotates into the plane of the π system as the bond is stretched and finally broken.

THE SYNTHESIS AND ELECTRON CAPTURE NEGATIVE ION
MASS SPECTROMETRY OF POLYCHLORINATED
DIPHENYL ETHERS AND DIBENZOFURANS

by
Yoon-Seok Chang

A Thesis
submitted to
Oregon State University

in partial fulfillment of
the requirements of the
degree of

Doctor of Philosophy

Completed September 10, 1990

Commencement June 1991

APPROVED:

Redacted for privacy

Professor of Chemistry in Charge of Major

Redacted for privacy

Head of Department of Chemistry

Redacted for privacy

Dean of Graduate School

Date thesis is presented: September 10, 1990

Typed by Yoon-Seok Chang

To my daughter, Sunny.

ACKNOWLEDGEMENTS

I would like to express my sincere gratitude to my research advisor, Professor Max L. Deinzer, for his guidance, constructive criticism, and encouragement throughout my graduate education.

Thanks are also extended to Professors Douglas Barofsky, Peter Freeman and Gerald Gleicher for their helpful suggestions.

I also thank National Institute of Health for the five year financial support.

Thanks also go to Ramnath Iyer, Belaid Mahiou, Brian Arbogast, Donald Griffin, James Laramee, who have contributed in so many ways to the work presented in this thesis.

Finally, I thank my Lord, Jesus Christ who has saved my life from the car accident in the first year in Corvallis and led me to finish the Ph.D work.

" If you abide in My word,
you are My disciples indeed.
And you shall know the truth,
and the truth shall make you free."

John 8:31-32

TABLE OF CONTENTS

	<u>Page</u>
I. INTRODUCTION	1
References	19
II. PHOTOCHEMISTRY OF IRGASAN-TRIFLATE: A SIMPLE CONVERSION OF AN AROMATIC HYDROXYL GROUP TO CHLORINE IN THE SYNTHESIS OF POLYCHLORINATED DIPHENYL ETHERS AND POLYCHLORINATED DIBENZOFURANS	23
Abstract	24
References	33
III. PHOTOCHEMISTRY OF IRGASAN-TRIFLATE II: MECHANISM OF THE CYCLIZATION	34
Abstract	35
Experimental	42
References	49
IV. REGIOSPECIFIC SYNTHESIS OF POLYCHLORINATED DIBENZOFURANS WITH CHLORINE-37 EXCESS	51
Summary	52
Introduction	53
Experimental Section	55
Results and Discussion	68
References	89
V. SYNTHESIS OF REGIOSPECIFIC CHLORINE-37 LABELED PENTACHLORODIBENZOFURANS AND MASS SPECTRAL EVIDENCE OF CHLORINE SCRAMBLING DURING MOLECULAR CHLORINATION	91
Summary	92

Experimental	97
References	102
VI. RELATIONSHIP OF MOLECULAR RADICAL ANION ABUNDANCE AND CALCULATED LOWEST UNOCCUPIED MOLECULAR ORBITAL ENERGIES FOR POLYCHLORINATED DIBENZOFURANS AND DIBENZODIOXINS IN ELECTRON CAPTURE NEGATIVE ION MASS SPECTROMETRY: EVIDENCE FOR NEGATIVE METASTABLE IONS	103
Abstract	104
Introduction	105
Experimental	107
Results and Discussion	111
References	120
VII. THEORY AND MASS SPECTROMETRY OF REDUCTIVE DECHLORINATION OF POLYCHLORODIBENZOFURANS UNDER ELECTRON CAPTURE NEGATIVE ION CONDITIONS	122
Abstract	123
Introduction	124
Experimental	126
Results	129
Discussion	132
References	152
VIII. BIBLIOGRAPHY	155
APPENDIX 1. MOLECULAR ORBITAL CALCULATIONS FOR ELECTRON AFFINITIES OF POLYCHLORINATED DIBENZOFURANS	166
References	179

APPENDIX 2. ELECTRON CAPTURE NEGATIVE ION MASS	
SPECTROMETRY OF 1,2,3,4-TETRACHLORODIBENZOFURAN	181
References	192
APPENDIX 3. ION-MOLECULE INTERACTIONS IN ELECTRON	
CAPTURE NEGATIVE ION MASS SPECTROMETRY OF	
OCTACHLORODIBENZOFURAN	193
References	200
APPENDIX 4. MISCELLANEOUS FIGURES	201

LIST OF FIGURES

<u>Figure</u>	<u>Page</u>
I.1 Schematic potential-energy diagrams for various modes of resonance electron capture.	5
I.2 Schematic potential-energy diagrams for ion-pair formation and dissociative electron capture.	6
II.1 Stern-Volmer plots of Irgasan-triflate for effects of naphthalene and 1,4-dinitrobenzene.	29
III.1 Products distribution from the photolysis of Irgasan-triflate in the presence of triethylamine.	45
III.2 Formation of 2,4,8-TrCDBF with variation in concentration of Irgasan-Triflate.	46
IV.1 Numbering system of PCDBF.	53
IV.2 2-D NMR COZY spectrum of 1(³⁷ Cl),6-DCDBF and 3(³⁷ Cl),6-DCDBF.	78
IV.3 NOE experiment of 2,3(³⁷ Cl),4-TrCDBF with irradiation of H ₁ .	85
IV.4 NOE experiment of 2,3(³⁷ Cl),4-TrCDBF with irradiation of H ₉ .	86
IV.5 NMR spectrum of 2,3,7(³⁷ Cl)-TrCDBF and 2,3(³⁷ Cl),8-TrCDBF.	88
V.1 Computer simulated (a and c) and experimental (b and d) molecular radical anions of 1,2,3,4,8(³⁷ Cl)-penta-CDBF (95% ³⁷ Cl) and octa-CDBF (43% ³⁷ Cl).	101
VI.1 Correspondence between molecular radical anion abundance and LUMO energies for (a) PCDBFs and (b) PCDDs. 120 °C ion source temperature, helium	

	reagent gas (0.7 mmHg). Error bars are quoted using a two standard deviation criterion.	117
VI.2	Chlorine atom loss by unimolecular dissociation of PCDD molecular radical anions versus LUMO energies of the neutral precursor.	118
VI.3	Schematic representation of the energy terms relating to the ionization, and dissociation of a chloroaromatic radical anion: EA, electron affinity of the neutral; DE, bond dissociation energy for $M^{\cdot-} - [M-Cl]^{-} + Cl^{\cdot}$; ρ , ionizing electron to neutral distance; δ , $[M-Cl]^{-}$ to Cl^{\cdot} separation.	119
VII.1	ECNI mass spectrum of 2,8(^{37}Cl)-di-CDBF (methane, 0.6 torr, 120 $^{\circ}C$).	145
VII.2	ECNI mass spectra of 2,3(^{37}Cl),7,8- (a) and 1,2,3(^{37}Cl),4-tetra-CDBF (b) (methane, 0.6 torr, 190 $^{\circ}C$).	145
VII.3	Source pressure effects on ECNI spectrum of 3(^{37}Cl),4-di-CDBF (methane, 120 $^{\circ}C$). TIC is arbitrary scale.	146
VII.4	Molecular ion abundances of tri-CDBFs vs. energy differences between LUMO- π and LUMO- σ .	147
VII.5	Calculated energies of 3,6-di-CDBF radical anion vs. C-Cl bond lengths.	148
VII.6	Free electron densities on departing chlorine from 3,6-di-CDBF radical anion.	149
VII.7	Calculated energies of 1,6- and 2,6-di-CDBF radical anions vs. C-Cl bond lengths.	150

VII.8 Calculated energies of 2,3,4-tri-CDBF radical
anion vs. C-Cl bond lengths.

151

LIST OF TABLES

<u>Table</u>		<u>Page</u>
I.1	Conventional synthetic routes for PCDBFs.	17
I.2	Conventional synthetic routes for PCDPEs.	18
II.1	Photolysis of Triflates in Cl_2/CCl_4 at 300 nm.	32
IV.1	Synthesis of PCDPEs and PCDBFs from condensation of chlorofluorobenzenes and aminophenols.	77
VII.1	Relative bond cleavage rates, calculated electron densities and energy differences of chlorine-37 labeled di-CDBFs.	142
VII.2	Relative bond cleavage rates and calculated electron densities of chlorine-37 labeled tri-CDBFs.	143
VII.3	Calculated LUMO energies of PCDBFs (AM1 method).	144

LIST OF APPENDIX FIGURES

<u>Figure</u>	<u>Page</u>
A.1.1 AM1 calculated geometries of radical anions of 1,2,3,4-tetra-CDBF with full optimization (a) and partial optimization (b).	175
A.1.2 CNDO calculated LUMO energies of neutral PCDBFs and PCDDs (Isomers are randomly selected).	176
A.1.3 MNDO and CNDO calculated LUMO energies of neutral PCDBFs.	177
A.1.4 MNDO calculated electron affinities and LUMO energies of neutral PCDBFs.	178
A.2.1 Chloride ion abundance of 1,2,3,4-tetra-CDBF as a function of source pressure of helium (120 °C) and methane (190 °C).	185
A.2.2 Total ion current of 1,2,3,4-tetra-CDBF as a function of source pressure (120 °C).	186
A.2.3 Chloride ion abundance of 1,2,3,4-tetra-CDBF as a function of source temperature (0.5 torr).	187
A.2.4 Total ion current of 1,2,3,4-tetra-CDBF as a function of source temperature (0.5 torr).	188
A.2.5 Relative negative ion abundance of 1,2,3,4-tetra-CDBF as a function of electron energy (helium, 0.5 torr, 120 °C).	189
A.2.6 Relative negative ion abundance of 1,2,3,4-tetra-CDBF as a function of GC eluting time of the peak (helium, 0.5 torr, 120 °C).	190
A.2.7 Relative negative ion abundance of octa-CDBF as a	

function of GC eluting time of the peak (helium, 0.5 torr, 120 °C).	191
A.3.1 ECNI mass spectrum of octa-CDBF in the presence of CD ₄ +O ₂ reagent gas (0.6 torr, 120 °C).	198
A.3.2 ECNI mass spectrum of octa-CDBF in the presence of CD ₄ reagent gas (0.6 torr, 120 °C).	199
A.4.1 ECNI mass spectra of di-CDBFs (methane, 0.5 torr, 120 °C).	202
A.4.2 ECNI mass spectra of tri-CDBFs (methane, 0.5 torr, 120 °C).	204
A.4.3 Calculated free electron densities of radical anions of PCDBFs (AM1, UHF).	206
A.4.4 Hi-resolution ECNI mass spectra of 2,3(³⁷ Cl),4- tri-CDBF (methane, 0.7 torr, 150 °C).	207
A.4.5 Hi-resolution ECNI mass spectra of 1,2,3(³⁷ Cl),4- tetra-CDBF (methane, 0.7 torr, 150 °C).	208
A.4.6 ECNI mass spectra of 2,3'(³⁷ Cl),6-tri-CDPE (a) and 2,4'(³⁷ Cl),6-tri-CDPE (b) (methane, 0.5 torr, 120 °C).	209
A.4.7 ¹ H- ¹³ C NMR spectrum of 2,3(³⁷ Cl),4-tri-CDBF.	210
A.4.8 AM1 calculated electron densities and C-Cl bond distances of radical anion of 2,3,4-TrCDBF with full optimization(a) and partial optimization(b).	211
A.4.9 Energy profiles of 1,2-di-CDBF radical anion calculated by AM1 UHF method.	212
A.4.10 Energy profiles of 2,3-di-CDBF radical anion calculated by AM1 UHF method.	213

A.4.11	Energy profiles of 3,4-di-CDBF radical anion calculated by AM1 UHF method.	214
A.4.12	Energy profiles of 1,6-di-CDBF radical anion calculated by AM1 UHF method.	215
A.4.13	Energy profiles of 2,6-di-CDBF radical anion calculated by AM1 UHF method.	216
A.4.14	Energy profiles of 3,6-di-CDBF radical anion calculated by AM1 UHF method.	217
A.4.15	Energy profiles of 2,7-di-CDBF radical anion calculated by AM1 UHF method.	218
A.4.16	Energy profiles of 1,4,7-tri-CDBF radical anion calculated by AM1 UHF method.	219
A.4.17	Energy profiles of 2,6,7-tri-CDBF radical anion calculated by AM1 UHF method.	220
A.4.18	Energy profiles of 2,3,8-tri-CDBF radical anion calculated by AM1 UHF method.	221
A.4.19	Energy profiles of 3,6-di-CDBF radical anion calculated by AM1 RHF method.	222
A.4.20	Free electron density changes on the departing chloride ion of 3,6-di-CDBF (AM1 RHF).	223
A.4.21	Energy profiles of 3,4-di-CDBF radical anion calculated by AM1 RHF method.	224

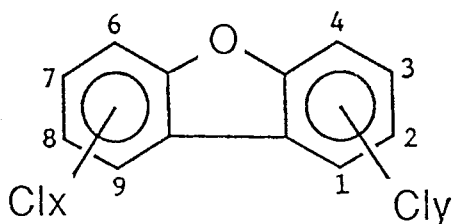
LIST OF APPENDIX TABLES

<u>Table</u>	<u>Page</u>
A.1.1 Calculated heats of formation of 2,3,7-tri-CDBF by various methods.	168
A.1.2 AM1 calculated total energies (TE) and heats of formation (HF) of selected PCDBFs.	173
A.1.3 Calculated LUMO energies of PCDBFs (AM1 method).	174

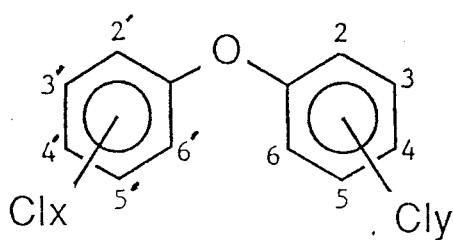
THE SYNTHESIS AND ELECTRON CAPTURE NEGATIVE ION
MASS SPECTROMETRY OF POLYCHLORINATED
DIPHENYL ETHERS AND DIBENZOFURANS

I. INTRODUCTION

Polychlorinated dibenzofurans (PCDBFs) and polychlorinated diphenyl ethers (PCDPEs) are a class of organic chemicals represented by the structural formulas shown below.



Polychlorinated Dibenzofuran
(PCDBF)



Polychlorinated Diphenylether
(PCDPE)

The analysis by mass spectrometry of PCDBFs has been the subject of this research effort, because these compounds are toxic and are present in the environment.¹ PCDPEs also have been of concern since they occur as contaminants in

chlorophenol preparations and are known to form PCDBFs by thermal, photochemical or metal-catalyzed reactions.² Their chemical counter-parts are polychlorinated dibenzo-p-dioxins (PCDDs).

These compounds have been involved in a number of incidences or in industrial accidents which have caused severe intoxication and environmental contamination. In earlier years, PCDBFs were identified mostly in technical products and in pesticides, most of which are not very widely used today anymore.³ Other sources of these toxic compounds, however, are incinerators⁴ of various types and exhaust fumes⁵ from cars running on leaded gasoline with halogenated additives. These chemicals can immediately penetrate living systems through various routes. Background levels of PCDBFs have been identified in fish and other aquatic organisms⁶, and in human adipose tissue samples⁷ as well as in samples of breast milk⁸.

Among the many isomers of PCDBFs, the highest biological activity has been shown by those congeners having chlorine substitution in the 2,3,7 and 8 positions.⁹ In order to assess the biological hazard presented by PCDBF mixtures it is necessary to know the structures and levels of such bioactive congeners present in the samples. Therefore, PCDBF analyses must be sensitive and congener-specific.

Mass spectrometry in combination with gas chromatography has been used most frequently for this purpose. Among various types of mass spectrometry electron capture negative ion

(ECNI) mass spectrometry is most suitable for the detection of trace levels of chlorinated compounds, largely because of the intrinsic sensitivity and specificity of the method for these compounds.¹⁰ In comparison to electron impact and positive ion modes, negative ion forming techniques provide very low detection limits for compounds with large electron affinities.¹¹ Since most halogenated aromatic compounds have high electron affinities this method is generally preferred for the trace analyses of these contaminants. Thus, the methods of ECNI mass spectrometry is ideally suit for the analyses of certain chlorinated wood preservatives and their by-products, other phenol preparations, and for various pollutants including nitroaromatic compounds from auto and diesel exhausts and emissions from incinerator fumes.¹

Electron attachment to suitable molecules occurs by ECNI mass spectrometry. High energy electrons (70~100 eV) are produced from a filament in the source that also contains a reagent gas whose primary function is to moderate the energy of the electrons and to produce a large population of low energy or nearly thermal energy electrons (0~15 eV).¹² These low energy electrons attach to the sample molecules to produce various ions according to the energetic or structural differences between parent molecules. Frequently, the molecular radical anion is the most intense peak in the spectrum.

Three major mechanisms of ionization occur in the ion

source by ECNI mass spectrometry. They include: (1) resonance electron capture, (2) dissociative electron capture and (3) ion-pair formation.

Resonance electron capture processes arise within a narrow range of electron energies, that is usually less than a few tenths of electron volts. In most cases the formation of the parent negative ion state reaches the maximum probability at ~ 0.0 eV.¹² That is there is no activation energy involved; the electronic and vibrational modes are coupled, and the very low energy electron drifts into the sample molecule and is captured to give a negative ion state. The cross sections and lifetimes of the resonance capture process are strongly dependent on the molecular structure and electron affinity.¹³ When the electron affinity of a molecule is less than 0 the unstable molecular radical anion $(AB^{\dot{-}})^*$ is more likely to disappear by autodetachment of the electron, i.e., by loss of the electron and a return of the molecule to the ground state (Figure I.1A). If the electron affinity is greater than 0 a stable molecular radical anion, AB^- may be formed provided excess energy of electron attachment is removed by a buffer gas at moderate pressures (0.1~1.0 torr).¹⁴ In this case the stabilized AB^- lives long enough ($>10^{-6}$ sec) to be observed by the usual mass spectrometry detection methods (Figure I.1B). Finally, if the electron affinity exceeds the dissociation energy of the AB^- , a new reaction channel becomes available, in which a

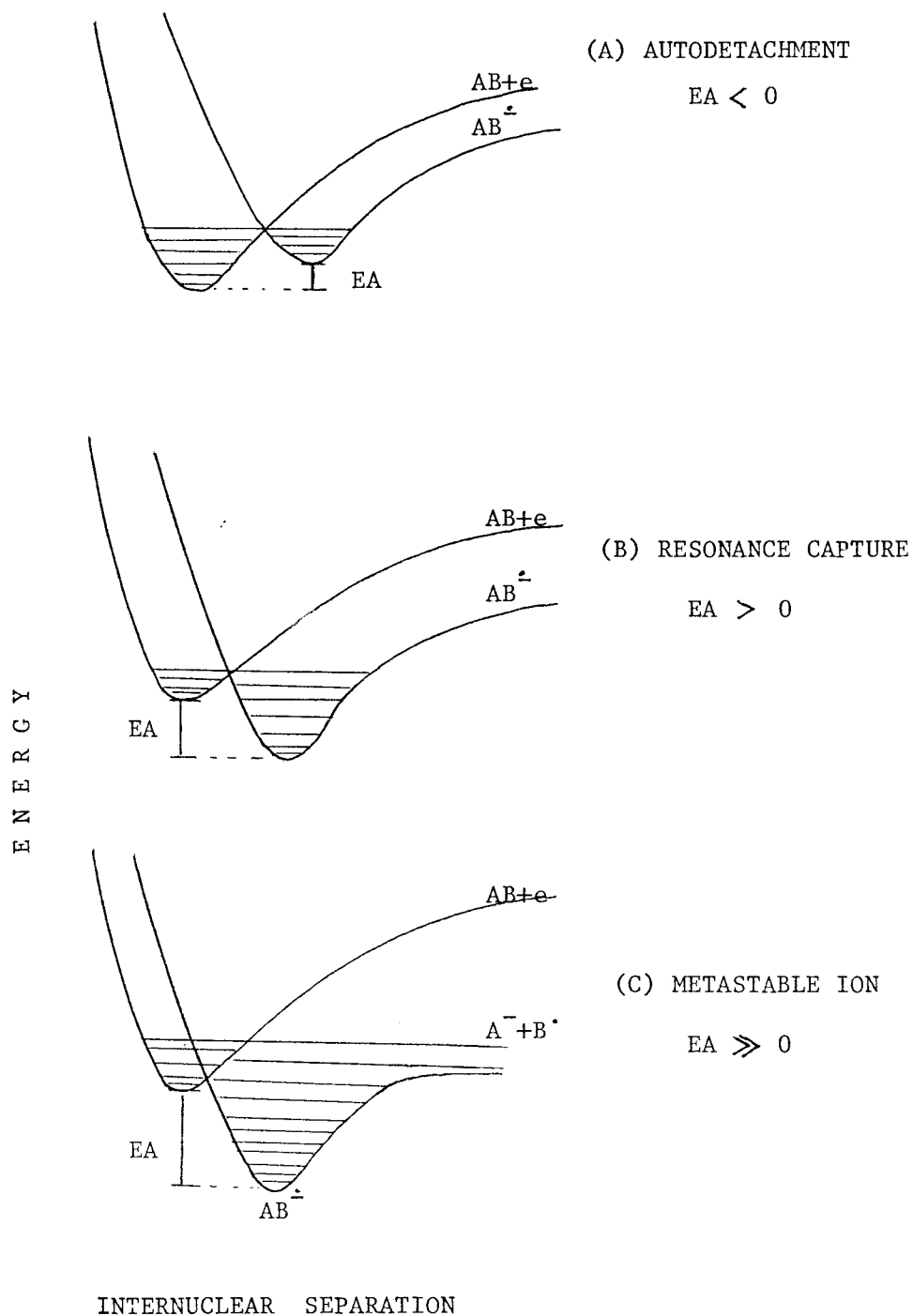


Figure I.1. Schematic potential-energy diagrams for various modes of resonance electron capture.

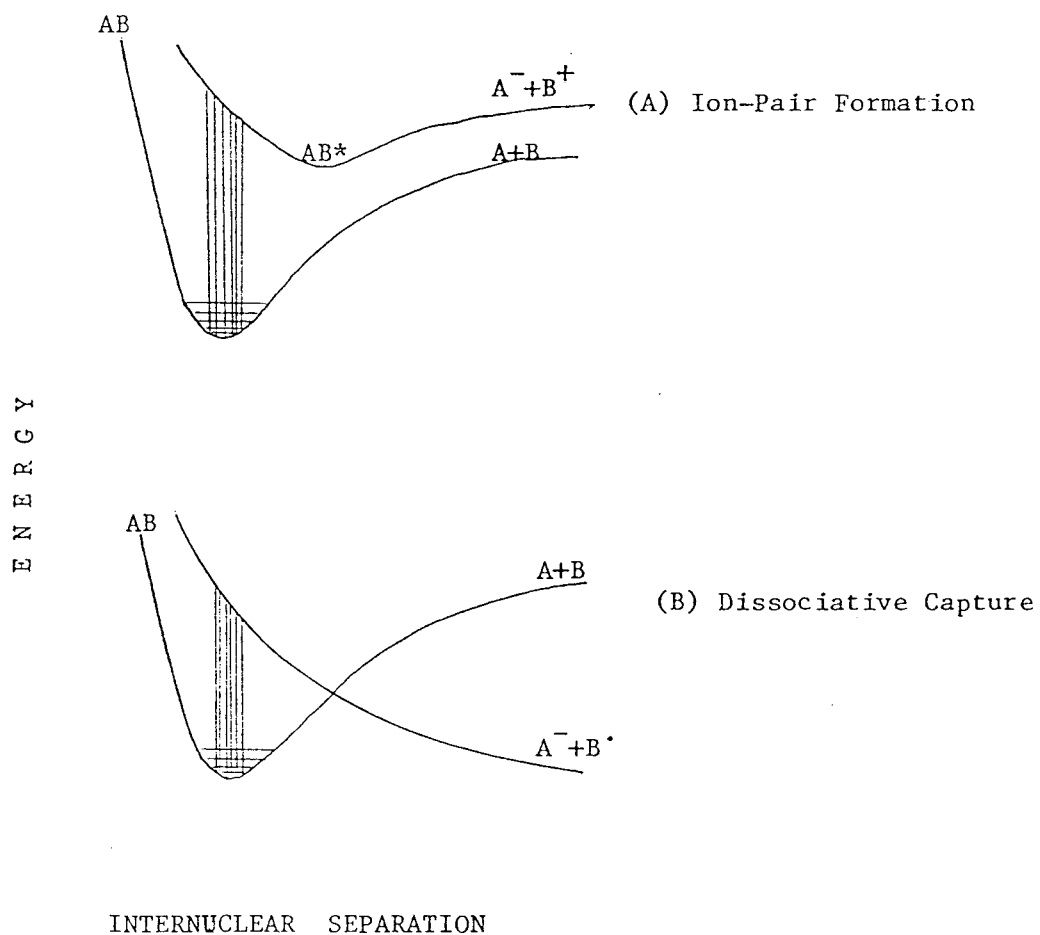


Figure I.2. Schematic potential-energy diagrams for ion-pair formation and dissociative electron capture.

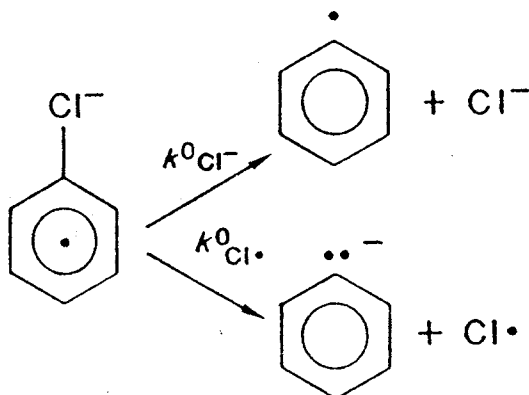
decreasing AB^- concentration would be expected (Figure I.1C). This event which can be detected by metastable ion analysis using B/E linked scanning has been observed with highly chlorinated compounds.¹⁵

Dissociative electron capture (Figure I.2B) takes place when capture of an electron leads a molecule to a repulsive state of $AB^{\dot{-}}$ which immediately dissociates into A^-+B^{\cdot} . The first step after the capture of an electron by the molecule is a vertical transition on the potential energy curve. This vertical transition called a Franck-Condon transition takes place with nuclear motion at rest or at the equilibrium value of r . This principle is based on the Born-Oppenheimer approximation which assumes the separation of nuclear and electronic motion.¹⁶ An ionizing electron may enter a π -LUMO (π type lowest unoccupied molecular orbital) but the dissociation is believed to occur from the σ^* state of the molecule. The molecular radical anion formed is unstable and if it exists at all it has a very short life time ($<10^{-9}$ sec). Since these short lifetimes are not easily measured, this process has long since been viewed as taking place in a single step, i.e., electron capture and bond breaking are synchronous.¹⁷

Ion-pair formation (Figure I.2A) is usually not involved in ECNI mass spectrometry since this is a relatively high energy process, and the mechanism is not well known. In this process the excited hot molecule dissociates into a positive

ion and a negative ion by the energy from electron bombardment.

In general electrons with low energies (~ 0.01 eV) usually correspond to resonance electron capture and those with higher energies (1-15 eV) correspond to dissociative electron capture. However, the channel between the two processes of dissociative capture and resonance capture can not be defined exactly since we assume that both processes involve a molecular radical anion in the initial stages after electron capture, regardless of the stability of these ions. These processes are not easily distinguished experimentally since to be detectable by conventional mass spectrometry the radical anions must have lifetimes greater than 10^{-5} sec. By field ionization kinetics¹⁸ ions with lifetimes as short as 10^{-9} sec may be studied. But mass spectrometry cannot be utilized for studying ions with rate constants greater than 10^9 sec⁻¹.



Scheme I.1

Studies in mass spectral fragmentation mechanisms have been conducted for both positive ions and negative ions. Hammett type relationships were found for daughter/parent ion ratios of molecule and the rho values allow location of the transition states in the bond cleavage processes.¹⁹ The Hammett study for chlorobenzenes under ECNI mass spectrometry conditions for two possible dissociative electron capture pathways (Scheme I.1) showed that the relative rates of Cl⁻ and Cl· atom losses are dependent upon the degree of chlorination and on the substitution pattern.²⁰ The branching ratio, $\log [(M-Cl)^-]/[Cl^-]$, is related to the sum of the σ substituents (eq. 1). The inaccuracies in the σ values, however, do not allow relationships to be drawn with respect to regiochemistry.

$$\log (k_{Cl^-}/k_{Cl\cdot}) = (\rho' - \rho)\Sigma\sigma + C \quad (1)$$

For halogenated aromatic compounds the branching ratios can also be correlated to energies of the low-lying unoccupied molecular orbitals. Dissociative electron capture products, (M-X)⁻ and X⁻ are related to the electron affinities²¹, and these in turn can be predicted from the lowest unoccupied molecular orbital (LUMO) energies.²² These energies vary according to the degree of halogenation.²³ Branching ratios for PCDDs are linearly related to the energies of several low-lying unoccupied molecular orbitals.²⁴ Correlations were also

found with calculated total energies of the neutral molecules, molecular radical anions and $(M-Cl)^{\cdot -}$ ion.

If total energies are calculated for the two possible dissociative electron capture pathways the energy difference reflects the relative rates of two processes and should be correlated with the branching ratios (eq.2).²⁵ This relationship assumes a knowledge about the chlorine which is ejected from the molecules under dissociative electron capture. The ultimate goal of this study is to be able to predict structural isomers of PCDBFs by using the branching ratios, measured under ECNI mass spectrometry conditions.

$$\log\left[\frac{(M-Cl)^{\cdot -}}{[Cl^{\cdot -}]}\right] \propto \{E(M-Cl)^{\cdot -} + E(Cl^{\cdot -}) - [E(M-Cl)^{\cdot} + E(Cl^{\cdot})]\} \quad (2)$$

The mechanism and kinetics of reductive carbon-halogen bond cleavages in halogenated aromatic molecules under electrochemical conditions have been studied by many researchers.²⁶ Few studies, however, were conducted in the gas phase.^{20,27} Correlations have been found between the reduction potentials and calculated orbital energies in solution. The calculations show that the process involves the transfer of an ionizing electron from a π^* orbital of ArX to a σ^* orbital of the C-X bond and finally to a p orbital of the halogen.

Andrieux and coworkers^{26a} proposed that the crossing point for the change in singly occupied molecular orbital (SOMO) from π^* to σ^* is the transition state for C-X bond cleavage.

However, Moreno et al.^{26b} suggested that the rate determining step in C-X bond cleavage is the stability of the σ -radical anion instead of the π^* - σ^* electron transition. Nevertheless, all these studies indicate that the molecular orbital calculations can be used to predict the location of an ionizing electron and to explain the bond cleavage process. On this basis the observed preferential C-Cl bond cleavages in chlorine-37 labeled compounds under ECNI conditions would be extremely helpful in an understanding of the mechanism of dissociation and its relationship to various molecular orbital properties, which can be calculated by semiempirical SCF methods. In order to carry out these studies, i.e., to identify the labile chlorines in PCDBFs under ECNI conditions, chlorinated compounds regiospecifically labeled with chlorine-37 must be synthesized.

Syntheses of PCDBFs and PCDPEs. Compared to PCDDs, considerably fewer PCDBF isomers have been synthesized.²⁸ A limited number of PCDBF isomers, including several carbon-13 and chlorine-37 labeled compounds, are commercially available²⁹, but very expensive. Because of this limitation, there has been widespread interest in the synthesis of specific PCDBF isomers.³⁰ All 38 isomers of tetra-CDBF have been synthesized by Mazer et al.⁹. The methods include pyrolysis of specific polychlorinated biphenyls (PCBs), ultraviolet (UV) photolysis of penta-CDBF isomers and chlorination by electrophilic substitution of specific tri-

CDBF isomers. The synthesis of all 87 PCDBF congeners containing 4~8 chlorine atoms were achieved by Bell and Gara³¹ via low temperature Pd-catalyzed cyclization of the appropriate PCDEs. Synthesis of mono- and dichloro compounds, however, are rarely reported.

Characterization of structures of PCDBFs has been done using several methods, including gas and liquid chromatography, mass spectrometry, proton and ¹³C NMR, and photolytic dechlorination coupled with pattern recognition techniques^{28d}. A few have been confirmed by single-crystal X-ray diffraction (XRD) method.³² Recently, Dunn et al.³³ reported a relationship between GC retention of PCDBFs and calculated molecular surface area.

The most common synthetic routes are shown in Table I.1. In many instances the pyrolysis of a PCB can lead to a number of PCDBFs, in many cases several with the same degree of chlorination (Table I.1.A). This method may prove useful in situations where only minute quantities of PCDBF isomers are required for reference purposes in GCMS analysis.³⁴ The formation of PCDBFs from the pyrolysis of PCBs may have environmental implications, because a large portion of PCB's used apparently are disposed of by way of incineration.³⁵ Experiments are carried out in the presence of air in sealed quartz ampoules at temperatures ranging from 550 to 850 °C. However, this synthesis is only semiselective, since there are a number of mechanisms by which PCBs may be converted to

PCDBFs.

The most common electrophilic chlorination of dibenzofuran involves FeCl_3/I_2 ,³⁶ and SbCl_5 ,³⁷ as catalysts. An improved chlorination method with $\text{Fe}/\text{Cl}_2/\text{CCl}_4$ was reported by Williams and Blanchfield³⁸. More recently, an efficient microscale chlorination procedure using a silica column was developed for the synthesis of isotopically labeled PCDDs³⁹ and PCDBFs⁴⁰. Direct chlorination of parent dibenzofuran (Table I.1.B) leads initially to 2,8-di-CDBF but further chlorination yields complex mixtures of the higher substituted compounds including highly toxic 2,3,7,8-tetra-CDBF. This method requires great efforts to separate the congeners.

Photolytic dechlorination of penta-CDBF (Table I.1.C) served as an alternative synthetic method for the formation of tetra-CDBF.⁴¹ The loss of chlorine may involve a homolytic bond cleavage in which the intermediate free radical apparently gains stabilization from the presence of the two vicinal chlorines at positions 2- and 4-, and perhaps some added stabilization from the biphenyl bond located para to it. For example, dechlorination of 1,2,3,4-tetra-CDBF showed that the 3-chlorine was the most easily lost, resulting in 1,2,4-tri-CDBF as the major trichloro compound formed. The second most abundant isomer formed was 1,3,4-tri-CDBF, resulting from the loss of the 2-chlorine. In this case the 2-chlorine also is surrounded by two vicinal chlorines and at the same time located para to the ether linkage.

An additional, convenient route is the cyclization of PCDPEs, of which a number of isomers are available. This reaction can be carried out photochemically^{28c,28g} (Table I.1.D), by a palladium acetate promoted reaction^{28e} (Table I.1.E) or by diazotization of suitably substituted o-phenoxyanilines^{28a} (Table I.1.F). The photoreaction usually involves two competing reaction pathways; dechlorination and cyclization. It has been shown that the dechlorination can be inhibited largely by using acetone as a solvent.^{28g} A major advantage of this methods is that it gives almost quantitative yields and it is easy to anticipate the product structures. However, the latter two methods give very low yields with highly chlorinated diphenyl ethers.

PCDPEs proved to be excellent precursors for the synthesis of PCDBFs via photochemical or organometallic cyclization as described in the beginning. Synthesis of PCDPEs has been extensively studied by Sundstrom and Hutzinger⁴² in 1976. The ether synthesis can be accomplished by several methods as shown in Table I.2.

The direct chlorination of dipheyl ether (Table I.2.A) can be carried out by using CCl_4 as solvent with SnCl_4 , FeCl_3 or AlBr_3 as catalysts or by using acetic acid without catalysts.⁴³ The substitution initially occur in the 2- and 4-positions. The chlorination reactions are usually performed without catalysts when low-chlorinated DPEs are to be synthesized. Decachloro-DPE can be obtained by treatment of

DPE with the BMC reagent ($\text{SO}_2\text{Cl}_2\text{-AlCl}_3\text{-S}_2\text{Cl}_2$).⁴⁴ It has been claimed that the usual ratio of para to ortho substitution of 4:1 obtained upon monochlorination of DPE can be increased to 9:1 by not using solvent or catalyst.⁴⁵ Increased amounts of meta isomers (64~80 %) can be obtained by heating the chlorination mixture with aluminum chloride or by chlorination in the gas phase.⁴⁶

The classical Ullmann method involves coupling of phenol salts with halogenated benzenes in the presence of copper catalysts (Table I.2.B). Cu_2Cl_2 and KI are used with diglyme while no catalysts are used when dimethyl sulfoxide is used. Sundstrom et al.⁴² developed a modification of the Ullmann method using diglyme as solvent to prepare chloro-nitro-DPEs in which the nitro groups were displaced by chlorine in the Ponomarenko reaction.

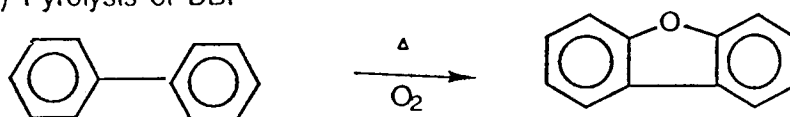
Other ether coupling syntheses can be accomplished by coupling of phenoxide ion and diaryliodonium salt (Table I.2.C) or by nucleophilic substitution of chlorobenzene with phenoxide ion (Table I.2.D). The latter method, however, gives very low yields unless the nucleophiles or electrophiles are activated.

A number of low-chlorinated DPEs have also been synthesized by exchange of amino groups for chlorine via the Sandmeyer reaction (Table I.2.E). However, the exchange of amino group in the position ortho to the ether linkage for chlorine was unsuccessful. Amino-chloro-DPEs can be converted

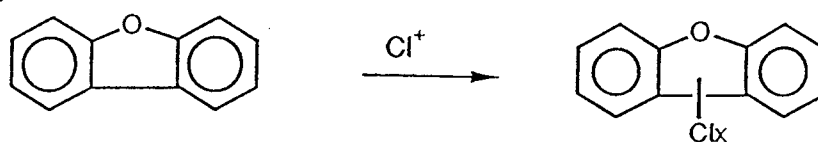
to chloro-DPEs by deamination via treatment with amyl nitrate in boiling tetrahydrofuran.⁴⁷

Table I.1. Conventional synthetic routes for PCDBFs.

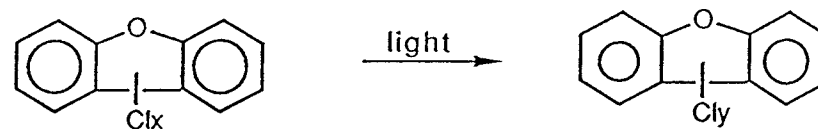
(A) Pyrolysis of DBF



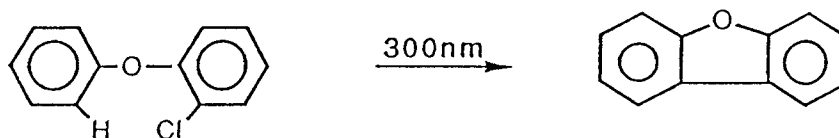
(B) Direct Chlorination



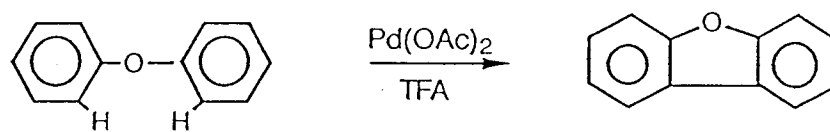
(C) Photodechlorination of PCDBF



(D) Photochemical Cyclization Of DPE



(E) Pd Catalyzed Cyclization Of DPE



(F) Deaminated Cyclization

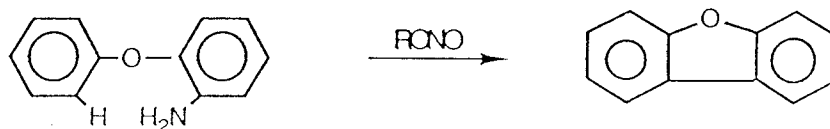
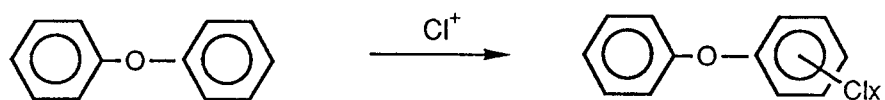
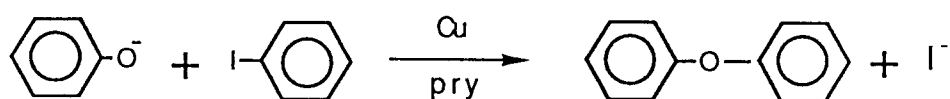


Table I.2. Conventional synthetic routes for PCDPES.

(A) Direct Chlorination of DPE



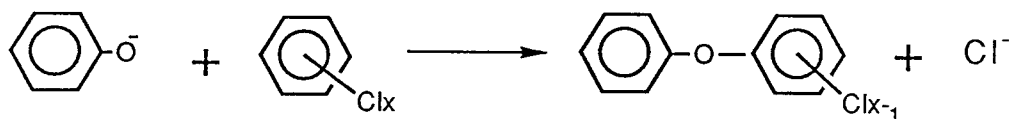
(B) Ullman Ether Synthesis



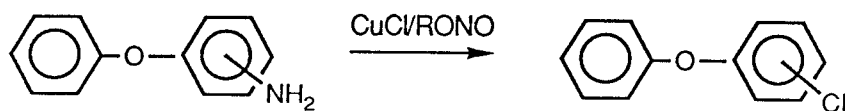
(C) Phenoxide Displacement Of Diaryliodonium salt



(D) Nucleophilic Displacement



(E) Sandmeyer Reaction



References

1. (a) Rappe, C. Halogenated Biphenyls, Terphenyls, Naphthalenes, Dibenzofurans and Related Products; Elsevier/North Holland Biomedical Press: New York, 1980.
(b) Rappe, C.; Choudhary, G.; Keith, L.H. Chlorinated Dioxins and Dibenzofurans in Perspective; Lewis Publishers: Chelsea, 1986.
(c) Choudhary, G.; Keith, L.H.; Rappe, C. Chlorinated Dioxins and Dibenzofurans in the Total Environment I and II; Butterworth Publishers: Woburn, 1983.
2. Busch, K.L.; Norstrom, Å.; Bursley, M.M.; Hass, J.R.; Nilsson, C.-A. Biomed.Mass Spectrom. 1979, 6, 157.
3. Rappe, C. Env. Sci. Technol. 1984, 16, 78 A.
4. Rappe, C.; Marklund, S.; Kjeller, L.O.; Bergqvist, P.A.; Hansson, M. In Chlorinated Dioxins and Dibenzofurans in the Total Environment Keith, L.H.; Rappe, C.; Choudhary, G., Eds.; Butterworth: Stoneham, 1984; Vol.II, p 401.
5. Marklund, S.; Rappe, C.; Tysklind, M.; Egeback, K.-E. Chemosphere 1986, 10, 355.
6. Rappe, C.; Buser, H.R.; Stalling, D.L.; Smith, L.M.; Dougherty, R.C. Nature 1981, 292, 524.
7. Rappe, C.; Bergqvist, P.-A.; Hansson, M.; Kjeller, L.-O.; Lindstrom, G.; Marklund, S.; Nygren, M. Banbury Report 18: Biological Mechanisms of Dioxin Action; Cold Spring Harbor Laboratory: New York, 1984; pp 17-25.
8. Fuerst, P.; Meemken, H.-A.; Groebel, W. Chemosphere 1986, 10, 381.
9. Mazer, T.; Hileman, F.; Noble, R.W.; Brooks, J.J. Anal. Chem. 1983, 55, 104.
10. Dougherty, R.C. Anal. Chem. 1981, 53, 625 A.
11. Larameé, J.A.; Arbogast, B.C.; Deinzer, M.L. Anal. Chem. 1986, 58, 2907.
12. Harrison, A.G. Chemical Ionization Mass Spectrometry; CRC Press: Boca Raton, 1983.
13. Christophorou, L.G. In Photon, Electron, and Ion Probes of Polymer Structure and Properties; Dwight, D.W.;

- Fabish, T.J.; Thomas, H.R. Eds.: American Chemical Society, Washington, D.C., 1981, pp 11-34.
14. Johnson, J.P.; McCorkle, D.L.; Christophorou, L.G.; Carter, I.G. J. Chem. Soc., Faraday Trans. II 1975, 71, 1742.
 15. Laramée, J.A.; Chang, Y-S.; Arbogast, B.C; Deinzer, M.L. Biomed. Mass Spectrom. 1988, 17, 63.
 16. Christophorou, L.G. Electron-Molecule Interactions and Their Applications; Academic Press, Inc.: Orlando, 1984; p 477.
 17. Naff, W.T.; Cooper, C.O.; Compton, R.N. J. Chem. Phys. 1968, 49, 2784.
 18. Schulten , H.-R. Int. J. Mass Specrom. Ion. Phys. 1979, 32, 97.
 19. a) McLafferty, F.W. Anal. Chem. 1959, 31, 447.
b) Bursey, M.M.; McLafferty, F.W. J. Am. Chem. Soc. 1966, 88, 529.
c) McLafferty, F.W.; Bursey, M.M. J. Org. Chem. 1968, 33, 124.
d) McLafferty, F.W.; Wachs, T J. Am. Chem. Soc. 1968, 89, 5043.
e) McLafferty, F.W.; Wachs, T.; Lifshitz, C.; Innorta, G.; Irving, P. J. Am. Chem. Soc. 1972, 92, 6867.
 20. Freeman, P.K.; Srinivasa, R.; Campbell, J.-A.; Deinzer, M.L. J. Am. Chem. Soc. 1986, 108, 5531.
 21. Christophorou, L.G.; Grant, M.W. Advances in Chemical Physics; Wiley-Interscience: New York, 1977; Vol. 36.
 22. Koopmans, T. Physica (The Hague) 1968, 104.
 23. Christophorou, L.G. Adv. Electron. Phys. 1978, 46, 55.
 24. Laramée, J.A.; Arbogast, B.C.; Deinzer, M.L. Anal. Chem. 1988, 60, 1937.
 25. Christophorou, L.G. EHP, Environ. Health Perspect. 1980, 36, 3.
 26. (a) Andrieux, C.P.; Savéant, J.M.; Su, K.B. J. Phys. Chem. 1986, 90, 3815.
(b) Moreno, M.; Gallardo, I.; Bertran, J. J. Chem. Soc., Perkin Trans. II 1989, 2017.
(c) Aalstad, B.; Parker, V.D. Acta Chem. Scand., Ser. B 1982, B 36, 47.

- (d) Beland, F.A.; Farwell, S.O.; Callis, P.R.; Geer, R.D. J. Electroanal. Chem. 1977, 78, 145.
- (e) Glidewell, C. Chemica Scripta 1985, 20, 142.
27. Mairanovsky, V.G. J. Electroanal. Chem. 1981, 125, 231.
28. a) Grey, A.P.; Dipinto, J.J.; Solomon, I.J. J. Org. Chem. 1976, 41, 2428.
b) Grey, A.P.; Cepa, S.P.; Solomon, I.J.; Aniline, O. J. Org. Chem. 1976, 41, 2435.
c) Norstrom, A.; Andersson, K.; Rappe, C. Chemosphere 1976, 5, 21.
d) Buser, H.R. J. Chromatog. 1976, 129, 303.
e) Norstrom, A.; Andersson, K.; Rappe, C. Chemosphere 1976, 5, 419.
f) Buser, H.R.; Bosshardt, H.-P.; Rappe, C. Chemosphere 1978, 7, 109.
g) Choudhry, G.F.; Sundstrom, G.; Wielen, R.W.M.; Hutzinger, H. Chemosphere 1977, 6, 327.
h) Lindahl, R.; Rappe, C.; Buser, H.R. Chemosphere 1980, 9, 351.
i) Gara, A.; Andersson, K.; Nilsson, C.-A.; Norstrom, A. Chemosphere 1981, 10, 365.
j) Hileman, F.D.; Hale, M.D.; Mazer, T.; Noble, R.W. Chemosphere 1985, 14, 601.
k) Humpfi, T. Chemosphere 1986, 15, 2003.
29. a) KOR Isotope (Cambridge, MA).
b) Cambridge Isotope (Woburn, MA).
c) Ultra Scientific (North Kingstown, RI).
30. Hutzinger, O.; Frei, R.W.; Meriam, E.; Pocciari, F., Eds. Chlorinate Dioxins and Related Compounds; Pergamon Press: New York, 1982.
31. Bell, R.A.; Gara, A. Chlorinated Dioxins and Dibenzofurans in Total Environment II; Butterworth-Ann Arbor Science: Boston, 1983.
32. Slonecker, P.J.; Cantrell, J.S. Anal. Chem. 1983, 54, 1543.
33. Dunn III, W.J.; Koehler, M.; Stalling, D.L.; Schwartz, T.R. Anal. Chem. 1986, 58, 1835.
34. Buser, H.R. Doctoral Dissertation 1978, University of Umea, Sweden.
35. Rappe, C.; Choudhary, G.; Keith, L.H. Chlorinated Dioxins and Dibenzofurans in Perspective; Lewis Publishers Inc.: Chelsea, 1986; Ch. 6, p 79.

36. Tomita, M.; Ueda, S.; Narisada, M. Yakugaku Zasshi 1959, 79, 186.
37. Denivelle, L.; Fort, R.; Van Hai, P. Bull. Soc. Chim. Fr. 1960, 1538.
38. Williams, D.T.; Blanchfield, B.J. J. Assoc. Off. Anal. Chem. 1972, 55, 93.
39. Lamparski, L.L.; Nestruck, T.J. Anal. Chem. 1982, 54, 402.
40. Peterson, R.G. Bull. Environ. Contam. Toxicol. 1987, 38, 416.
41. Mazer, T.; Hileman, F.D. Chemosphere 1982, 11, 651.
42. Sundstrom, G.; Hutzinger, O. Chemosphere 1976, 5, 305.
43. Wengarten, H; Schisla, R.M. J. Org. Chem. 1962, 27, 4103.
44. Hutzinger, O.; Jamieson, W.D.J.; Safe, S.; Zitko, V.Z. J. Assoc. Off. Anal. Chem. 1973, 56, 982.
45. U. S. 3, 022, 252, Feb. 20, 1962, (Chem. Abstr. 1962, 58, 7174e), 45.
46. Engelsma, J.W.; Kooljman, E.C. Rec. Trav. Chim. 1961, 80, 526.
47. Cadogan, J.I.G.; Molina, G.A. J. Chem. Soc. Perkin Trans. I. 1973, 541.

II. PHOTOCHEMISTRY OF IRGASAN-TRIFLATE:
A SIMPLE CONVERSION OF AN AROMATIC HYDROXYL GROUP
TO CHLORINE IN THE SYNTHESIS OF POLYCHLORINATED
DIPHENYL ETHERS AND POLYCHLORINATED DIBENZOFURANS

Yoon-Seok Chang, Jung-Suk Jang, and Max L. Deinzer

Department of Chemistry
Oregon State University
Corvallis, Oregon 97331

Tetrahedron, 1990, 46, 4161.

Photolysis and synthesis were performed by Jung-Suk Jang. Product identification and data interpretation were done by Yoon-Seok Chang.

Abstract

Several chlorophenoxy phenols were converted to their triflates by reaction with trifluoromethanesulfonyl chloride. The triflates undergo triplet sensitized photolytic cyclizations at 300 nm in acetone to give chlorodibenzofurans or singlet state substitution reactions in carbon tetrachloride saturated with chlorine gas to give the corresponding chlorine substituted diphenyl ethers. 2-Chloro-3-hydroxy dibenzofuran was similarly converted to the 2,3-dichlorodibenzofuran. The mechanism for displacement of triflate by chlorine appears to involve chlorine-arene π complexation.

In recent years the polychlorinated dibenzofurans (PCDBFs), along with their dibenzo-p-dioxin counterparts, have been the subject of an intense research effort because of their high toxicity as contaminants in the environment.¹ In connection with our efforts to synthesize polychlorinated diphenyl ethers (PCDPEs) and PCDBFs for mass spectrometric studies² we sought to replace the hydroxyl group of polychlorinated phenoxy phenols (PCPPs) with chlorine. The PCPPs had been prepared previously in this laboratory.³ These compounds also have been isolated from commercial pentachlorophenols as impurities.⁴

5-Chloro-2-(2,4-dichlorophenoxy)phenol 1, a commercial pesticide, called Irgasan DP300, CIBA-GEIGY Co., was chosen as the starting material in one example. Irradiation of a degassed 10^{-3} M acetone solution of Irgasan triflate 2⁵ at 300 nm gave complete conversion to 2,4,8-trichlorodibenzofuran (2,4,8-TrCDBF) 3⁶. A yield of 88 % of 2,2',4,4'-tetrachlorodiphenyl ether 4⁷ was obtained when irradiated in chlorine saturated carbon tetrachloride. Compound 4 also could be readily converted to 2,4,8-TrCDBF 3 in acetone solution. Photolysis of PCDPEs in acetone resulting in its cyclization to form PCDBFs has been known as the major photoconversion pathway.⁸ However, the detailed mechanism for conversion is still obscure. It was proposed⁹ that acetone acts as a triplet photosensitizer due to its high triplet energy ($E_T = 79\text{--}82$ kcal/mol)¹⁰ and that the excited triplet state of the

substrate is responsible for the cyclization via single electron transfer. The yield of photoproduct 3 was low in other organic solvents¹¹ and the formation of 3 in acetone was quantitatively quenched in the presence of triplet quencher, naphthalene, for which the Stern-Volmer plot was linear. Particularly efficient nonlinear quenching was also observed with 1,4-dinitrobenzene, in which a secondary process is involved such as electron transfer or singlet energy quenching (Figure II.1). In this case the ortho-triflate group is much superior to the other ortho-chlorine as a leaving group during cyclization.

Traditional chlorination reagents¹² including SOCl_2 , POCl_3 , PCl_5 and $(\text{C}_6\text{H}_5)_3\text{PCl}_2$ ¹³ for substituting a chlorine for a hydroxyl group are often used, but the conditions involve high temperatures. Conversion of the hydroxyl group to an amino functionality via diethylphosphate¹⁴ followed by diazotization and chlorination¹⁵ is also well known. In the latter steps dechlorination or hydrogen atom abstraction are often observed. The preparation of 4 from the photolysis of 2 in Cl_2/CCl_4 solution is a new and milder procedure for this transformation.

The mechanism of this photolytic chlorine-substitution may include π -complexation between the triflate compound and chlorine atom followed by ipso substitution. It has been found that in the typical photolytic chlorination condition the chlorine atom forms a π -molecular complex with arenes.

Electron-poor arenes that have lower π -basicities than benzene form weaker Cl/arene π -complexes and these π -complexes can rearrange to σ -molecular complexes followed by ipso substitution.¹⁶ Ipso substitution of bromine or iodine (X=Br, I) by chlorine is well known.¹⁷ In some cases chlorine atom can also be captured on the other benzene ring to undergo displacement of chlorinated phenoxy radical bearing the triflate group to give a polychlorobenzene (Scheme II.2, pathway a).

The experiments also were carried out with the chlorine-37 enriched compound and significant loss of chlorine-37 excess was observed (from 95% to 65%) (Entry 5 of Table II.1). This provides additional evidence for π -complexation prior to the ipso substitution. Table II.1 shows some transformations of hydroxy compounds to the corresponding chloro compounds.

A typical experimental procedure for the chlorine substitution reaction is as follows. A hydroxy compound is dissolved in acetone and anhydrous potassium carbonate is added. The mixed solution is stirred with a magnetic bar at room temperature and trifluoromethanesulfonyl chloride solution in acetone is slowly added. After completion of the reaction, the product is isolated by a silica-gel column. The triflate compound is dried and redissolved (usually, 10^{-2} M concentration) in carbon tetrachloride solution saturated with chlorine gas and photolyzed in a pyrex tube at 300 nm for 1 - 2 hours. The solution is concentrated down and

chromatographed on a preparative silica TLC plate or on a HPLC column.

Acknowledgement. We gratefully acknowledge support from the National Institutes of Health, NIEHS ES00040 and NIEHS ES00210. We also thank Dr. Ramnath Iyer for helpful discussion. This paper is issued as technical paper No. 9249 from the Agricultural Experimental Station.

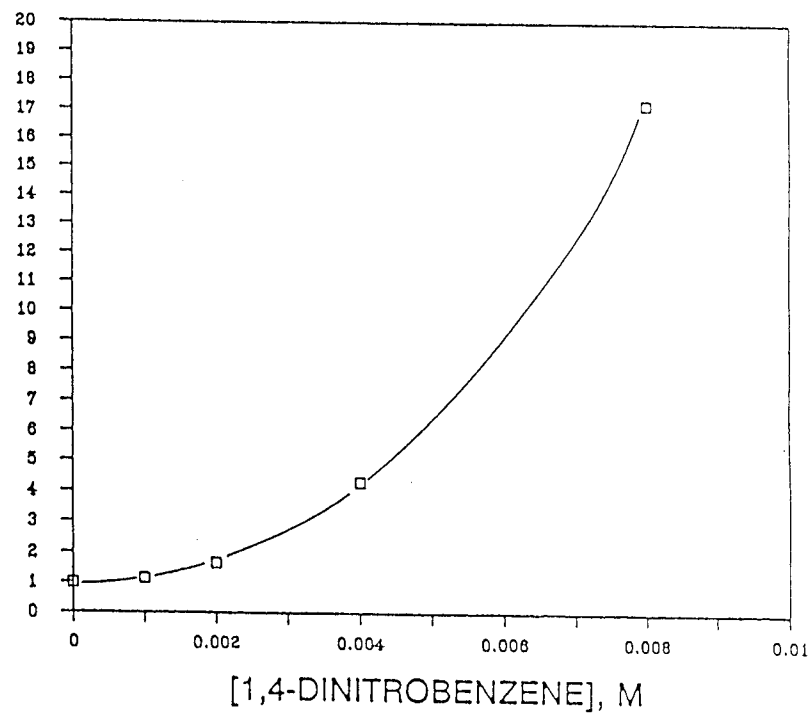
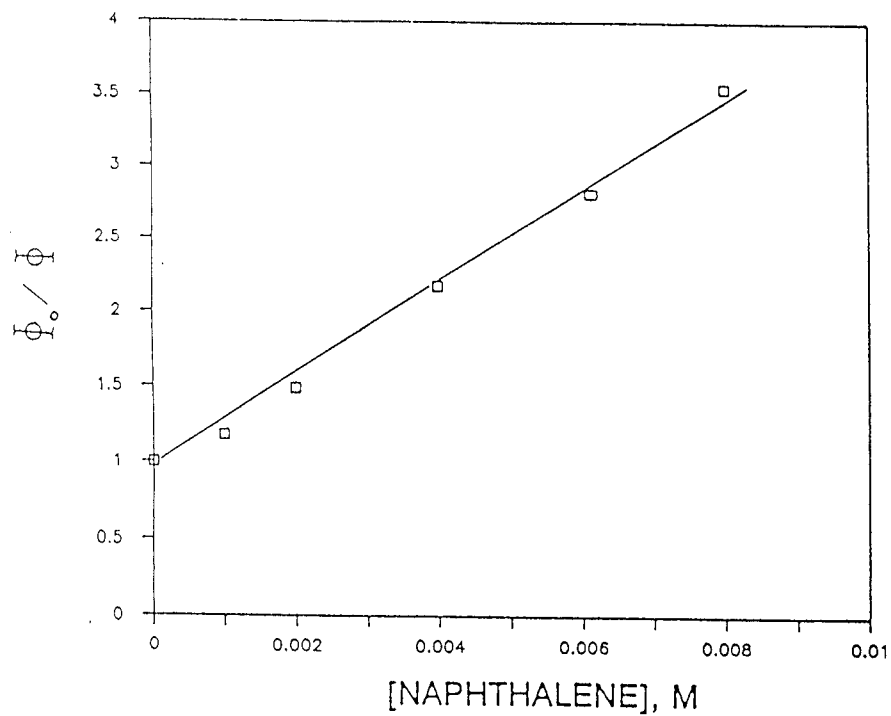
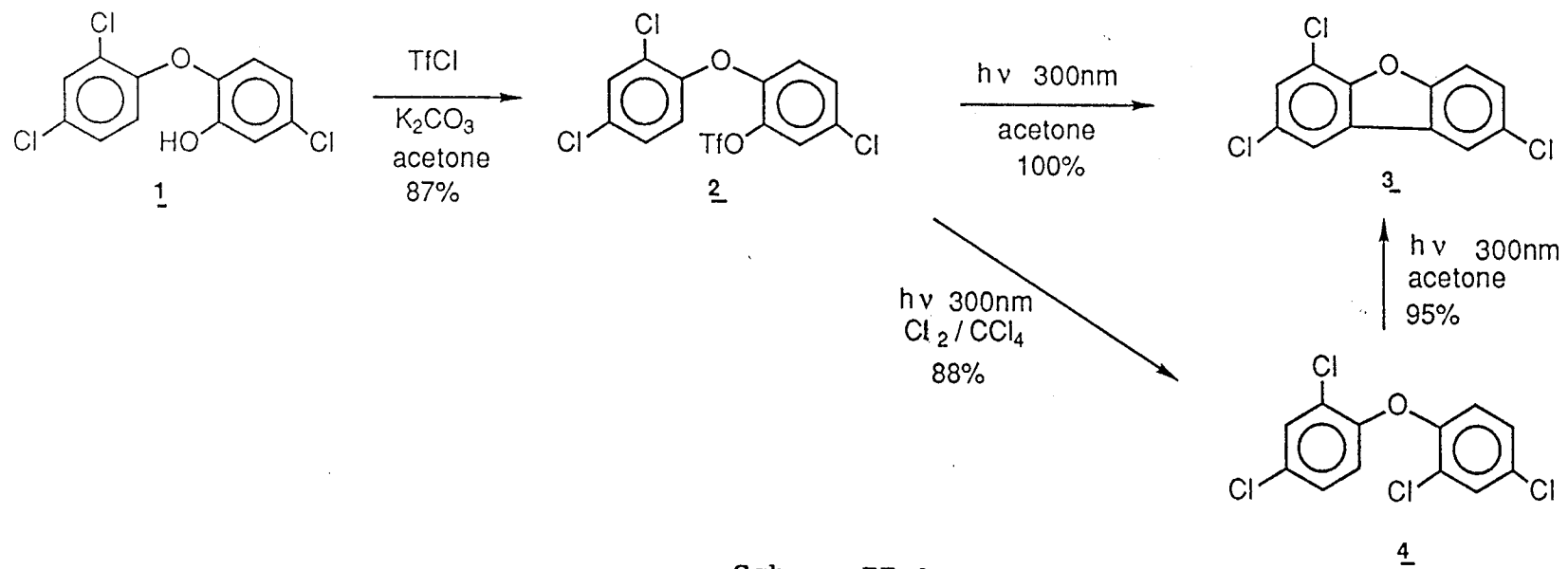
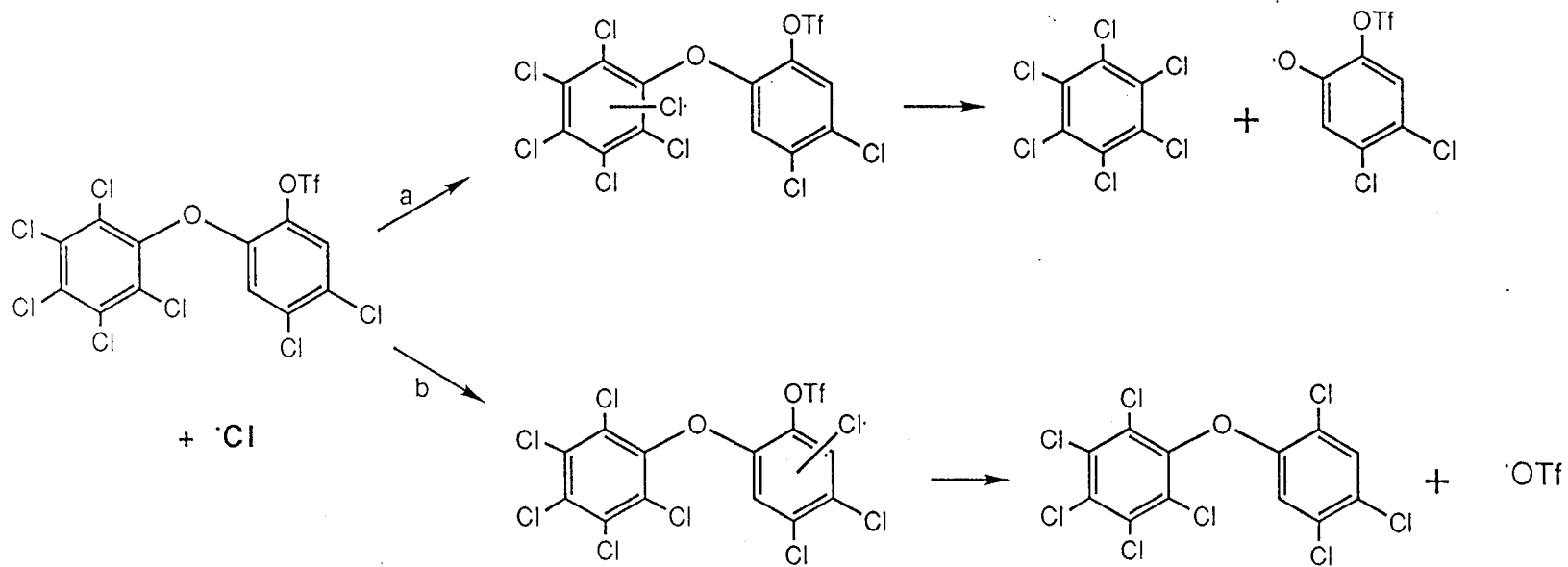


Figure II.1. Stern-Volmer plots of Irgasan-triflate for effects of naphthalene and 1,4-dinitrobenzene.

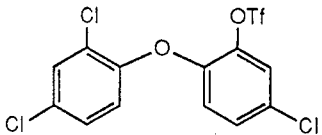
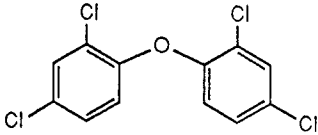
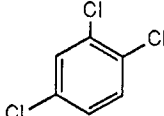
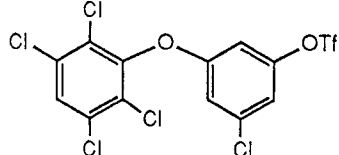
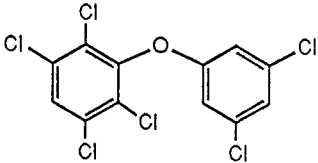
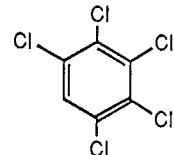
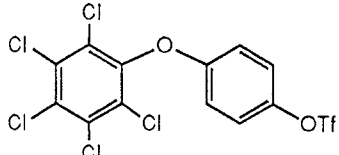
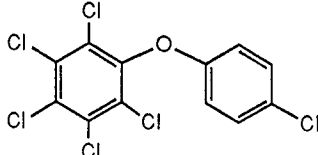
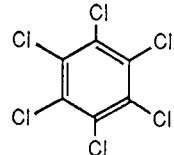
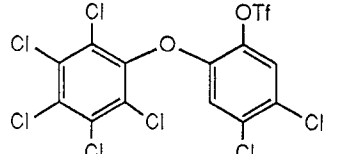
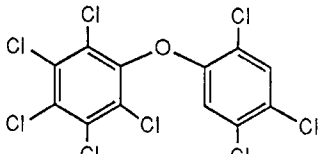
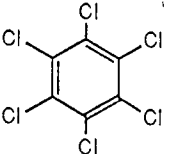
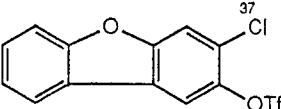
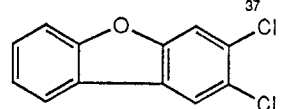


Scheme II.1



Scheme II.2

Table II.1. Photolysis of Triflates in Cl_2/CCl_4 at 300 nm.

Entry	Triflates	Photo Products	Yield (%) PCDPEs
1		 +  8:1	88
2		 +  15:1	75
3		 +  1.2:1	42
4		 +  1.3:1	40
5			91

References

1. Keith, L. H.; Rappe, C.; Choudhary, G. Chlorinated Dioxins and Dibenzofurans in the Total Environments I and II Ann Arbor Science, Butterworth, 1985.
2. Laramee, J. A.; Chang, Y-S.; Arbogast, B. C.; Deinzer, M. L. Biomed. Environ. Mass Spectrom. 1988, 17, 63.
3. Kolonko, K. J.; Deinzer, M. L.; Miller, T. L. Synthesis 1984, 2, 133.
4. Schwertz, B. A.; Keeler, P. A.; Gehring, P. J. Toxicol. Appl. Pharmacol. 1974, 28, 151.
5. ^1H NMR (400MHz, CD_3COCD_3) δ 7.69(dd,2H), 7.47(td,2H), 7.26(d,1H), 7.06(d,1H)
6. ^1H NMR (400MHz, CD_3COCD_3) δ 8.24(d,1H), 8.19(dd,1H), 7.73(d,1H), 7.71(dd,1H), 7.51(t,1H)
7. ^1H NMR (400MHz, CD_3COCD_3) δ 7.67(d,2H), 7.42(dd,2H), 7.07(d,2H)
8. Choudhry, G. G.; Sundstrom, G.; Wielen, F. W.; Hutzinger, O. Chemosphere 1977, 6, 327.
9. Freeman, P. K.; Jonas, V. J. J. Agric. Food Chem. 1984, 32, 1307.
10. Murov, S. L. (Ed.) Handbook of Photochemistry Marcel Dekker, Inc., New York, 1973.
11. Acetonitrile (16.5%), Toluene (15.2%), Methanol (12.3%), Hexane (8.5%).
12. Brown, G. S. In The Chemistry of the Hydroxyl Group; Partai, S., Ed., Wiley, New York, 1971, part 1, pp. 593.
13. Wiley, G. A.; Hershkowitz, R. L.; Rein, B. M.; Chung, B. C. J. Am. Chem. Soc. 1964, 86, 964.
14. Rossi, R. A.; Bunnett, J. F. J. Org. Chem. 1972, 37, 3570.
15. Doyle, M. P.; Siefried, B.; Dellaria, J. F. J. Org. Chem. 1977, 42, 2426.
16. Raner, K. D.; Lusztyk, J.; Ingold, K. U. J. Am. Chem. Soc. 1989, 111, 3652. References are therein.
17. Traynham, J. G. Chem. Rev. 1979, 79, 323.

III. PHOTOCHEMISTRY OF IRGASAN-TRIFLATE II:
MECHANISM OF THE CYCLIZATION

Yoon-Seok Chang, Jung-Suk Jang, and Max L. Deinzer

Department of Chemistry
Oregon State University
Corvallis, Oregon 97331

Tetrahedron, submitted.

Photolysis and synthesis were performed by Jung-Suk Jang. Product identification and data interpretation were done by Yoon-Seok Chang.

Abstract

5-Chloro-2-(2,4-dichlorophenoxy)phenol was converted to its triflate by reaction with trifluoromethanesulfonyl chloride. The triflate undergoes triplet sensitized photolytic cyclization at 300 nm in acetone to give 2,4,8-trichlorodibenzofuran in 100% yield. The mechanism of this efficient photocyclization reaction is discussed.

Polychlorinated dibenzofurans (PCDBFs) and polychlorinated diphenyl ethers (PCDPEs), along with chlorinated dioxins, have been of great concern because these compounds are toxic and are present in the environment.¹ These compounds have been involved in a number of incidents or in industrial accidents which caused severe intoxication or environmental contamination.² PCDPEs proved to be excellent precursors for the synthesis of PCDBFs via photochemical³ or organometallic cyclization reaction⁴. The photoreaction usually involves two competing reaction pathways; dechlorination and cyclization. It has been shown that the dechlorination can be inhibited largely by using acetone as a solvent.³ A major advantage of this method is that it gives almost quantitative yields and it is easy to anticipate the product structures. Nevertheless, the detailed mechanism for conversion is still obscure.

Recently we reported a new photochemical method for the conversion of an aromatic hydroxyl group to chlorine in the synthesis of PCDBFs and PCDPEs.⁵ The method was developed from the initial photo-reaction of triflate derivative of 5-chloro-2-(2,4-dichlorophenoxy)phenol, a commercial pesticide, called Irgasan DP300. A yield of 88% of 2,2',4,4'-tetrachlorodiphenyl ether was obtained from Irgasan-triflate when irradiated in chlorine-saturated carbon tetrachloride. Meanwhile, irradiation of a 10^{-3} M acetone solution of Irgasan-triflate 1 at 300 nm gave complete conversion to 2,4,8-

trichlorodibenzofuran (2,4,8-TrCDBF) 2. The latter result is a new synthetic route for the conversion of ortho-hydroxydiphenyl ethers to PCDBFs via triflate intermediates.

The involvement of a triplet state for the cyclization reaction of 1, due to the high triplet energy of acetone ($E_T=79\sim 81$ kcal/mol)⁶, was verified⁵; the yield of photoproduct 2 was low in other organic solvents⁷ and the formation of 2 in acetone was quenched in the presence of triplet quencher, naphthalene ($E_T=61$ kcal/mol)⁶, for which the Stern-Volmer plot was linear. Nonlinear quenching was observed in the presence of 1,4-dinitrobenzene.

These photo-sensitization reactions should involve two species in the triplet state: the sensitizer, acetone, and the Irgasan-triflate. Quenching experiments must, therefore, take into account both triplets, and it can be shown by steady state conditions that the quantum yield ratio is dependent on a quadratic concentration in quencher.⁸ The fact that the Stern-Volmer plot is linear for naphthalene as quencher suggests that the quencher interacts only with the reactive triplet state of 1 and that the rate constant for quenching of triplet acetone is or approaches zero. This suggests that naphthalene has a triplet energy state closer to Irgasan-triflate than does acetone. The results for 1,4-dinitrobenzene as quencher are consistent with quenching of both triplets. However, this may equally well indicate secondary processes such as electron transfer or singlet

energy transfer.⁹

It is possible that cyclization to 2 involves direct homolysis of the C-O bond of the triflate group and cyclization of the resulting radical. However, it is unlikely that the triplet energy of 1 is sufficient to cleave the C-O bond homolytically.¹⁰ The dissociation energy of the C-O bond in anisole is 100 kcal/mol.¹¹ A better model for comparison would be benzene triflate, and MMX calculations suggest that the C-O bond energy for this compound is 82 kcal/mol. Therefore, the possibility of an intermolecular electron transfer mechanism¹² was explored as being involved in the formation of a radical anion from the triplet excited state of 1. Loss of a triflate anion to give a sigma radical 5 would follow and cyclization could occur (Scheme III.1). The sigma radical is the well known Pschorr-type intermediate¹³. Alternatively, the intermediate 4¹⁴ could cyclize to a new tricyclic radical anion 6, which leads to the product 2 with loss of a hydrogen atom and a triflate anion.¹⁵ If intermediate 4 abstracts a hydrogen atom first, then it leads to the formation of diphenyl ether 3. To test for cyclization from the radical anion, irradiation experiments were carried out in the presence of an electron donor, triethylamine.¹⁶

In the range of low triethylamine concentrations (0.2~2-fold excess) the rate of disappearance of starting material 1 did not change noticeably with increasing concentration of triethylamine. The rate of formation of dichlorodibenzofuran,

instead, did increase with a concomitant decrease in the amount of 2,4,8-TrCDBF, 2 produced (Figure III.1). The dichlorodibenzofuran is considered to be formed from 2 upon further electron transfer from triethylamine and not directly from the starting material 1. Therefore, the photocyclization reaction was not enhanced by triethylamine. At high concentration of triethylamine (>50-fold excess), however, 2,4,4'-trichlorodiphenyl ether (2,4,4'-TrCDPE) 3 was formed exclusively. The intermediate 4 (or 5) abstracts a hydrogen atom more readily from triethylamine radical cation in the excimer cage.¹⁷ These results suggest that the radical anion intermediate is not a precursor of the cyclized products but rather of the diphenyl ether 3. It is worth noting that these results also are consistent with electron capture negative ion chemical ionization mass spectrometry¹⁸ of compound 1, which shows a base peak at m/z 148 for triflate anion but no evidence of cyclized product $(M-TfOH)^-$ with m/z 270.

But, it was also shown that 1 is a "self-quencher" in the production of 2, which suggests that low concentration of 1 is more favorable for the efficient formation of chemically useful excited triplet state (Figure III.2). This also excludes excimer formation from intermolecular electron transfer reaction as a mechanism of 2 production. The mechanism of the acetone sensitized photocyclization of 1 appears, therefore, not to involve the radical anion or sigma-radical intermediate which is common in the Pschorr-type

cyclization reaction and the 1,4-dinitrobenzene quenching studies may involve quenching of the triplet states of both sensitizer and Irganox-1010 as expected.

A possible mechanism involving an intramolecular electron transfer¹⁹ in which in the excited triplet state one electron is transferred, through space or by polarization, from the relatively electron rich ring to the more electron deficient ring containing the triflate group also needs to be considered. After formation of an intramolecular exciplex, the triflate anion would be expelled and the ortho radical could form a furan ring where return to aromaticity would favor the departure of a proton (Scheme III.2). The intramolecular electron transfer would be most efficient when two π systems face each other. However, the ability of species to have two π systems parallel to each other is not a prerequisite for the formation of a charge transfer complex.^{20,21}

The possibility of concerted ring closure by the π orbital overlapping of two ortho carbons during ring rotation of 1 is not feasible because of the steric effect of the triflate group which would not allow close approach of the rings for good π orbital overlap. Theoretical studies²² and ¹³C NMR data²³ of PCDEs show that the ring rotation within the molecule is hindered by the steric and electrostatic interactions of chlorine atoms in ortho positions. Likewise, the large triflate group in the ortho position would be

expected to hinder rotation and induce a higher energy pathway. On the other hand an ortho chlorine in one ring and an ortho hydrogen in the other might be brought into closer proximity. But loss of HCl during ring closure is not observed and this mechanism seems unlikely.

Experimental

Instrumentation. NMR spectra were obtained on a Bruker AM 400 MHz. Analytical GC-MS analyses were performed on a Finnigan 4023 quadrupole mass spectrometer in the electron impact mode. A 30 m DB-1301 (J & W, 0.25 mm i.d.) capillary column with splitless injection technique was used. HPLC analyses and separations were carried out using a Beckman 421 HPLC equipped with a dual pump system and a variable UV detector (254 nm wavelength was used). A preparative reverse-phase column (Sephadex C-18, 250x10 mm) was used. Photolyses were carried out in a Rayonet merry-go-round reactor equipped with eight 300 nm Rull lamps. A cooling fan was installed on the top of the reactor and air was blown over the apparatus during photolysis. The photolysis temperature was about 25~28 °C.

Materials. Spectral grade acetone (Baker), triethylamine (Aldrich, 99%), 18-crown-6 (Aldrich, 99.5%) and trifluoromethanesulfonyl chloride (Aldrich, 99%) were used without further purification.

Synthesis of Irgasan-triflate. Irgasan (10 mmol, 2.9 g) was dissolved in acetone (50 mL) and anhydrous potassium carbonate (12 mmol, 3.5 g) was added with a catalytic amount of 18-crown-6. The mixed solution was stirred at room temperature and trifluoromethanesulfonyl chloride (12 mmol, 2.0 g) in acetone (5 mL) was added slowly. After completion

of the reaction, the solution was concentrated and the product was isolated from a preparative silica TLC (EM Science, 2 mm, 20x20 cm) with hexane as an eluting solvent (87% yield). Irgasan-triflate 1 (EIMS; m/e 422(21), 420(22), 252(100), 250(64), 189(20), ¹H NMR; CD₃COCD₃; δ 7.69(dd,2H), 7.47(td,2H), 7.26(d,1H), 7.06(d,1H)).

Photolysis of Irgasan-triflate. To an acetone solution of Irgasan-triflate (10⁻² M concentration) varying amounts of triethylamine was added to give concentrations ranging from 10⁻³ to 10⁻¹ M. Sample solutions (5 ml each) were added to quartz tubes (170x15 mm) and degassed using four freeze-pump-thaw cycles. The tubes were sealed in vacuo. The solutions were photolyzed at 300 nm for 3 hours. At end of the reaction period the product ratios were determined by GCMS. After the GCMS analyses the solutions were concentrated and chromatographed on a preparative silica TLC or on a reverse-phase HPLC column. Further product structural assignments were made by proton NMR. When the non-labeled compounds were commercially available or previously reported, comparisons of ¹H NMR or GC retention times also were used. 2,4,8-TrCDBF 2 (EIMS; m/e 272(98), 270(100), 207(32), 137(35), 86(20), ¹H NMR; CD₃COCD₃; δ 8.24(d,1H), 8.19(dd,1H), 7.73(d,1H), 7.71(dd,1H), 7.51(t,1H)). 2,4,4'-TrCDPE 9 (EIMS; m/e 274(98), 272(100), 236(75), 202(90), 75(52), ¹H NMR; CD₃COCD₃; δ 7.64(d,1H), 7.42(m,3H), 7.15(d,1H), 7.02(dd,2H)).

Acknowledgement. We gratefully acknowledge support from the National Institutes of Health, NIEHS ES00040 and NIEHS ES00210. We also thank Drs. Peter Freeman and Ramnath Iyer for helpful discussion. This paper is issued as technical paper No.9249 from the Agricultural Experimental Station.

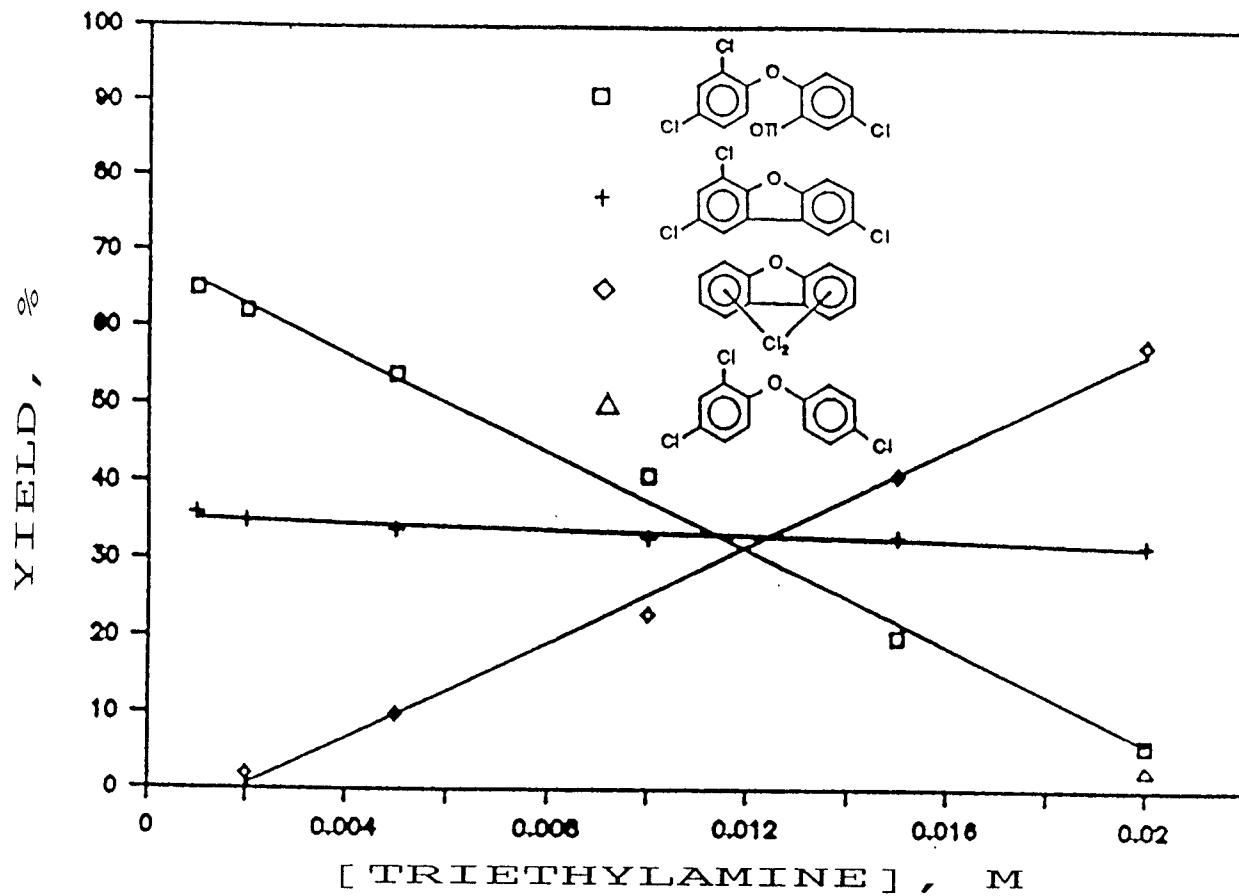


Figure III.1. Products distribution from the photolysis of Irgasan-triflate in the presence of triethylamine.

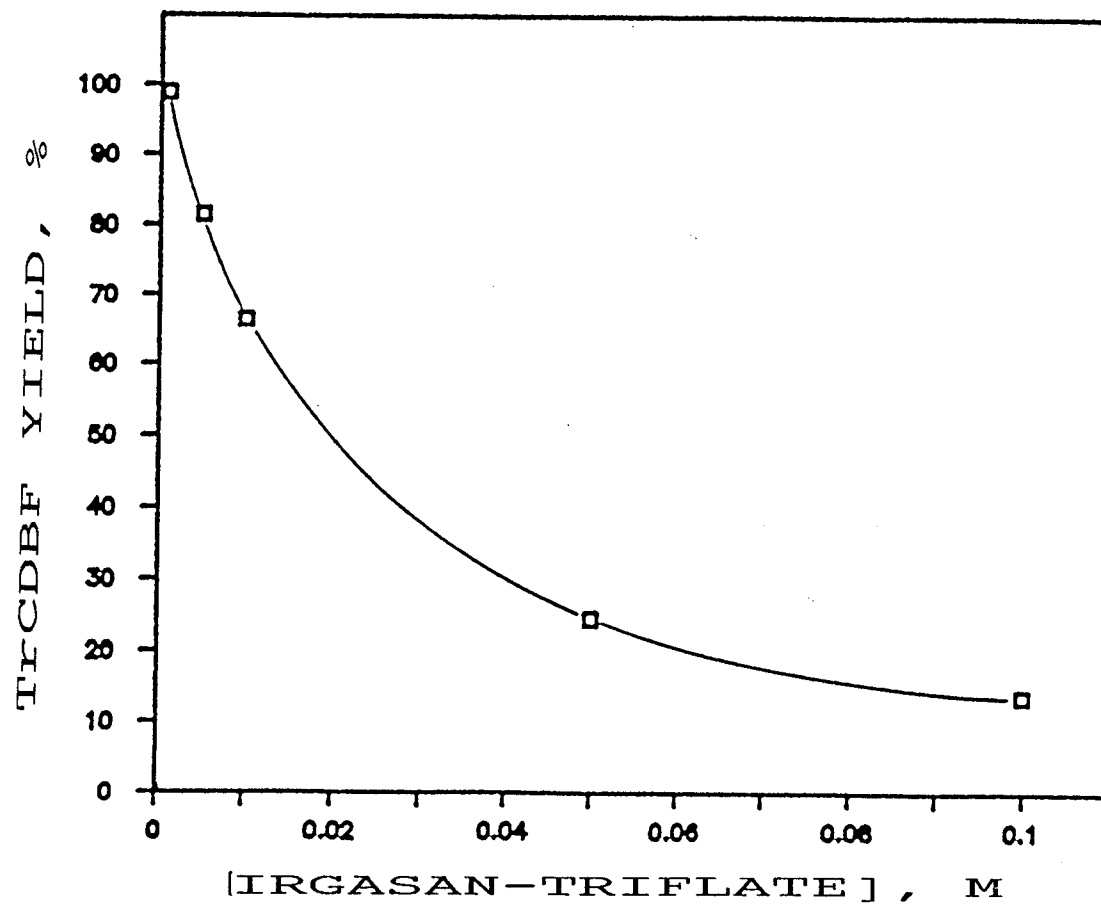
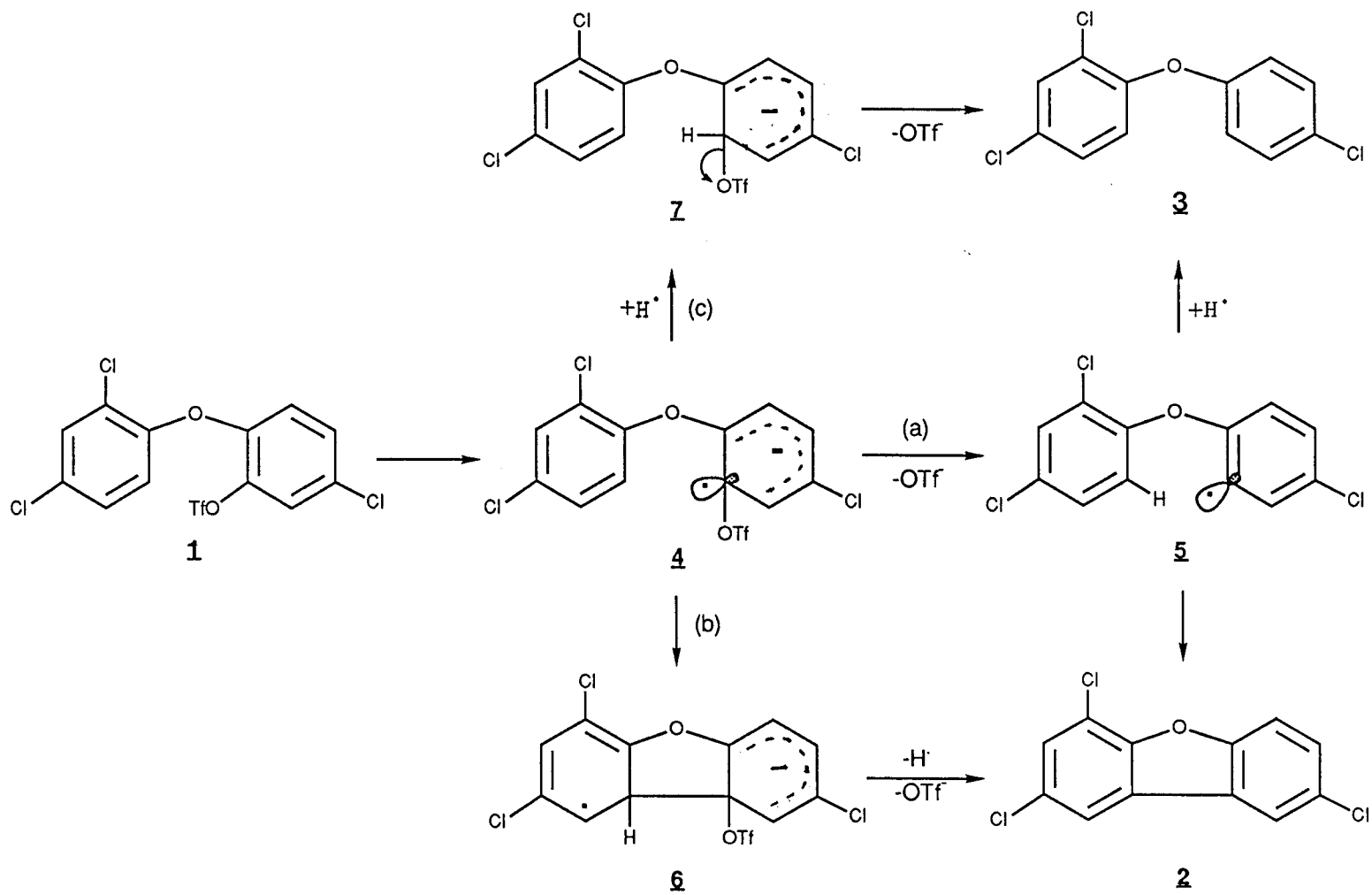
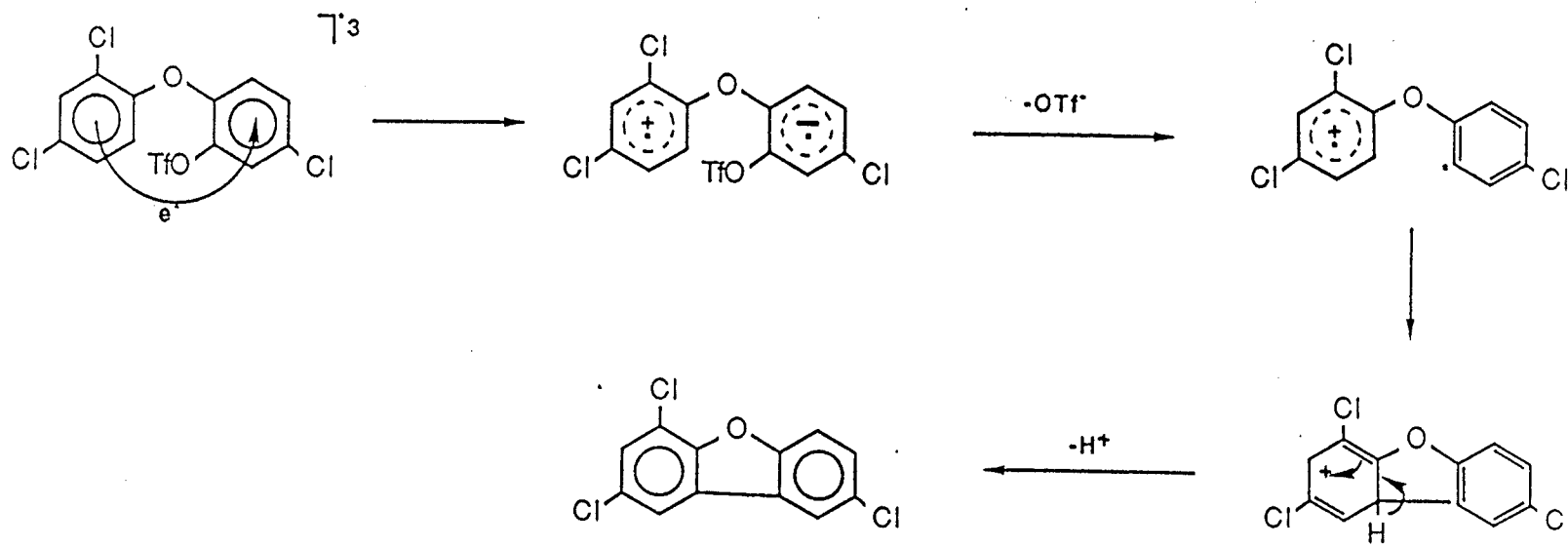


Figure III.2 Formation of 2,4,8-TrCDBF with variation in concentration of Irgasan-Triflate.



Scheme III.1



Scheme III.2

References

1. Keith, L.H.; Rappe, C.; Choudhary, G. Chlorinated Dioxins and Dibenzofurans in the Total Environments I and II; Butterworth Publishers: Woburn, 1983.
2. Rappe, C. Env. Sci. Technol. 1984, 16, 78 A.
3. Choudhry, G.F.; Sundstrom, G.; Wielen, R.W.M.; Hutzinger, H. Chemosphere 1977, 6, 327.
4. Norstrom, A.; Andersson, K.; Rappe, C. Chemosphere 1976, 5, 419.
5. Chang, Y-S.; Jang, J-S.; Deinzer, M.L. Tetrahedron 1990, 46, 4161.
6. Murov, S.L. Handbook of Photochemistry; Marcel Dekker, Inc.: New York, 1973.
7. Acetonitrile (16.5%), Toluene (15.2%), Methanol (12.3%), Hexane (8.5%).
8. Kavarnos, G.J.; Turro, N.J. Chem. Rev. 1986, 86, 401.
9. Schanze, K.S.; Sauer, K. J. Am. Chem. Soc. 1988, 110, 1180.
10. Freeman, P.K.; Jonas, V. J. Agric. Food Chem. 1984, 32, 1307.
11. Benson, S.W. Thermochemistry Kinetics, 2nd ed.; Wiley: New York, 1976.
12. Freeman, P.K.; Srinivasa, R. J. Agric. Food Chem. 1983, 31, 775.
13. Pschorr, R. Chem. Ber. 1896, 29, 496.
14. Freeman, P.K.; Srinivasa, R.; Campbell, J.-A.; Deinzer, M.L. J. Am. Chem. Soc. 1986, 108, 5531.
15. We thank a reviewer for pointing this out.
16. Fery-Forgues, S.; Lavabre, D.; Paillous, N. J. Org. Chem. 1987, 52, 3381.
17. There was no incorporation of deuterium in 6 when acetone-d₆ was used as solvent.

18. Harrison, A.G. Chemical Ionization Mass Spectrometry; CRC Press: Boca Raton, 1983.
19. Chow, Y.L.; Danen, W.C.; Nelsen, S.F.; Rosenblatt, D.H. Chem. Rev. 1978, 78, 243.
20. (a) De Schryver, F.C.; Beans, N. Adv. Photochem. 1977, 10, 359.
(b) Ide, R.; Sakata, Y.; Misumi, S.; Okada, T.; Mataga, N. J. Chem. Soc., Chem. Commun. 1972, 1009.
21. Grabowski, Z.R.; Dobkowski, J. J. Pure Appl. Chem. 1983, 55, 245.
22. Pitea, D.; Ferrazza, A. J. Mol. Str. 1988, 92, 141.
23. Edlund, U.; Norstrom, A. Org. Magn. Reson. 1977, 9, 196.

IV. REGIOSPECIFIC SYNTHESIS OF POLYCHLORINATED
DIBENZOFURANS WITH CHLORINE-37 EXCESS

Yoon-Seok Chang and Max L. Deinzer

Department of Chemistry
Oregon State University
Corvallis, Oregon 97331

Journal of Labelled Compounds and Radiopharmaceuticals,
in print.

Summary

The synthesis of regiospecifically chlorine-37 labeled di- and trichlorodibenzofurans is described. The strategy for introducing a chlorine-37 label regiospecifically has been to reduce the nitro derivative to the corresponding amine. The amine is converted to the diazonium salt with t-butyl nitrite, and this product is converted to the final product via the Sandmeyer reaction with chlorine-37 labeled cuprous chloride.

Key words: Chlorine-37 labeled polychlorinated dibenzofuran

Introduction

Polychlorinated dibenzofurans (PCDBFs) constitute a family of organic chemicals represented by the structural formula and numbering system shown in Figure IV.1. There is

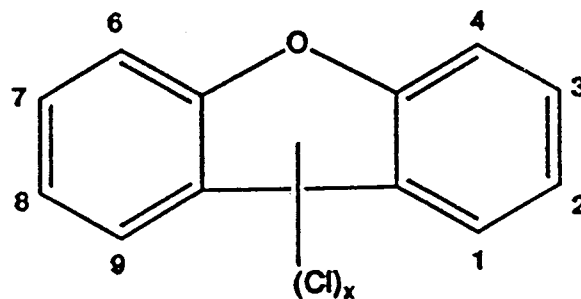


Figure IV.1. Numbering system of PCDBF

considerable interest in PCDBFs because they are major contaminants in technical grade pentachlorophenol, a biocide used extensively in the wood products industry.¹ PCDBFs also have been detected among the pyrolysis products of polychlorinated biphenyls and chlorinated benzenes.² The extraordinary toxicity of some PCDBFs that has been demonstrated through animal experiments³ and to some extent through accidental exposure of humans to these compounds⁴, have prompted efforts to develop convenient analytical and synthetic procedures to study this class of compounds in a more controlled way.

Our own efforts have been directed largely towards an understanding of the mechanism of dechlorination in electron capture negative ion mass spectrometry (ECNIMS) and the development of analytical protocols for their analyses that are both sensitive and specific with respect to positional

isomers. It has been shown, for example, that a linear correlation exists between the branching ratio, $\log [(M-Cl)^-]/[Cl^-]$ and the energies of low-lying unoccupied molecular orbitals for polychlorinated dibenzo-p-dioxins (PCDDs) under the ECNIMS conditions.⁵ On this basis it was hypothesized, and later confirmed, that branching ratios can be related to differences in the energy of products formed provided one knows the position from which the chlorine atom or ion is lost during dissociative electron capture. A similar correlation has been observed for PCDBFs.⁶ Attempts to identify the labile chlorines of PCDBFs under ECNIMS conditions has led to the synthesis of chlorine-37 labeled regiospecific isomers. General methods for the syntheses of dichloro- and trichloroisomers are described.

Experimental Section

Instrumentation. NMR spectra were obtained on a Bruker AM 400 MHz. Analytical GC-MS analyses were performed on a Finnigan 4023 quadrupole mass spectrometer in the EI mode. A 30 m DB-1301 (J & W, 0.25 mm i.d.) capillary column with splitless injection technique was used. Exact mass measurements were made on a Kratos MS50 high resolution mass spectrometer in the EI mode. HPLC analyses and separations were carried out using a Beckman 421 HPLC equipped with a dual pump system and a variable UV detector (254 nm wavelength was used). A preparative reverse-phase column (Sephadex C-18, 250 X 10 mm) was used. Photolyses were carried out in a Rayonet merry-go-round reactor equipped with eight 300 nm Rull lamps.

Materials. Spectral grade solvents were used without further purification. Chlorine gas was purchased from Matheson Co. (99.5%, Newark, CA). Anhydrous Cu^{37}Cl was prepared from Na^{37}Cl by the procedure of Tubandt et al.⁷ Na^{37}Cl was purchased from Isotec Inc. (95.6% ^{37}Cl enriched, Miamisburg, OH).

Product Analyses. Large scale (more than 200 mg) chromatographic preparations were carried out on a column (2 x 40 cm) of silica CC-7 special (Mallinckrodt) or silica 60 (EM Reagents) with hexane/dichloromethane (7:3) as eluting solvent. Most small scale products (less than 200 mg) were purified on preparative silica TLCs (EM science, 2 mm, 20 x

20 cm) with hexane/dichloromethane (6:4) or hexane/chloroform (9:1) as developing solvents. Further separations, if necessary, were achieved by reverse-phase HPLC. A mixture of water (30%) and methanol (70%) was used, and the methanol ratio was increased gradually to 95% in 30 min. The flow rate was 2.5 mL/min. 1(³⁷Cl),6-Dichloro-DBF and 3(³⁷Cl),6-dichloro-DBF were collected by repeated separation of the mixture with collection of the individual fractions on a Gilson Model FC-80 fraction collector. Structural assignments for the intermediate compounds and final chlorine-37 labeled PCDBFs were made by various NMR techniques, including ¹H, ¹³C, ¹H-¹H, ¹H-¹³C, NOE and relay experiments. When the non-labeled compounds were commercially available or previously reported, comparisons of ¹H NMR or GC retention times were used. Exact masses for all final products were determined by peak matching techniques (PFK was used as the reference) on a high resolution mass spectrometer set at a resolving power of 12,000 resolution.

Synthesis of Cu³⁷Cl. Equimolar amounts (10 mmol each) of anhydrous cupric sulfate (Aldrich) and Na³⁷Cl (Isotec Inc.) were added in 10 mL of water in a 50 mL three-necked round bottom flask. Sulfur dioxide gas (Atheson Inc.) was bubbled slowly (1 mL/sec) into the stirred solution. A precipitate of Cu³⁷Cl fell out as a white crystalline product, which was washed with SO₂-water. After drying by filter suction, the crystalline material was put under high vacuum and heated over

110 °C until completely dry. The chlorine-37 isotope enrichment of Cu^{37}Cl was determined by high resolution mass spectrometry in the fast atom bombardment mode. For these studies it was 95.6%.

Nitration of Dibenzofuran. A suspension of dibenzofuran (0.17 g, 1.0 mmol) in 20 mL of THF was stirred at room temperature and treated with 4 mL of trifluoroacetic anhydride followed by solid ammonium nitrate (0.8 g, 1.0 mmol). After stirring for 12 h or longer, the mixture was poured into 100 mL water and extracted with chloroform (2 x 100 mL). The product ratios were measured by GCMS analysis using the EI mass spectrometry mode. The solution was concentrated and chromatographed on a silica column with hexane/dichloromethane (5:95). By TLC, the first spot gives a product, 2-nitro-DBF which has the following spectral data: EIMS; m/e 213(100), 167(25), 155(22), 139(63), ^1H NMR; CD_3COCD_3 ; δ 9.08(d), 8.46(dd), 8.37(dd), 7.88(d), 7.77(dd), 7.68(td), 7.53(td). The second spot, due to 3-nitro-DBF, has the following spectral data: EIMS; m/e 213(100), 183(24), 167(25), 139(65), ^1H NMR; CD_3COCD_3 ; δ 8.54(d), 8.39(d), 8.33(dd), 8.30(dd), 7.78(dd), 7.70(td), 7.53(td). The remaining spots included a mixture of 3-, 1-, and 4-nitro-DBFs.

Typical Procedure for Reduction of Nitro Group to Amino Group. Granular tin (Aldrich, 30 mesh, 3 g, 25 mmol) was added to a warm solution of the nitro compound (1 mmol) dissolved in methanol (10-20 mL). Concentrated hydrochloric

acid (10-20 mL) was added drop-wise with stirring at a rate so as to maintain a gentle reflux. The mixture was refluxed for 0.5-2 hours, after which the solution was allowed to cool to room temperature and poured into 100 mL of water. The aqueous mixture was then adjusted to a pH of about 8 with a concentrated sodium hydroxide solution. Tin hydroxide was filtered off and the solution was extracted with chloroform (2 x 100 mL). The combined solution was concentrated and chromatographed on a preparative TLC plate with dichloromethane.

Conversion of Amine to Chlorine-37 Compound. Anhydrous Cu^{37}Cl (20 mg, 0.2 mmol), *t*-butyl nitrite (0.1 g, 1 mmol) and anhydrous acetonitrile (5 mL) were added to a 25 mL three-necked round-bottom flask, which was cooled on an ice bath. The amine (0.1 mmol) in acetonitrile (10 mL) was slowly added under rapid stirring. As the amine was added, the reaction solution turned black with evolving nitrogen. After the addition was completed, the reaction mixture was slowly warmed to room temperature or, if necessary, to 60 °C. The completion of reaction was checked by TLC or GCMS. The final reaction mixture was initially passed through a small-scale neutral alumina column (disposable pipets were used) and further purified on a preparative silica TLC plate or by reverse phase HPLC. Typical range of yields of pure chlorine-37 labeled dichloro-DBFs was 42-95%.

General Method for Surface Chlorination. A Kontes #K-

420000 chromatographic column with a stainless steel tee was used for the chlorination. The column was packed with sodium sulfate (1.5 g) followed by silica gel (3 g). A solution of dibenzofuran was added to the top of the column and dispersed further with a portion of acetone. Another glass wool plug was then placed about 5 cm above the packing. The acetone was completely evaporated with nitrogen gas and chlorine gas was slowly bubbled through the column. (The chlorine gas flow was not measured but maintained at the same rate throughout all the reactions.) Heating tape around the column was used to increase the reaction temperature. The chlorine gas was turned off at the end of the reaction period and the column was purged with nitrogen to remove the residual chlorine. The tee was removed from the column and products were eluted with acetone (100 mL).

2(³⁷Cl),6-Dichloro-DBF. 1,3-Dichloro-2-fluorobenzene (Aldrich, 1 g, 6.1 mmol), 4-aminophenol (Aldrich, 1 g, 9.2 mmol), dried potassium carbonate (EM science, 2 g, 14.5 mmol), 18-crown-6 (Aldrich, 50 mg, 0.19 mmol), and acetonitrile (50 mL) were refluxed for 2 days. The mixture was filtered and the residue washed with hot acetonitrile (50 mL). The combined solution was concentrated and chromatographed on a silica column. 4'-Amino-2,6-dichloro-DPE (280 mg, 1.1 mmol, 18% yield) has the following spectral data: EIMS; m/e 255(62), 253(100), 183(15), 108(86), ¹H NMR; CDCl₃; δ 7.38(d, 2H), 7.09(m, 2H), 6.37(dq), 6.18(m, 2H), 3.54(b, NH₂). The

amino group was converted to chlorine to give 2,4'(³⁷Cl),6-trichloro-DPE [EIMS; m/e 276(69), 274(100), 239(12), 204(86), 202(56), 113(21), 75(30), ¹H NMR; CD₃COCD₃; δ 7.61(d, 2H), 7.39(q, 2H), 7.14(dq), 6.90(t), 6.81 (dq)]. The ether (27 mg, 0.1 mmol) was dissolved in acetone (10⁻³ M) and photolyzed at 300 nm for 3 hours. The product was concentrated and pure dichloro-DBF (95% yield) was collected by reverse-phase HPLC [EIMS; m/e 240(32), 238(100), 175(13), 119(10) 87(10), ¹H NMR; CD₃COCD₃; δ 8.22(d), 8.15(dd), 7.77(d), 7.63(dd), 7.61(dd), 7.45(t)]. Exact mass calculated for C₁₂H₆OCl³⁷Cl: 237.9766; HRMS: 237.9766.

1(³⁷Cl),6-Dichloro-DBF and 3(³⁷Cl),6-Dichloro-DBF.
Procedures were the same as those for the synthesis of 2(³⁷Cl),6-dichloro-DBF. The final photoproducts were separated by reverse-phase HPLC from repeated collections. The ratio of two compounds 1.2:1 (98% photolysis yield) and the structure of each compound was confirmed by 2D NMR. [3'-Amino-2,6-dichloro-DPE: EIMS; m/e 255(31), 253(50), 218(22), 183(100), 92(20), 65(22), ¹H NMR; CDCl₃; δ 7.38 (d, 2H), 7.09 (m, 2H), 6.37(dq), 6.18(m, 2H), 3.54(b, NH₂)]. [2,4'(³⁷Cl),6-trichloro-DPE: EIMS; m/e 278(14), 276(77), 274(100), 239(14), 204(78), 202(53), ¹H NMR; CD₃COCD₃; δ 7.61(d, 2H), 7.39(q, 2H), 7.14(dq), 6.90(t), 6.81(dq)]. [1(³⁷Cl),6-dichloro-DBF: EIMS; m/e 240(32), 238(100), 175(13), 119(10), 87(100), ¹H NMR; CD₃COCD₃; δ 8.32(dd), 7.76(dd), 7.68(dd), 7.65(t), 7.52(td,2H)]. Exact mass calculated for C₁₂H₆OCl³⁷Cl: 237.9766;

HRMS: 237.9766. [$3(^{37}\text{Cl})$],6-dichloro-DBF: EIMS; m/e 240(30), 238(100), 175(13), 119(10), 87(10), ^1H NMR; CD_3COCD_3 ; δ 8.18(d), 8.12(dd), 7.88(d), 7.63(dd), 7.51(dd), 7.46(td)]. Exact mass calculated for $\text{C}_{12}\text{H}_6\text{OCl}^{37}\text{Cl}$: 237.9766; HRMS: 237.9766.

2,7(^{37}Cl)-Dichloro-DBF. 3-Nitro-DBF (43 mg, 0.2 mmol) was chlorinated by chlorine gas in a silica column at room temperature for 1.5 h. After rinsing the column with acetone (100 mL), the solution was concentrated and chromatographed on a preparative silica TLC plate. The major compound isolated was 2-chloro-7-nitro-DBF (41 mg, 83% yield) [EIMS; m/e 249(30), 247(100), 217(22), 201(20), 173(55), 138(20), ^1H NMR; CD_3COCD_3 ; δ 8.57(d), 8.45(d), 8.38(s), 8.36(dd), 7.85(d), 7.71(dd)]. The nitro compound was reduced by Sn/HCl in methanol for 1 h and the crude product was diazotized and chlorinated with Cu^{37}Cl . 2,7(^{37}Cl)-dichloro-DBF (74% yield) was isolated from a preparative TLC plate [EIMS; m/e 240(38), 238(100), 175(20), 137(15), 87(17), ^1H NMR; CD_3COCD_3 ; δ 8.21(d), 8.18(d), 7.80(d), 7.70(d), 7.58(dd), 7.49(dd)]. Exact mass calculated for $\text{C}_{12}\text{H}_6\text{OCl}^{37}\text{Cl}$: 237.9766; HRMS: 237.9766.

3(^{37}Cl),4-Dichloro-DBF. 3-Nitro-DBF (120 mg, 0.6 mmol) was reduced by Sn/HCl in methanol for 2 h. The crude mixture was chromatographed on a preparative TLC plate. The major spot was (22 mg, 0.1 mmol) 3-amino-4-chloro-DBF [EIMS; m/e 219(28), 217(100), 126(15), 109(20), ^1H NMR; CDCl_3 ; δ 7.75(dd),

7.57(dd), 7.51(dd), 7.31(td), 7.25(td), 6.57(d), 3.58(b, NH₂)]. The lower spot was (72 mg, 0.4 mmol) 3-amino-DBF [EIMS; m/e 183(100), 154(15), 127(15), 92(20), 77(16), ¹H NMR; CDCl₃; δ 7.79(dd), 7.69(d), 7.47(dd), 7.32(td), 7.27(td), 6.85(d), 6.69(dd), 3.97(b, NH₂)]. 3-Amino-4-chloro-DBF was diazotized and chlorinated with Cu³⁷Cl to yield 3(³⁷Cl),4-dichloro-DBF (81% yield) [EIMS; m/e 240(32), 238(100), 175(15), 137(15), 119(18), ¹H NMR; CD₃COCD₃; δ 7.93(dd), 7.78(d), 7.66(dd), 7.52(td), 7.45(d), 7.39(td)]. Exact mass calculated for C₁₂H₆OCl³⁷Cl: 237.9766; HRMS: 237.9766.

1,2(³⁷Cl)-Dichloro-DBF. A solution of 4-nitro-DPE (Ultra Scientific Co., 150 mg, 0.7 mmol) and 2 equivalents of palladium acetate in acetic acid (50 mL) was heated to reflux for 24 h. The solvent was evaporated and the residue redissolved in chloroform (100 mL). After filtration and concentration, 2-nitro-DBF was isolated from a preparative TLC plate (133 mg, 89% yield) [EIMS; m/e 213(100), 183(14), 167(28), 155(12), 139(70), ¹H NMR; CD₃COCD₃; δ 9.08(d), 8.46(dd), 8.37(dd), 7.88(d), 7.77(dd), 7.68(td), 7.53(td)]. 2-Nitro-DBF (105 mg, 0.5 mmol) was reduced by Sn/HCl in methanol for 2 h. 2-Amino-DBF was isolated as the major product from a preparative TLC plate (67 mg, 0.4 mmol) [EIMS; m/e 184(12), 183(100), 154(10), 127(12), 91(15), ¹H NMR; CDCl₃; δ 7.79(dd), 7.69(d), 7.48(dd), 7.34(td), 7.25(td), 6.85(d), 6.69(dd), 3.85(b, NH₂)]. 2-Amino-1-chloro-DBF, upper spot from TLC plate (13 mg, 0.06 mmol), has the following spectral

characteristics: EIMS; m/e 219(31), 217(100), 154(12), 126(10), ^1H NMR; CDCl_3 ; δ 8.36(dd), 7.53-7.45(m, 2H), 7.36(td), 7.33(d), 6.92(d), 4.04(b, NH_2). 2-Amino-1-chloro-DBF was diazotized and chlorinated with Cu^{37}Cl to give 1,2(^{37}Cl)-dichloro-DBF (42% yield) [EIMS; m/e 240(32), 238(100), 175(18), 119(15), 87(22), ^1H NMR; CD_3COCD_3 ; δ 8.41(dd), 7.72(dd), 7.70(d, 2H), 7.66(td), 7.51(td)]. Exact mass calculated for $\text{C}_{12}\text{H}_6\text{OCl}^{37}\text{Cl}$: 237.9766; HRMS: 237.9766.

2,3(^{37}Cl)-Dichloro-DBF. 3-Amino-2-methoxy-DBF (Aldrich, 107 mg, 0.5 mmol) was diazotized and chlorinated with Cu^{37}Cl . 3(^{37}Cl)chloro-2-methoxy-DBF (94 mg, 75% yield) was isolated from a preparative TLC plate [EIMS; m/e 234(100), 219(75), 191(34), 126(25), ^1H NMR; CD_3COCD_3 , δ 8.10(dd), 7.85(s), 7.73(s), 7.61(dd), 7.52(td), 7.38(td), 4.00(s, CH_3)]. 3(^{37}Cl)chloro-2-methoxy-DBF (94 mg), boron tribromide (1 mL), and dichloromethane (15 mL) were refluxed for 2 hours. Dichloromethane (20 mL) and water (20 mL) were slowly added. The layers were separated in a separatory funnel and the water layer extracted with 20 mL of dichloromethane. The dichloromethane phase was dried over anhydrous sodium sulfate, filtered, and concentrated. The product was chromatographed on a preparative silica column to give 3(^{37}Cl)-chloro-2-hydroxy-DBF (72 mg, 84% yield). This compound was dissolved in acetone (10 mL) and potassium carbonate (0.2 g, 1.5 mmol) was added. The mixed solution was stirred with a magnetic bar at room temperature and trifluoromethanesulfonyl chloride

solution in acetone (1 M, 10 mL) was slowly added. After completion of the reaction, 3(³⁷Cl)-chloro-2-triflate-DBF was isolated by preparative TLC (105 mg, 88% yield) [EIMS; m/e 352(35), 219(100), 191(36), 126(30), ¹H NMR; CDCl₃; δ 8.38(s), 8.23(dd), 8.03(s), 7.70(dd), 7.63(td), 7.47(td)]. The triflate compound was redissolved in carbon tetrachloride saturated with chlorine gas (10⁻² M) and photolyzed in a pyrex tube at 300 nm for 1 hour. The crude solution was initially passed through a small alumina column to remove impurities. Final 2,3(³⁷Cl)-dichloro-DBF was isolated from a preparative TLC plate (91% yield) [EIMS; m/e 240(32), 238(100), 236(42), 175(20), 173(27), 137(25), 87(34), ¹H NMR; CDCl₃; δ 8.01(s), 7.89(dd), 7.67(s), 7.55(dd), 7.49(td), 7.36(td)]. Exact mass calculated for C₁₂H₆OCl³⁷Cl: 237.9766; HRMS: 237.9766.

2(³⁷Cl),8-Dichloro-DBF. 4-Amino-4-chloro-DPE (Western Chemical, 220 mg, 1.0 mmol) was diazotized and chlorinated with Cu³⁷Cl, and 4(³⁷Cl),4-dichloro-DPE was isolated from a preparative TLC plate (198 mg, 83% yield) [EIMS; m/e 242(33), 240(100), 177(24), 175(18), 168(15), 75(18), ¹H NMR; CD₃COCD₃; δ 8.68(dd, 4H), 8.31(dd, 4H)]. The solution of the ether and 2 equivalents of palladium acetate in acetic acid (30 mL) was refluxed for 12 h. The solvent was evaporated and the residue redissolved in chloroform. After filtration and concentration 2(³⁷Cl),8-dichloro-DBF was isolated from a preparative TLC plate (52%). The product was further purified by reverse-phase HPLC and purity was checked by GCMS, and no impurities

were detected [EIMS; m/z 240(33), 238(100), 175(13), 119(12)]. ^1H NMR; CD_3COCD_3 ; δ 8.22(d,2H), 7.69(d,2H), 7.56(dd,2H)]. Exact mass calculated for $\text{C}_{12}\text{H}_6\text{OCl}^{37}\text{Cl}$: 237.9766; HRMS: 237.9766.

2,3(^{37}Cl),4-Trichloro-DBF. 3-Amino-DBF (45 mg, 0.3 mmol) in a 50 mL round bottom flask was added by Cl_2/CCl_4 (10 mL) and stirred for 3 minutes. At the end of the reaction, aqueous sodium bisulfite was added to quench the reaction. Chloroform (50 mL) and water (50 mL) were added to the mixture. After shaking, the chloroform layer was separated, washed with water (50 mL), and dried with anhydrous sodium sulfate. The solution was concentrated and chromatographed by preparative TLC with chloroform/ hexane (9:1). 3-Amino-2,4-dichloro-DBF was isolated as the major product (62 mg, 82% yield) [EIMS; m/e 253(73), 251(100), 151(13), 126(23), 125(23), 76(14), ^1H NMR; CDCl_3 ; δ 7.71(dd), 7.70(s), 7.49(dd), 7.33(td), 7.26(td), 4.67(b, NH_2)]. 3-Amino-2,4-dichloro-DBF was diazotized and chlorinated with Cu^{37}Cl . 2,3(^{37}Cl),4-Trichloro-DBF was separated from 2,4-dichloro-DBF by reverse-phase HPLC (49% yield) [2,4-Dichloro-DBF: EIMS; m/e 238(65), 236(100), 173(34), 137(23), 86(25), ^1H NMR; CDCl_3 ; δ 7.91(dd), 7.83(d), 7.65(dd), 7.54(td), 7.47(dd), 7.39(td)] [2,3(^{37}Cl),4-Trichloro-DBF: EIMS; m/e 274(72), 272(100), 209(28), 137(30), 136(15), 104(15), ^1H NMR; CD_3COCD_3 ; δ 7.97(s), 7.91(dd), 7.65(dd), 7.55(td), 7.41(td)]. Exact mass calculated for $\text{C}_{12}\text{H}_5\text{OCl}_2^{37}\text{Cl}$: 271.9376; HRMS: 271.9376.

1,2(³⁷Cl),3-Trichloro-DBF. Chlorination of 2-amino-DBF (165 mg, 0.9 mmol) was performed as described for 3-amino-DBF. A reaction time of 5 minutes gave mostly 2-amino-1,3-dichloro-DBF (176 mg, 78% yield) [EIMS; m/e 253(63), 251(100), 188(12), 126(12), ¹H NMR; CDCl₃; δ 8.31(dd), 7.53-7.44 (m, 2H), 7.46(s), 7.34(td), 4.39(b, NH₂)]. 2-Amino-1,3-dichloro-DBF was diazotized and chlorinated with Cu³⁷Cl. 1,2(³⁷Cl),3-trichloro-DBF was further purified by reverse-phase HPLC (56% yield) [EIMS; m/e 274(62), 272(100), 209(25), 137(20), ¹H NMR; CD₃COCD₃; δ 8.35(dd), 7.76(s), 7.75(dd), 7.69(td), 7.53(td)]. Exact mass calculated for C₁₂H₅OCl₂³⁷Cl: 271.9376; HRMS: 271.9377.

2,3,7(³⁷Cl)-Trichloro-DBF. 3-Nitro-DBF (215 mg, 1 mmol) was chlorinated in a silica column with chlorine gas at 60 °C for 1.5 h. The acetone-eluted solution was concentrated and 2,3-dichloro-7-nitro-DBF was collected by reverse-phase HPLC. This compound was then reduced with Sn/HCl in methanol for 30 minutes. The crude mixture was diazotized and chlorinated with Cu³⁷Cl (30% overall yield) [EIMS; m/e 274(70), 272(100), 209(15), 137(14), ¹H NMR; CD₃COCO₃; δ 8.40(s), 8.19(d), 7.98(s), 7.81(d), 7.49(dd)]. Exact mass calculated for C₁₂H₅OCl₂³⁷Cl: 271.9376; HRMS: 271.9376.

2,3(³⁷Cl),8-Trichloro-DBF. 3(³⁷Cl)-Chloro-DBF was prepared from the 3-nitro-DBF through reduction, diazotization and chlorination with Cu³⁷Cl by the same methods described above to give 69% overall yield [EIMS; m/e 204(100), 139(20),

102(15), ^1H NMR; CD_3COCD_3 ; δ 8.12(d, 2H), 7.74(d), 7.68(dd), 7.58(td), 7.43(dd), 7.42(td)]. 3(^{37}Cl)-chloro-DBF (42 mg, 0.2 mmol) was chlorinated in a silica column with chlorine gas at room temperature for 0.5 h. The acetone solution was concentrated and chromatographed by reverse-phase HPLC to collect 2,3(^{37}Cl),8-trichloro-DBF (22% yield) [EIMS; m/e 274(72), 272(100), 209(16), 137(15), ^1H NMR; CD_3COCD_3 ; δ 8.44(s), 8.26(d), 7.99(s), 7.72(d), 7.61(dd)]. Exact mass calculated for $\text{C}_{12}\text{H}_5\text{OCl}_2^{37}\text{Cl}$: 271.9376; HRMS: 271.9376 Extreme caution should be taken throughout the reaction since the major product is the very toxic 2,3(^{37}Cl),7,8-tetrachloro-DBF.

Results and Discussion

Strategy of Chlorine-37 Labeling on the Dibenzofuran Molecule. Sandmeyer-type chlorination of amino aromatics is well known and a very efficient process.⁸ We have used this method to introduce a chlorine-37 label regiospecifically into the dibenzofuran molecule. The amine is converted to the diazonium salt by *t*-butyl nitrite, and conversion of this product to the chloride is accomplished by chlorine-37 labeled cuprous chloride by the method of Doyle et al.⁹ This is a modification of the Sandmeyer reaction. Excess amino compounds and *t*-butyl nitrite were used relative to Cu³⁷Cl (45.6 % enriched) to assure maximum incorporation of chlorine-37. In general, no loss of isotopic enrichment was found during the Sandmeyer reaction. Equimolar amounts of substrate, *t*-butyl nitrite and nonlabeled cuprous chloride gave yields in the range 42-95 %.

Synthesis of Dichlorodibenzofurans. A series of 1,6-, 2,6-, and 3,6-dichloro-DBFs with chlorine-37 on positions 1, 2 or 3 (Scheme IV.1) were synthesized. A strategy developed previously¹⁰ for synthesis of chlorinated phenoxy phenols was adapted. This method yields products with chlorines in one of the rings at the ortho positions where they are required for cyclization to the dibenzofuran system. The amino group, like the methoxy group in the synthesis of phenoxyphenols,

should increase the nucleophilicity of the phenoxide ion during the reaction.

An aminophenol, a chlorinated fluorobenzene in the presence of potassium carbonate, and 18-crown-6 was refluxed in acetonitrile for two days. Chlorines on the activated aromatic substrate were required to be symmetrically placed around the fluorine for reaction to take place. For example, 2,6-dichloro-, 2,3,5,6-tetrachloro-, and 2,3,4,5,6-pentachlorofluorobenzene reacted to form the diphenyl ether (DPE). Unsymmetrically substituted chlorofluorobenzenes failed to react. The higher chlorinated fluorobenzene gave higher yield of product (Table IV.1) because of its greater electrophilicity. Conversion of the chlorinated aminodiphenyl ether to the diazonium salt, with *t*-butyl nitrite and introduction of chlorine-37 by displacement of the diazonium group with Cu^{37}Cl , was carried out in one step.

The photochemical conversion of the chlorine-37 labeled trichloro-DPE was carried out at 300 nm in acetone, which acts as a triplet sensitizer.¹¹ The triplet-sensitized cyclization reaction gave almost 100% product, but in the absence of acetone or other triplet sensitizer the yields of dibenzofuran were poor. No loss of label was encountered in the synthesis, and the use of Cu^{37}Cl with 95% atom excess of chlorine-37 yielded a product with the same atom excess of isotope. Two products from the cyclization of 2,3'(^{37}Cl),6-trichloro-DPE were successfully separated by reverse phase HPLC and their

structures were confirmed by 2-D NMR COZY spectroscopy (Figure IV.2).

The introduction of a nitro group at the desired position of the dibenzofuran gave the starting material for the synthesis of several chlorinated dibenzofurans with chlorine-37 at key positions. Among the known nitrating agents, ammonium nitrate in the presence of trifluoroacetic anhydride¹² was found to be most effective for synthesis of mononitrodibenzofuran. The major products were 3-nitro-DBF (72 %) and 2-nitro-DBF (16 %). The 2-nitro-DBF can also be obtained from the commercially available 4-nitro-DPE (Ultra Scientific Co.) by palladium acetate-promoted cyclization.¹³

With 3-nitro-DBF as starting material and a silica surface as catalyst¹⁴, chlorination proceeded to give 7-chloro-3-nitro-DBF (Scheme IV.2). Reduction of the nitro group with tin in hydrochloric acid¹⁵ followed by diazotization and chlorination with Cu^{37}Cl gave 3(³⁷Cl),7-dichloro-DBF. In the reduction step, some 3-amino-4,7-dichloro-DBF was formed as well. This was observed to be a general phenomenon when nitrodibenzofurans were reduced with tin in the presence of large amounts of concentrated hydrochloric acid¹⁶, and it turned out to be a useful reaction for the preparation of isomers which were otherwise very difficult to obtain.

Approximately twenty percent of the reduction product obtained from 3-nitro-DBF was 3-amino-4-chloro-DBF (Scheme IV.2). Diazotization and chlorination of this compound gave

3,4(³⁷Cl)-dichloro-DBF. In the same way, 1,2(³⁷Cl)-dichloro-DBF was obtained from 2-nitro-DBF (Scheme IV.3).

Chlorine-37 labeled 2,3-dichloro-DBF was prepared from commercially available 3-amino-2-methoxy-DBF (Scheme IV.4). After conversion of the amino group to chlorine-37, this reaction was demethylated with boron tribromide and the resultant phenolic compound converted to the triflate. Chlorination of this compound with chlorine gas in carbon tetrachloride under photolytic conditions at 300 nm gave a good yield of 2,3(³⁷Cl)-dichloro-DBF.¹⁷ The photolytic conversion involving the singlet state proceeded smoothly to give the product in high yield. However, loss of chlorine-37 enrichment was observed (from 95 % to 65 %) after photolysis reaction.

The commercially available 4-amino-4'-chloro-DPE was easily converted to 4,4'(³⁷Cl)-dichloro-DPE (Scheme IV.5), which in turn could be converted to the dibenzofuran by the method of Åkermark et al.¹², that involved cyclization in acetic acid with the aid of palladium acetate.

Synthesis of Trichlorodibenzofurans. Among the possible trichlorodibenzofurans the 1,2,3- and 2,3,4-trichloro-DBFs are particularly difficult to synthesize because the conventional chlorination of dibenzofuran always gives chlorinated products which have an equal distribution of chlorines on the two rings, e.g., 2,8-, 2,3,8-, 2,3,7,8-, etc.¹⁸ The 2,3,4- isomer

has been synthesized by Safe¹⁹ by the condensation of 2,3,4,5-tetrachloroaniline and anisole, followed by demethylation and base-catalyzed cyclization. The overall yield after the three reaction steps was approximately 1 %.

Electrophilic chlorination of aminodibenzofuran followed by substitutive deamination reaction is one method to introduce chlorines in the ring bearing the amino group.²⁰ This reaction is efficient because of the electron-releasing effect of the amino group. Generally, amines are very reactive towards electrophilic halogenation. The reaction may be carried out without catalysts and most often cannot be controlled to provide monochlorinated products.²¹ For reactions in the absence of a catalyst, the attacking entity is chlorine molecule which has been polarized by the ring. Evidence for molecular chlorine as the attacking species is provided by the fact that acids, bases, and other ions, especially chloride ion, accelerate the rate about equally.²²

The chlorination of 3-amino-DBF was carried out in Cl_2/CCl_4 solution at room temperature without catalyst. The reactions proceeded very rapidly. In 3 minutes a dichloro-compound was formed exclusively, and in 5 minutes a mixture of dichloro- and trichloro- compound in a ratio of 1:0.4 was obtained (Scheme IV.6).

The trichloro compound was identified as 3-amino-1,2,4-trichloro-DBF. 3-Amino-2,4-dichloro-DBF was then diazotized and chlorinated with Cu^{37}Cl . The reaction gave a dichloro-DBF

and a trichloro-DBF in the ratio of 0.7:1. The mass spectrum of the dichloro- compound showed that the compound had only natural isotopic abundance of chlorine, indicating that deamination had occurred. This was observed to be a general phenomenon when the amino group had neighboring chlorines. Lowering the initial temperature decreased the amounts of deamination products considerably. The solvent, acetonitrile, could be a hydrogen source in the deamination reaction; this was confirmed by the deuterium incorporation when acetonitrile- d_3 was used as solvent.

By the above method 2-amino-DBF was chlorinated and 1,2(^{37}Cl),3-trichloro-DBF and 1,2(^{37}Cl),3,4-tetrachloro-DBF were obtained (Scheme IV.7). The rate of chlorination of this compound was somewhat slower than that of the 3-amino-DBF.

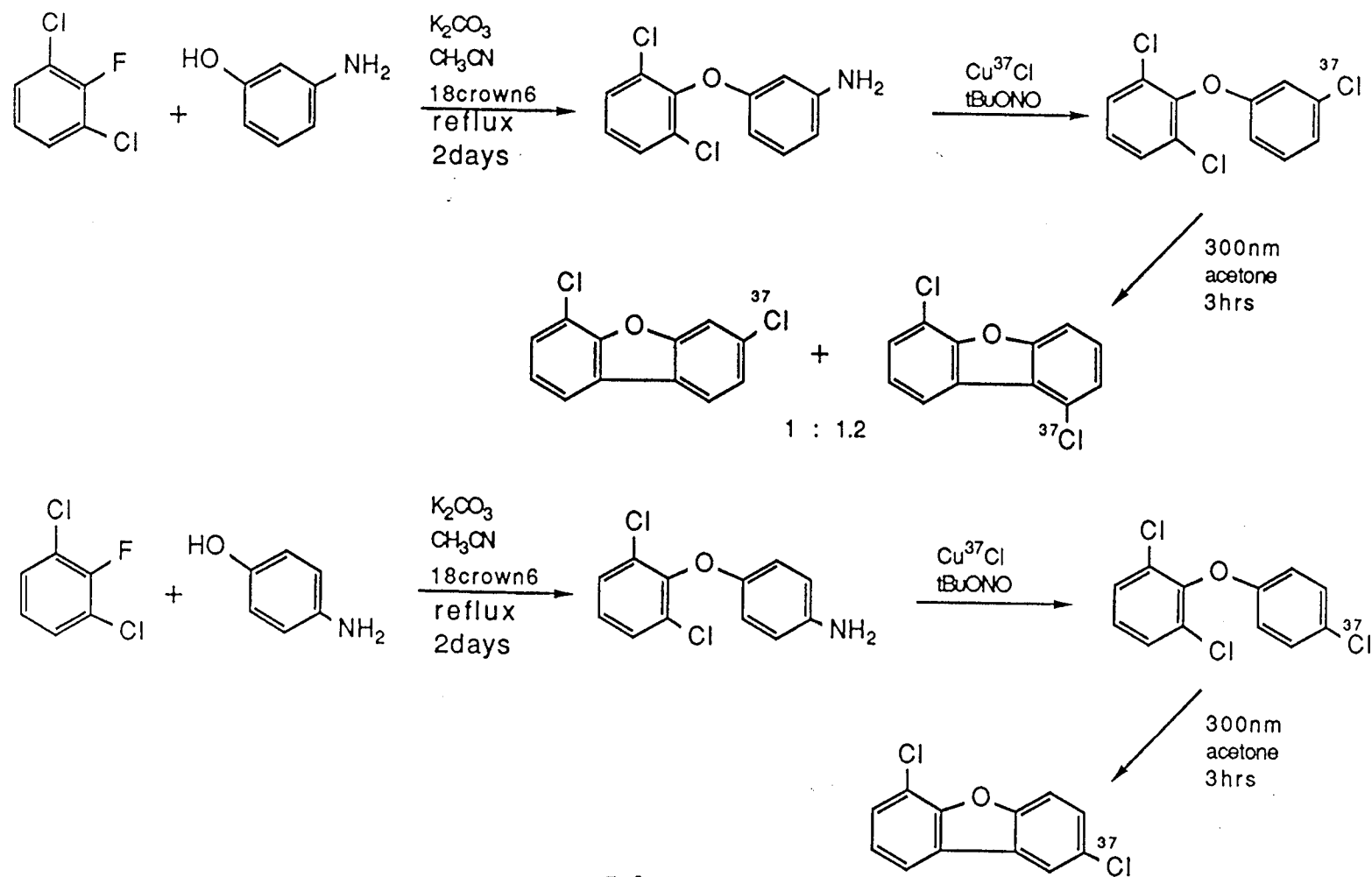
The structure of the 2,3,4-trichloro-DBF was determined by 2-D NMR with the help of the NOE technique. The proton NMR spectrum showed four coupled hydrogens and one singlet. Four hydrogens coupled to one another are present in one ring and the single proton is in the ring with the three chlorines. AM1 calculation of the neutral molecule indicates that protons 1 and 9 should be 2.88 Å apart. This distance is sufficiently close to be able to observe an NOE if these protons are both present.²³ A strong NOE was observed by irradiation of the singlet (Figure IV.3). Thus, this proton must be within 3.0 Å of another proton, which is H_9 . This was confirmed by irradiation of the H_9 doublet which shows an NOE for H_1 (Figure

IV.4). The structure of the product must, therefore be 2,3,4-trichloro-DBF. The remaining protons were assigned by noting that H₉ showed a slight NOE upon irradiation of H₁, and H₆ and H₇ were assigned by ¹H-¹H homonuclear and ¹H-¹³C heteronuclear correlations. A further experiment was performed to confirm the location of chlorine-37 on the 3-position. Photolytic dechlorination with triethylamine gave 2,4-dichloro-DBF exclusively, which was shown by mass spectrometry to have only two natural chlorines. Therefore, there was no regiochemical scrambling of the chlorine-37.

By use of the silica based chlorination, 3-nitro-DBF and 3(³⁷Cl)-chloro-DBF were chlorinated. The chlorination of 3-nitro-DBF occurred at positions 7 and 8, while the chlorination of 3(³⁷Cl)-chloro-DBF gave chlorine incorporation at positions 2 and 8 (Scheme IV.8). These two different regiochemistries yielded 2,3,7(³⁷Cl)- and 2,3(³⁷Cl),8-trichloro-DBFs respectively and allowed a comparison to be made of the reactivity of the C₃ position with and without the effects of a neighboring chlorine in the ECNI mass spectrometry. In both cases, however, extreme caution was exercised since the highly toxic 2,3(³⁷Cl),7,8-tetrachloro-DBF can be produced. The two structures could be identified easily by ¹H NMR because of the ortho and meta coupling, respectively, of protons H₇ or H₈ to H₉ (Figure IV.5). The most down-field protons are H₁.

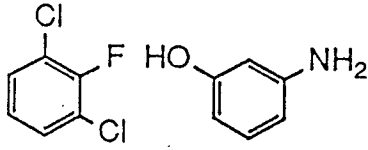
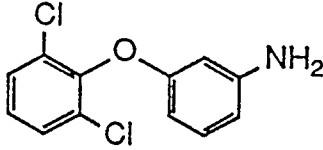
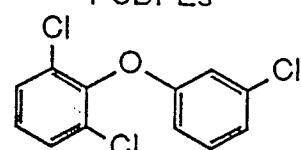
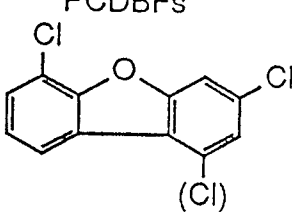
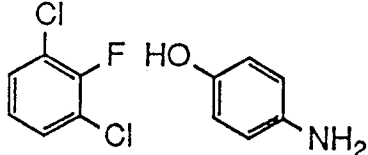
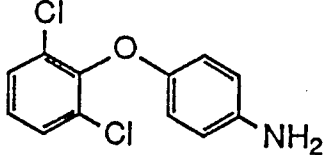
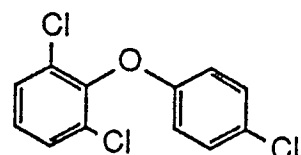
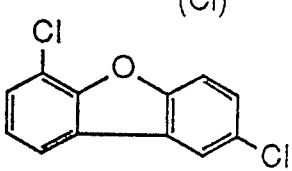
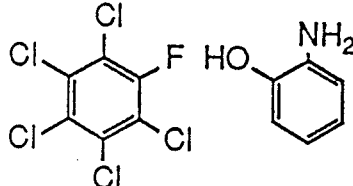
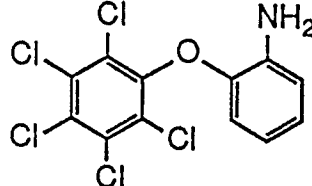
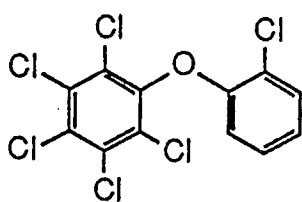
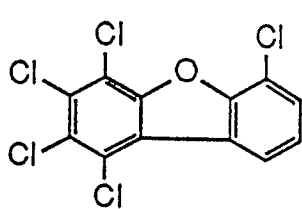
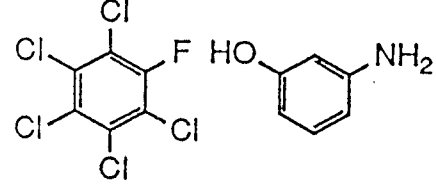
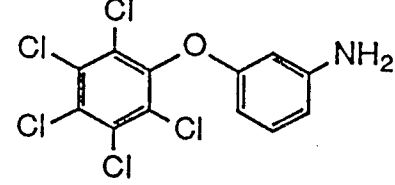
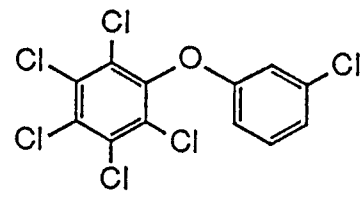
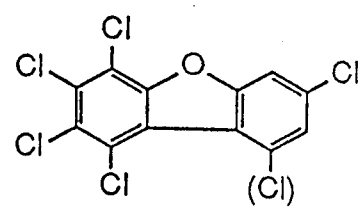
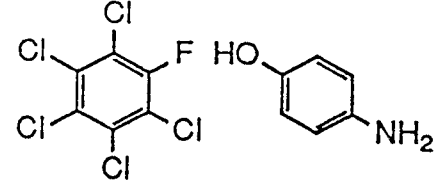
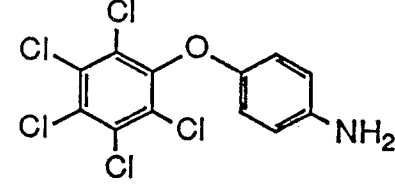
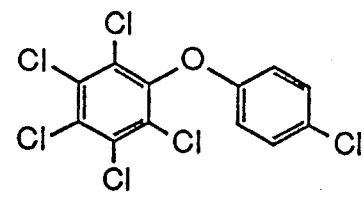
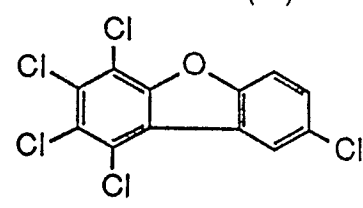
Acknowledgement. We gratefully acknowledge support from

the National Institutes of Health, NIEHS ES00040 and NIEHS ES00210. We also wish to thank Rodger Kohnert for NMR analysis and Jung-Suk Jang for the photolysis work. The Bruker AM 400 NMR spectrometer was purchased in part through grants from the National Science Foundation (CHE-8216190) and from the M. J. Murdock Charitable Trust to Oregon State University. This is Oregon Agricultural Experiment Station Publication No. 9276.



Scheme IV.1

Table IV.1. Synthesis of PCDPEs and PCDBFs from condensation of chlorofluorobenzenes and aminophenols.

Reactants	Products	yield(%)	PCDPEs	PCDBFs
		15		
		18		
		71		
		65		
		68		

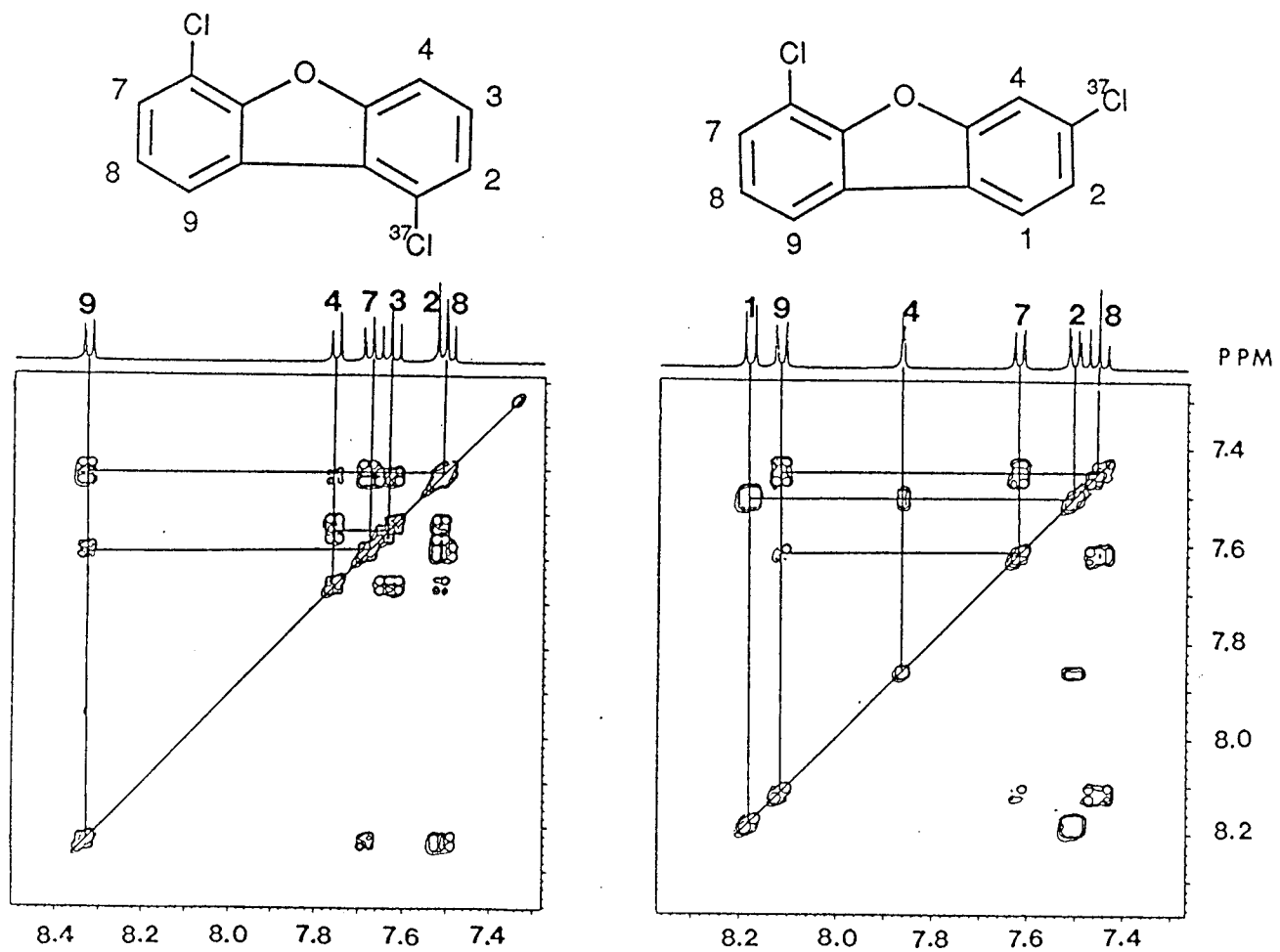
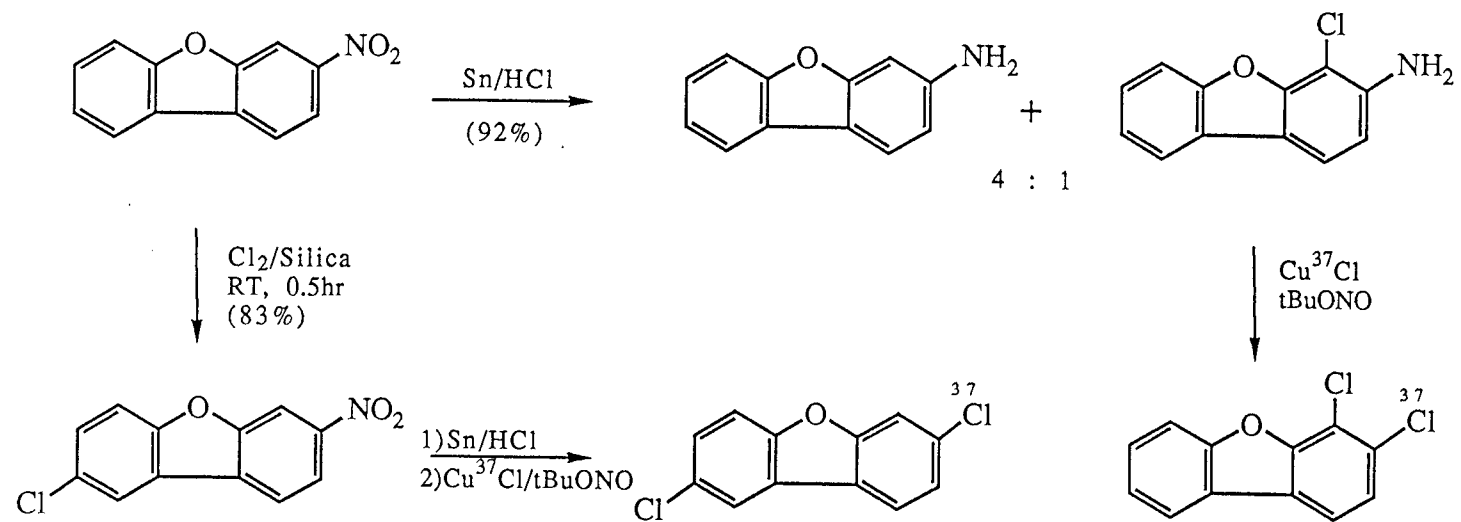
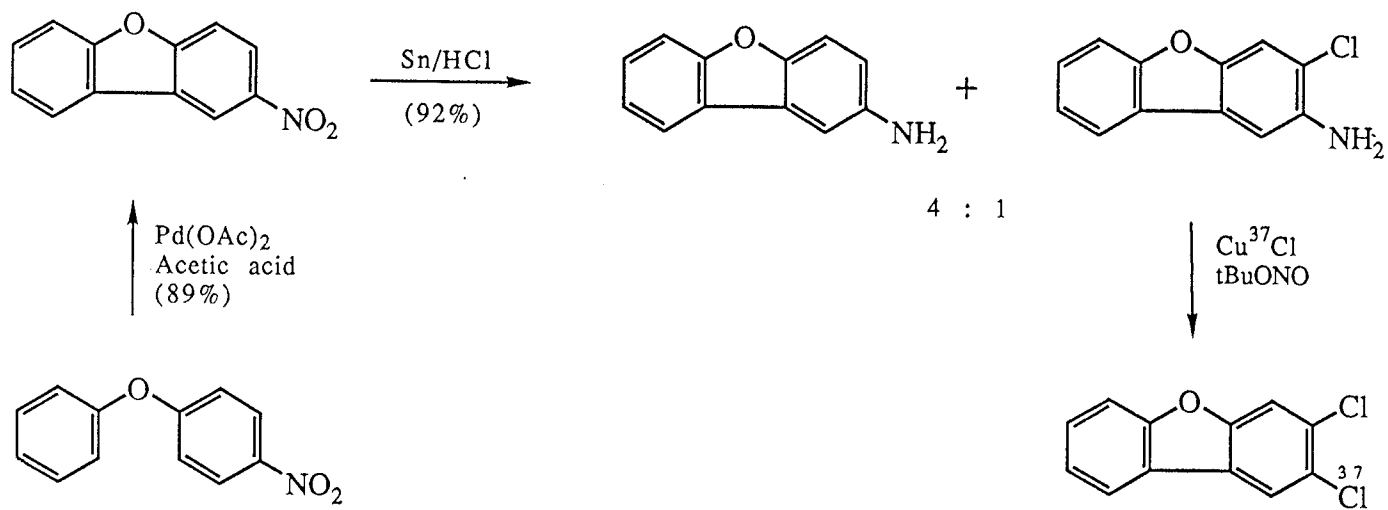


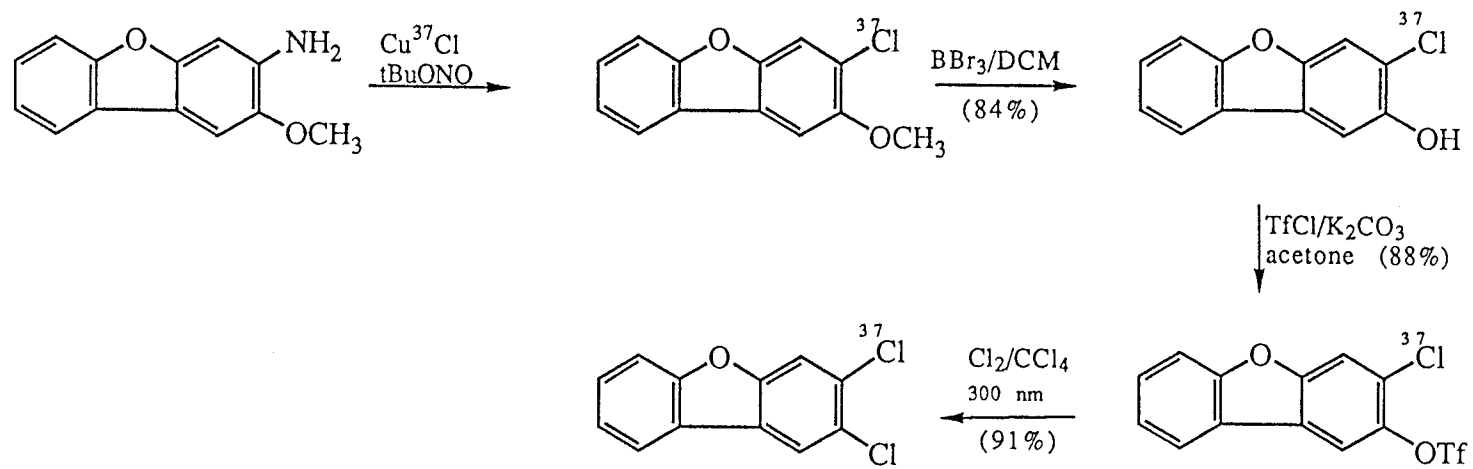
Figure IV.2. 2-D NMR COZY spectrum of 1(³⁷Cl),6-DCDBF and 3(³⁷Cl),6-DCDBF.



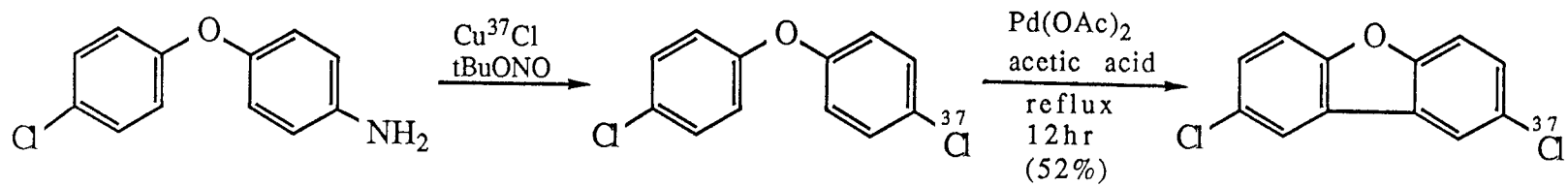
Scheme IV.2



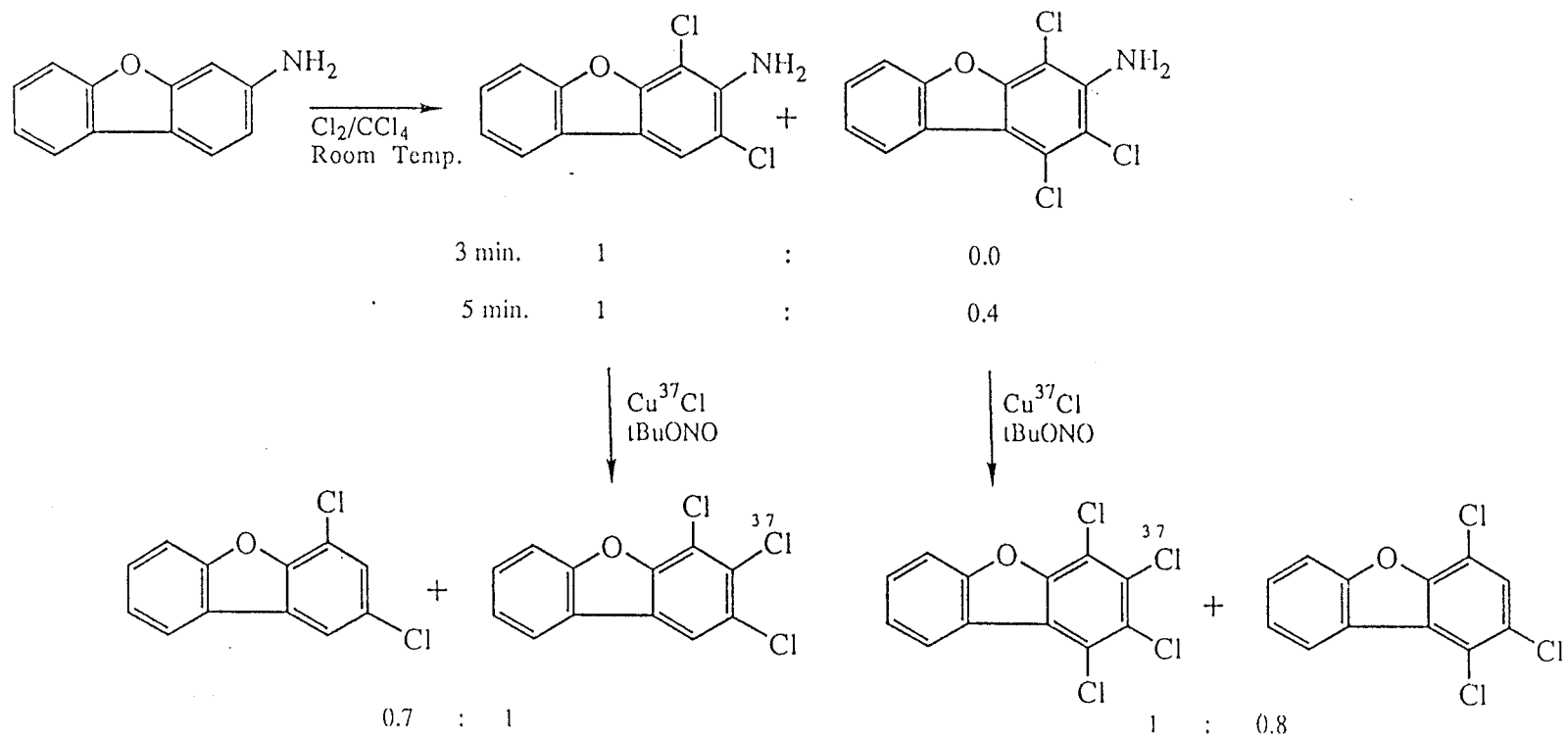
Scheme IV.3



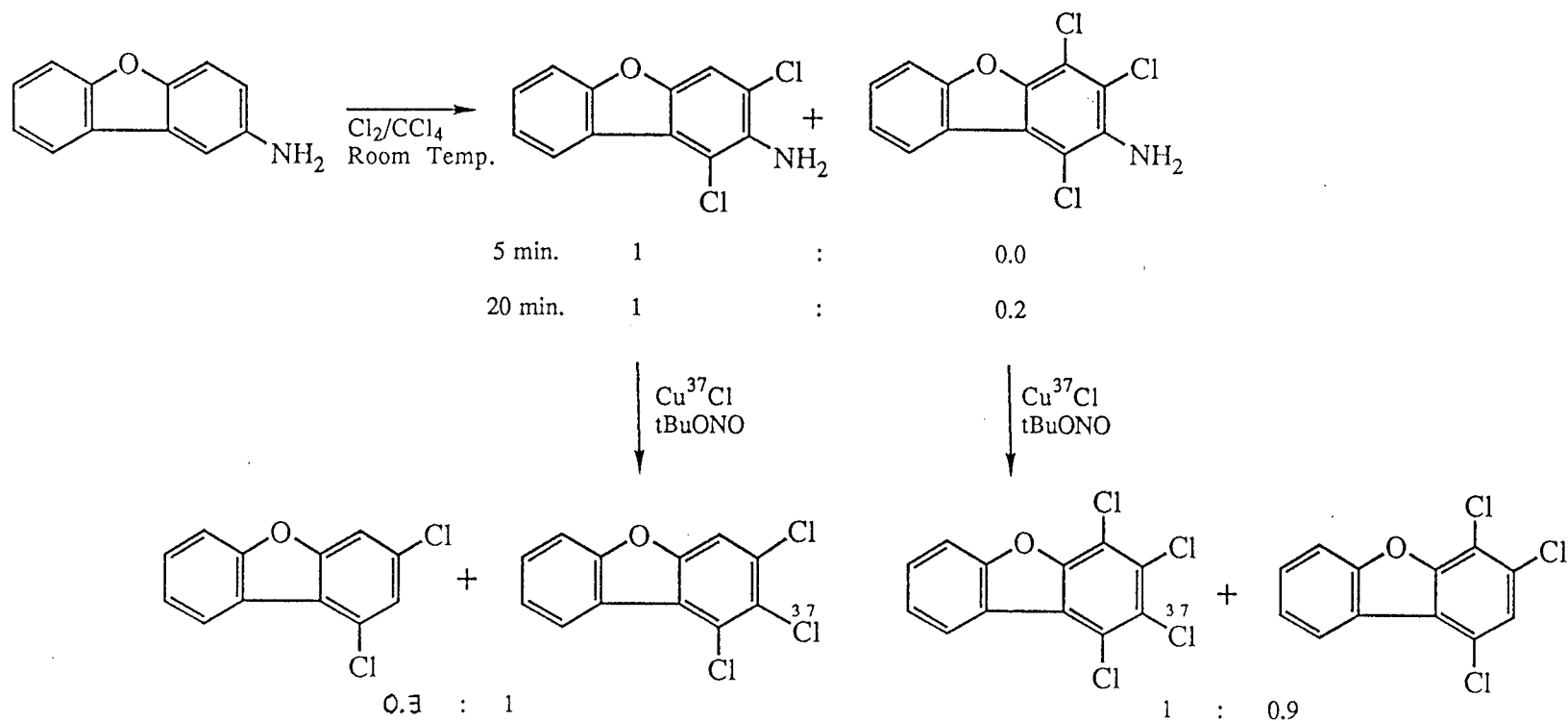
Scheme IV.4



Scheme IV.5



Scheme IV.6



Scheme IV.7

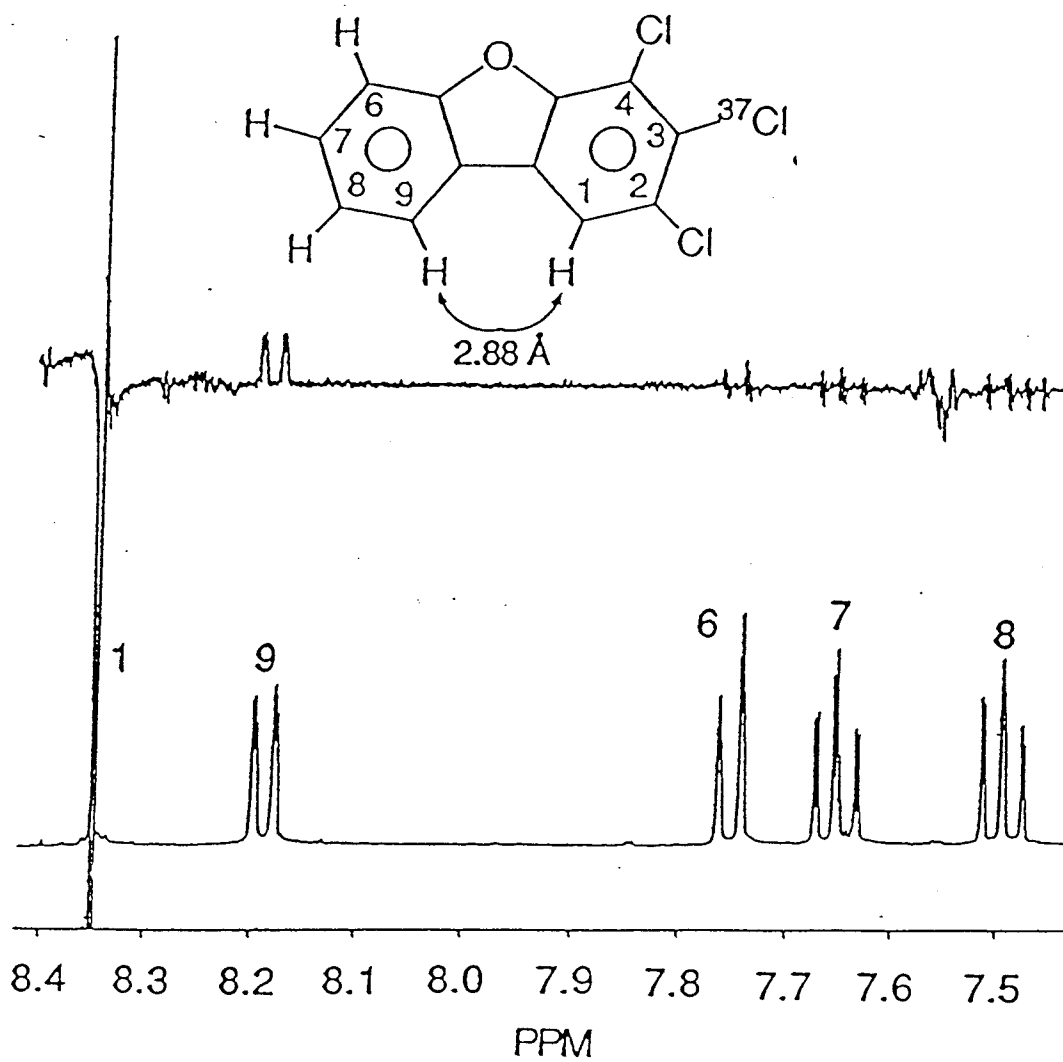


Figure IV.3. NOE experiment of 2,3(³⁷Cl),4-TrCDBF with irradiation of H1.

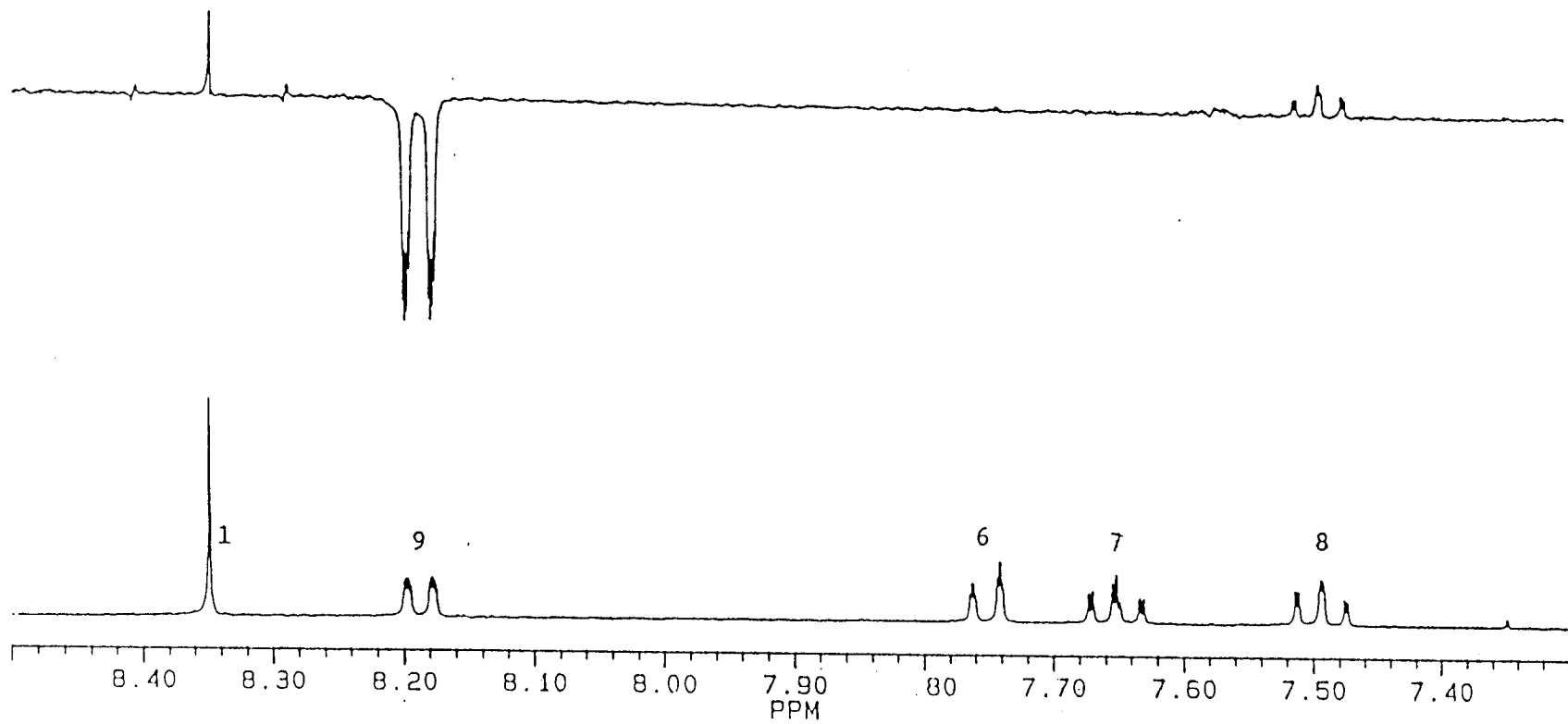
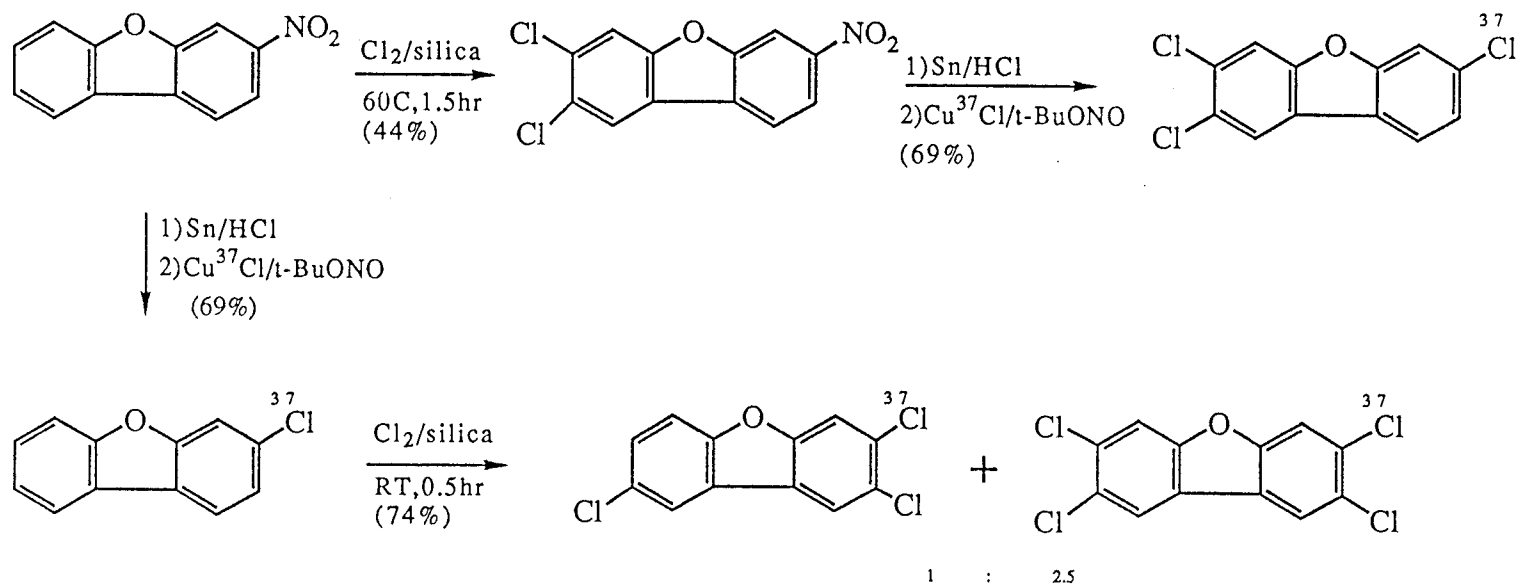


Figure IV.4. NOE experiment of 2,3(³⁷Cl),4-TrCDBF with irradiation of H₉.



Scheme IV.8

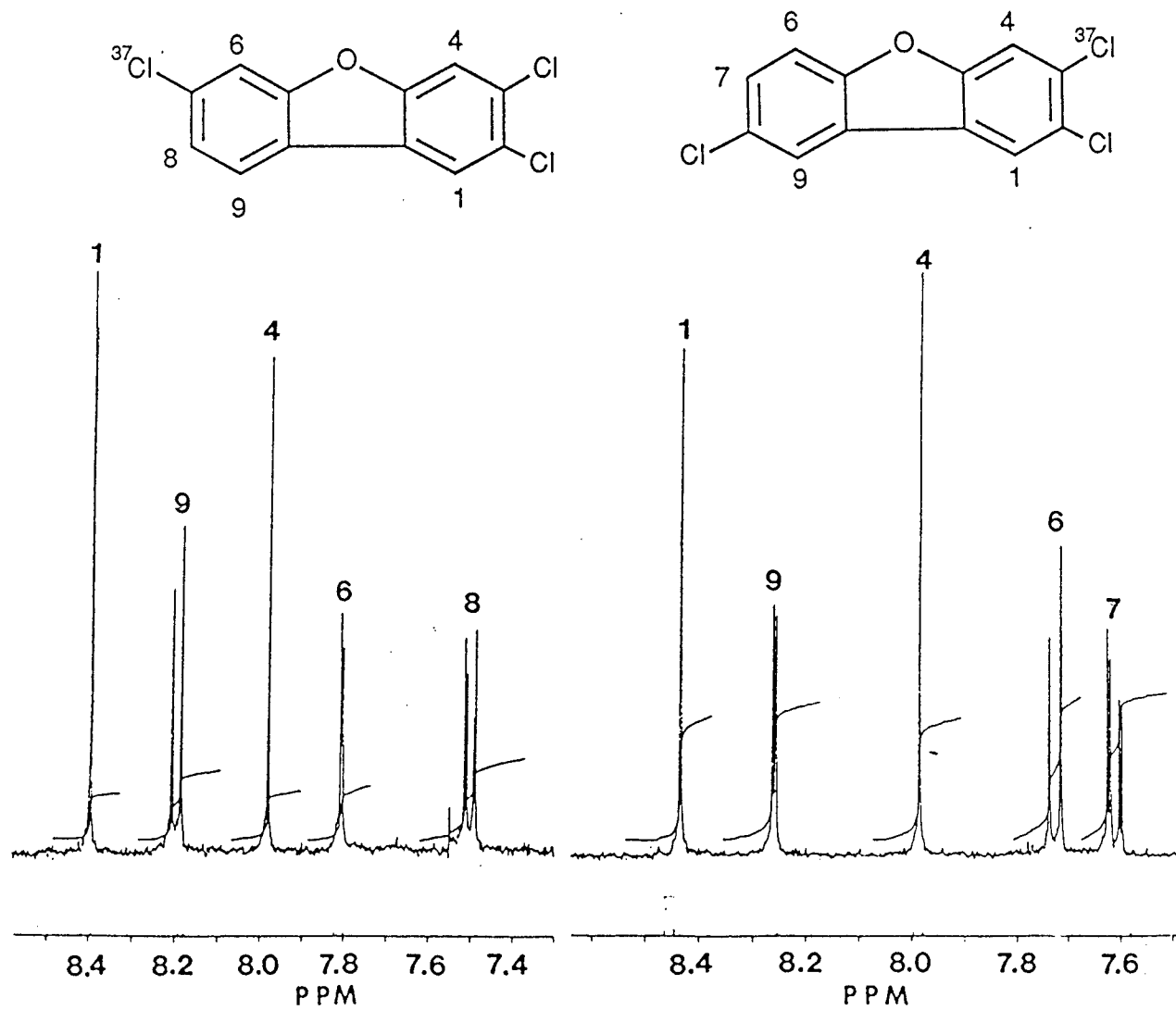


Figure IV.5. NMR spectrum of 2,3,7(^{37}Cl)-TrCDBF and 2,3(^{37}Cl),8-TrCDBF.

References

1. Rappe, C.; Gara, A.; Buser, H.R. Chemosphere 1978, 7, 981.
2. (a) Morita, M.; Nakagawa, J.; Rappe, C. Bull. Env. Contam. Toxicol. 1978, 19, 665.
(b) Buser, H.R.; Rappe, C. Chemosphere 1979, 8, 157.
3. Polychlorinated Dibenzo-p-dioxins NRCC No. 18576, National Council of Canada, 1981.
4. Ryan, J.J.; Lizotte, R.; Lau, B.P.-Y. Chemosphere 1985, 14, 697.
5. Laramée, J.A.; Arbogast, B.C.; Deinzer, M.L. Anal. Chem. 1988, 60, 1937.
6. Laramée, J.A.; Chang, Y-S.; Arbogast, B.C.; Deinzer, M.L. Biomed. Environ. Mass Spectrom. 1988, 17, 63.
7. Tubandt, C.; Rindtorff, E.; Jost, W.Z. anorg. allg. Chem. 1927, 165, 195.
8. (a) Meerwein, H.; Buchner, E.; van Emster, K. J. prakt. Chem. 1939, 152, 237.
(b) Dickerman, S.C.; Weiss, K.; Ingberman, A.K. J. Org. Chem. 1956, 21, 380.
(c) Dickerman, S.C.; DeSouza, D.J.; Jacobson. N. J. Org. Chem. 1969, 34, 710.
(d) Galli, C. J. Chem. Soc., Perkin Trans. 2 1982, 1139.
9. Doyle, M.P.; Siegfried, B.S.; Dellaria, J.F. J. Org. Chem. 1977, 42, 2426.
10. Kolonko, K.J.; Deinzer, M.L.; Miller, T.L. Synthesis, 1981, 2, 133.
11. Freeman, P.K.; Jonas, V. J. Agric. Food Chem. 1984, 32, 1307.
12. Oliver, J.E.; Ruth, J.M. Chemosphere 1983, 12, 1497.
13. Åkermark, B.; Ebersson, L.; Jonsson, E.; Petersson, E. J. Org. Chem. 1975, 40, 1365.
14. (a) Lamparski, L.L.; Nestricks, T.J. J. Anal. Chem. 1982, 54, 402.
(b) Peterson, R.G. Bull. Environ. Contam. Toxicol. 1987, 38, 416.

15. Chae, K.; Cho, L.K.; McKinney, J.D. J. Agric. Food Chem. 1977, 25, 1207.
16. Furniss, B.S.; Hannaford, A.J.; Rogers, V.; Smith, P.W.G.; Tatchell, A.L. Vogel's Textbook of Practical Organic Chemistry 4th Ed.; Longman Scientific & Technical, 1987, p 658.
17. Chang, Y-S.; Jang, J-S.; Deinzer, M.L. Tetrahedron 1990, 46, 4161.
18. Gray, A.P.; Dipinto, V.M.; Solomon, I.J. J. Org. Chem. 1976, 41, 2428.
19. Safe, S.H.; Safe, L.M. J. Agric. Food Chem. 1984, 32, 68.
20. Chang, Y-S.; Deinzer, M.L. Synth. Commun. in press.
21. de la Mare, P.B.D.; Hall, D.J. Chem.Soc., Perkin Trans. II 1977, 106.
22. March, J. Advanced Organic Chemistry; Wiley Interscience: New York, 1985, p 477.
23. Sanders, J.K.M.; Hunter, B.K. Modern NMR Spectrometry; Oxford University Press: Oxford, 1988.

V. SYNTHESIS OF REGIOSPECIFIC CHLORINE-37 LABELED
PENTACHLORODIBENZOFURANS AND MASS SPECTRAL EVIDENCE
OF CHLORINE SCRAMBLING DURING MOLECULAR CHLORINATION

Yoon-Seok Chang and Max L. Deinzer*

Department of Chemistry
Oregon State University
Corvallis, Oregon 97331

Journal of Labelled Compounds and Radiopharmaceuticals,
submitted.

Summary

Four pentachlorodibenzofurans with four chlorines in one ring were synthesized and labeled regiospecifically with chlorine-37 at positions 6, 7, 8, and 9. These were further chlorinated on a silica column with chlorine gas which yielded a mixture of hexa-, hepta- and octachlorodibenzofuran congeners. However, this post-chlorination reaction occurred with loss of chlorine-37 label. The mechanism of the chlorination reaction is discussed.

Key Words: Chlorine-37 labeled, pentachlorodibenzofuran, octachlorodibenzofuran, molecular chlorination.

Elucidation of the mechanisms responsible for regiospecific chlorine loss from substituted benzenes¹, polychlorinated dibenzo-p-dioxins (PCDDs)², and polychlorinated dibenzofurans (PCDBFs)³ under electron capture negative ion mass spectrometry conditions is an ongoing effort in this laboratory. Incorporation of a chlorine-37 label at key positions should allow for the determination of the chlorine atom or ion lost during a dissociative electron capture event. This paper reports on the synthesis of regiospecifically labeled chlorine-37 penta-CDBFs and the results from molecular chlorination of these compounds for the preparation of higher chlorinated congeners.

By using the method developed previously for the synthesis of chlorophenoxyphenols⁴, three isomers of aminopentachlorodiphenyl ethers were prepared via coupling of pentachlorofluorobenzene with ortho-, meta- and para-aminophenols in 75~88% yields. The aminophenols are good nucleophiles because of the electron releasing ability of the amino group.

Cyclization of these aminochlorodiphenyl ethers to aminochlorodibenzofurans under photolytic conditions was unsuccessful. Thus, the amino group was first converted to chlorine-37 via the Sandmyer reaction⁵ using copper chloride-37 (95.5% ³⁷Cl excess). The resulting chlorine-37 labeled hexachlorodiphenyl ethers (HxCDPEs) were photolyzed in acetone at 300 nm which resulted in cyclization to dibenzofuran by

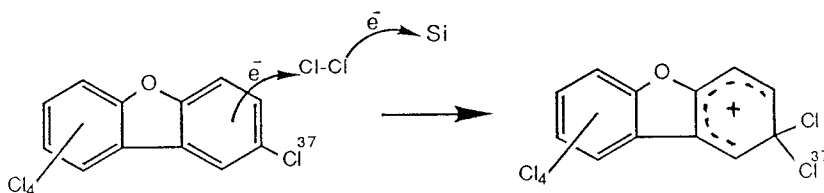
loss of HCl. These acetone-sensitized photocyclization reactions⁶ were very efficient and almost all of the diphenyl ethers were converted to the pentachlorodibenzofurans, 1,2,3,4,6(³⁷Cl)-, 1,2,3,4,7(³⁷Cl)-, 1,2,3,4,8(³⁷Cl)- and 1,2,3,4,9(³⁷Cl)-penta-CDBF (Scheme V.1). A close examination of the molecular ion isotope cluster in mass spectrometry showed no loss of chlorine-37 in the reaction.

The chlorine-37 labeled pentachlorodibenzofurans were further chlorinated to give higher chlorination products. The newly reported technique⁷ for chlorination of PCDDs and PCDBFs using a silica supporting matrix was used. Purification by HPLC and identification by GCMS showed higher chlorinated products were obtained including hexa-CDBFs, hepta-CDBFs and octa-CDBF. The temperature of the silica column governs the final product congener distribution (Scheme V.2). Higher temperatures yield higher chlorinated products in these reaction. However, significant loss of chlorine-37 label occurs during chlorination. The higher the degree of chlorination, the greater the loss of chlorine-37 observed. For example, the octachlorodibenzofuran obtained from chlorination of 1,2,3,4,8(³⁷Cl)-penta-CDBF showed chlorine-37 loss from 95% to 43% (Figure V.1).

The mechanism of molecular chlorination of aromatic compounds at low temperature involves an initial step which consists of a rapidly reversible formation of a π -complex between the reactants. The aromatic ring acquires a positive

charge by single electron transfer to the chlorine molecules.⁸ The π -complex then rearranges to a σ -complex. The results from chlorination of penta-CDBFs show that the reaction is more regiospecific at higher temperature, indicating that the σ -complex formed by free-radical attack predominates. This discrimination is not quite so apparent for further chlorination of the hexa-CDBFs. The product distribution, in fact, is more random at higher temperature, suggesting that regiospecificity via a σ -complex is significantly less important.

It has been known that activated alumina and silica have electron acceptor properties, and the formation of radical cations of aromatic hydrocarbons adsorbed on alumina have been observed by ESR.⁹ Satoh and coworkers reported copper(II) halide halogenation of aromatic hydrocarbons on alumina and silica gel.¹⁰ They postulated the reaction mechanism to involve one electron transfer to the alumina or silica gel. The loss of chlorine-37, likewise, may result from aromatic radical cation formation by electron transfer from penta-CDBF to the chlorine molecule followed by one electron transfer to the silica support.



Possible intramolecular migration of chlorine-37 was tested under photolytic dechlorination reaction conditions¹¹ for the octachlorodibenzofuran product which was enriched by chlorine-37 at the 3-position. It was observed that the dechlorinated products, 1,2,4,6,7,8,9-hepta-CDBF and 1,2,4,6,8,9-hexa-CDBF, have the same chlorine-37 enrichment as that of the precursor octachlorodibenzofuran, indicating there was no intramolecular migration of chlorine during the chlorination reactions.

Experimental

The general method and experimental conditions for chlorine-37 labeling on dibenzofuran and the synthesis of regiospecific chlorine-37 labeled di-, tri- and tetrachlorodibenzofurans are described elsewhere.¹²

Structural characterizations for penta-CDBFs and their chlorinated products were made by GC retention time comparison using a DB-5 column according to the procedure of Bell and Gara¹³. The two penta-CDBF isomers prepared by cyclization of 2,3,3'(³⁷Cl),4,5,6-HxCDPE were separated on a preparative silica TLC plate with 100% hexane and the structures were verified by proton NMR. 1,2,3,4,7(³⁷Cl)-Penta-CDBF: CD₃COCD₃; δ 8.40(d), 7.95(d), 7.60(dd). 1,2,3,4,9(³⁷Cl)-Penta-CDBF: CD₃COCD₃; δ 7.81(dd), 7.70(t), 7.59(dd).

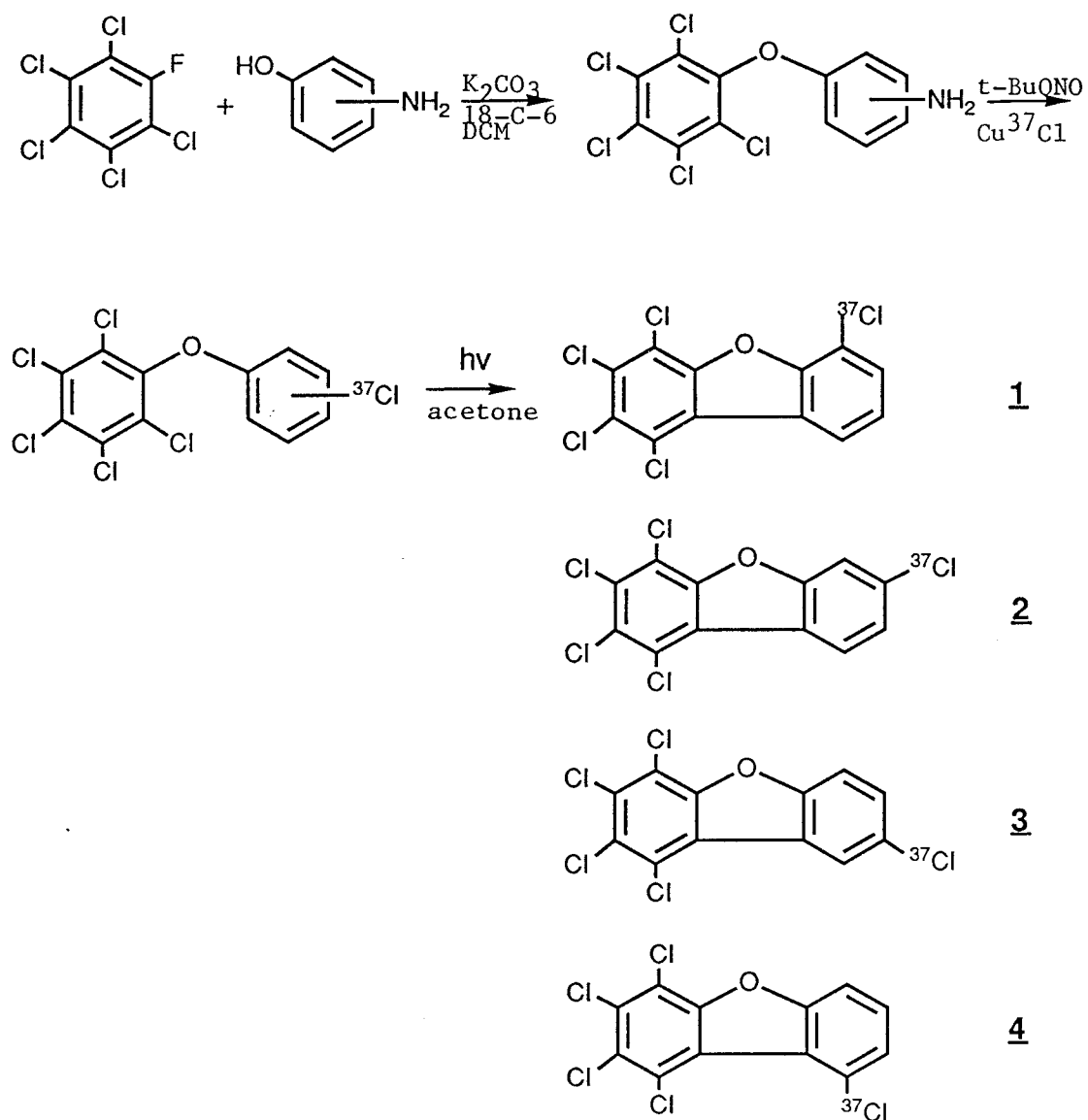
2,2'(³⁷Cl),3,4,5,6-HxCDPE: EIMS; m/e 378(42), 308(80), 306(100), 113(40), 75(100), ¹H NMR; CD₃COCD₃; δ 7.60(dd), 7.24(td), 7.16(td), 6.82(dd). 2,3,3'(³⁷Cl),4,5,6-HxCDPE: EIMS; m/e 378(22), 308(80), 306(100), 113(55), 75(78), ¹H NMR; CD₃COCD₃; δ 7.40(t), 7.18(dd), 7.10(t), 6.90(dd). 2,3,4,4'(³⁷Cl),5,6-HxCDPE: EIMS; m/e 378(44), 308(80), 306(100), 113(50), 75(100), ¹H NMR; CD₃COCD₃; δ 7.38(dd), 7.02(dd). Exact mass calculated for C₁₂H₄O₁Cl₅³⁷Cl₁: 375.83638; high resolution masses for three isomers: 375.8363±0.0001.

The quantity of isotope loss was determined by comparison of the molecular ion clusters obtained experimentally to those generated via a binomial expansion. The calculation is based

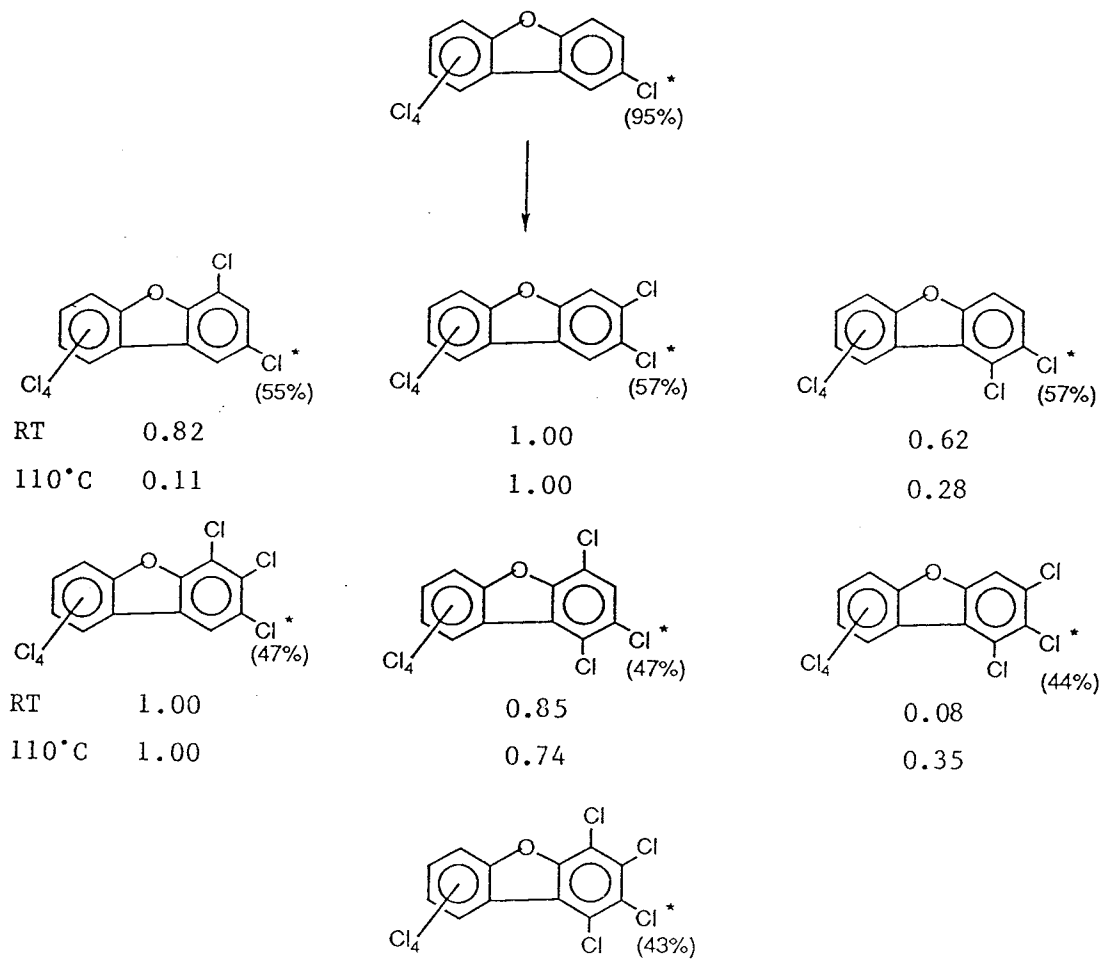
on the equation $(x+y)^m(a+b)^n$, where m is number of natural chlorines with percent abundances $x:y$ and n is the number of isotope-enriched chlorines with percent abundances $a:b$. Excellent agreement between the calculated and experimental isotope patterns was observed (Figure V.1).

Acknowledgement

We thank NIH for support ES00040. We also thank Jung-Suk Jang for assistance in the photolysis works. This is publication No.9353 from the Oregon Agricultural Experimental Station.



Scheme V.1



Scheme V.2

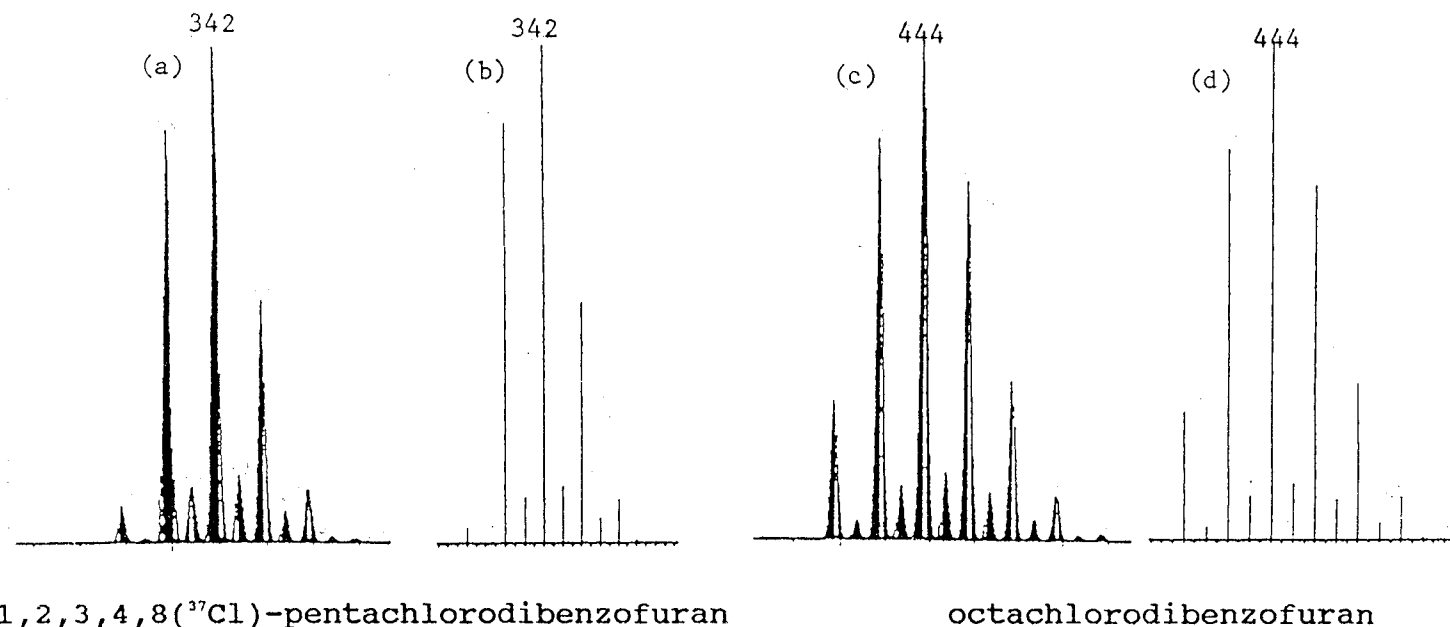


Figure V.1. Computer simulated (a and c) and experimental (b and d) mass spectra of molecular radical anions for 1,2,3,4,8(³⁷Cl)-penta-CDBF (95% ³⁷Cl) and octa-CDBF (43% ³⁷Cl).

References

1. Freeman, P.K.; Srinivasa,R.; Campbell, J.-A.; Deinzer, M.L. J. Am. Chem. Soc. 1986, 108, 5531.
2. Larameé, J.A.; Arbogast, B.C.; Deinzer, M.L. Anal. Chem. 1988, 60, 1937.
3. Larameé, J.A.; Chang, Y-S.; Arbogast, B.C.; Deinzer, M.L. Biomed. Environ. Mass Spectrom. 1988, 17, 63.
4. Kolonko, K,J.; Deinzer, M.L.; Miller, T.L. Synthesis 1981, 2, 133.
5. Doyle, M.P.; Siegfried, B.S.; Dellaria, J.F. J. Org. Chem. 1977, 42, 2426.
6. Chang, Y-S.; Jang, J-S.; Deinzer, M.L. Tetrahedron 1990, 46, 4161.
7. Lamparski, L.L.; Nestricks, T.J. Anal. Chem. 1982, 54, 402.
8. a) Kooyman, E.C. Halogenation of Aromatic Compound In Advances in Radical Chemistry Vol.1; Logos: London, 1965, p 151.
b) Tanko, J.M.; Anderson, F.E. J. Am. Chem. Soc. 1988, 110, 3525.
9. Flodchart, B.D.; Swsay, I.M.; Pink, R.C. J. Chem. Soc., Chem. Commun. 1980, 439.
10. Kodomari, K.; Satoh, H.; Yoshitomi, S. Nippon Kagaku Kaishi 1986, 1813.
11. Choudhary, G.; Keith, L.H.; Rappe, C. Chlorinated Dioxins and Dibenzofurans in the Total Environment I; Ann Arbor Science: Butterworth, 1985, p 35.
12. Chang, Y-S.; Deinzer, M.L. J. Labelled Compd. Radiopharm. in press.
13. Keith, L.H.; Rappe, C.; Choudhary, G. Chlorinated Dioxins and Dibenzofurans in the Total Environment II; Butterworth Publishers: Stoneham, 1985, p 10.

VI. RELATIONSHIP OF MOLECULAR ANION ABUNDANCE AND
CALCULATED LOWEST UNOCCUPIED MOLECULAR ORBITAL ENERGIES
FOR POLYCHLORINATED DIBENZOFURANS AND DIBENZODIOXINS IN
ELECTRON CAPTURE NEGATIVE ION MASS SPECTROMETRY:
EVIDENCE FOR NEGATIVE METASTABLE IONS

James Laramée, Yoon-Seok Chang, Brian Arbogast and Max Deinzer

Department of Chemistry
Oregon State University
Corvallis, Oregon 97331

Biomedical and Environmental Mass Spectrometry, 1988, 17, 63.

Dioxins were investigated by James Laramée and Dibenzofurans were studied by Yoon-Seok Chang. Mass measurements were performed by Brain Arbogast.

Abstract

Relationships were found between experimentally measured molecular radical anion abundances and calculated lowest unoccupied molecular orbital energies (ϵ_{LUMO}) for polychlorodibenzofurans and polychlorodibenzo-p-dioxins. Anion abundances were measured using standard mass spectrometric techniques, while ϵ_{LUMO} were calculated by the 'Complete Neglect of Differential Overlap' method. Polychlorodibenzofurans with calculated $\epsilon_{\text{LUMO}} > 2.0$ eV show 0 % molecular radical anion and those with $\epsilon_{\text{LUMO}} < 1.4$ eV show >80 % molecular radical anion abundance. Similarly, the molecular radical anion is absent for polychlorodibenzo-p-dioxins with calculated $\epsilon_{\text{LUMO}} > 2.0$ eV. A trend towards greater molecular radical ion relative abundance appears for $2.0 \text{ eV} > \epsilon_{\text{LUMO}} > 1.0$ eV and a maximum is reached around 1 eV, whereupon the molecular ion abundance diminishes with lower ϵ_{LUMO} . B/E linked scan analysis indicates that chlorodioxins with $\epsilon_{\text{LUMO}} < 1$ eV give increasing amounts of metastable anions.

Introduction

Electron capture negative ion chemical ionization (ECNICI) mass spectrometry is particularly attractive for the analyses of electrophilic compounds with low-lying antibonding orbitals.¹ It has been assumed that two distinct pathways account for the production of negative ions. In general, resonance capture of electrons with near thermal energies by neutral molecules yields molecular radical anions, and dissociative capture with electrons of somewhat higher energy yields fragment ions.² However, observation of metastable ions from certain radical anions³ suggests that fragmentation of the molecular radical ions can also occur.

The mode of decomposition and nature of the fragmentation ions formed must strongly depend upon the details of molecular structure. Formation of an aromatic molecular radical anion generally is assumed to involve capture of an ionizing electron in the π system.⁴ If the product ion is stabilized relative to the neutral ground state molecule, the electron affinity of the neutral is positive and the ion produced is long-lived ($>10^{-6}$ s).⁵ If the ionization electron is captured by the neutral and the energy of the ion produced lies above the ground state of the neutral, the electron affinity for the process is negative and the ion will be short-lived ($<10^{-6}$ s) because it undergoes autodetachment or fragmentation.⁶ Between these extremes there must be a channel for production

of transient ions. We investigated two classes of chlorinated aromatics in an effort to show a relationship between molecular ion intensities and calculated LUMO energies, and in the course of these investigations discovered that certain congeners produce transient molecular ions.

Experimental

Chemicals

The chemicals used were either purchased from commercial suppliers (>97 % purity by gas chromatographic (GC) analysis), or synthesized in-house (>99 % purity by GC analysis). The helium buffer gas was purified by molecular sieves and Pt/Pd getter trapping followed by oxy-trap scrubbing.

Synthesis

1,2,3-Trichlorodibenzofuran (1,2,3-TrCDBF), 1,2,4,8-tetrachlorodibenzofuran (1,2,4,8-TCDBF), 1,2,7,8-TCDBF, 2,3,6,8-TCDBF, 2,3,7,8-TCDBF, 1,2,3,7,9-pentachlorodibenzofuran (1,2,3,7,9-PCDBF) and 1,2,3,6,7,9-hexachlorodibenzofuran (1,2,3,6,7,9-HCDBF) were prepared by photolysis from their respective precursor polychlorodiphenyl ethers, which were obtained from commercial sources. The photolysis of the ethers was performed in a Rayonet merry-go-round reactor equipped with eight 300 nm Rull lamps. Precursor ethers were dissolved in acetone (1 mg 10 ml⁻¹), degassed through four freeze-pump-thaw cycles, and then irradiated for 30 min. The reactor temperature was maintained at 50±5 °C throughout the irradiation. Purification and separation of products was accomplished by either reverse-phase high-performance liquid chromatography (HPLC) (Sephadex C-18, 150 x 4.6 mm) or reverse-phase thin-layer chromatography

(TLC) (EM HPTLC RP-18 F254).

Molecular Orbital Calculations

LUMO energies were calculated using the published 'Complete Neglect of Differential Overlap' (CNDO) method.⁷ The CNDO version used in these studies was adapted to an IBM-PC and parameterized to include the second-row elements.⁸ Accelerator hardware and software (Microway, Inc.) were used to decrease the program run-time. Input geometries were chosen from X-ray diffraction data when these data were available. Equilibrium geometries were located, with full optimization of all geometrical variables, using the published 'Modified Neglect of Diatomic Overlap' (MNDO) method⁹ when X-ray data were not available. This was done for the unsubstituted and chlorinated dibenzofurans up through trichlorodibenzodioxin. In addition, the total energy of octachlorodioxin was monitored as C-Cl bond lengths and interannular ring separation were varied. Conformations were examined with an interactive graphic system.

Mass Spectrometry

Measurements were made on the Finnigan 4023 (4500 ion source) and Kratos MS50RF spectrometers employing quadrupole electric field and magnetic deflection analysis, respectively. Samples were analyzed under NICI conditions. Helium was used as reagent gas¹⁰ and its pressure was monitored with a capacitive

manometer attached to the ion source via a static line. Ion currents were recorded from m/z 30 through the molecular anion region. A minimum of 14 measurements were recorded on two or more independent occasions. The results typically agreed to better than 5 %. Furthermore, reproducibility checks between the Kratos and Finnigan spectrometers were made after a delay of 4 months, and agreement was better than 10%.

For both spectrometers, a constant ionization source temperature of 120 °C was used. Temperature measurements were made using a Pt-sensor calibrated to DIN standard 43760 located inside the ion source block. The temperature regulation was ± 3 °C for the Finnigan spectrometer and ± 10 °C for the Kratos spectrometer.

For a quadrupole type mass spectrometer, the transmission efficiency is dependent upon the mass of the ion, axial ion energy, and the extraction potentials.¹¹ The following procedure was used throughout the work. The lens closest to the ion source was adjusted to give both a symmetric peak and maximum ion current for m/z 35. The next lens was set to 130 eV; the final lens potential was adjusted for maximum M^+ ion current. Typically the potential ratios of this symmetric lens were 1:20:15.

Solutions of samples (50 $\mu\text{g ml}^{-1}$ in nonane or toluene which had been refluxed with sodium metal and redistilled) were admitted to the quadrupole mass spectrometer via a GC inlet. Once the retention time of the analyte was known, 2

μL of various congeners and isomers was mixed in the syringe and coinjected in order to reduce the effects of short-term instrument drifts on the measurements. A 30 m x 0.25 mm i.d. DB-5 silica capillary column (J & W Scientific) with splitless injection was used. Spectrometer conditions were: 100 eV electron energy, 0.3 mA total emission, and an axial ion energy of 5.0 ± 0.1 eV. Spectra were recorded on a NOVA-3-mini-computer operating under INCOS software. The Kratos instrument was operated with 100 eV electron energy, 10 μA trap current and 8 keV ion translational energy. The magnet was scanned at a rate of 30 s/decade. Solutions of samples were evaporated in a disposable crucible. A direct insertion probe was used to introduce the crucible into the ionization source. A modified post-acceleration detector was operated at 15 keV, and spectra were recorded with DS-90 software.

Results and Discussion

Koopmans' theorem¹² asserts that the one-electron energy of the highest occupied orbital is reasonable approximation to the ionization potential of an atom or molecule. This implies a correspondence between the electron affinity (EA) of a molecule and the orbital energy of the lowest unoccupied molecular orbital (ϵ_{LUMO}).¹³

Previous studies¹⁴ have shown a qualitative relationship between the number and relative positions of the negative ion states and the LUMO energies calculated by CNDO and other molecular orbital procedures. As a rule, organic compounds with conjugated unsaturated systems such as aromatics possess low-lying LUMOs which may accept an electron to produce the radical anion.¹⁻³ If electronegative groups are present the electron withdrawing effect further lowers the ϵ_{LUMO} and the electron affinity becomes increasingly positive.¹⁵

We selected the CNDO method for calculations of LUMO energies since it is sufficiently simple for application to large molecules, ~100 minimal basis functions.¹⁶ Although MNDO would have been a more desirable calculation method, the MNDO version available to us was restricted to 75 minimal basis functions, and was thus limited to calculations no larger than trichlorodibenzodioxin and pentachlorodibenzofuran.

Polychlorodibenzofurans show little or no molecular radical anions for neutral congeners and isomers whose

calculated LUMO energies are above 1.6 eV (Figure VI.1). This includes mono- and dichlorodibenzofurans. A large difference is observed between 2,4-dichlorodibenzofuran which shows no $M^{\cdot-}$ and 2,4,8-trichlorodibenzofuran which yields almost 90 % $M^{\cdot-}$, despite a difference of only 0.3 eV in LUMO energies. The introduction of just one chlorine atom onto a given isomeric structure apparently causes a significant increase in the stability of the ion. All polychlorodibenzofurans tested in this study with three or more chlorines show relative $M^{\cdot-}$ abundances of >80 %. There is, however, a slight trend towards lower $M^{\cdot-}$ relative abundance for congeners whose calculated LUMO energies are below 1 eV. Thus, 1,2,4,8-tetrachlorodibenzofuran whose $\epsilon_{LUMO} = 0.95$ eV shows a maximum $M^{\cdot-}$ of about 98% relative abundance; 1,2,3,4,6,7,8-heptachlorodibenzofuran and octachlorodibenzofuran with lower ϵ_{LUMO} show 87 % and 90 % $M^{\cdot-}$, respectively.

Polychlorodibenzodioxin isomers and congeners whose calculated LUMO energies are greater than 2 eV show no $M^{\cdot-}$ (Figure VI.1). An intermediate group of compounds with $0.8 < \epsilon_{LUMO} < 1.8$ eV show a trend towards increasing $M^{\cdot-}$ relative abundance with a maximum of 95 % for 1,2,3,4,7-pentachlorodibenzodioxin. Polychlorodioxin congeners with ϵ_{LUMO} 0.8 eV showed decreasing $M^{\cdot-}$ relative abundance. Chlorines introduced into the 1,2,3,4,7-dioxin isomer caused a systematic reduction in molecular ion intensities with octachlorodioxin showing only 13 % $M^{\cdot-}$. This trend followed

the decreasing calculated ϵ_{LUMO} values.

The initial trend of increasing M^{\cdot} relative abundance can be understood in terms of increasingly positive electron affinities as chlorines are introduced. The maximum that is observed in the LUMO energy/ M^{\cdot} abundance relationship is not as readily understood. The electron affinities should continue to become more positive with further increase in the numbers of chlorine atoms, and the excess energies, resulting from introduction of the ionizing electron, should find an increasing density of vibrational states in which to be dissipated.

Using octachlorodioxin as a model, the effects of C-Cl bond length and interannular ring separation on calculated LUMO energies were tested. CNDO calculated bond lengths (C-Cl) compare well against X-ray diffraction data:³⁰ 1.64 Å and 1.715 Å, respectively. Interannular ring angle variations of 40° influence ϵ_{LUMO} by 0.2 eV. Hence, the effects of reasonable geometry variations are not sufficient to account for the changes observed in the M^{\cdot} abundance.

Since some of the input geometries used for CNDO calculations were obtained from MNDO results, the ability of MNDO to reproduce experimental geometries was also examined. Accuracy of the predicted geometries was tested using dibenzofuran. The agreement between published X-ray crystallographic data and calculated bond lengths and bond angles were better than ± 0.1 Å and $\pm 0.5^{\circ}$, respectively.

The effects of ion transmission efficiency were also probed since quadrupole mass spectrometers show a tendency to discriminate against higher masses.¹⁷ When $M^{\cdot-}$ abundances measured on a Finnigan instrument were compared to those measured on a Kratos MS50 magnetic sector instrument, there was essentially no difference in measured $M^{\cdot-}$ ion abundances.

A test for metastable ion decomposition carried out by B/E linked scanning¹⁸ showed no $[M-Cl]^{\cdot-}$ from $M^{\cdot-}$ for compounds with $\epsilon_{LUMO} > 1$ eV. However, increasing relative abundance of $[M-Cl]^{\cdot-}$ was observed from $M^{\cdot-}$ decomposition with decreasing LUMO energies. Octachlorodibenzofuran showed very little $M^{\cdot-}$ decomposition consistent with the fact that a high $M^{\cdot-}$ relative abundance was recorded for this compound. These data suggested that the barrier for $[M-Cl]^{\cdot-}$ dissociation is different for dibenzodioxin substrates than for dibenzofurans.

The results can be rationalized as a feature of the electron capture process. Upon greater chlorination, an increasing EA of the neutral yields a corresponding increase in the internal energy of $M^{\cdot-}$ available for dissociation. When the EA exceeds the dissociation energy of the molecular radical anion to form $[M-Cl]^{\cdot-}$, a new reaction channel becomes available (Figure VI.3). Thus, a decreasing $M^{\cdot-}$ concentration would then be expected with increasing EA values, as observed (Figure VI.2). It should be noted that loss of Cl^{\cdot} for form $[M-Cl]^{\cdot-}$ anion is symmetry forbidden. Simply stretching a σ bond in a π radical anion is disallowed if strict planarity

is imposed. A bent C-C-Cl bond in the transition state, with rehybridization allowing localization of an electron pair in the σ orbital as the chlorine atom departs, has been suggested previously.¹⁹ This requirement for non-planarity signifies that more than Koopmans' theorem is needed to understand fragmentation rates. An account of the perturbing effects by the captured electron would also have to involve the reorganization and correlation energies. These corrections at the CNDO level of approximation are not reliable.

Consistent with past assumptions, dissociative electron capture occurs for compounds whose LUMO energies are relatively high.²⁰ And compounds with lower LUMO energies undergo resonance electron capture and give increasing amounts of $M^{\cdot-}$ until a maximum is reached. The lower chlorinated isomers (mono- to tri-) also exhibit varying degrees of $[M-Cl]^{\cdot-}$ concentrations. Further chlorine substitution which lowers the LUMO energies do not result in high $M^{\cdot-}$ abundance as expected. This has been clearly demonstrated for polychlorodibenzodioxins. Instead, increasing amounts of metastable ion decomposition are observed and one is forced to conclude there is another high-energy channel available for dissipation of the internal energy resulting from electron capture by certain molecules. The data for polychlorodibenzofurans (Figure VI.1a) also hints at a maximum in $M^{\cdot-}$ relative abundance around 1 eV.

Acknowledgements

We gratefully acknowledge support from the National Institutes of Health, NIEHS ES00040 and NIEHS ES00210. We also wish to thank Dr Thomas Koenig (University of Oregon) for helpful discussion. Oregon Agricultural Experimental Station paper No. 8208.

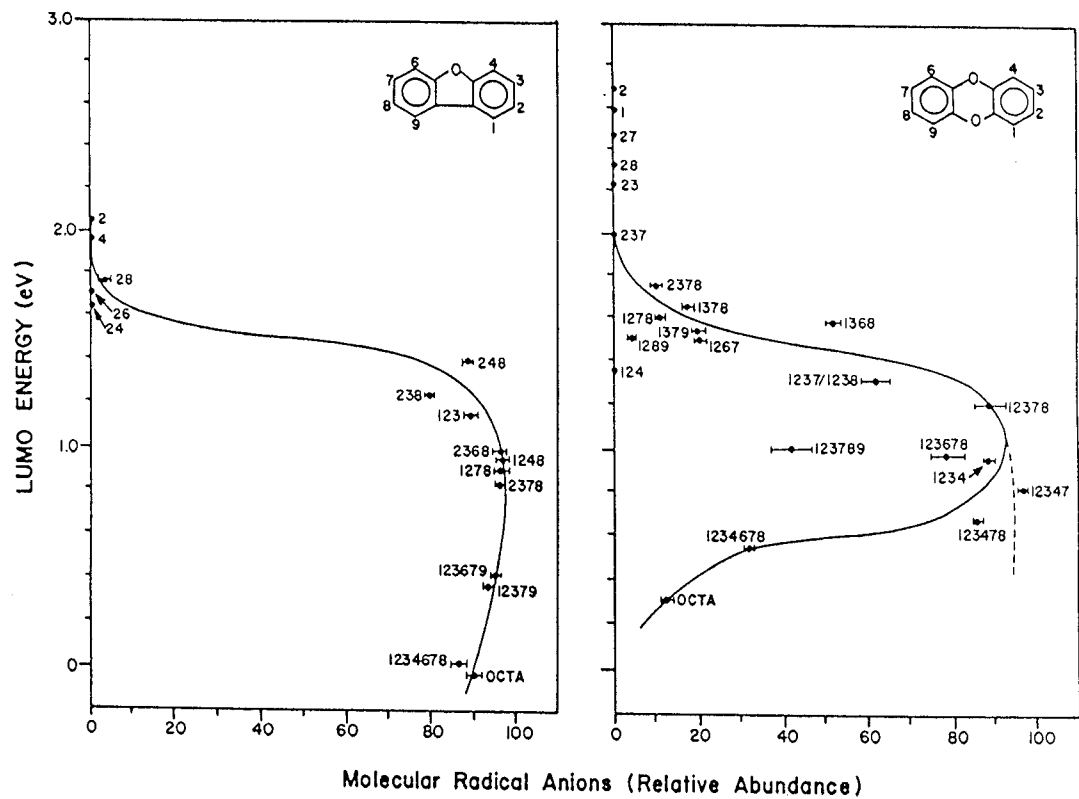


Figure VI.1. Correspondence between molecular radical anion abundance and LUMO energies for (a) PCDBFs and (b) PCDDs. 120 °C ion source temperature, helium reagent gas (0.7 mmHg). Error bars are quoted using a two standard deviation criterion.

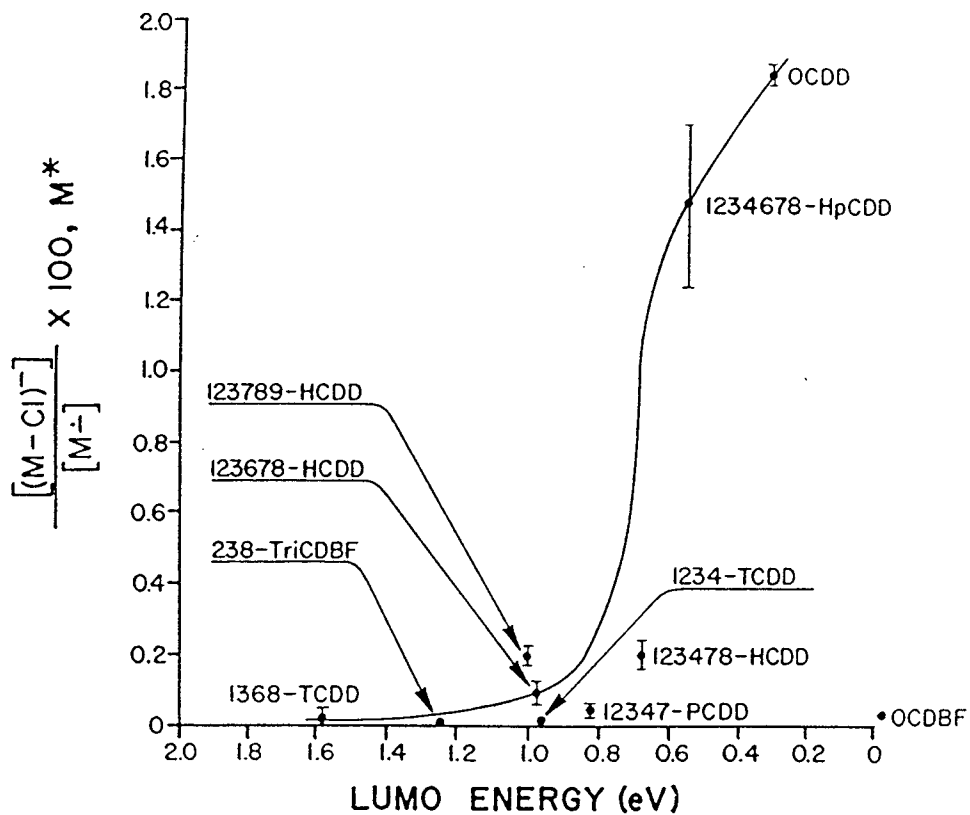


Figure VI.2. Chlorine atom loss by unimolecular dissociation of PCDD molecular radical anions versus LUMO energies of the neutral precursor.

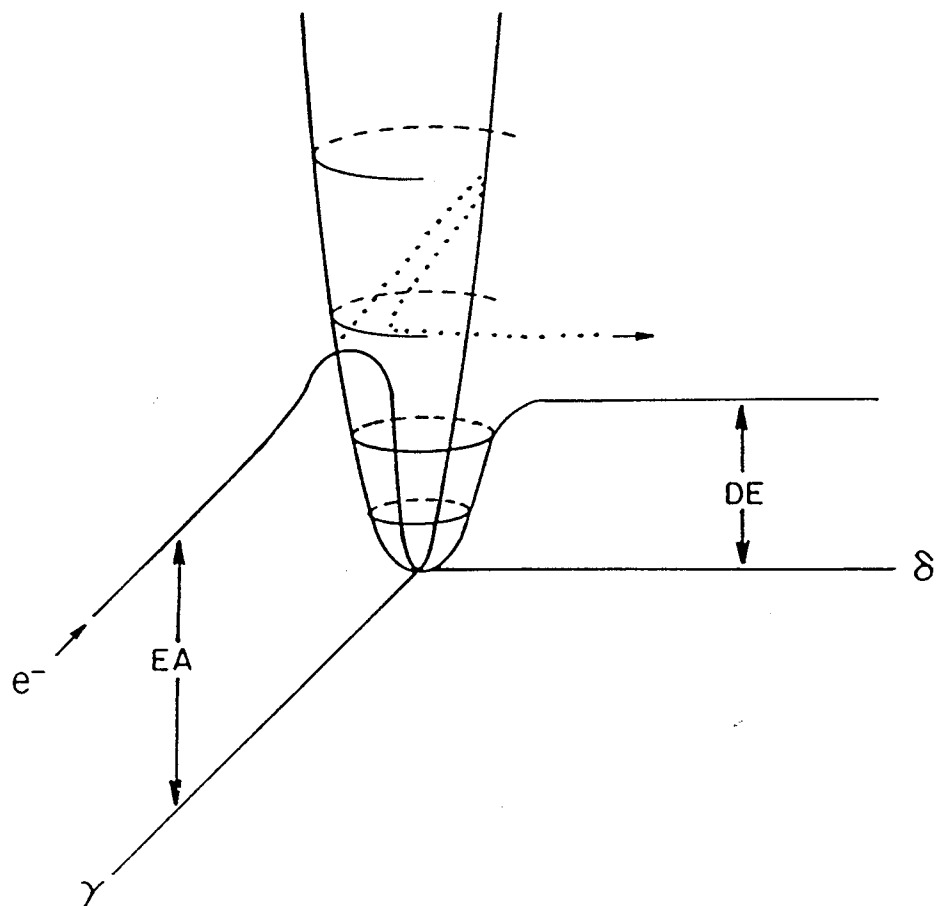


Figure VI.3. Schematic representation of the energy terms relating to the ionization, and dissociation of a chloroaromatic radical anion: EA, electron affinity of the neutral; DE, bond dissociation energy for $M^{\cdot-} \rightarrow [M-Cl]^- + Cl^{\cdot}$; γ , ionizing electron to neutral distance; δ , $[M-Cl]^-$ to Cl^{\cdot} separation.

References

1. Budzikiewicz, H. Angew. Chem. Int. Ed. Engl. 1981, 20, 624.
2. Christophorou, L.G. Atomic and Molecular Radiation Physics; Wiley-Interscience: London, 1971, Ch. 6 and 7.
3. a) Bowie, J.H. Environ. Health Perspect. 1980, 36, 89, and references therein.
b) Bowie, J.H. in Mass Spectrometry ed. Johnstone, R. A. W.; Arrowsmith: Bristol, 1979, Ch. 11.
4. (a) Christophorou, L.G.; Grant, M.W.; McCorkle, D.L. Advances in Chemical Physics; Wiley-Interscience: New York, 1977, p 413.
(b) Christophorou, L.G. Environ. Health Perspect. 1980, 36, 3.
(c) Cooper, C.D.; Naff, W.T.; Compton, R.N. J. Chem. Phys. 1975, 63, 2752.
(d) Szulejko, J.E.; Howe, I.; Benyon, J.H.; Schlunegger, U.P. Org. Mass Spectrom. 1980, 15, 263.
5. Johnson, J.P.; McCorkle, D.L.; Christophorou, L.G.; Carter, J.G. J. Chem. Soc., Faraday Trans. II 1975, 71, 1742.
6. Naff, W.T.; Cooper, C.O.; Compton, R.N. J. Chem. Phys. 1968, 49, 2784.
7. a) Pople, J.A.; Beveridge, D.L. Approximate Molecular Orbital Theory; McGraw-Hill: New York, 1970.
b) Pople, J.A.; Santry, D.P.; Segal, G.A. J. Chem. Phys. 1965, 43, S129, S136.
c) Pople, J.A.; Segal, G.A. J. Chem. Phys. 1966, 44, 3289.
8. CNDO/INDO computational package with Z-matrix program, QCMP 001.
9. a) MNDO extended version with geometry optimization, QCMP 002.
b) Dewar, M.J.S.; Thiel, W. J. Am. Chem. Soc. 1977, 99, 4899.
c) Dewar, M.J.S.; Thiel, W. J. Am. Chem. Soc. 1977, 99, 4907.
d) Dewar, M.J.S.; McKee, M.L. J. Am. Chem. Soc. 1977, 99, 5231.
e) Dewar, M.J.S.; Rzepa, H.S. J. Am. Chem. Soc. 1978, 100, 58.

10. Laramée, L.A.; Arbogast, B.C.; Deinzer, M.L. Anal. Chem. 1988, 58, 2907.
11. Dawson, P.H. Quadrupole Mass Spectrometry and Its Applications; Elsevier: Amsterdam, 1976.
12. Koopman, T. Physica 1933, 104.
13. Pople, J.A.; Beveridge, D.L. Approximate Molecular Orbital Theory; McGraw-Hill: New York, 1970.
14. a) Christophorou, L.G.; McKorkle, D.L.; Carter, J.G. J. Chem. Phys. 1974, 60, 3779.
b) Jordan, K.D.; Burrow, P.D.; Accts. Chem. Res. 1978, 11, 341.
c) Younkin, J.M.; Smith, L.J.; Compton, R.N. Theoret. Chem. Acta 1976, 41, 157.
d) Burrow, P.D.; Michejda, J.A.; Jordan, K.D. J. Am. Chem. Soc. 1976, 98, 6392.
e) Frazier, J.R.; Christophorou, L.G.; Carter, J.G.; Scheinler, H.C. J. Chem. Phys. 1978, 69, 3907.
f) Nenner, I.; Schulz, G.J.; J. Chem. Phys. 1975, 62, 1747.
g) Pisanias, M.N.; Christophorou, L.G.; Carter, J.G.; McCorkle, D.L. J. Chem. Phys. 1973, 2110.
15. Kebarle, P.; Chowdhury, S. Chem. Rev. 1987, 87, 513.
16. Pople, J.A. Acc. Chem. Res. 1970, 3, 217.
17. Dawson, P.H. Quadrupole Mass Spectrometry and Its Applications; Elsevier: Amsterdam, 1976.
18. McLafferty, F.W. Tandem Mass Spectrometry; Wiley-Interscience: New York, 1989, Ch. 9.
19. Freeman, P.K.; Srinivasa, R.; Campbell, J.-A.; Deinzer, M.L. J. Am. Chem. Soc. 1986, 108, 5531.
20. Naff, W.T.; Compton, R.N.; Cooper, C.D. J. Chem. Phys. 1971, 54, 212.

VII. THEORY AND MASS SPECTROMETRY OF REDUCTIVE
DECHLORINATION OF POLYCHLORODIBENZOFURANS UNDER
ELECTRON CAPTURE NEGATIVE ION CONDITIONS

Yoon-Seok Chang and Max L. Deinzer

Department of Chemistry
Oregon State University
Corvallis, Oregon 97331

Analytical Chemistry, submitted.

Abstract

A series of regiospecific chlorine-37 enriched di-, tri- and tetrachlorodibenzofurans were ionized under ECNI conditions. The relative abundance of chloride ion ejected from each of the positions could be determined from the chlorine-35/chlorine-37 ion ratios. The C₃-Cl bond is most reactive for almost all chlorodibenzofurans. With the AM1 method C-Cl bond stretching-energy profiles were developed for each isomer. And the C-Cl bond most likely to be cleaved could be correctly predicted by this method. The calculated heats of formation of the chlorodibenzofuran product radicals after bond dissociation, as well as the activation energies for C-Cl bond dissociation yielded qualitatively correct predictions with the bonds cleaved experimentally under ECNI conditions. But quantitative correlations with respect to the relative rates of bond cleavages and calculated intrinsic electronic properties of the molecules were not found.

Introduction

One-electron reduction of halogenated aromatic compounds by electron capture negative ion (ECNI) mass spectrometry can take place to give a radical anion which has a long lifetime ($>10^{-6}$ s).¹ The subsequent reaction of the molecular radical anion may undergo cleavage of the carbon-halogen bond to give $(M-X)^{\cdot-}$ or $X^{\cdot-}$.² More often, however, halogenated aromatics capture an electron which leads immediately to loss of a halogen atom as anion or radical. This dissociation is believed to take place in a single step, i.e., the electron transfer and bond breaking are synchronous.³ The structural differences between the parent molecules lead to a wide range in the rates of fragmentation and in the regiochemistry of bond breaking in the radical anion.

Branching ratios, $\log [(M-Cl)^{\cdot-}]/[Cl^{\cdot-}]$, of polychlorinated dibenzo-*p*-dioxins (PCDDs) under ECNI conditions have been measured and correlated with CNDO-calculated total energies of the two dissociative electron capture pathways.⁴ Similar results were observed for polychlorinated dibenzofurans (PCDBFs).⁵ Implicit in these studies is the assumption that chlorine loss from the molecule under ECNI conditions is regioselective.

With the advent of powerful computers semiempirical molecular orbital calculations have often been used to predict structures, energies and other properties of large organic

molecules and reactive species. With the help of chlorine-37 regiospecific labeled PCDBFs and these molecular orbital calculations, the regioselective dechlorination of PCDBFs have been examined in an attempt to better understand the dissociative electron capture process in ECNI mass spectrometry. The ultimate goal of this study is to investigate the qualitative relationship between the intrinsic electronic properties of PCDBFs and the observed carbon-chlorine bond cleavage under ECNI conditions.

Experimental

Molecular Orbital Calculations. Most MO calculations were performed using a newly developed AM1 (Austin Model 1) method⁶ since the AM1 method is known to be generally superior to MNDO, especially in calculations of radical species.⁷ Some calculations were carried out by MNDO (Modified Neglect of Diatomic Overlap)⁸ or CNDO (Complete Neglect of Differential Overlap)⁹ methods for comparison.

The AM1 version used in this study was adapted to a FPS (Floating Point System) super computer interfaced to a vax 11/780. The MNDO and CNDO versions were adapted to an IBM-PC and parameterized to include the second-row elements. Accelerator hardware and software (Microway, Inc.) were used to decrease the program run time. Closed-shell systems (neutrals or anions) were calculated using the RHF (Restricted Hartree-Fock) method whereas open-shell calculations (radicals or radical anions) were carried out using the UHF (Unrestricted Hartree-Fock) method.

Mass Spectrometry. Measurements were made on a Finnigan 4023 (4500 ion source) instrument employing quadrupole electric field and a Kratos MS50RF spectrometer using magnetic deflection analysis. Samples were analyzed under negative chemical ionization (NCI) conditions. Methane was used as reagent gas¹⁰ at 0.6 torr. The pressure was monitored with a

capacitive manometer attached to the ion source via a static line. Ion currents were recorded from m/z 30 through the molecular anion region. A minimum of 4 measurements were recorded on two or more different occasions. The results typically agreed to within better than $\pm 5\%$. Moreover, reproducibility checks between the Kratos and Finnigan instruments were made after a delay of 3 months, and agreement was within $\pm 10\%$.

For both instruments, a constant ionization source temperature of $120\text{ }^\circ\text{C}$ was used. Temperature measurements were made using a Pt-sensor located inside the ion source block. The temperature regulation was $\pm 3\text{ }^\circ\text{C}$ for the Finnigan instrument and $\pm 10\text{ }^\circ\text{C}$ for the Kratos spectrometer.

For a quadrupole mass spectrometer, the transmission efficiency is dependent upon the mass of the ion, axial ion energy, and the extraction potentials.¹¹ The following procedure was used throughout this study. The lens closest to the ion source was adjusted to give both a symmetric peak and a maximum ion current for m/z 35. The next lens was set to 130 eV; the final lens potential was adjusted for maximum M^- ion current. Typically the potential ratios of this symmetric lens system were 1:20:15.

Samples in acetone were admitted to the quadrupole mass spectrometer via a GC inlet. A 30 m x 0.25 mm i.d. DB-5 silica capillary column (J & W Scientific) with splitless injection was used. Spectrometer conditions were: 70 eV

electron energy, 0.3 mA total emission, and an axial ion energy of 5.0 ± 0.1 eV. Spectra were recorded on a NOVA-3-mini-computer operating under INCOS software.

The Kratos instrument was operated with 100 eV electron energy, 10 μ A trap current and 8 keV ion translational energy. The magnet was scanned at a rate of 30 s/decade. Solutions of samples were evaporated in a disposable crucible. A direct insertion probe was used to introduce the crucible into the ionization source. A modified post-acceleration detector was operated at 15 keV, and spectra were recorded with DS-90 software.

Synthesis. The chlorine-37 regiospecifically labeled PCDBFs used in this study were synthesized as described elsewhere.¹² The strategy for introducing a chlorine-37 label is to reduce a nitro derivative to the corresponding amine and converting the amine to the diazonium salt with *t*-butyl nitrite. This product is converted to the chloro derivative via the Sandmyer reaction using chlorine-37 labeled copper chloride. Typically, chlorine-37 excess at a given position was 95%.

Results

A series of regiospecific chlorine-37 enriched di-, tri- and tetrachlorodibenzofurans were ionized under ECNI conditions. The relative abundance of chloride ion ejected from each of the positions was determined from the observed $[\text{}^{35}\text{Cl}^-]/[\text{}^{37}\text{Cl}^-]$ ratios by solving the simultaneous equations,

$$\begin{array}{rclcl} ax & + & cy & = & I_a \\ bx & + & dy & = & I_b \end{array}$$

where I_a is the relative intensity of ${}^{35}\text{Cl}^-$ ion and I_b is the relative intensity of ${}^{37}\text{Cl}^-$ ion obtained from the mass spectrum. The coefficient c is the relative excess of chlorine-35 and d is the relative excess of chlorine-37 at the labeled position. In most cases the chlorine-37 enrichment achieved regiospecifically was ~95 %. In these cases c is 0.05 and d is 0.95. The value x is the fraction of chlorine loss from the unenriched position(s) and y is the fraction of chlorine loss from the position enriched with chlorine-37. Natural chlorine is assumed to have an abundance ratio $[\text{}^{35}\text{Cl}^-]:[\text{}^{37}\text{Cl}^-]$ of 3:1. Therefore, a is 0.75 and b is 0.25 for dichlorodibenzofurans, and 1.50 and 0.50 respectively for trichlorodibenzofurans. Loss of chlorine from two unlabeled positions in trichlorodibenzofurans cannot be distinguished by this method.

Results from ECNI mass spectrometry of dichlorodibenzofuran show there is no detectable chlorine-37

isotope effect¹³: 50% chloride ion comes from each of the two positions in the symmetrical isomer, 2,8(³⁷Cl)-di-CDBF (Figure VII.1). In each of the unsymmetrical isomers it is clear that loss of one of the chloride ions is preferred (Table VII.1). Position 3 (or 7) is most reactive as shown by comparison of the chloride ion losses from 2,7(³⁷Cl)- and 3(³⁷Cl),6-di-CDBFs under ECNI conditions. When both chlorines are in the same ring, the 3-position is still most reactive as shown by the results for the 2,3(³⁷Cl)- and 3(³⁷Cl),4-isomers. The 2-position is more reactive than the 1- or 6-positions as shown by analysis of 1,2(³⁷Cl)- and 2(³⁷Cl),6-di-CDBFs. However, the 1-position is very close in reactivity to the 6-position as shown by 1(³⁷Cl),6-di-CDBF.

The results from ECNI mass spectrometry of trichlorodibenzofurans show that the C₃-Cl bond (or C₇-Cl bond) generally is still most labile. Thus, 49% and 63% respectively of total chloride ion is lost from positions 3 and 7 in the 2,3(³⁷Cl),8-trichloro and 2,6,7(³⁷Cl)-trichloro isomers (Table VII.2). A slight excess of chloride ion also is lost from position 7 in the 1,4,7(³⁷Cl)-trichloro isomer. In the 2,3(³⁷Cl),4-trichloro isomer an additional steric effect¹⁴ for C₃-Cl bond cleavage might be expected. However, the mass spectrum shows there is no noticeable preference for loss of chlorine-37 from the C₃ relative to the chlorines at the C₂ and C₄ positions, suggesting that there is no significant steric relief for the chloride ion loss from the

radical anion. Rate enhancement from maximum steric relief also is not apparent from the results for the 1,2(³⁷Cl),3-isomer as the middle C-Cl bond is ruptured only 13% of the time. These results also indicate that the electronic properties of substituted molecules are altered by substitution with three adjacent chlorines.

The results from ECNI mass spectrometry of two tetrachlorodibenzofurans, 1,2,3(³⁷Cl),4- and 2,3(³⁷Cl),7,8-, show that the C₃-Cl bond also is most labile than any other bonds (Figure VII.2). Chloride ion losses from 3 positions of 1,2,3(³⁷Cl),4- and 2,3(³⁷Cl),7,8-tetra-CDBF are 35% and 37%, respectively.

Effects of pressure and temperature on the ECNI mass spectra, especially the ratio of [³⁵Cl⁻]/[³⁷Cl⁻], of PCDBFs were tested with several congeners. The sensitivity and the ratio of chloride ion vs. molecular ion vary significantly with variation in ion source pressure and temperature, but the [³⁵Cl⁻]/[³⁷Cl⁻] ratio, i.e., the relative bond cleavage rate, changes by less than 5% within the range of 0.3~1.2 torr pressure and 100~190 °C source temperature (Figure VII.3). This is within experimental error of the measurement.

Discussion

For studying the reduction mechanism of haloaromatics it is important first to establish which orbital (σ or π) receives the ionizing electron. It has been demonstrated that there is a relationship between the π -LUMO energies and the product distribution, i.e., the branching ratios of chloride and $(M-Cl)^{\cdot -}$ ions versus the molecular radical anion abundances.²

In studies of the reduction of organohalogen compounds using a simple MO method Fukui et al.¹⁵ suggested that the LUMO for conjugated organic polyhalogenated compounds might be a σ rather than a π orbital since the LUMO- σ (Lowest σ -type unoccupied MO) energy levels decrease with increasing chlorine substitution and the LUMO- π (Lowest π -type unoccupied MO) levels do not change significantly. There seems not to be a connection between the half-wave reduction potentials and the LUMO- π states, either. Beland and coworkers¹⁶ also suggested on the basis of CNDO/2 calculations that the ionizing electron is accepted in the σ -orbital of chlorobenzenes.

If electron capture is represented as the addition of an electron to a σ antibonding orbital of the molecule, then a given C-Cl bond surely would be weakened and the C-Cl bond cleavage should proceed quickly. The electron density in the antibonding orbital is localized in the C-Cl bonds. In this case there may exist meaningful correlations between the LUMO-

σ electron densities and the observed distribution of products. The electron density distribution in the LUMO- σ , calculated for the neutral chlorobenzenes, correctly predicted the major electrochemical reduction products and gave reasonable estimates of the amount of each isomer formed.¹⁶ However, these arguments are unsatisfactory when a more sophisticated MO calculation method, i.e., the MNDO method is used. MNDO calculations predict almost all chlorobenzenes to have lower LUMO- π energy states and the ionizing electron is assumed to enter the π antibonding orbital.¹⁷

The most recently described method, i.e., the AM1 method, has been used to calculate LUMO energies of PCDBFs (Table VII.3) and the question of electron localization has been examined. These results show that with increasing chlorine substitution both σ and π LUMO energies decrease but the average energy differences between LUMO- π and LUMO- σ remain about 1.8 eV. In each case the LUMO- π energy is lower and an average difference in energies of 1.8 eV between the σ and π LUMOs would indicate the ionizing electron enters the π antibonding orbital.

For PCDBFs with chlorines distributed over both aromatic rings, i.e., 2,8-, 2,3,8-, 2,3,7,8-, etc., the calculated energy differences between LUMO- π and LUMO- σ are greater than they are for 1,2-, 1,2,3-, 1,2,3,4-, etc. This suggests that the former isomers should form more stable π -electron complexes. The large relative abundance of molecular ions in

the ECNI mass spectrum of 2,8-di-CDBF (Figure VII.1) and of other isomers can be explained in part by the large energy difference between the LUMO- π and LUMO- σ . One can further show that a correlation exists between $E(\text{LUMO-}\sigma) - E(\text{LUMO-}\pi)$ and the relative molecular ion abundances for a series of trichlorodibenzofurans (Figure VII.4).

A better method to predict the orbital into which the ionizing electron enters would be to add the electron and determine what orbital is predicted to be singly occupied in the radical anion. This can be achieved by open shell calculations which give the energy of the singly occupied molecular orbital (SOMO). It is immediately obvious that the SOMO in each PCDBF is a π orbital (Table VII.3). Furthermore, the energy difference between the SOMO and σ -LUMO is much greater (~ 7.3 eV) than the energy difference between the σ -LUMO and π -LUMO in the neutral molecule (~ 1.8 eV). This indicates that the thermal electron under ECNI conditions goes into the π antibonding orbital and electron transition from π^* to σ^* is energetically unfavorable.

Since the ionizing electron is presumed to enter the π antibonding orbital of the molecule the unpaired electron distribution in the radical anion should be important to assess the relative strength of bonds and reactivities.¹⁸ The electron density in the radical anion can be estimated from MO calculations¹⁹ and verified experimentally by ESR spectroscopy²⁰. Eisch and coworkers, for example, explained

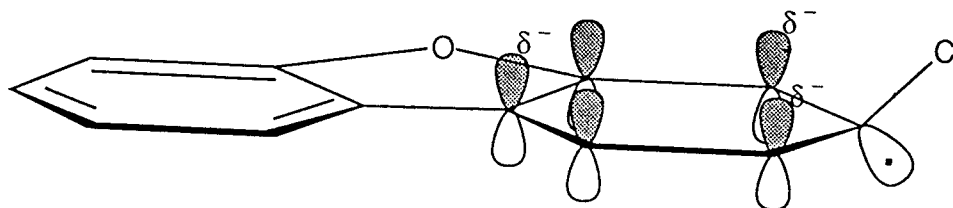
the reactivity of demethylation reactions of radical anions from dimethyl-dibenzothiophenes on the basis of the charge repulsions in the carbon-carbon bonds.²¹ The electrochemical reductive cleavage rates of carbon-halogen bonds have been correlated with the free electron density at the carbon sites of the bond breaking as estimated by simple Huckel molecular orbital calculations.²²

AM1 calculations of PCDBFs show that the electron densities in the radical anions are relatively higher at the C₃ (or C₇) position. It is clear that the calculated electron densities are generally higher at the carbon atom from which the chlorine preferentially departs under ECNI conditions. The higher reactivity of C₃-Cl (or C₇-Cl) bond cleavage can be expected on the basis that the extra electron localized at C₃ is more likely to undergo transition to the σ^* C₃-Cl orbital through a lower energy pathway. However, the correlation of the departing chlorine with electron densities is at best very rough, and it should not be expected to be better since cleavage of the C-Cl bond directly from the π^* state is a forbidden process.²³

One may examine the internal energies of the ions as the bonds stretch and finally break. The degree of progress of the bond cleavage reaction can be represented by variation of the bond length, i.e., kinetic bond stretching calculations can be used to visualize the actual bond cleavage process.²⁴ These calculations show that the process involves the transfer

of an unpaired electron from a π^* orbital of the aromatic system (ArX) to a σ^* orbital in the C-X bond and finally to a p orbital of the halogen.

Since an ionizing electron should go into the LUMOs of halogenated aromatic compounds to give a π^* state under ECNI conditions, the electron must be transferred to the σ antibonding orbital in order to break the carbon-halogen bond. Though the transition from π^* to σ^* is a forbidden process it can take place due to vibronic coupling between the π^* orbital of the aromatic ring and the π character of the σ^* orbital of the C-Cl bond.^{24b} The cleavage process itself may involve a "bent" bond²⁵ in the transition state (I).²⁶



(I)

With the AM1 UHF method the heats of formation (ΔH_f) of the PCDBFs were calculated as a function of the C-Cl bond length undergoing cleavage. Increase of the C-Cl bond distance in the radical anion of 3,6-DCDBF, for example, gives rise to a quick increase in energy in the radical anion so that it becomes unstable (Figure VII.5). At the transition

state the energy is at a maximum, at which point the high electron affinity of chlorine becomes significant and the energy of the system is reduced with departure of the chloride ion. This change appears smooth for cleavage of the C₃-Cl bond but not for cleavage of the C₆-Cl bond. The latter shows a sharp discontinuity in energy in the electron transition from π^* to σ^* at a bond distance around 2.6 Å. Initially the extra electron is fairly delocalized in the π system of the molecule, but after the transition state the electron is strongly localized in the σ orbital of the C-Cl bond.

The π^* - σ^* transition occurs earlier (~2.2 Å) as shown on the reaction coordinate diagram for the C₃-Cl bond cleavage process, and at this point the SOMO orbital is mixed with both π and σ orbital contributions. The system finally stabilizes when the C-Cl bond length has increased to around 2.9 Å and bond breaking occurs to give a dibenzofuran radical and a chloride anion. This can also be visualized from Figure VII.6 which shows the free electron density on the departing chloride ion. At the points of π^* - σ^* transition, charge density on the departing chloride ion has increased dramatically due to the high electron affinity of chlorine.²⁷

The bond stretching-energy profiles for each dichlorodibenzofuran showed that the C-Cl bond which was found to rupture more easily would have been predictable on the basis of the lower energy pathway. This is reflected in the ΔE_a values (Table VII.1). A quantitative correlation,

however, was not forthcoming. The difference in the energies for rupture of the C-Cl bonds of 1,6-, and 2,6-di-CDBFs are small as are the experimental bond cleavages for the two C-Cl bonds in each (Figure VII.7). And the large differences in the experimental C-Cl bond cleavages for the 3,6- and 3,4- isomers are also reflected in the largest activation energy differences. But in each of these cases the calculated energy differences are reversed from the experimental cleavage rates, and worse, the energy differences for C-Cl cleavages of the 2,7-, 2,3- and 1,2- isomers are smallest while the bond cleavage rate differences for these isomers are quite large.

The differences in the calculated heats of formation, H_f , of the aromatic monochlorodibenzofuran radical products also showed that the more stable radical is the one more likely to be produced under ECNI conditions. In this case the largest H_f was calculated for 3,4-di-CDBF and it was found experimentally that this compound showed the largest difference in relative C-Cl bond cleavage rates (Table VII.1). While the expected radical stabilities were consistent with the more abundant products that were observed, again it was not possible to show a correlation with the differences in the heats of formation. However, since the activation energies or heats of formation of the final products are calculated to be lower for the more reactive bond sites, the bond cleavage reactions appear to be most dependent on the stability of σ -radical anion. Other attempts to find energy terms, i.e. π_{SOMO}^-

σ_{LUMO} etc., to correlate with experimental data were not successful because of the very small calculated energy differences.

Andrieux and coworkers^{24c} suggested that the crossing point for the change in SOMO from π^* to σ^* could be the transition state for C-X bond dissociation. Thus, the rate constant for C-X bond dissociation was suggested to be a function of the energy difference between σ^* and π^* states. The results also indicate that the activation, as represented by the energy at the crossing point, is correlated with the energy of the π^* orbital. Moreno et al.^{24a,24b}, however, suggested that the rate determining step of C-X bond cleavage is dependent on the stability of the σ -radical anion instead of the π^* - σ^* electronic transition.

Unfortunately, there is no simple way to label the three positions in the trichlorodibenzofuran isomers independently and only one of the three positions in each case was labeled. However, bond-stretching energy profiles similar to that for 2,3,4-tri-CDBF (Figure VII.8), showed the energy pathway to be lowest when the labeled position was the most reactive. And in the case of the 2,3,4- isomer, the labeled 3-position yielded less than a statistical amount of chloride ion product under ECNI conditions. The energy diagram, in fact, suggests that the 2-position is the most reactive. This is also reflected in that the calculated activation energy, E_a (Table VII.2) for loss of the chloride ion at the 2-position is 29.8

kcal/mol and the activation energies for loss of chloride ion from the 3- and 4- positions are 41.0 and 44.4 kcal/mol, respectively. The C₇-Cl bond that is preferentially cleaved from both 1,4,7- and 2,6,7-tri-CDBFs was calculated to have the lowest activation energy for cleavage in each case. For the 2,3,8-isomer the chloride ion lost, i.e. the chlorine at the 3-position has a slightly higher (0.4 kcal/mol) activation energy for cleavage than does the chlorine at the 2-position. Again, for the trichlorodibenzofurans there was no apparent quantitative correlation between the chlorines that were actually lost and any intrinsic property of the molecule that could be calculated.

Two tetrachlorodibenzofurans both labeled at the 3-position also were analyzed. The symmetrical 2,3(³⁷Cl),7,8-tetra-CDBF when analyzed under ECNI conditions lost 37% chloride ion from the 3-position, while the 1,2,3(³⁷Cl),4-isomer lost only 35% from the 3-position. As already demonstrated by the 2,3(³⁷Cl),4-tri-CDBF, the regiochemistry is greatly altered by the complete substitution of one ring.

In conclusion, regiospecific chloride ion losses from various isomers of di-, tri- and tetra-chlorodibenzofurans were predictable for ECNI mass spectrometry conditions. The high reactivity of C₃-Cl bond cleavage in several cases could be explained on the basis of the relatively high π electron density on the C₃ carbon and its easier transition to the σ^* C-Cl bond. In every case the kinetic bond stretching

calculations provide good pictures for the bond cleavage processes that actually take place. Lower activation energy with smoother $\pi^*-\sigma^*$ electron transition was shown to be reflected in the higher reactivity in the bond cleavage. However, quantitative correlations between the experimental reactivities with calculated values such as electron densities, activation energies or product stabilities were not totally satisfactory. Better calculation methods such as ab initio method are needed to estimate these molecular properties.

Acknowledgement. This work is supported by the National Institutes of Health (NIEHS ES00210 and NIEHS ES00040). This paper is issued as technical paper No. 9251 from the Oregon Agricultural Experimental Station.

Table VII.1. Relative bond cleavage rates, calculated electron densities and energy differences of chlorine-37 labeled di-CDBFs.

Di-DBFs	Bond cleavage ^a	electron density ^b	H_f (M-Cl) ^c	E_a ^d	
2,8(³⁷ Cl)-	C ₂ /C ₈	1.00	1.00	(C ₂ -C ₈) 0.00	0.0
1(³⁷ Cl),6-	C ₁ /C ₆	1.04	1.20	(C ₆ -C ₁) 1.42	7.0
2(³⁷ Cl),6-	C ₂ /C ₆	1.13	1.00	(C ₆ -C ₂) 2.52	3.1
3(³⁷ Cl),6-	C ₃ /C ₆	1.86	1.60	(C ₆ -C ₃) 2.61	38.4
2,7(³⁷ Cl)-	C ₇ /C ₂	1.33	1.60	(C ₂ -C ₇) 1.10	1.7
3(³⁷ Cl),4-	C ₃ /C ₄	4.56	1.50	(C ₄ -C ₃) 2.77	13.9
2,3(³⁷ Cl)-	C ₃ /C ₂	1.38	2.00	(C ₂ -C ₃) 0.17	1.5
1,2(³⁷ Cl)-	C ₂ /C ₁	1.56	1.29	(C ₁ -C ₂) 1.28	2.4

^a Ratio of bond cleavage rates of the two C-Cl bonds under ECNI condition (methane, 0.6 torr, 120 °C).

^b Ratio of π electron densities on the two C-Cl bonds in radical anion, calculated by AM1 method.

^c Difference of calculated heats of formation (kcal/mol) of two (M-Cl).

^d Difference of calculated activation energies (kcal/mol) in two C-Cl bond cleavage processes.

Table VII.2. Relative bond cleavage rates and calculated electron densities of chlorine-37 labeled tri-CDBFs.

TrCDBFs	e ⁻ Density ^a	Cl-37 Loss ^b	Ea ^c
1,2(³⁷ Cl),3-	0.08	0.39	C ₁ 35.5 C ₂ 38.9 C ₃ 25.4
2,3(³⁷ Cl),4-	0.55	0.93	C ₂ 29.8 C ₃ 41.0 C ₄ 44.4
2,3,7(³⁷ Cl)-	0.42	0.87	C ₂ 26.1 C ₃ 25.0 C ₇ 39.5
2,3(³⁷ Cl),8-	0.64	1.47	C ₂ 25.5 C ₃ 25.9 C ₈ 38.2
1,4,7(³⁷ Cl)-	0.39	1.11	C ₁ 77.8 C ₄ 64.5 C ₇ 29.3
2,6,7(³⁷ Cl)-	0.52	1.89	C ₂ 65.0 C ₆ 68.8 C ₇ 29.1

^a Fraction of electron density on carbon bearing chlorine-37 relative to all carbons bearing chlorine, calculated by the AM1 method.

^b Relative rate (normalized) of chlorine-37 loss under ECNI conditions (methane, 0.6 torr, 120 °C). The value 1 is 33.3% loss of chlorine.

^c Calculated activation energies (kcal/mol) for each C_a-Cl bond cleavage.

Table VII.3. Calculated LUMO energies of PCDBFs (AM1 method).

PCDBFs	Neutral (eV)			Radical Anion (eV)	
	LUMO- π	LUMO- σ	$\epsilon(\pi-\sigma)^a$	SOMO(π)	LUMO- σ
DBF	-0.4065	2.1410	2.5475	-1.7721	6.6708
1	-0.6029	1.1891	1.7920	-2.0269	5.4353
2	-0.5997	1.2624	1.8621	-2.0640	5.2572
3	-0.6488	1.1422	1.7910	-2.0725	5.1480
4	-0.5877	1.2831	1.8708	-2.0285	5.3909
1,2	-0.7655	0.9370	1.7025	-2.2902	5.0353
1,6	-0.7608	1.0787	1.8395	-2.2572	5.1306
2,3	-0.8158	0.9332	1.7490	-2.3208	4.9376
2,6	-0.7606	1.1304	1.8910	-2.2831	5.0164
2,7	-0.8285	1.0260	1.8545	-2.3265	4.8661
2,8	-0.7875	1.1577	1.9452	-2.3189	5.0201
3,4	-0.8070	0.9241	1.7311	-2.2912	5.0066
3,6	-0.8121	1.0394	1.8515	-2.2922	4.8778
1,2,3	-0.9739	0.5883	1.5622	-2.5445	4.6474
1,4,7	-0.9918	0.8435	1.8353	-2.5161	4.6253
2,3,4	-0.9687	0.6670	1.6357	-2.5352	4.7386
2,3,7	-1.0246	0.8097	1.8343	-2.5520	4.5704
2,3,8	-0.9852	0.8300	1.8152	-2.5468	4.6917
2,6,7	-0.9748	0.8104	1.7852	-2.5228	4.7206
1,2,3,4	-1.1362	0.4589	1.5951	-2.7620	4.5319
2,3,7,8	-1.1693	0.7022	1.8715	-2.7535	4.4055
1,2,3,4,6	-1.2646	0.3830	1.6476	-2.9180	4.3489
2,3,4,7,8	-1.3007	0.4878	1.7885	-2.9357	4.2194
1,2,3,4,6,7	-1.4222	0.2998	1.7220	-3.0841	4.0478
1,2,3,4,6,7,8	-1.5527	0.2319	1.7846	-3.2489	3.8899
OCDBF	-1.6459	0.2072	1.8531	-3.3952	3.7585

^a E(LUMO- σ) - E(LUMO- π) (eV).

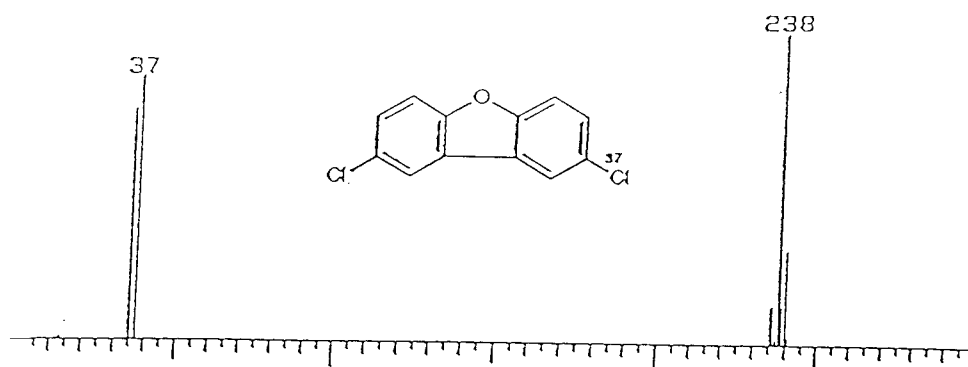


Figure VII.1. ECNI mass spectrum of 2,8(^{37}Cl)-di-CDBF (methane, 0.6 torr, 120 °C).

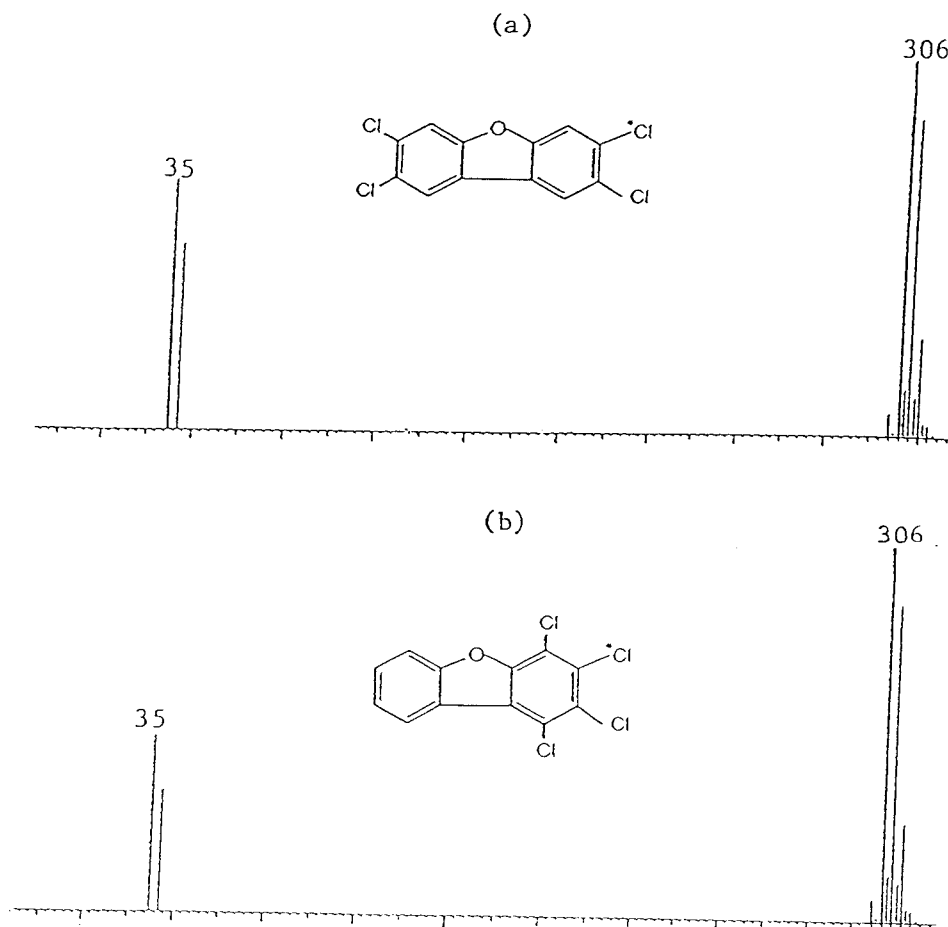


Figure VII.2. ECNI mass spectra of 2,3(^{37}Cl),7,8- (a) and 1,2,3(^{37}Cl),4-tetra-CDBF (b) (methane, 0.6 torr, 190 °C).

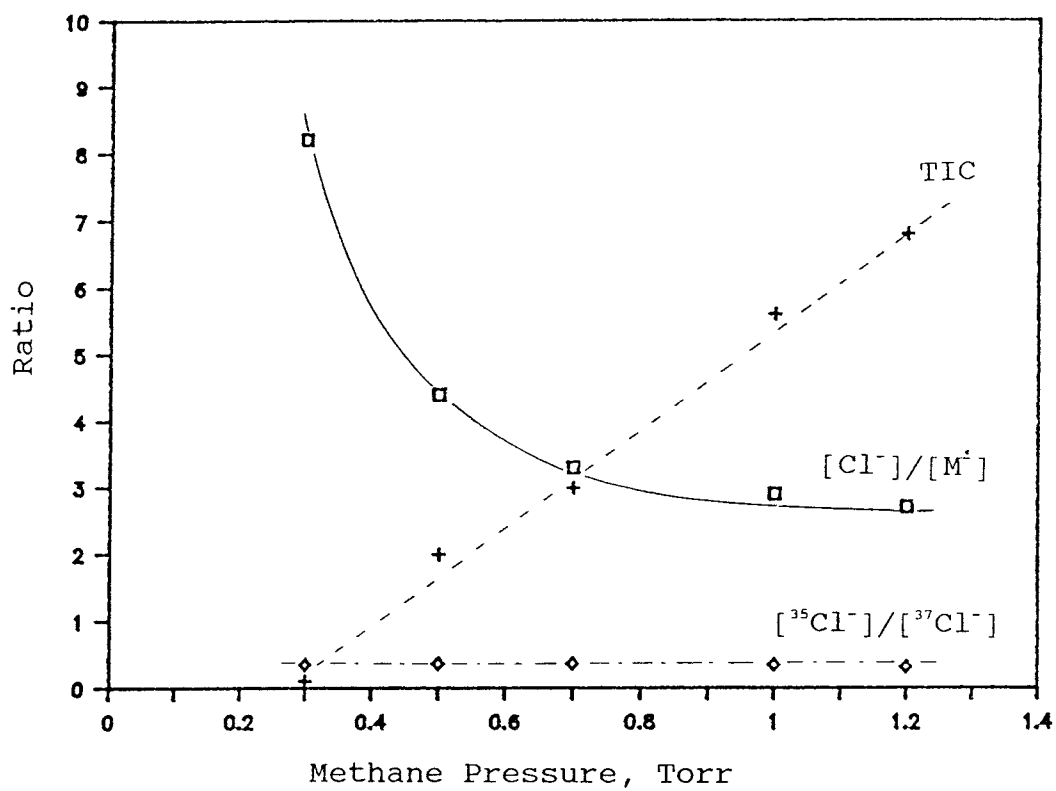


Figure VII.3. Source pressure effects on ECNI spectrum of $3(^{37}Cl),4\text{-di-CDBF}$ (methane, 120°C). TIC is arbitrary scale.

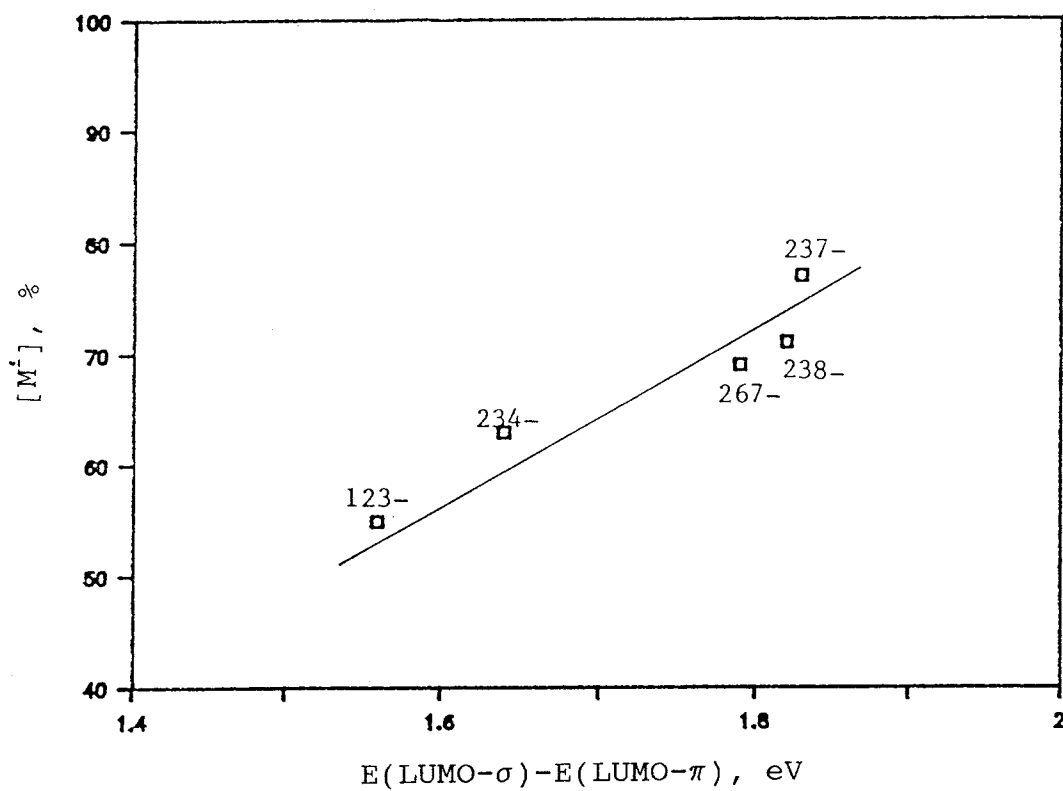


Figure VII.4. Molecular ion abundances of tri-CDBFs vs. energy differences between LUMO- π and LUMO- σ .

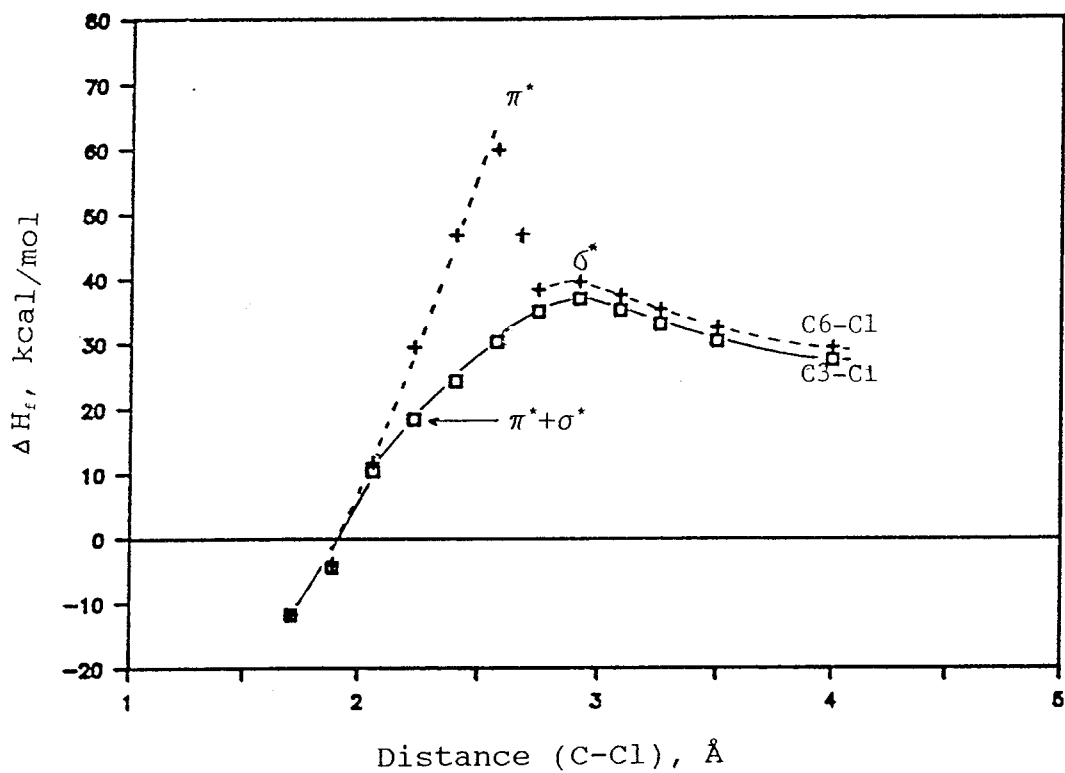


Figure VII.5. Calculated energies of 3,6-di-CDBF radical anion vs. C-Cl bond lengths.

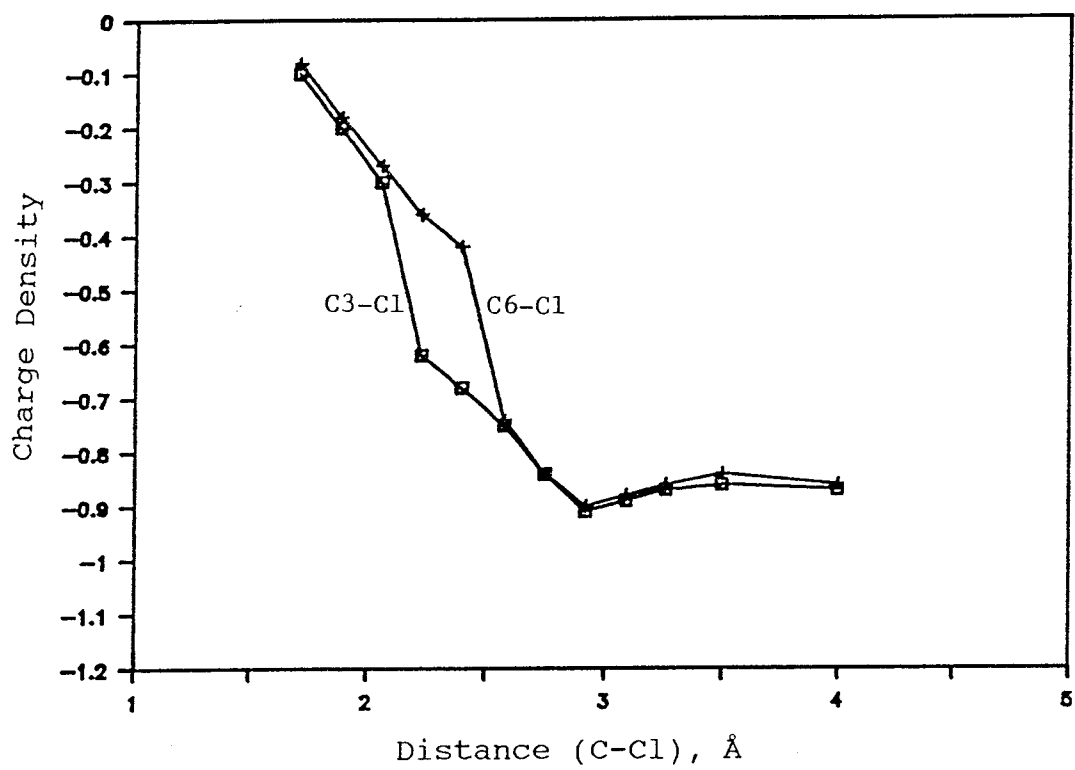


Figure VII.6. Free electron densities on departing chlorine from 3,6-di-CDBF radical anion.

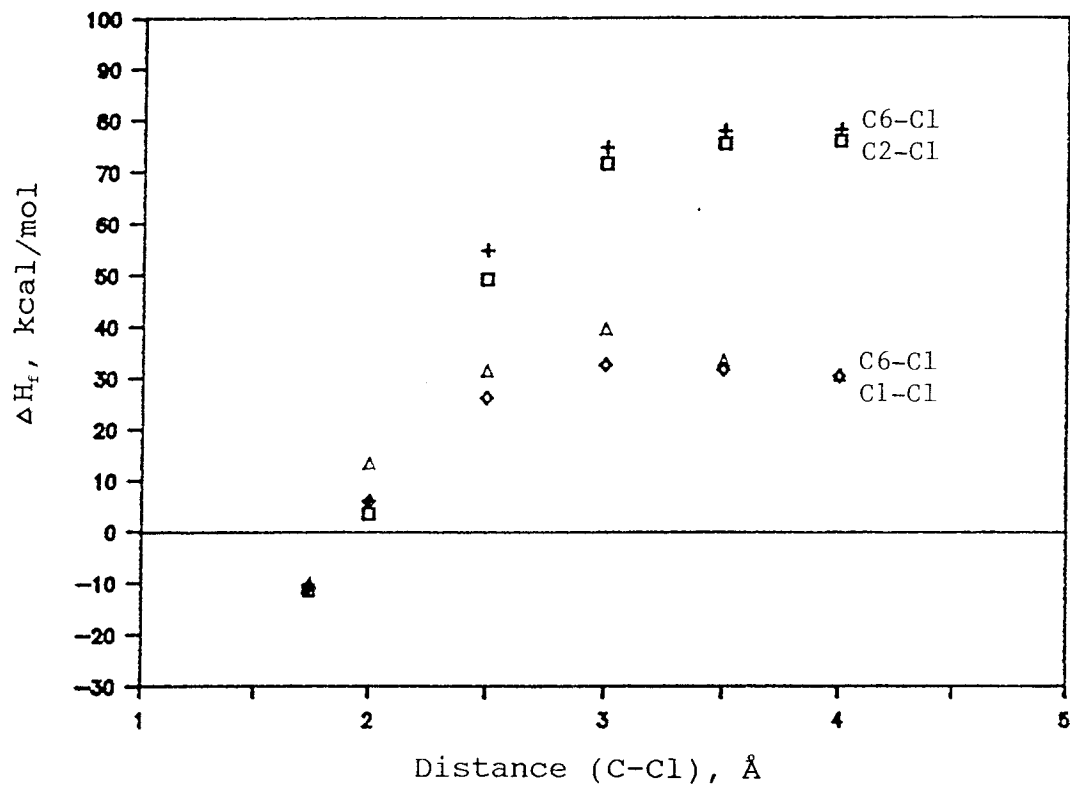


Figure VII.7. Calculated energies of 1,6- and 2,6-di-CDBF radical anions vs. C-Cl bond lengths.

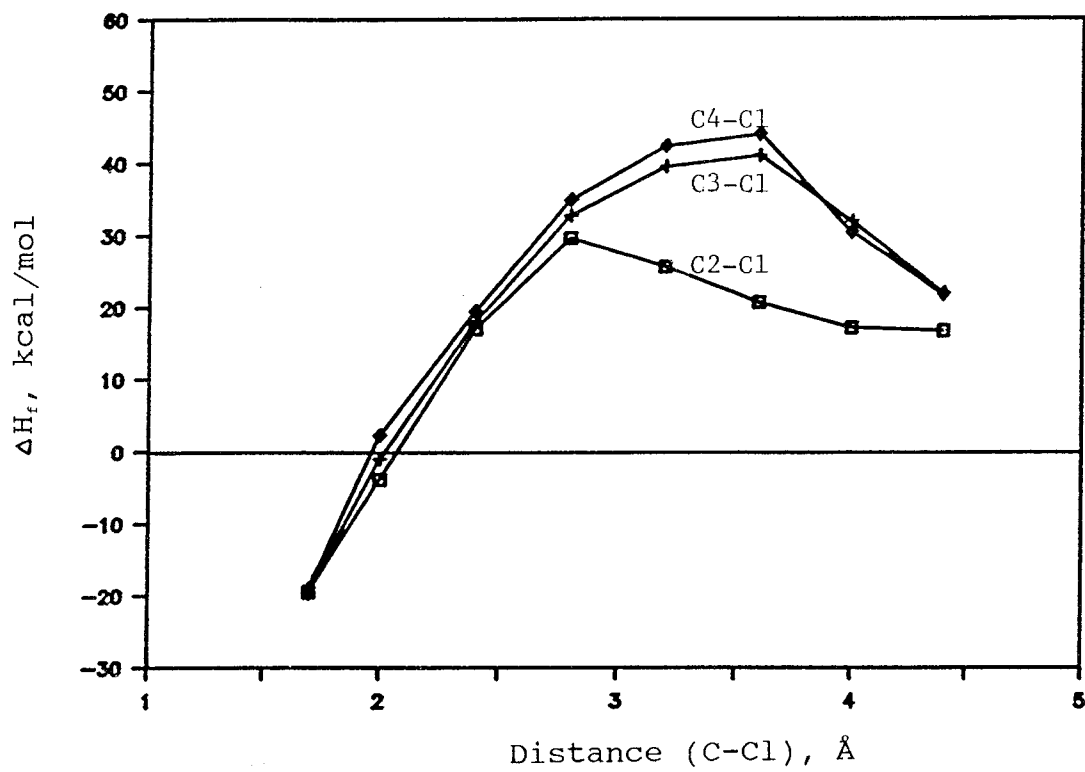


Figure VII.8. Calculated energies of 2,3,4-tri-CDBF radical anion vs. C-Cl bond lengths.

References

1. Johnson, J.P.; McCorkle, D.L.; Christophorou, L.G.; Carter, J.G. J. Chem. Soc., Faraday Trans. II 1975, 71, 1742.
2. Larameé, J.A.; Chang, Y-S.; Arbogast, B.C.; Deinzer, M.L. Biomed. Environ. Mass Spectrom. 1988, 17, 63.
3. Naff, W.T.; Cooper, C.O.; Compton, R.N. J. Chem. Phys. 1968, 49, 2784.
4. Laramee, J.A.; Arbogast, B.C.; Deinzer, M.L. Anal. Chem. 1988, 60, 1937.
5. Unpublished work.
6. Dewar, M.J.S.; Zoebisch, E.G.; Healy, E.F.; Stewart, J.J. J. Am. Chem. Soc. 1985, 107, 3902.
7. Dewar, M.J.S.; Rzepa, H.S. J. Am. Chem. Soc. 1978, 100, 784.
8. (a) Dewar, M.J.S.; Thiel, W. J. Am. Chem. Soc. 1977, 99, 4899.
(b) Dewar, M.J.S.; Thiel, W. J. Am. Chem. Soc. 1977, 99, 4907.
(c) Dewar, M.J.S.; McKee, M.L. J. Am. Chem. Soc. 1977, 99, 5231.
(d) Dewar, M.J.S.; Rzepa, H.S. J. Am. Chem. Soc. 1978, 100, 58.
9. (a) Pople, J.A.; Beveridge, D.L. Approximate Molecular Orbital Theory; McGraw-Hill: New York, 1970.
(b) Pople, J.A.; Santry, D.P.; Segal, G.A. J. Chem. Phys. 1965, 43, S 129, S 136.
(c) Pople, J.A.; Segal, G.A. J. Chem. Phys. 1966, 44, 3289.
10. Laramee, J.A.; Arbogast, B.C.; Deinzer, M.L. Anal. Chem. 1988, 58, 2907.
11. Dawson, P.H. Quadrupole Mass Spectrometry and Its Applications; Elsevier: Amsterdam, 1976.
12. Chang, Y-S.; Deinzer, M.L. J. Labelled Compd. Radiopharm. in press.
13. Zakett, D.; Flynn, R.G.A.; Cooks, R.G. J. Phys. Chem. 1978, 82, 2359.

14. Mazer, T.; Hileman, F.D. Chemosphere 1982, 11, 161.
15. Fukui, K.; Morokuma, K.; Kato, H.; Yonezawa, T. Bull. Chem. Soc. Jap. 1963, 36, 47.
16. Beland, F.A.; Farwell, B.S.O.; Callis, P.R.; Geer, R.D. J. Electroanal. Chem. 1977, 78, 145.
17. Glidewell, C. Chemica Scripta 1985, 20, 142.
18. Levine, I.N. Quantum Chemistry; Allyn and Bacon, Inc.: Boston, 1983, p 483.
19. Clark, T. A Hand Book of Computational Chemistry; Wiley Interscience: New York, 1985, p 162.
20. Bowers, K.W. In Radical Ions; Kaiser, E.T.; Kevan, L., Ed.; Wiley Interscience: New York, 1968, p 232.
21. Eisch, J.J.; Hallenbeck, L.E.; Han, K.I. J. Am. Chem. Soc. 1986, 108, 7763.
22. (a) Alwair, K.; Grimshaw, J. J. Chem. Soc. Perkin Trans. II 1973, 1150.
(b) Alwair, K.; Grimshaw, J. J. Chem. Soc. Perkin Trans. II 1973, 1811.
(c) Grimshaw, J.; Trocha-Grimshaw, J. J. Electroanal. Chem. 1974, 56, 443.
(d) Gores, G.; Koeppe, C.E.; Bartak, D.E. J. Org. Chem. 1979, 44, 380.
23. Amatore, C.; Oturan, M.A.; Pinson, J.; Savéant, J.M.; Thiébault, A. J. Am. Chem. Soc. 1985, 107, 3451.
24. (a) Moreno, M.; Gallardo, I.; Bertran, J. J. Chem. Soc. Perkin Trans. II 1989, 2017
(b) Casado, J.; Gallardo, I.; Moreno, M. J. Electroanal. Chem. 1987, 219, 197.
(c) Andrieux, C.P.; Saveant, J.M.; Su, K.B. J. Phys. Chem. 1986, 90, 3815.
(d) Aalstad, B.; Parker, V.D. Acta Chem. Scand., Ser. B 1982, B36, 47.
(e) Parker, V.D. Acta Chem. Scand., Ser. B 1981, B35, 595.
25. Streiweiser, A.; Mares, F.; J. Am. Chem. Soc. 1968, 90, 2444.
26. Freeman, P.K.; Srinivasa, R.; Campbell, J.-A.; Deinzer, M.L. J. Am. Chem. Soc. 1986, 108, 5531.

27. Olthoff, J.K.; Tossell, J.A.; Moore, J.H. J. Chem. Phys. 1985, 83, 5637.

VIII. BIBLIOGRAPHY

- Alstad, B.; Parker, V.D. Acta Chem. Scand., Ser. B 1982, B36, 47.
- Akermark, B.; Ebersson, L; Jonsson, E.; Peterson, E. J. Org. Chem. 1975, 40, 1365.
- Alwair, K.; Grimshaw, J. J. Chem. Soc., Perkin Trans. II 1973, 1150.
- Alwair, K.; Grimshaw, J. J. Chem. Soc., Perkin Trans. II 1973, 1811.
- Amatore, C.; Oturan, M.A.; Pinson, J.; Saveant, J.M.; Thiebault, A. J. Am. Chem. Soc. 1985, 107, 3451.
- Andrieux, C.P.; Saveant, J.M.; Su, K.B. J. Phys. Chem. 1986, 90, 3815.
- Bartmess, J.E. Mass Spectrom. Rev. 1989, 8, 297.
- Beland, F.A.; Farwell, B.S.O.; Callis, P.R.; Geer, R.D. J. Electroanal. Chem. 1977, 78, 145.
- Bell, R.A.; Gara, A. Chlorinated Dioxins and Dibenzofurans in Total Environment; Butterworth-Ann Arbor Science: Boston, 1983.
- Benkovic, S.J.; Benkovic, P.A.; Comfort, D.R. J. Am. Chem. Soc. 1969, 91, 1860.
- Bowers, K.W. Radical Ions; Kaiser, E.T.; Kevan, L., Ed.; Wiley-Interscience: New York, 1968, p 232.
- Bowie, J.H. Mass spectrometry; Johnstone, R.A.W., Ed.;

- Arrowsmith: Bristol, 1979, Ch. 11.
- Bowie, J.H. Environ. Health Prospect. 1980, 36, 89.
- Brown, G.S. The Chemistry of the Hydroxyl Group; Partai, S., Ed.; Wiley-Interscience: New York, 1971, p 593.
- Budzikiewicz, H. Angew. Chem. Int. Ed. Engl. 1981, 20, 624.
- Budzikiewicz, H. Mass Spectrom. Rev. 1986, 5, 345.
- Budzikiewicz, H. Org. Mass Spectrom. 1988, 23, 561.
- Burrow, P.D.; Michejda, J.A.; Jordan, K.D. J. Am. Chem. Soc. 1976, 98, 6392.
- Burse, M.M.; McLafferty, F.W. J. Am. Chem. Soc. 1966, 88, 529.
- Buser, H.R. Doctoral Dissertation 1978, University of Umea, Sweden.
- Buser, H.R.; Bosshardt, H.-P.; Rappe, C. Chemosphere 1978, 7, 109.
- Buser, H.R.; Rappe, C. Chemosphere 1979, 8, 157.
- Buser, H.R. J. Chromatog. 1976, 129, 303.
- Cadogan, J.I.G.; Molina, G.A. J. Chem. Soc. Perkin Trans. I. 1973, 541.
- Casado, J.; Gallardo, I.; Moreno, M. J. Electroanal. Chem. 1987, 219, 197.
- Chae, K.; Cho, L.K.; McKinney, J.D. J. Agric. Food Chem. 1977, 25, 1207.
- Chang, Y-S.; Jang, J-S.; Deinzer, M.L. Tetrahedron in press.
- Chang, Y-S.; Deinzer, M.L. Synth. Commun. in Press.
- Choudhry, G. F.; Sundstrom, G.; Wielen, R.W.M.; Hutzinger, H.

- Chemosphere 1977, 6, 327.
- Chow, Y.L.; Danen, W.C.; Nelson, S.F.; Rosenblatt, D.H. Chem. Rev. 1978, 78, 243.
- Christophorou, L.G.; Grant, M.W.; McCorkle, D.L. Advances in Chemical Physics; Wiley: New York, 1977, p 413.
- Christophorou, L.G.; McCorkle, D.L.; Carter, J.G. J. Chem. Phys. 1974, 60, 3779.
- Christophorou, L.G.; Grant, M.W. Advances in Chemical Physics; Wiley: New York; 1977, Vol. 36.
- Christophorou, L.G. Electron-Molecule Interactions and Their Applications; Academic Press: Orlando, 1984, p 477.
- Christophorou, L.G. Environ. Health Prospect. 1980, 36, 3.
- Christophorou, L.G. Adv. Electron. Phys. 1978, 46, 55.
- Christophorou, L.G. EHP, Environ. Health Prospect. 1980, 36, 3.
- Christophouou, L.G. Atomic and Molecular Radiation Physics; Wiely: London, 1971, Ch. 6 and 7.
- Clark, D.T.; Murrell, J.N.; Tedder, J.M. J. Am. Chem. Soc. 1963, 1250.
- Clark, T. A Handbook of Computational Chemistry; Wiley: New York, 1985, Ch. 3.
- Cooper, C.D.; Naff, W.T.; Compton, R.N. J. Chem. Phys. 1975, 63, 2752.
- Dawson, P.H. Quadrupole Mass Spectrometry and Its Applications; Elesevier: Amsterdam, 1976.
- de la Mare, P.B.D.; Hall, D. J. Chem. Soc., Perkin Trans. II

- 1977, 106.
- Dawson, P.H. Quadrupole Mass Spectrometry and Its Applications; Elsevier: Amsterdam, 1976.
- de Schryver, F.C.; Beans, N. Adv. Photochem. 1977, 10, 359.
- Deinzer, M.; Griffin, D.; Miller, T.; Lamberton, J.; Freeman, F.; Jonas, V. Biomed. Mass Spectrom. 1982, 9, 85.
- Dennivelle, L.; Fort, R.; Van Hai, P. Bull. Soc. Chim. Fr. 1960, 1538.
- Dewar, M.J.S.; Thiel, W. J. Am. Chem. Soc. 1977, 99, 4907.
- Dewar, M.J.S.; Zoebisch, E.G.; Healy, E.F.; Stewart, J.J. J. Am. Chem. Soc. 1985, 107, 3902.
- Dewar, M.J.S.; Thiel, W. J. Am. Chem. Soc. 1977, 99, 4899.
- Dewar, M.J.S.; Rzepa, H.S. J. Am. Chem. Soc. 1978, 100, 784.
- Dewar, M.J.S.; Rzepa, H.S. J. Am. Chem. Soc. 1978, 100, 58.
- Dewar, M.J.S.; McKee, M.L. J. Am. Chem. Soc. 1977, 99, 5231.
- Dickerman, S.C.; Weiss, K.; Ingberman, A.K. J. Org. Chem. 1956, 21, 380.
- Dickerman, S.C.; DeSouza, D.J.; Jacobson, N. J. Org. Chem. 1969, 34, 710.
- Dougherty, R.C. Nature 1981, 292, 524.
- Dougherty, R.C. Anal. Chem. 1981, 53, 625 A.
- Doyle, M.P.; Siegfried, B.S.; Dellaria, J.F. J. Org. Chem. 1977, 42, 2426.
- Dunn III, W.J.; Koehler, M.; Stalling, D.L.; Schwartz, T. R. Anal. Chem. 1986, 58, 1835.
- Edlund, U.; Norstrom, A. Org. Magn. Reson. 1977, 9, 196.

- Eisch, J.J.; Hallenbeck, L.E.; Han, K.I. J. Am. Chem. Soc. 1968, 108, 7763.
- Engelsma, J.W.; Kooljman, E.C. Rec. Trav. Chim. 1961, 80, 526.
- Feurst, P.; Meemken, H.-A.; Grobel, W. Chemosphere 1986, 10, 381.
- Floodchart, B.D.; Swsay, I.M.; Pink, R.C. J. Chem. Soc., Chem. Commun. 1980, 439.
- Frazier, J.R.; Christophorou, L.G.; Carter, J.G.; Scheinler, H.C. J. Chem. Phys. 1978, 69, 3907.
- Freeman, P.K.; Jonas, V. J. Agric. Food Chem. 1984, 32, 1307.
- Freeman, P.K.; Srinivasa, R. J. Agric. Food Chem. 1983, 31, 775.
- Freeman, P.K.; Srinivasa, R.; Campbell, J.-A.; Deinzer, M.L. J. Am. Chem. Soc. 1986, 108, 5531.
- Fukui, K.; Morokuma, K.; Kato, H.; Yonezawa, T. Bull. Chem. Soc. Jap. 1963, 36, 47.
- Furniss, B.S.; Hanaford, A.J.; Rogers, V.; Smith, P.W.G.; Galli, C. J. Chem. Soc., Perkin Trans. II 1982, 1139.
- Gara, A.; Andersson, K.; Nilsson, C.-A.; Norstrom, A. Chemosphere 1981, 10, 365.
- Gerdil, R.; Lucken, E.A.C. J. Am. Chem. Soc. 1965, 87, 213.
- Gores, G. Koeppe, C.E.; Bartak, D.E. J. Org. Chem. 1979, 44, 380.
- Grabowski, Z.R.; Dobkowski, J. J. Pure Appl. Chem. 1983, 55, 245.
- Grey, A.P.; Cepa, S.P.; Solomon, I.J.; Aniline, O. J. Org.

- Chem. 1976, 41, 2435.
- Grey, A.P.; Dipinto, J.J.; Solomon, I.J. J. Org. Chem. 1976, 41, 2428.
- Grimshaw, J.; Trocha-Grimshaw, J. J. Electroanal. Chem. 1974, 56, 443.
- Hameka, H.F. J. Org. Chem. 1987, 52, 5025.
- Hansson, M. In Chlorinated Dioxins and Dibenzofurans in the Total Environment, Keith, L.H.; Rappe, C.; Choudhary, G., Eds.; Butterworth: Woburn, 1983.
- Harrison, A.G. Chemical Ionization Mass Spectrometry; CRC Press: Boca Raton, 1983, p 22.
- Hileman, F.D.; Hale, M.D.; Mazer, T.; Noble, R.W. Chemosphere 1985, 14, 601.
- Humpfi, T. Chemosphere 1986, 15, 2003.
- Hutzinger, O.; Jamieson, W.D.J.; Safe, S.; Zitko, V.Z. J. Assoc. Off. Anal. Chem. 1973, 56, 982.
- Hutzinger, O.; Frei, R.W.; Meriam, E.; Pocciari, F., Eds. Chlorinate Dioxins and Related Compounds; Pergamon Press: New York, 1982.
- Ide, R.; Sakata, Y.; Misumi, S.; Okada, T.; Mataga, N. J. Chem. Soc., Chem. Commun. 1972, 1009.
- Johnson, J.P.; McCokle, D.L.; Christophorou, L.G.; Carter, J.G. J. Chem. Soc., Faraday Trans. II 1975, 71, 1742.
- Jordan, K.D.; Burrow, P.D. Accts. Chem. Res. 1978, 11, 341.
- Kavarnos, G.J.; Turro, N.J. Chem. Rev. 1986, 86, 401.
- Kebarle, P.; Chowdhury, S. Chem. Rev. 1987, 87, 513.

- Keith, L.H.; Rappe, C.; Choudhary, G. Chlorinated Dioxins and Dibenzofurans in the Total Environments I and II; Ann Arbor Science: Butterworth, 1985.
- Kodomari, K.; Satoh, H.; Yoshitomi, S. Nippon Kagaku Kaishi **1986**, 1813.
- Kolonko, K.J.; Deinzer, M.L.; Miller, T.L. Synthesis **1984**, *2*, 133.
- Koopman, T. Physica **1933**, 104.
- Kooyman, E.C. Halogenation of Aromatic Compound In Advances in Radical Chemistry; Vol 1; Logos: London, 1965, p 151.
- Lamparski, L.L.; Nesterick, T.J. Anal. Chem. **1982**, *54*, 402.
- Laramee, J.A.; Arbogast, B.C.; Deinzer, M.L. Anal. Chem. **1988**, *60*, 1937.
- Laramee, J.A.; Chang, Y.-S.; Arbogast, B.C.; Deinzer, M.L. Biomed. Environ. Mass Spectrom. **1988**, *17*, 63.
- Laramee, J.A.; Arbogast, B.C.; Deinzer, M.L. Anal. Chem. **1986**, *58*, 2907.
- Levine, I.N. Quantum Chemistry; Allyn and Bacon Inc.: Boston, 1983, pp 483-486.
- Lindahl, R.; Rappe, C.; Buser, H.R. Chemosphere **1980**, *9*, 351.
- March, J. Advanced Organic Chemistry; Wiley Interscience: New York, 1985, p 477.
- Marklund S.; Rappe, C.; Tysklind, M.; Egeback, K.-E.; Chemosphere **1986**, *10*, 355.
- Mazer, T.; Hileman, F.D. Chemosphere **1982**, *11*, 651.
- Mazer, T.; Hileman, F.; Noble, R.W.; Brooks, J.J. Anal. Chem.

- 1983, 55, 104.
- McLafferty, F.W.; Wachs, T.; Lifshitz, C.; Innorta, G.;
Irving, P. J. Am. Chem. Soc. 1972, 92, 6867.
- McLafferty, F.W.; Wachs, T. J. Am. Chem. Soc. 1968, 89, 5043.
- McLafferty, F.W. Tandem Mass Spectrometry; Wiley-Interscience:
New York, 1987, Ch. 9.
- McLafferty, F.W.; Bursey, M.M. J. Org. Chem. 1968, 33, 124.
- McLafferty, F.W. Anal. Chem. 1959, 31, 447.
- Meerwein, H.; Buchner, E.; van Emster, K. J. Prakt. Chem.
1939, 152, 237.
- Moreno, M.; Gallardo, I.; Bertran, J. J. Chem. Soc., Perkin
Trans. II 1989, 2017.
- Morita, M.; Nakagawa, J.; Rappe, C. Bull. Env. Contam.
Toxicol. 1978, 19, 665.
- Murov, S.L. Handbook of Photochemistry; Marcel Dekker Inc.:
New York, 1973.
- Naff, W.T.; Cooper, C.O.; Compton, R.N. J. Chem. Phys. 1968,
49, 2784.
- Naff, W.T.; Compton, R.N.; Cooper, C.D. J. Chem. Phys. 1971,
54, 212.
- Nenner, I.; Schulz, G.J. J. Chem. Phys. 1975, 62, 1747.
- Norstrom, A.; Andersson, K.; Rappe, C. Chemosphere 1976, 5,
21.
- Norstrom, A.; Andersson, K.; Rappe, C. Chemosphere 1976, 5,
419.
- Oliver, J.E.; Ruth, J.M. Chemosphere 1983, 12, 1497.

- Olthoff, J.K.; Tossell, J.A.; Moore, J.H. J. Chem. Phys. 1985, 83, 5637.
- Parker, V.D. Acta Chem. Scand., Ser. B 1981, B35, 595.
- Peterson, R.G. Bull. Environ. Contam. Toxicol. 1987, 38, 416.
- Pisaniyas, M.N.; Christophorou, L.G.; Carter, J.G.; McCorkle, D.L. J. Chem. Phys. 1973, 2110.
- Pitea, D.; Ferrazza, A. J. Mol. Str. 1988, 92, 141.
- Pople, J.A.; Segal, G.A. J. Chem. Phys. 1966, 44, 3289.
- Pople, J.A.; Beveridge, D.L. Approximate Molecular Orbital Theory; McGraw-Hill: New York, 1970.
- Pople, J.A. Acc. Chem. Res. 1970, 3, 217.
- Pople, J.A.; Santry, D.P.; Segal, G.A. J. Chem. Phys. 1965, 43, S129, S136.
- Pschorr, R. Chem. Ber. 1986, 29, 496.
- Raner, K.D.; Lusztyk, J.; Ingold, K.U. J. Am. Chem. Soc. 1989, 111, 3652.
- Rappe, C.; Buser, H.R.; Stalling, D.L.; Smith, L.M.; Rappe, C. Env. Sci. Technol. 1984, 16, 78 A.
- Rappe, C.; Marklund, S.; Kjeller, L.L.; Bergqvist, P.A.;
- Rappe, C.; Gara, A.; Buser, H.R. Chemosphere 1978, 7, 981.
- Rappe, C. Halogenated Biphenyls, Terphenyls, Naphthalenes, Dibenzofurans and Related Products; Elsevier/North Holland Biomedical Press: New York, 1980, pp 48-68.
- Rappe, C.; Bergqvist, P.-A.; Hansson, M.; Kjeller, L.-O.; Lindstrom, G.; Marklund, S.; Nygren, M. Banbury Report 18: Biological Mechanisms of Dioxin Action; Cold Spring

- Harbor Laboratory: New York, 1984, pp 17-25.
- Rappe, C.; Choudhary, G.; Keith, L.H. Chlorinated Dioxins and Dibenzofurans in Perspective; Lewis Publishers Inc.: Chelsea, 1986, Ch. 6, p 79.
- Rossi, R.A.; Bunnett, J.F. J. Org. Chem. 1972, 37, 3570.
- Ryan, J.J.; Lizotte, R.; Lau, B.P.-Y. Chemosphere 1985, 14, 697.
- Safe, S.H.; Safe, L.M. J. Agric. Food Chem. 1984, 32, 68.
- Sanders, J.K.M.; Hunter, B.K. Modern NMR Spectrometry; Oxford University Press: Oxford, 1988.
- Schulten, H.-R. Int. J. Mass Spectrom. Ion Phys. 1979, 32, 97.
- Schwartz, B.A.; Keeler, P.A.; Gehring, P.J. Toxicol. Appl. Pharmacol. 1974, 28, 151.
- Sears, L.J.; Grimsrud, E.P. Anal. Chem. 1989, 61, 2523.
- Slonecker, P.J.; Cantrell, J.S. Anal. Chem. 1983, 54, 1543.
- Sundstrom, G.; Hutzinger, O. Chemosphere 1976, 5, 305.
- Szulejko, J.E.; Howe, I.; Benyon, J.H.; Schlunegger, U.P. Org. Mass Spectrom. 1980, 15, 263.
- Tanko, J.M.; Anderson, F.E. J. Am. Chem. Soc. 1988, 110, 3525.
- Tatchell, A.L. Vogel's Textbook of Practical Organic Chemistry 4th Ed.; Longman Scientific & Technical, 1987, p 658.
- Tomita, M.; Ueda, S.; Narisada, M. Yakugaku Zasshi 1959, 79, 186.
- Traynham, J.G. Chem. Rev. 1979, 79, 323.
- Wengerten, H.; Schisla, R.M. J. Org. Chem. 1962, 27, 4103.
- Wiley, G.A.; Hershkowitz, R.L.; Rein, B.M.; Chung, B.C. J. Am.

Chem. Soc. 1964, 86, 964.

Williams, D.T.; Blanchfield, B.J. J. Assoc. Off. Anal. Chem.
1972, 55, 93.

Younkin, J.M.; Smith, L.J.; Compton, R.N. Theort. Chem. Acta
1976, 41, 157.

Zakett, D.; Flynn, R.G.A.; Cooks, R.G. J. Phys. Chem. 1978,
82, 2359.

APPENDICES

APPENDIX 1. MOLECULAR ORBITAL CALCULATIONS
FOR ELECTRON AFFINITIES OF POLYCHLORINATED DIBENZOFURANS

Electron Affinities (EAs) of molecules are most important in negative ion chemistry including electron capture negative ion (ECNI) mass spectrometry.¹ When $EA < 0$ a Franck-Condon transition² (vertical transition on the potential-energy curve without changes in the nuclear separation and velocity of relative nuclear motion) leads to an unstable molecular anion M^{*-} which may disappear by autodetachment or by dissociation to $(M-X)^{\cdot-} + X^-$. When $EA > 0$, if the excess energy of M^{*-} is distributed into the vibrational modes of the anion, a significant lifetime ($>10^{-6}$ s) for the molecular anion can be obtained and collisional stabilization can occur more readily.

EA measurements for polychlorinated dibenzofurans (PCDBFs) are not available. With the advent of powerful computers semiempirical MO calculations have often been used to predict structures, energies and other properties of large organic molecules. By using these MO calculation methods the EAs of PCDBFs have been estimated and the electron capture processes of PCDBFs in ECNI mass spectrometry could be better understood. Several semiempirical SCF calculational methods are examined and their calculated EA values are discussed.

Calculation methods. Most MO calculations were performed using a recently developed AM1 (Austin Model 1) method³ since the AM1 method is known to be generally superior to MNDO,

especially in radical calculations. Some calculations were carried out by MNDO (Modified Neglect of Diatomic Overlap)⁴ or CNDO (Complete Neglect of Differential Overlap)⁵ methods for comparison. The major weakness of MNDO is its tendency towards an excessive stabilization of the π orbitals in aromatic compounds.⁶ This weakness is much improved in the AM1 method.

The AM1 version used in this study was adapted to a FPS (Floating Point System) super computer interfaced to a vax 11/780. The MNDO and CNDO versions were installed in an IBM-PC and an accelerator (Microway, Inc.) was added to decrease the program run time.

Closed-shell systems (neutrals or anions) were calculated using the RHF (Restricted Hartree-Fock) method. Open-shell calculations (radicals or radical anions) were carried out using the UHF (Unrestricted Hartree-Fock) method since the UHF method has been known to give more realistic estimates of spin densities for radicals and it was also found that the UHF calculations converge more readily than the corresponding RHF calculations.⁷ One major problem with the UHF calculations is that of spin contamination where the UHF wave function mixes in states of higher spin.⁸ For example, when the spin contamination is significant the RHF results are usually in better agreement with experimental data than the UHF results.⁹ Nevertheless, it is difficult to state which is best as there is no experimental data available for comparison of radical

anion stabilities.

Table A.1.1. Calculated heats of formation for 2,3,7-tri-CDBF by various methods.

Program	Method	Charge State	Optimiz.	HF(kcal/mol)
MNDO	RHF	neutral	yes	-4.22
AM1	"	"	yes	18.40
MNDO	"	rad.anion	yes	-45.21
AM1	"	"	yes	-15.49
AM1	"	"	no	-10.67
MNDO	UHF	"	yes	-56.72
AM1	"	"	yes	-23.70
AM1	"	"	no	-18.63

Several calculations were carried out for a neutral molecule and a radical anion of 2,3,7-tri-CDBF to compare the AM1 and MNDO methods including the difference of UHF and RHF methods (Table A.1.1). The results show that the MNDO method gives much lower energies in either neutral or radical anion calculations and the UHF method gives about 10 kcal/mol lower energies than the RHF method does. Comparisons were also made between the two possible states of radical anion, i.e., the same geometry as the optimized neutral molecule and the optimized geometry that comes from the minimization of the energy. The first one, which represents the Frank-Condon transition, is about 5 kcal/mol higher in energy than that of

the energy minimized structure. Table A.1.2 shows total energies and heats of formation of some PCDBF neutrals and radical anions, calculated by the AM1 method.

Another interesting observation in radical anion calculations of PCDBFs is that slight changes in input geometry of some isomers can induce large changes in bond orders, electron distributions or types of orbital energy. The assumption of planarity of the benzene ring, by setting the dihedral angles at 0° , must be used carefully.¹⁰ For example, radical anion calculations of 1,2,3,4-tetra-CDBF with and without full geometry optimization give very different results, especially in the C_3 -Cl bond order (Figure A.1.1). In the planar structure the electron density is largely localized in the C_3 -Cl bond and the bond length is much greater than the other C-Cl bonds. This kind of difference could be observed with isomers which have neighboring chlorines; for example, 1,2,3-, 2,3,4-, 1,2,3,4-, etc.

Electron Affinity (EA). Although the effort to measure EAs of atoms, molecules and radicals stretches over many decades, it is only recently that the accuracy of the data has become satisfactory even for small chemical species. Christophorou et al.¹ extensively reviewed the literature and discussed the methods and EA values. According to the authors, methods used to determine EAs have been divided into three broad groups: theoretical, semiempirical and experimental.

One simple method for estimation of the EA of molecules is the use of Koopman's Theorem (KT)¹¹; the electron energy of the highest occupied molecular orbital ϵ_{HOMO} is a good approximation to the ionization potential of the molecule. Similarly, the EA can be approximated from the energy of the lowest unoccupied molecular orbital, ϵ_{LUMO} , since the LUMO is the virtual orbital into which the ionizing electron enters. These EA values obtained through Koopman's Theorem are significantly different from reliable experimental data mainly because of the omission of charge redistribution and electron reorganization. This implies a correspondence between the EA of a molecule and the orbital energy of the LUMO, ϵ_{LUMO} , with use of "reorganization energy (δ)" corrections (eq.1). The value δ is very small and can be negligible for the highly polar molecules and quite large for nonpolar molecules. Younkin et al.¹² provided a better correlation equation by using a least-squares method (eq.2). In this study a relationship between the LUMO energies and EAs, calculated by MNDO for a variety of aromatic hydrocarbons was developed (eq.3).¹³ The results show that the reorganization energy is well accounted for by the MNDO method.

$$\text{EA(M)} = -\epsilon_{\text{LUMO}} - \delta \quad (1)$$

$$\text{EA(M)} = -0.95\epsilon_{\text{LUMO}} - 1.9 \text{ eV} \quad (2)$$

$$\text{EA(M)} = -1.17\epsilon_{\text{LUMO}} - 0.52 \text{ eV} \quad (3)$$

The CNDO method was initially used for calculation of LUMO energies of PCDBFs since the method is sufficiently

simple for application to large molecules; ~100 minimal basis functions may be used.¹⁴ The CNDO calculated LUMO energies of neutral PCDBFs and PCDDs were compared and PCDBFs show about 0.6 eV lower LUMO energies than those of PCDDs (Figure A.1.2). This can be expected from the structural preference of PCDBFs for delocalization of electrons between the two phenyl rings. However, the CNDO method yields lower values compared to the MNDO method (~2.2 eV) and AM1 method (~1.8 eV) (Figure A.1.3). LUMO energies of selected neutral PCDBFs and PCDDs calculated by the AM1 method are shown in Table A.1.3.

Generally, the EA value of a neutral molecule is also defined as the difference in energy between the neutral molecule plus an electron at infinity and the molecular negative ion when both are in their ground electronic, vibrational, and rotational states.¹⁵ Since electronic and nuclear motion in molecules are treated as if independent of one another in the Born-Oppenheimer approximation, electron attachment to molecules proceeds in the Frank-Condon region, which involves vertical transitions between potential-energy curves from the equilibrium positions of the atoms. Therefore, geometries of radical anions can be approximated by optimized geometries of neutral molecules. The AM1 method has been used to calculate the heats of formation of neutral molecules and its adiabatic negative ions of PCDBFs. By using these calculated heats of formation, the adiabatic EAs of PCDBFs have been obtained. These calculated EAs are about 0.4

eV lower than the LUMO energies of its neutral molecules (Figure A.1.4). The difference of 0.4 eV might be responsible for the reorganization energy, if these two values are correct.

In conclusion, the AM1 method is generally superior to the other methods; MNDO and CNDO, for calculation of the EA values of PCDBFs. Even though better results could be obtained by calculations for the energy difference between neutral and radical anion, the ϵ_{LUMO} is still a good approximation to assess the EA of PCDBF.

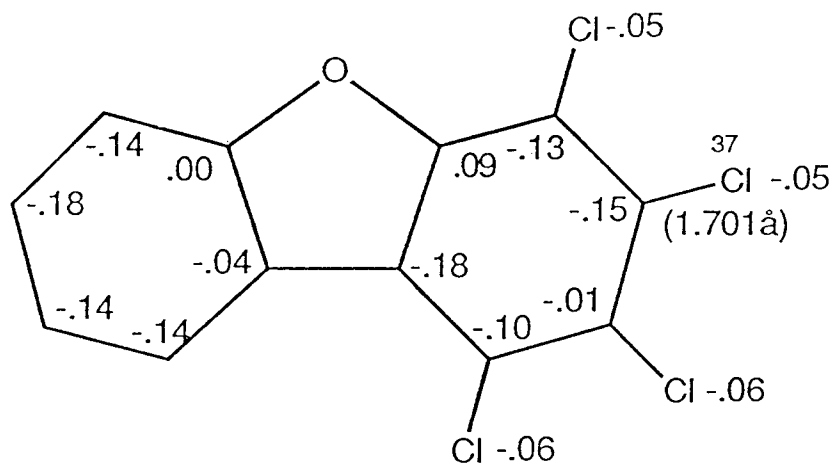
Table A.1.2. AM1 Calculated Total Energies (TE) and Heats of Formation (HF) of Selected PCDBFs.

Compound	Total Energy		Heat of Formation	
	Neutral	Anion	Neutral	Anion
DBF	-1965.06	-1966.18	36.35	10.65
1	-2325.14	-2326.49	30.07	-1.01
2	-2325.26	-2326.52	29.65	-1.84
3	-2325.15	-2326.54	29.77	-2.29
4	-2325.09	-2326.43	31.25	0.37
1,2	-2685.26	-2686.72	24.92	-11.08
1,6	-2685.16	-2686.71	25.09	-10.61
2,3	-2685.27	-2686.77	24.68	-12.24
2,6	-2685.27	-2686.74	24.79	-11.40
2,7	-2685.23	-2686.85	23.17	-13.96
2,8	-2685.24	-2686.70	23.08	-12.50
3,4	-2685.11	-2686.68	26.11	-10.23
3,6	-2685.26	-2686.75	24.86	-11.71
1,2,3	-3045.15	-3046.95	20.49	-20.90
1,4,7	-3045.22	-3047.01	18.99	-22.30
2,3,4	-3045.10	-3046.70	21.52	-19.64
2,3,7	-3045.24	-3047.07	18.39	-23.69
2,3,8	-3045.25	-3047.06	18.26	-23.42
2,6,7	-3045.29	-3046.97	19.66	-21.52
1,2,3,4	-3405.07	-3407.06	17.67	-28.14
2,3,7,8	-3405.24	-3407.21	13.78	-31.57
1,2,3,4,6	-3765.07	-3767.21	13.04	-36.20
2,3,4,7,8	-3765.18	-3767.35	10.56	-39.32
1,2,3,4,6,7	-4125.09	-4127.39	8.18	-44.94
1,2,3,4,6,7,8	-4485.07	-4487.52	4.02	-52.66
OCDBF	-4844.85	-4847.44	4.46	-55.31

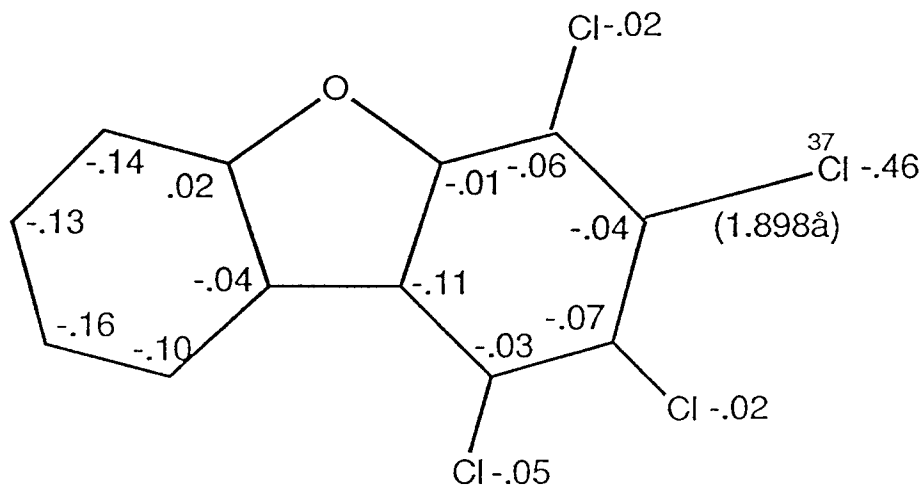
Table A.1.3. Calculated LUMO energies of PCDBFs (AM1 method).

PCDBFs	Neutral (eV)			Radical Anion (eV)	
	LUMO- π	LUMO- σ	$\epsilon(\pi-\sigma)^a$	SOMO(π)	LUMO- σ
DBF	-0.4065	2.1410	2.5475	-1.7721	6.6708
1	-0.6029	1.1891	1.7920	-2.0269	5.4353
2	-0.5997	1.2624	1.8621	-2.0640	5.2572
3	-0.6488	1.1422	1.7910	-2.0725	5.1480
4	-0.5877	1.2831	1.8708	-2.0285	5.3909
1,2	-0.7655	0.9370	1.7025	-2.2902	5.0353
1,6	-0.7608	1.0787	1.8395	-2.2572	5.1306
2,3	-0.8158	0.9332	1.7490	-2.3208	4.9376
2,6	-0.7606	1.1304	1.8910	-2.2831	5.0164
2,7	-0.8285	1.0260	1.8545	-2.3265	4.8661
2,8	-0.7875	1.1577	1.9452	-2.3189	5.0201
3,4	-0.8070	0.9241	1.7311	-2.2912	5.0066
3,6	-0.8121	1.0394	1.8515	-2.2922	4.8778
1,2,3	-0.9739	0.5883	1.5622	-2.5445	4.6474
1,4,7	-0.9918	0.8435	1.8353	-2.5161	4.6253
2,3,4	-0.9687	0.6670	1.6357	-2.5352	4.7386
2,3,7	-1.0246	0.8097	1.8343	-2.5520	4.5704
2,3,8	-0.9852	0.8300	1.8152	-2.5468	4.6917
2,6,7	-0.9748	0.8104	1.7852	-2.5228	4.7206
1,2,3,4	-1.1362	0.4589	1.5951	-2.7620	4.5319
2,3,7,8	-1.1693	0.7022	1.8715	-2.7535	4.4055
1,2,3,4,6	-1.2646	0.3830	1.6476	-2.9180	4.3489
2,3,4,7,8	-1.3007	0.4878	1.7885	-2.9357	4.2194
1,2,3,4,6,7	-1.4222	0.2998	1.7220	-3.0841	4.0478
1,2,3,4,6,7,8	-1.5527	0.2319	1.7846	-3.2489	3.8899
OCDBF	-1.6459	0.2072	1.8531	-3.3952	3.7585

^a $E(\text{LUMO}-\sigma) - E(\text{LUMO}-\pi)$ (eV).



(a) nonplanar structure



(b) planar structure

Figure A.1.1. AM1 calculated geometries of radical anions of 1,2,3,4-tetra-CDBF with full optimization (a) and partial optimization (b).

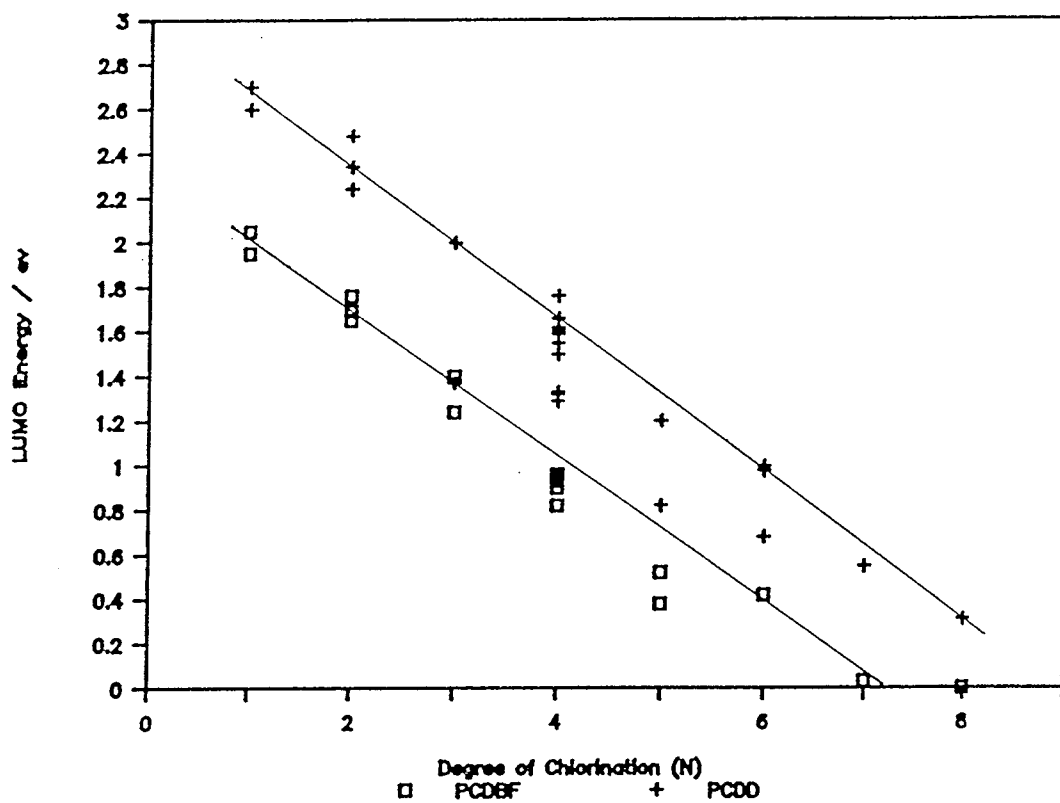


Figure A.1.2. CNDO calculated LUMO energies of neutral PCDBFs and PCDDs (Isomers are randomly selected).

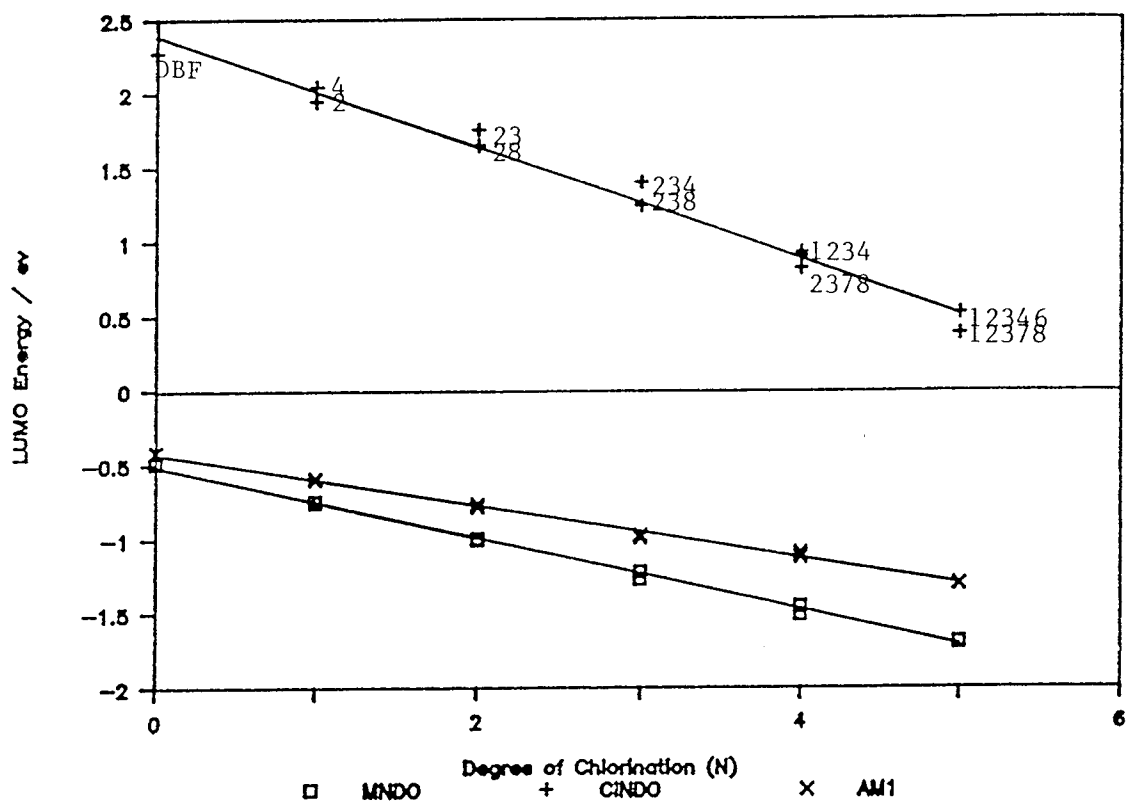


Figure A.1.3. MNDO and CNDO calculated LUMO energies of neutral PCDBFs.

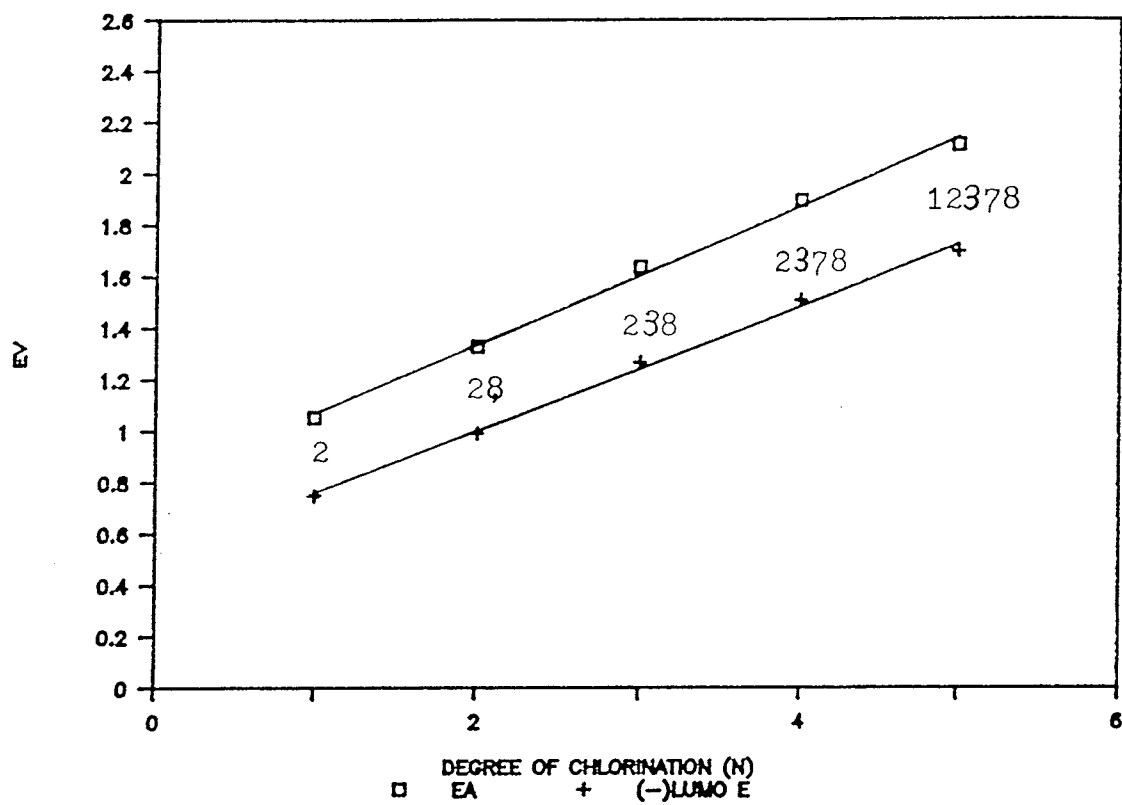


Figure A.1.4. MNDO calculated electron affinities and LUMO energies of neutral PCDBFs.

References

1. Christodoulides, A.A.; McCorkle, D.L.; Christophorou, L.G. In Electron-Molecule Interactions and Their Application, Vol. 1"; Christophorou, L.G., Ed.; Academic Press: Orlando, 1984; Chap. 6.
2. Mark, T.D. In "Electron-Molecule Interactions and Their Applications Vol. 1"; Christophorou, L.G., Ed.: Academic Press: Orlando, 1984; p 277.
3. Dewar, M.J.S.; Zoebisch, E.G.; Healy, E.F.; Stewart, J.J. J. Am. Chem. Soc. 1985, 107, 3902.
4. 1) Dewar, M.J.S.; Thiel, W. J. Am. Chem. Soc. 1977, 99, 4899.
2) Dewar, M.J.S.; Thiel, W. J. Am. Chem. Soc. 1977, 99, 4907.
3) Dewar, M.J.S.; McKee, M.L.; J. Am. Chem. Soc. 1977, 99, 5231.
4) Dewar, M.J.S.; Rzepa, H.S. J. Am. Chem. Soc. 1978, 100, 58.
5. a) Pople, J.A.; Beveridge, D.L. Approximate Molecular Orbital Theory; McGraw-Hill: New York, 1970.
b) Pople, J.A.; Santry, D.P.; Segal, G.A. J. Chem. Phys. 1965, 43, S 129, S 136.
c) Pople, J.A.; Segal, G.A. J. Chem. Phys. 1966, 44, 3289.
6. Dewar, M.J.S.; Rzepa, H.S. J. Am. Chem. Soc. 1978, 100, 784.
7. Hameka, H.F. J. Org. Chem. 1987, 52, 5025.
8. Pacansky, J.; Liu, B.; Defrees, D. J. Org. Chem. 1986, 51, 3720.
9. Farnell, J.; Pople, J.A.; Random, L. J. Phys. Chem. 1983, 87, 79.
10. Hameka, H.F. J. Org. Chem. 1987, 52, 5025.
11. Koopmans, T. Physica 1934, 1, 104.
12. Younkin, J.M.; Smith, L.J.; Compton, R.N. Theor. Chim. Acta 1976, 41, 157.
13. Unpublished work.
14. Pople, J.A. Acc. Chem. Res. 1970, 3, 217.

15. Christophorou, L.G. Atomic and Molecular Radiation Physics; Wiley Interscience: New York, 1971.

APPENDIX 2. ELECTRON CAPTURE NEGATIVE ION

MASS SPECTROMETRY OF 1,2,3,4-TETRACHLORODIBENZOFURAN

Production of high levels of reagent ions initiated by electron impact ionization of the reagent gas is influenced by several conditions. Previously, we reported the electron capture negative ion (ECNI) mass spectrometry of 1,2,3,4-tetrachlorodibenzo-p-dioxin (1,2,3,4-TCDD).¹ The results showed that the competition between resonance electron capture and dissociative electron capture is influenced by the reagent gas pressure, mass of the collision gas, and the ionization potential of the reagent gas. Helium reagent gas was found to give the most intense molecular ion, and the most linear ion abundance over a large pressure range.

A careful investigation of the ECNI mass spectrometry of 1,2,3,4-tetrachlorodibenzofuran (1,2,3,4-TCDBF) with variation of controllable parameters including reagent gas pressure, source temperature, electron energy and time dependent GC peak analysis has been carried out. The results from helium reagent gas are discussed.

Ion Source Pressure. Ion source pressure affects relative ion abundances in a complex manner. In the low-pressure region, before substantial ion current is produced, an enhancement in molecular ion relative to fragment ion abundance was observed for a variety of compounds.² This behavior was attributed to an enhancement of M^+ production due

to electron thermalization or collisional stabilization of M^- ion. The relative abundances of the molecular anion and chloride ions produced from 1,2,3,4-TCDBF remain relatively constant over a measured pressure range of 0.1~1.9 torr, with the molecular ion dominating the spectrum (Figure A.2.1). A closer examination of the chloride ion abundances which have compensating relationship with molecular ion abundances shows no chloride ion at pressures between 0.1~0.3 torr. This is followed by a slow increase of chloride ion production at higher pressures with a maximum of 3.4 % at 2.1 torr. The detectable total ion current increases dramatically and reaches a maximum at 0.7 torr at which point it begins to diminish again (Figure A.2.2). For helium gas, therefore, the pressure range of 0.7~0.9 torr gives the maximum TIC. As observed previously for 1,2,3,4-TCDD, a higher pressure of helium gas, in comparison to hydrogen, argon and xenon, is needed in the ionization source to achieve the maximum total ion current. The effect of reagent gas pressure upon resonance capture as compared to two dissociative electron capture channels is not significant. Lower source pressure gives a total ion current predominantly composed of the molecular anion, and higher source pressures yield greater dissociative capture with less molecular anion current but greater total ion current.

Ion Source Temperature. Lowering the ion source temperature is generally found to decrease fragmentation and

enhance molecular ion abundance.³ This effect has been attributed to a decrease in ion internal energy and subsequent rate of dissociative reactions.⁴ Hence, the effect of source temperature on electron attachment negative ion production is more profound at higher temperatures. Ion source temperature of 150 °C shows relatively large molecular ion abundances (99.5 %) (Figure A.2.3). However, total ion current dropped very sharply from 80 °C at which point a maximum TIC is observed (Figure A.2.4).

Electron Energy. In the electron impact mode other conditions being constant, the extent of ionization by the electron beam increases rapidly with electron energy from 10 eV to approximately 20 eV for most organic compounds.⁵ Most reference spectra are obtained and reported at 70 eV, because at that level the perturbations in electron energy have negligible effects on ion production and because reproducible fragment ion patterns are obtained at that energy level. In contrast, the electron energy in the chemical ionization mode could be greater than 70 eV and there will be an effective penetration of the electrons into the relatively high pressure reagent gas. Typically the ion current increases to a constant value as the filament's electron energy is increased above about 100 eV and the filament's electron energy has a minor effect on relative ion abundances. The results of 1,2,3,4-TCDBF show that TIC is most abundant at the range of 40~60 eV and relative ion abundance is almost constant over

a wide range from 25 eV at which helium could begin to be ionized (Figure A.2.5). Therefore, the ionizing electron energy does not change much of transition probability of the electron capture modes of 1,2,3,4-TCDBF meanwhile the high energy electrons could have more possibilities of penetration into the reagent gas without ionization reactions producing less TIC.

Sample concentration. Variations in mass spectra resulting from changes in sample concentration may be subtle, as in cases where ion abundances vary across a chromatographic peak, or they may be quite dramatic, as in cases where new ions appear and dominate the spectrum. The less dramatic variations are often present when ions attributed to wall reactions are involved and result in tailing ion chromatograms associated with ions generated by this mechanism.⁶ Under constant temperature, pressure and electron energy, the relative abundance of molecular and chloride ions of 1,2,3,4-TCDBF varies only within $\pm 1.5\%$ (Figure A.2.6), whereas the M^- and $(M-HCl)^-$ ions of octa-CDBF vary significantly as the GC peak elutes into the ion source (Figure A.2.7).

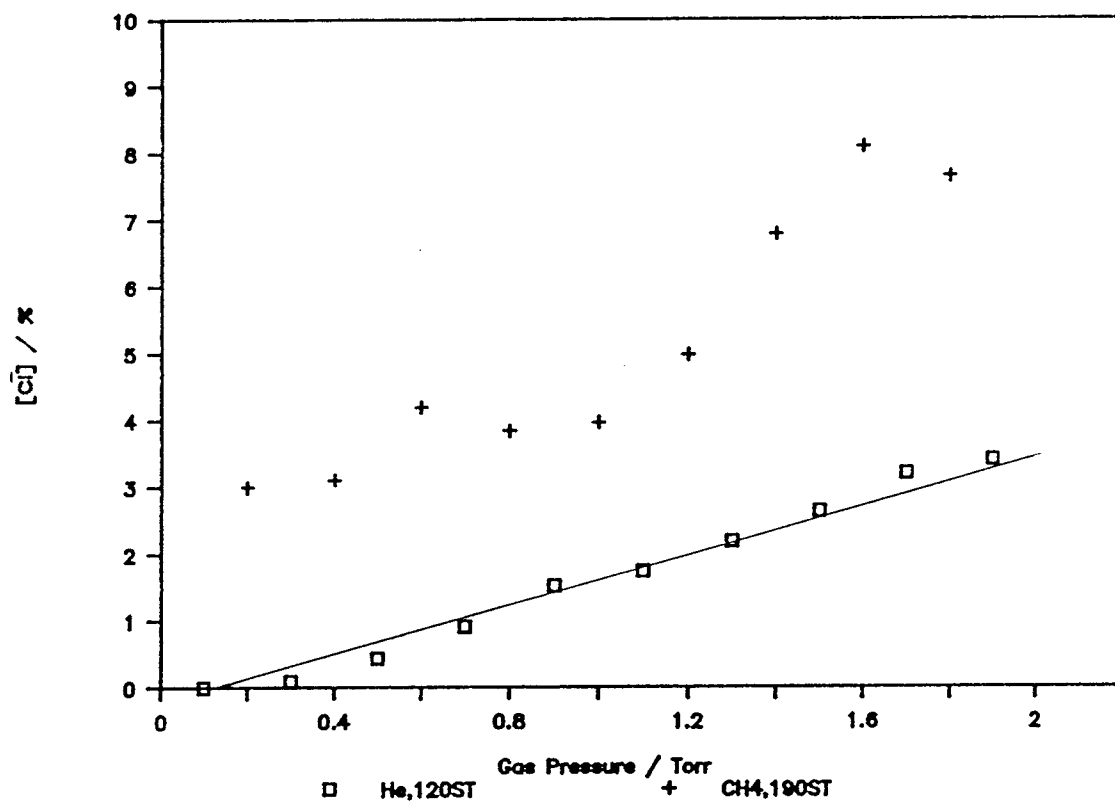


Figure A.2.1. Chloride ion abundance of 1,2,3,4-tetra-CDBF as a function of source pressure of helium (120 °C) and methane (190 °C).

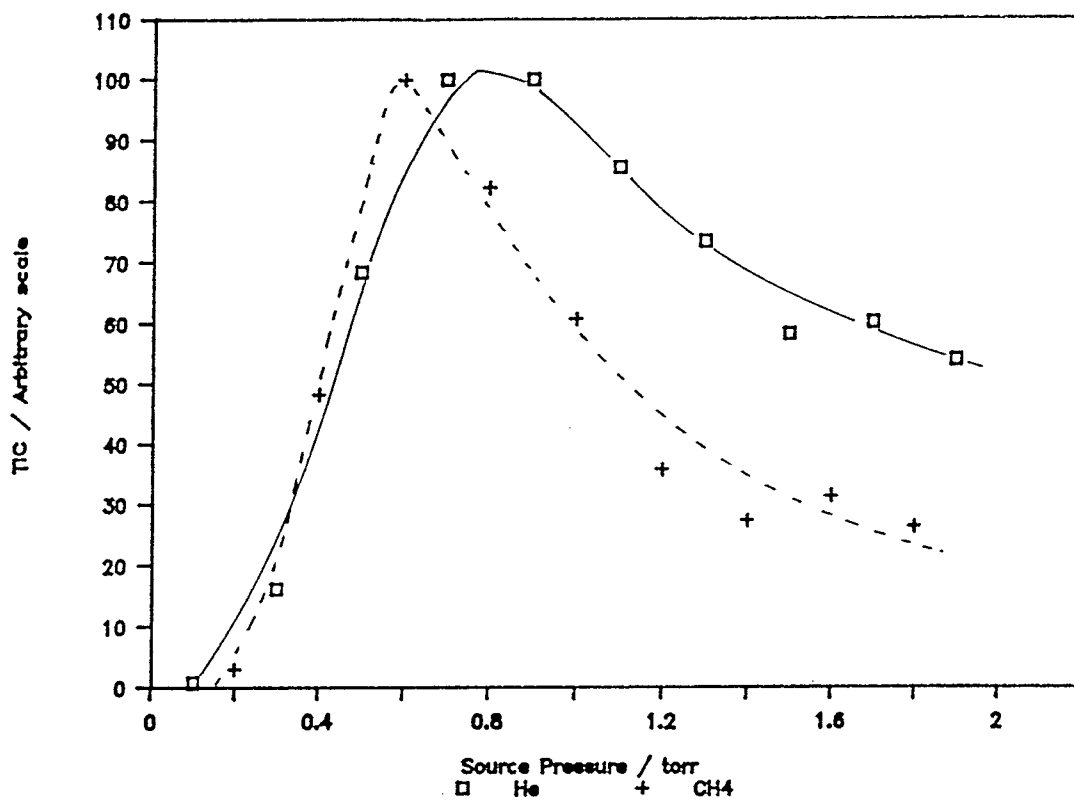


Figure A.2.2. Total ion current of 1,2,3,4-tetra-CDBF as a function of source pressure (120 °C).

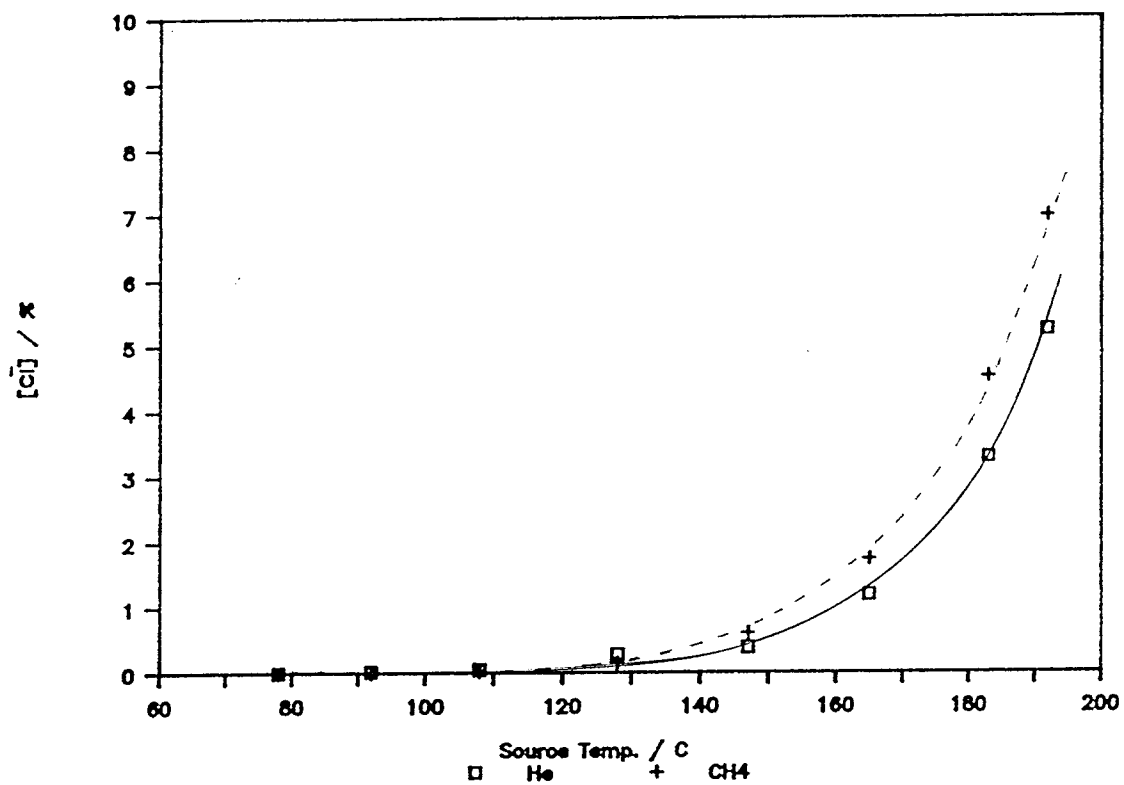


Figure A.2.3. Chloride ion abundance of 1,2,3,4-tetra-CDBF as a function of source temperature (0.5 torr).

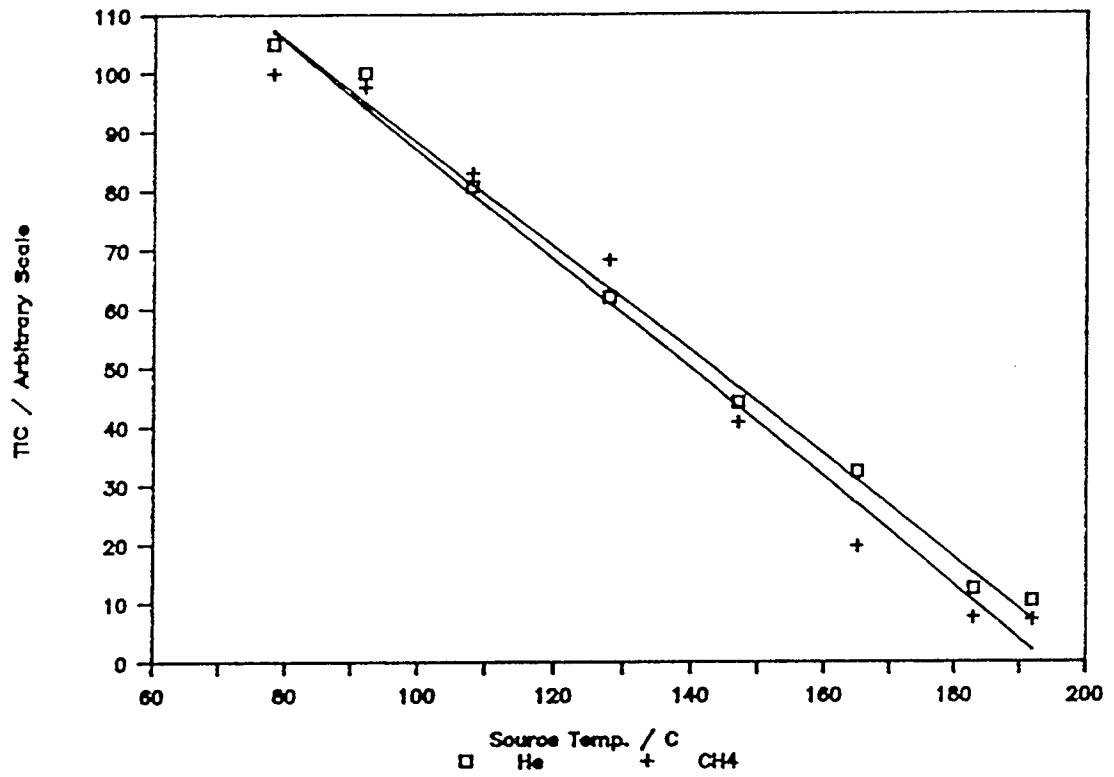


Figure A.2.4. Total ion current of 1,2,3,4-tetra-CDBF as a function of source temperature (0.5 torr).

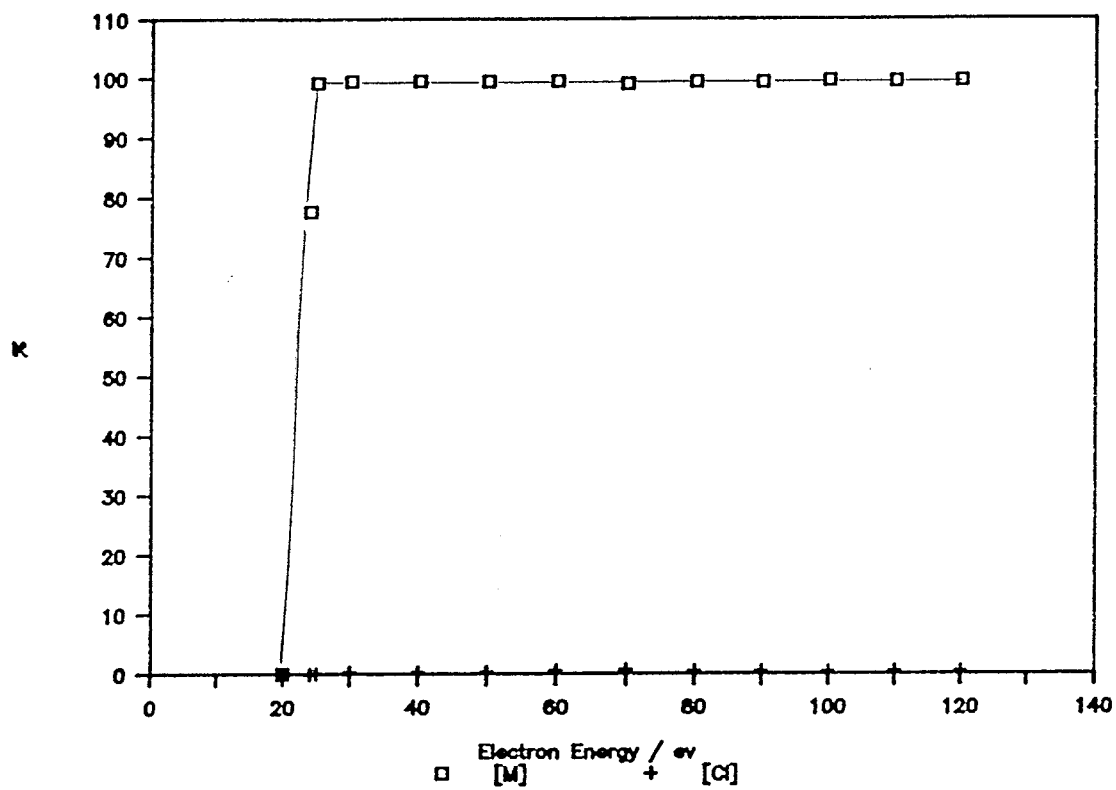


Figure A.2.5. Relative negative ion abundance of 1,2,3,4-tetra-CDBF as a function of electron energy (helium, 0.5 torr, 120 °C).

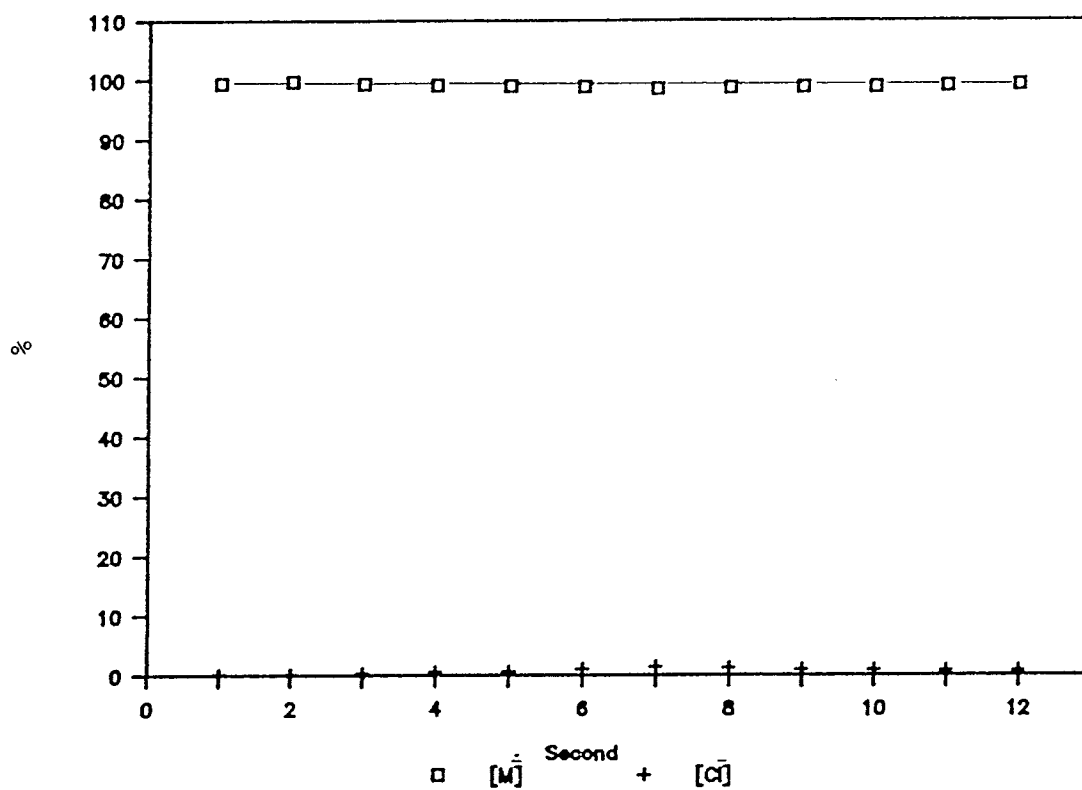


Figure A.2.6. Relative negative ion abundance of 1,2,3,4-tetra-CDBF as a function of GC eluting time of the peak (helium, 0.5 torr, 120 °C).

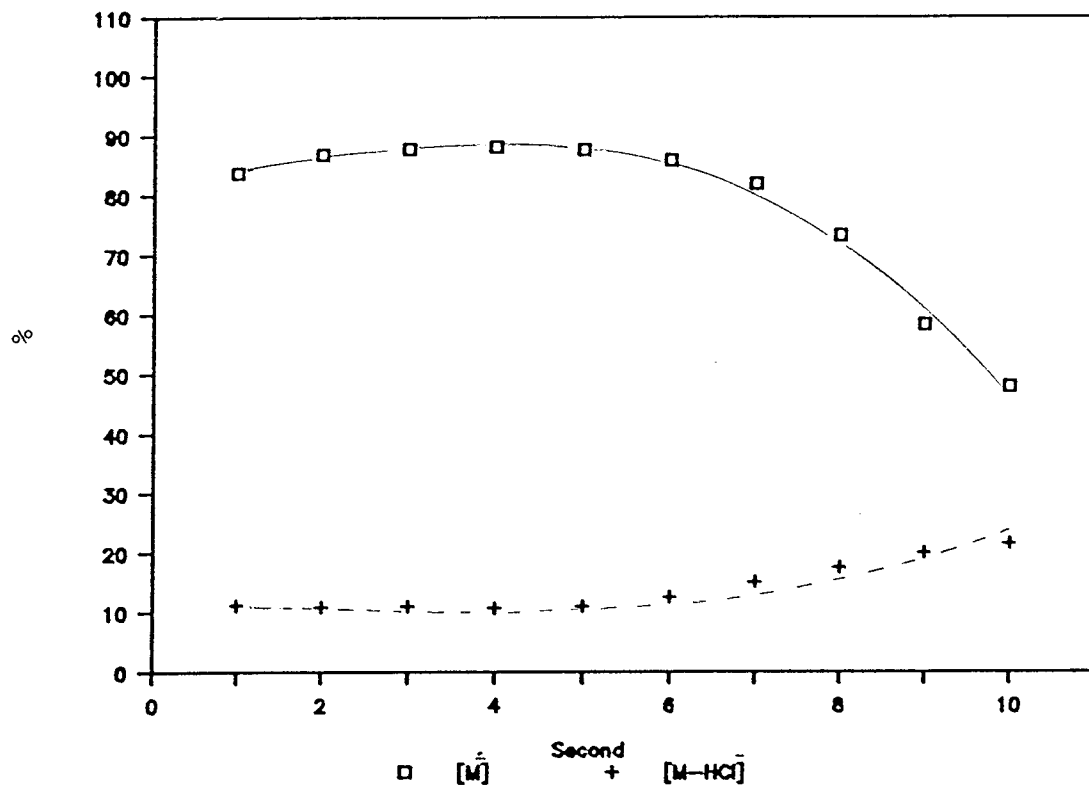


Figure A.2.7. Relative negative ion abundance of octa-CDBF as a function of GC eluting time of the peak (helium, 0.5 torr, 120 °C).

References

1. Laramée, J.A.; Arbogast, B.C.; Deinzer, M.L. Anal. Chem. 1986, 58, 2907.
2. Stemmler, E.A.; Hites, R.A. Electron Capture Negative Ion Mass Spectra of Environmental Contaminants and Related Compounds; VCH publisher: New York, 1988.
3. Stemmler, E.A.; Hites, R.A. Biomed. Mass. Spectrom. 1988, 15, 659.
4. Compton, R.N.; Christophorou, L.G.; Hurst, G.S.; Reinhardt, P.W.J. Chem. Phys. 1966, 45, 4634.
5. Watson, J.T. Introduction to Mass Spectrometry: Raven Press; New York, 1984, p 184.
6. Sears, L.J.; Campbell, J.-A.; Grimsrud, E.P. Biomed. Environ. Mass Spectrom. 1987, 14, 401.

APPENDIX 3. ION-MOLECULE INTERACTIONS IN ELECTRON CAPTURE
NEGATIVE ION MASS SPECTROMETRY OF OCTACHLORODIBENZOFURAN

In mass spectrometry, radicals formed during the ionization process cannot be observed directly.¹ However, radicals produced as fragments of decomposition conceivably could be ionized in a second process for example, by capture of a low energy electron to give an anion in electron capture negative ion (ECNI) mass spectrometry. The low concentration of such radicals in the ion source would make the probability of capturing an electron by radicals very low. Nevertheless, in chemical ionization (CI) mass spectrometry it is more common to see the effects of radicals present in the source on the mass spectra.²

The first observation of radicals under CI conditions was made by McEwen and Rudat³. They found that 7,7,8,8-tetracyano-quinodimethane (TCNQ) reacted with radicals formed in a CI plasma by attachment, or by attachment with loss of one or more cyano groups. These studies clearly showed that the radical population produced in a hydrocarbon plasma under CI conditions is sufficiently high to be trapped and the products ionized and observed. Blom and Munson⁴ observed protonated ethane ions in a methane plasma under positive CI conditions. They postulated that ethane was produced by methyl radical combination reactions apparently occurring on the metal surfaces of the ion source. Changing the surface

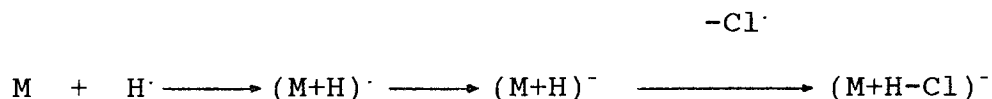
metal from aluminum (aluminum oxide) to stainless steel and then to gold reduced the amount of protonated ethane observed.

Ions of the type $(M+O-Cl)^-$ are often observed in the spectrum of chlorinated aromatic hydrocarbons.⁵ These ions can be produced by a displacement reaction between the resonance electron capture (EC) product, M^- , and trace levels of oxygen. The small amount of oxygen introduced into the ion source acts as a reagent gas as in chemical ionization. This secondary process in EC spectra is well-understood and can be controlled by careful attention to ion source conditions. The site of displacement of chlorine in a benzene ring is known to be ortho or para to a methoxy group, with para being the preferred site.⁶ Meta chlorines act to stabilize the displacement at these sites. Usually, molecular anions could be observed only when the concentration of oxygen is extremely low, or under low pressure conditions when the frequency of collision of M^- with oxygen would be low.

Such ion-molecule interactions also are observed in ECNI mass spectrometry of polychlorinated dibenzofurans (PCDBFs). The oxygen containing deuterated methane spectra of octa-CDBF showed a large amount of $(M-Cl+O)^-$ peaks with molecular ion M^- (Figure A.3.1). Oxygen traps remove almost all $(M-Cl+O)^-$ peaks and $(M+D-Cl)^-$ seems to be a dominant fragmentation ion. However, close examination of $(M+D-Cl)^-$ peaks shows that these are composed of $(M-Cl)^-$, $(M+H-Cl)^-$ and $(M+D-Cl)^-$ (Figure A.3.2). This indicates that there is still an ion-molecule

interaction with hydrogen that is responsible for the $(M+H-Cl)^-$ in the CD_4 atmosphere. This observation is further confirmed by the spectra of octa-CDBF in the presence of D_2 , which also gives $(M-Cl)^-$, $(M+H-Cl)^-$, $(M+D-Cl)^-$.

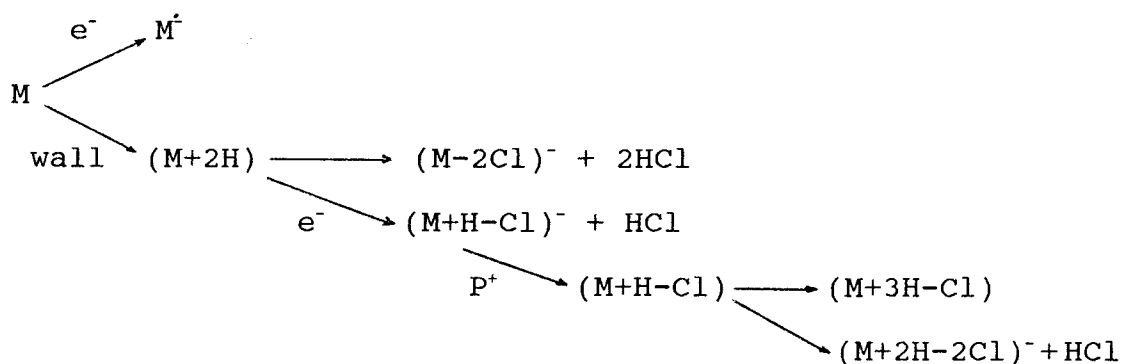
Stemmler and Hites⁷ reported the methane spectra of twenty four bridged polycyclic chlorinated pesticides. An unusual feature of these spectra was that prominent ions corresponding to the species $(M+nH-nCl)^-$ differing by 34 mass units (where $n=1$ to 5), were observed for many compounds. They suggested that these ions reflect involvement of free radicals (Scheme A.3.1). It is significant to note, however, that reactions of hydrogen atoms only, and not alkyl radicals were indicated by the spectra of these compounds. This mechanism is doubtful because it would require a low probability ionization process to occur and the loss of chlorine atoms is not favored over the loss of chloride ion.



Scheme A.3.1

Other unusual features of the spectra of polycyclic chlorinated pesticides were reported.⁸ For example, using CD_4 as the reagent gas produced $(M+D-Cl)^-$ ions (33 amu loss) as expected, but produced in equal abundance $(M+H-Cl)^-$ ions (34

amu loss). This suggests a source of hydrogen other than the reagent gas. Changing the reagent gas from a hydrocarbon gas to argon or nitrogen does not eliminate the $(M-34)^-$ ions. The authors suggested this was because hydrogen sources such as water were still present. It should be noted that $(M+H-X)^+$ cations also have been observed in EI spectra. A mechanism with intermediacy of $(M+H)^-$ was excluded because such a species has never been observed.



Scheme A.3.2

Sears and Grimsrud⁹ recently observed that fluoranil and chloranil produce $(M+H-F)^-$ and $(M+H-Cl)^-$ ions, respectively, under ECNI conditions with methane reagent gas. These authors proposed an alternative mechanism for radical addition to explain the results.¹⁰ The proposed mechanism involves successive and repeated electron capture and neutralization by ion-ion recombination steps (Scheme A.3.2). This mechanism is most feasible since the rate constants for the various reaction steps, including the electron capture and the ion-

ion recombination reactions, considerably exceed the diffusion controlled rate constants. The high rate constants allow several reaction steps to occur during the lifetime of a sample molecule in the CI ion source.

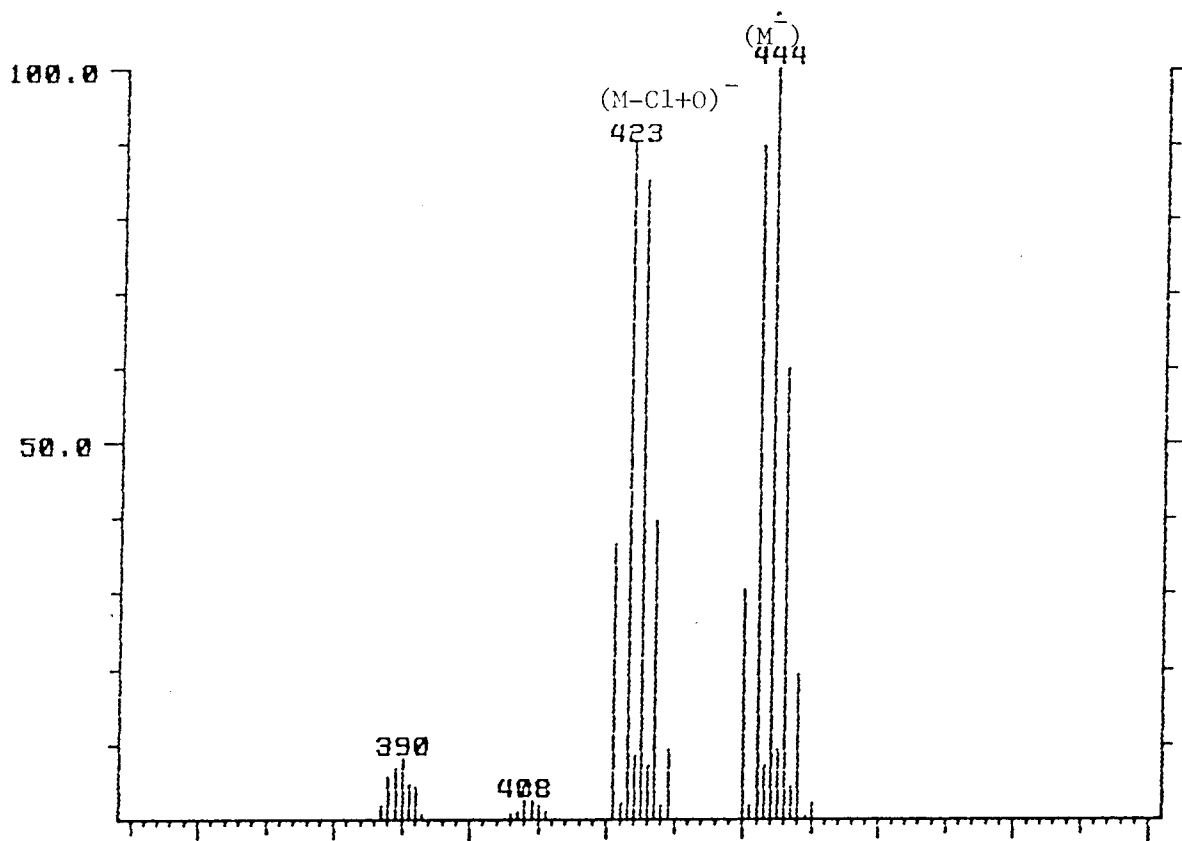


Figure A.3.1. ECNI mass spectrum of octa-CDBF in the presence of CD_4+O_2 reagent gas (0.6 torr, 120 °C).

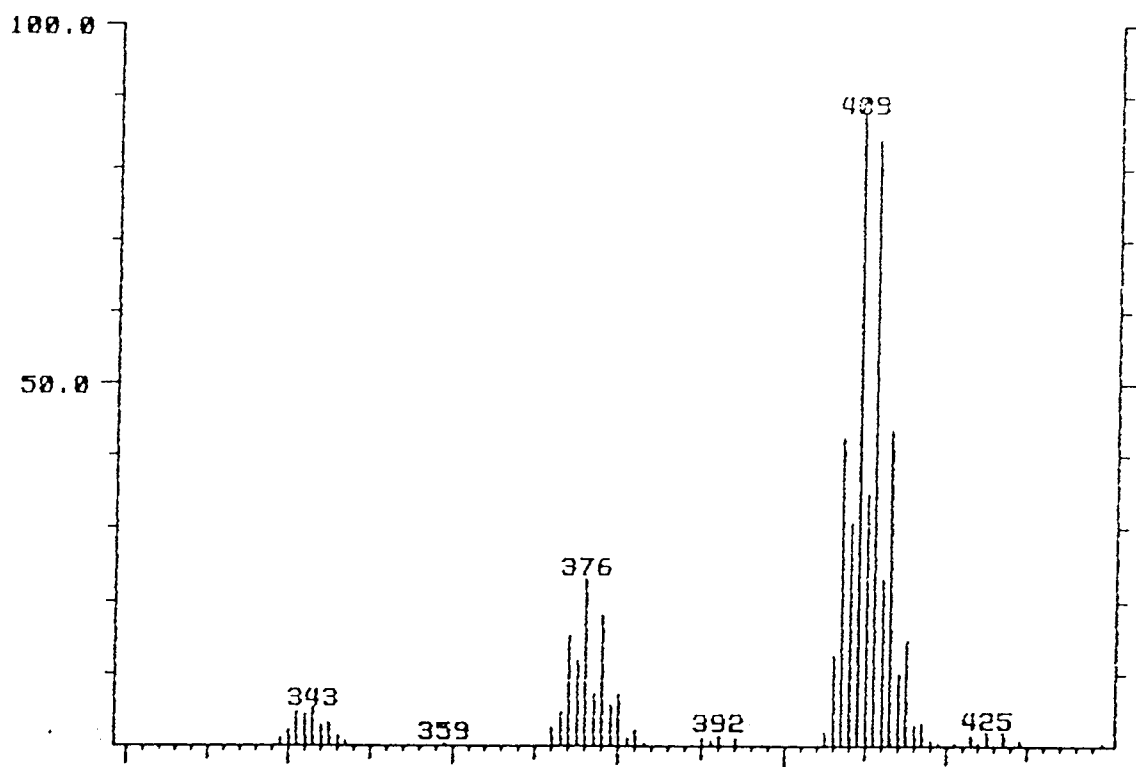


Figure A.3.2. ECNI mass spectrum of octa-CDBF in the presence of CD₄ reagent gas (0.6 torr, 120 °C).

References

1. (a) McEwen, C.N. Mass Spectrom. Rev. 1986, 5, 521.
(b) Budzikiewicz, H. Org. Mass Spectrom. 1988, 561.
2. Budzikiewicz, H. Org. Mass Spectrom. 1988, 23, 561.
3. (a) McEwen, C.N.; Rudat, M.A. J. Am. Chem. Soc. 1979, 101, 6470.
(b) Rudat, M.A. J. Am. Chem. Soc. 1981, 103, 4343.
4. Blom, K.; Munson, B. Int. J. Mass Spectrom., Ion Phys. 1982, 43, 17.
5. Grimsrud, E.P.; Chowdhury, S.; Kebarle, P. Int. J. Mass Spectrom., Ion Phys. 1986, 68, 57.
6. Busch, K.L.; Hass, J.R.; Bursley, M.M. Org. Mass Spectrom. 1978, 13, 604.
7. Stemmler, E.A.; Hites, R.A. Anal. Chem. 1985, 57, 684.
8. Deinzer, M.; Griffin, D.; Miller, T.; Lamberton, J.; Freeman, P.; Jonas, V. Biomed. Mass Spectrom. 1982, 9, 85.
9. Sears, L.J.; Grimsrud, E.P. 34th Annual Conferences on Mass Spectrometry and Allied Topics, June, 1986.
10. (a) Sears, L.J.; Campbell, J.-A.; Grimsrud, E.P. Biomed. Environ. Mass Spectrom. 1987, 14, 401.
(b) Sears, L.J.; Grimsrud, E.P. Anal. Chem. 1989, 61, 2523.

APPENDIX 4. MISCELLANEOUS FIGURES

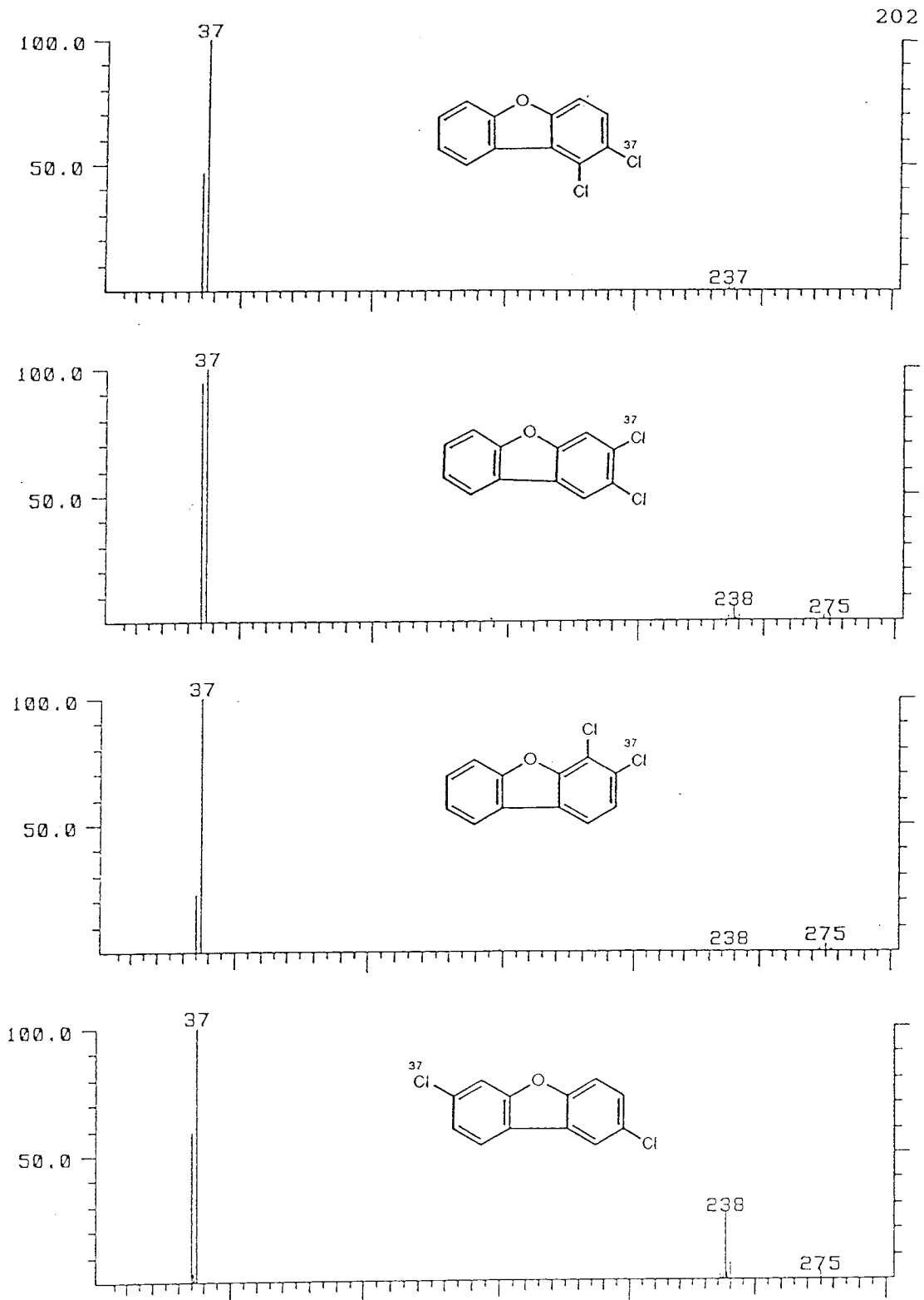


Figure A.4.1. ECNI mass spectra of di-CDBFs (methane, 0.5 torr, 120 °C).

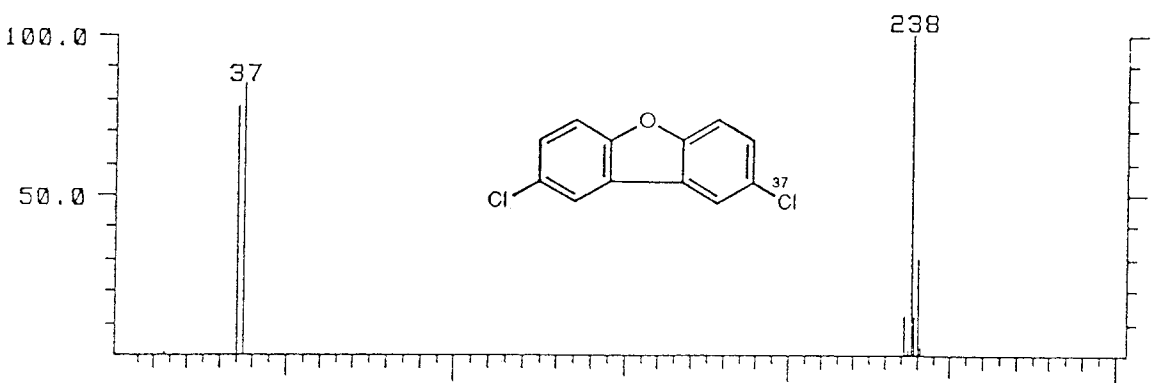
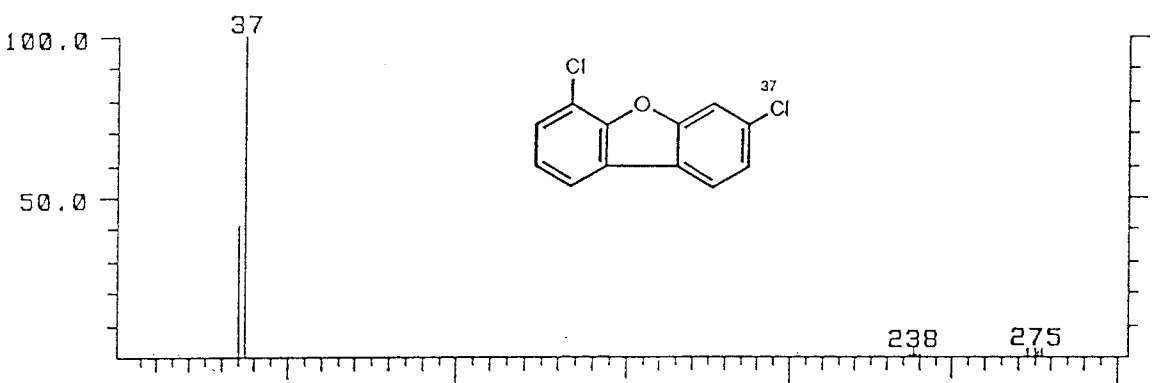
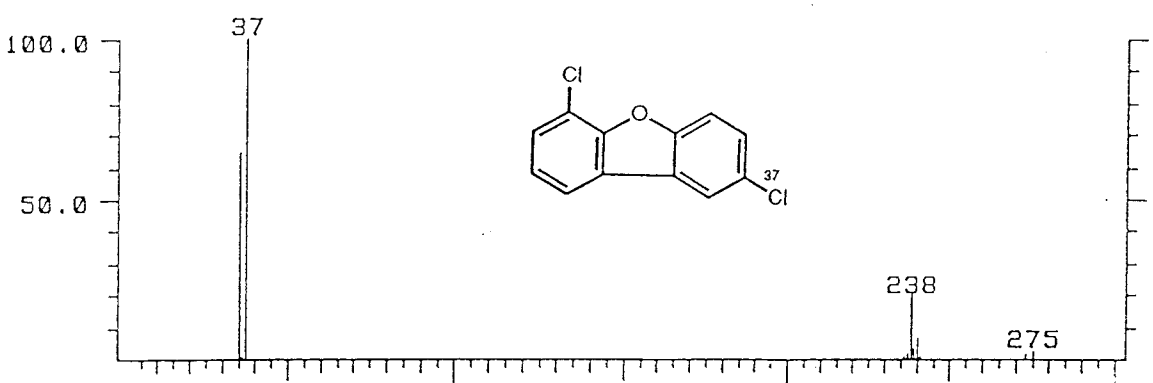
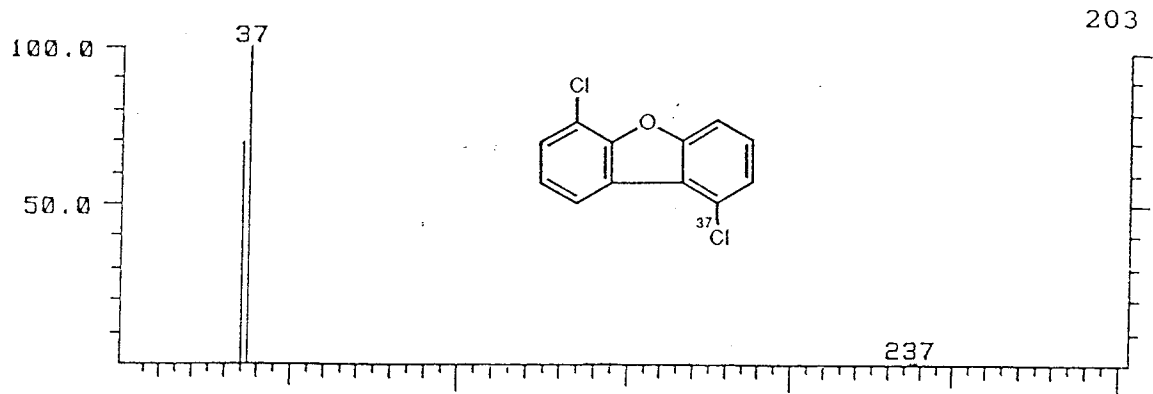


Figure A.4.1. Continued.

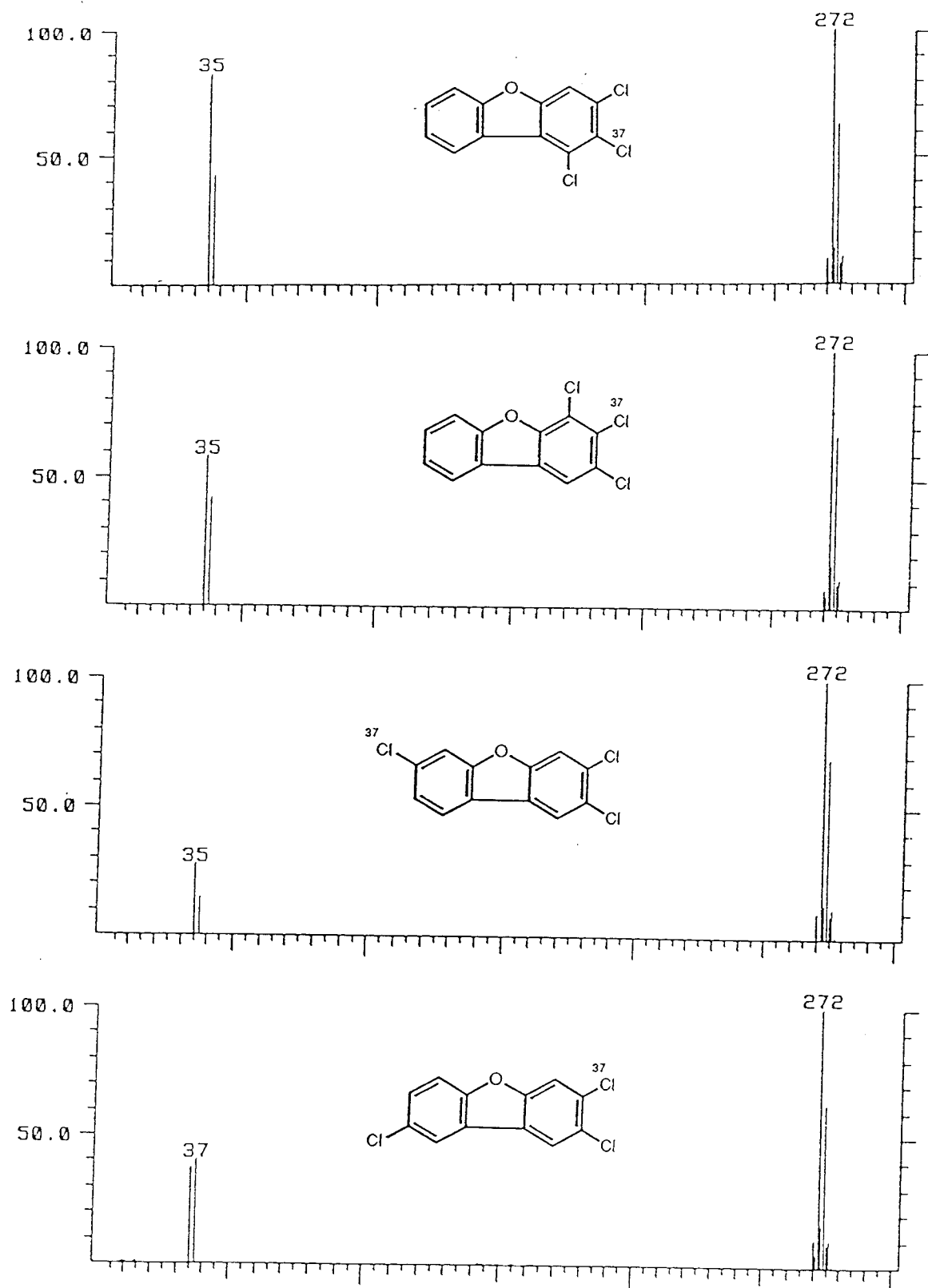


Figure A.4.2. ECNI mass spectra of tri-CDBFs (methane, 0.5 torr, 120 °C).

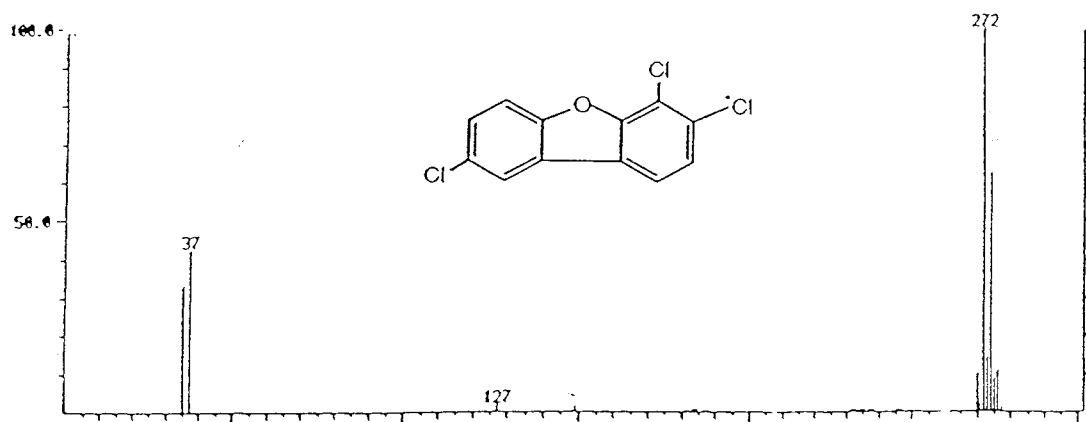
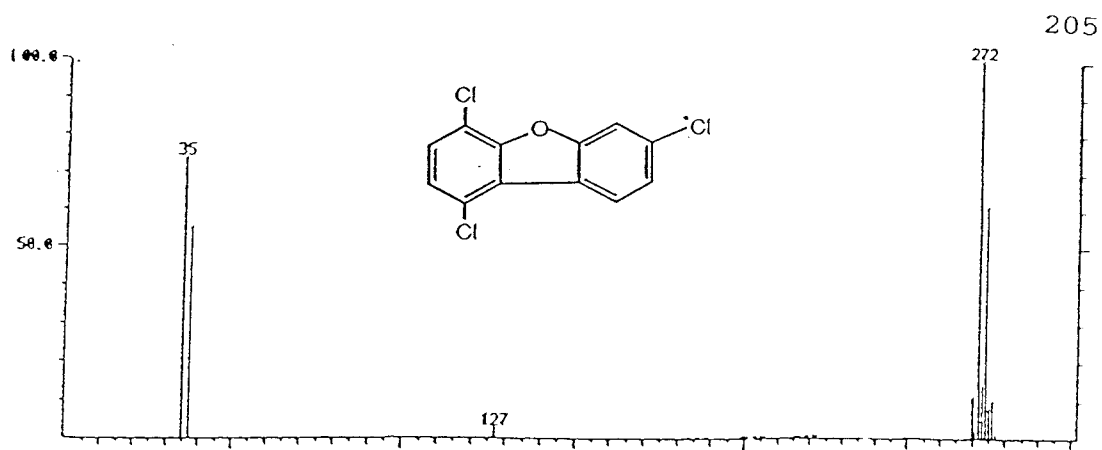


Figure A.4.2. Continued.

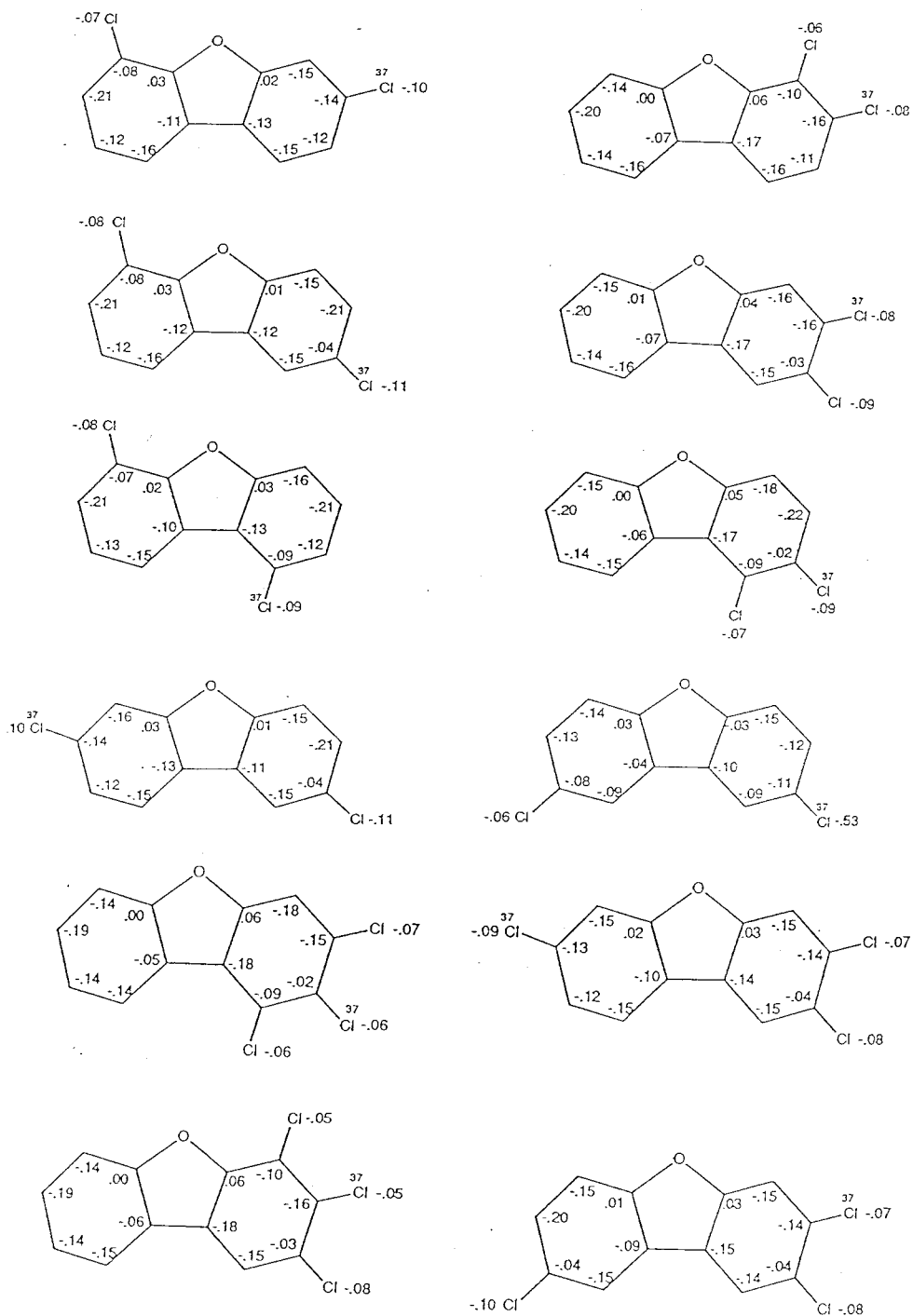


Figure A.4.3. Calculated free electron densities of radical anions of PCDBFs (AM1, UHF).

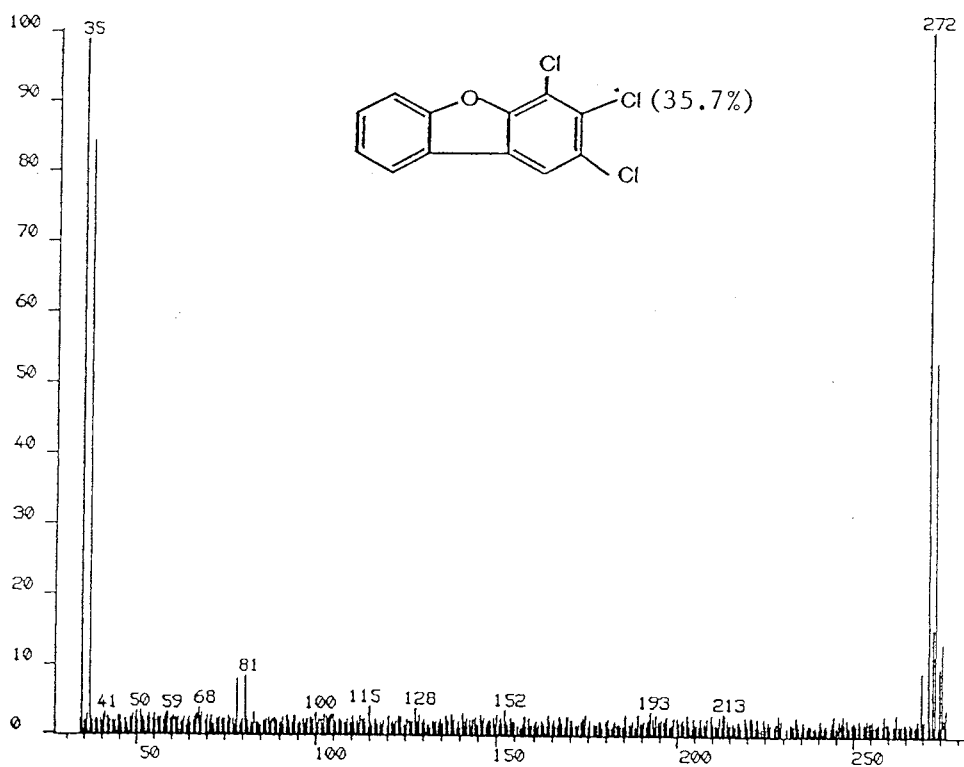


Figure A.4.4. Hi-resolution ECNI mass spectra of 2,3(^{37}Cl),4-tri-CDBF (methane, 0.7 torr, 150 °C).

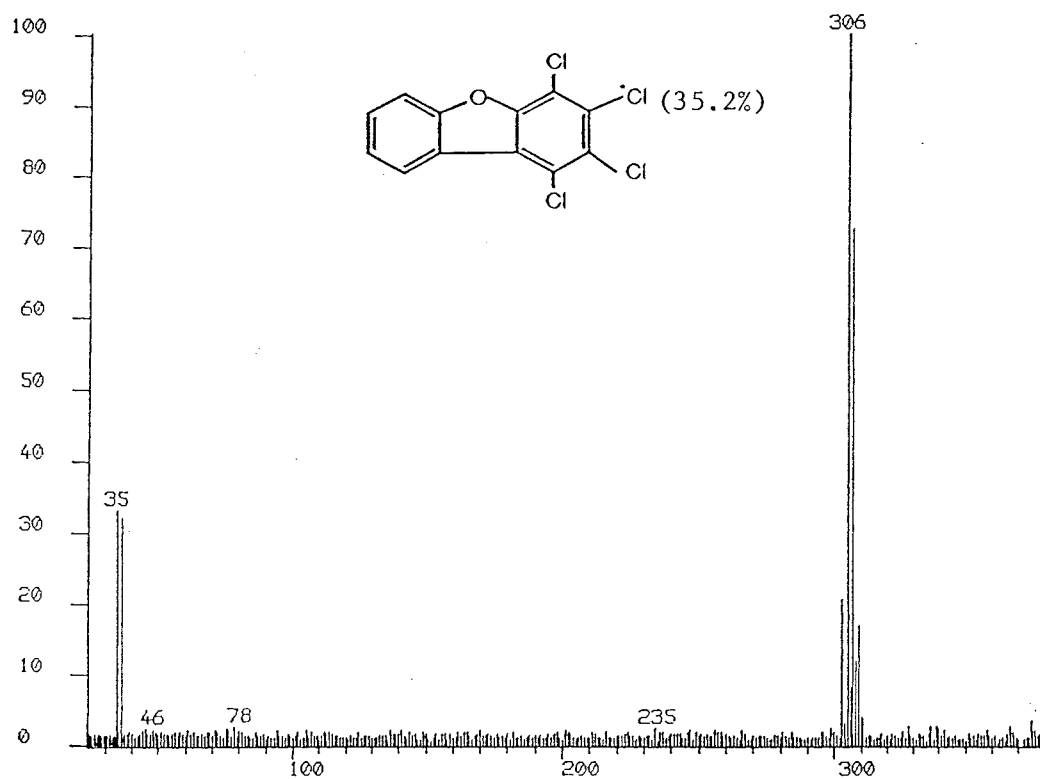


Figure A.4.5. Hi-resolution ECNI mass spectra of 1,2,3(^{37}Cl),4-tetra-CDBF (methane, 0.7 torr, 150 °C).

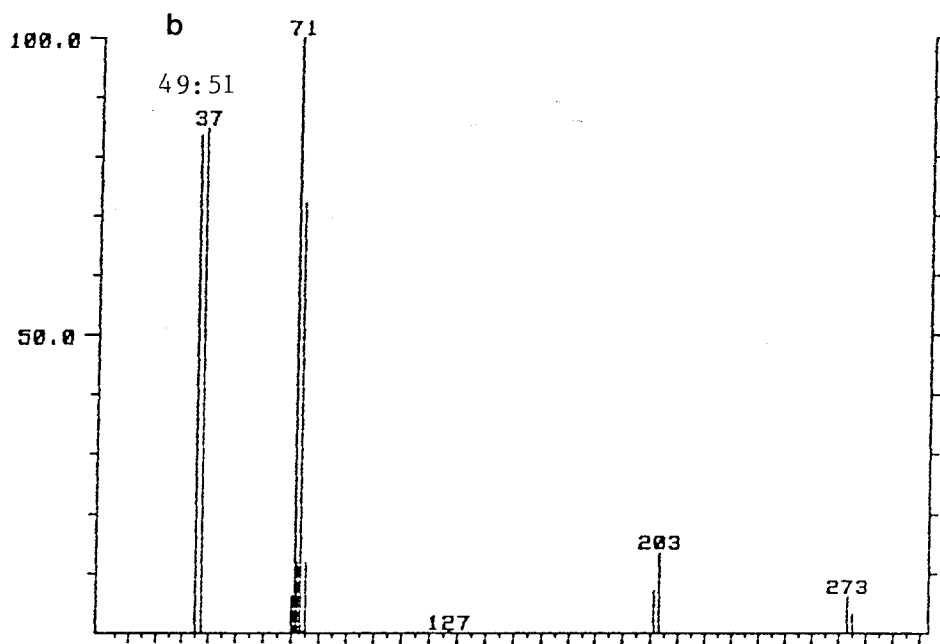
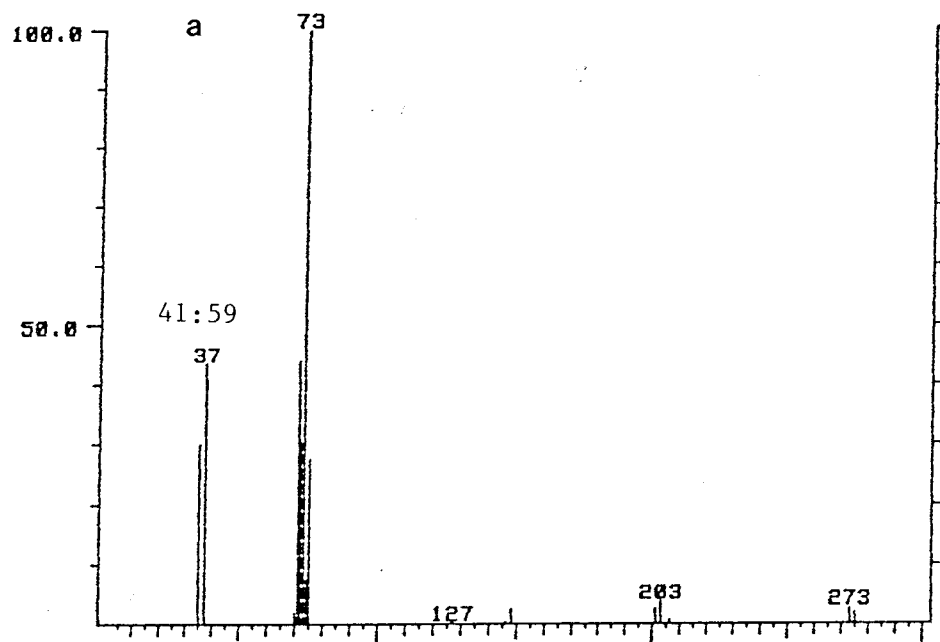


Figure A.4.6. ECNI mass spectra of 2,3'(³⁷Cl),6-tri-CDPE (a) and 2,4'(³⁷Cl),6-tri-CDPE (b) (methane, 0.5 torr, 120 °C).

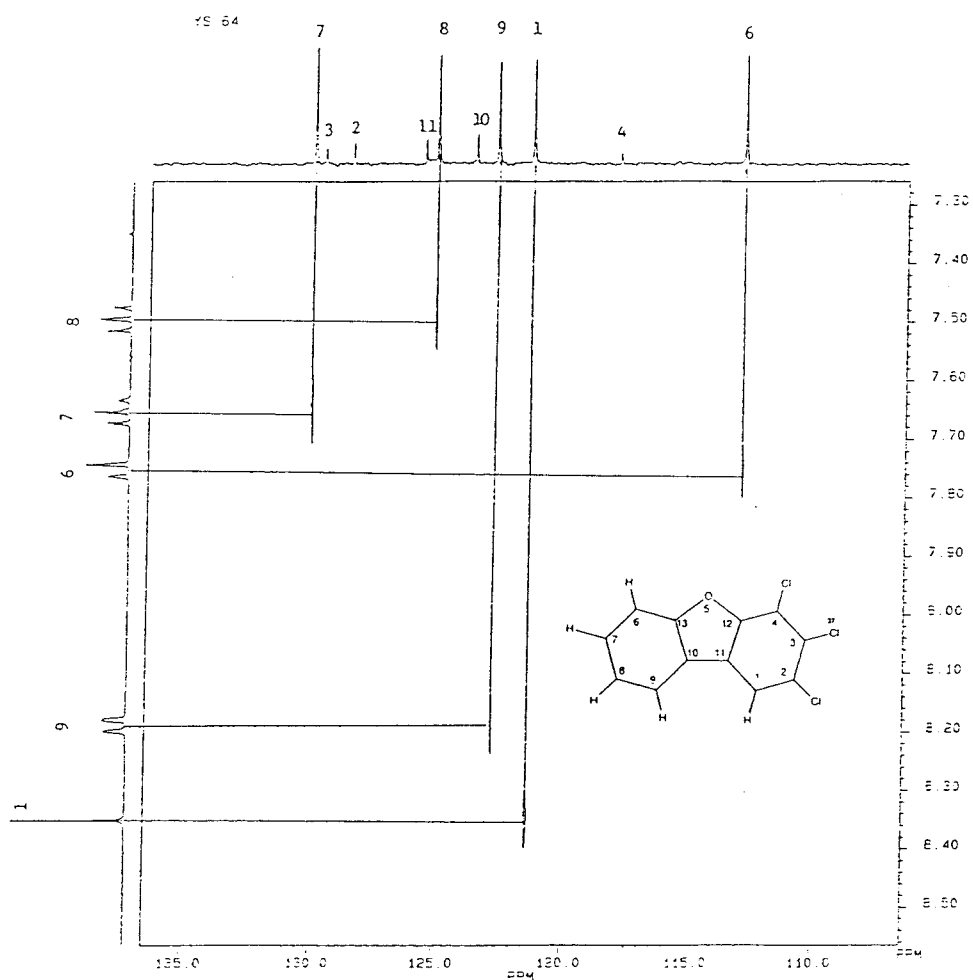
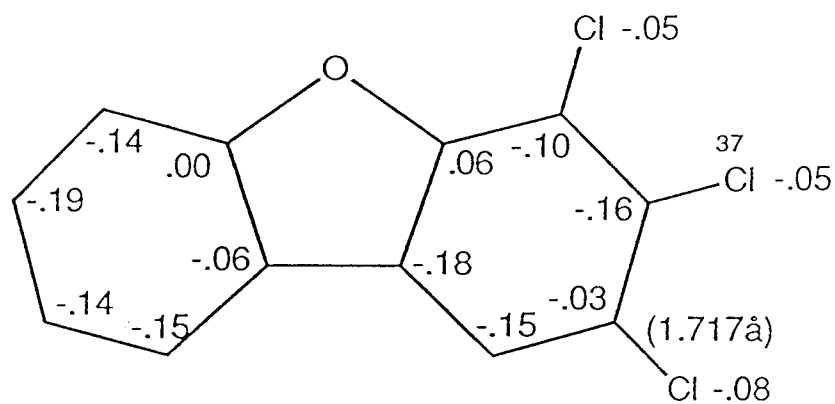
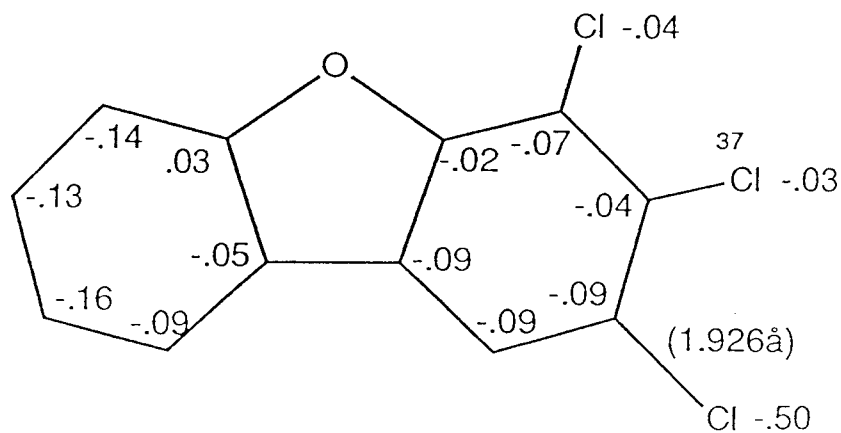


Figure A.4.7. ^1H - ^{13}C NMR spectrum of 2,3(^{37}Cl),4-tri-CDBF.



(a) nonplanar structure



(b) planar structure

Figure A.4.8. AM1 calculated electron densities and C-Cl bond distances of radical anion of 2,3,4-TrCDBF with full optimization (a) and partial optimization (b).

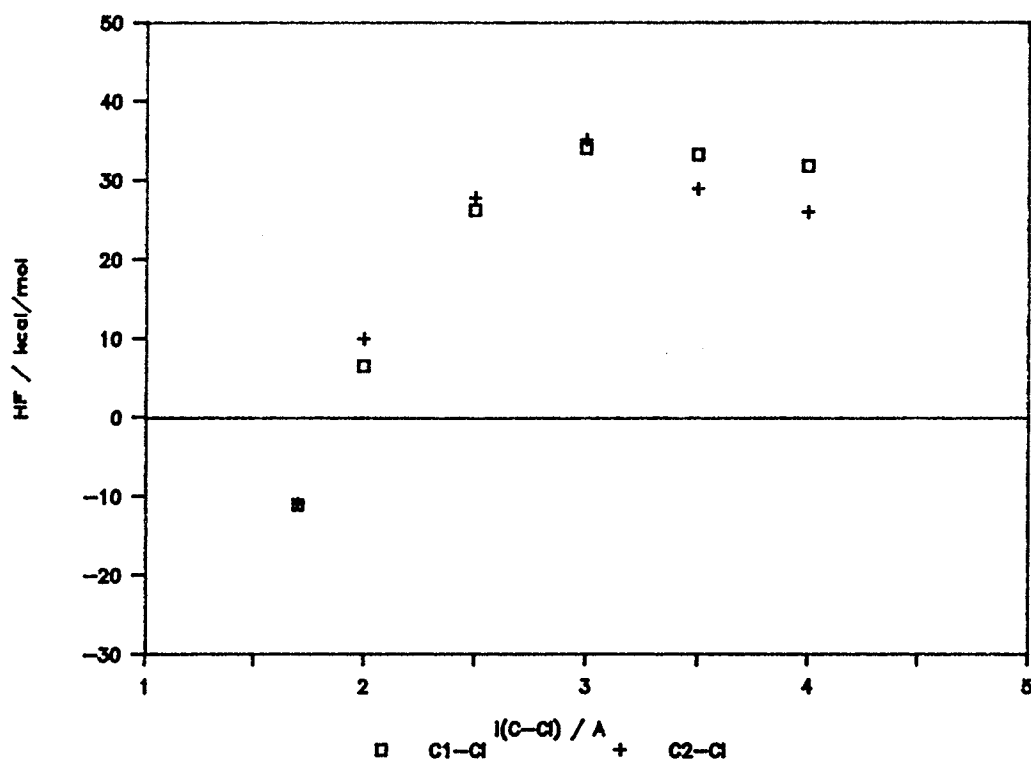


Figure A.4.9. Energy profiles of 1,2-di-CDBF radical anion calculated by AM1 UHF method.

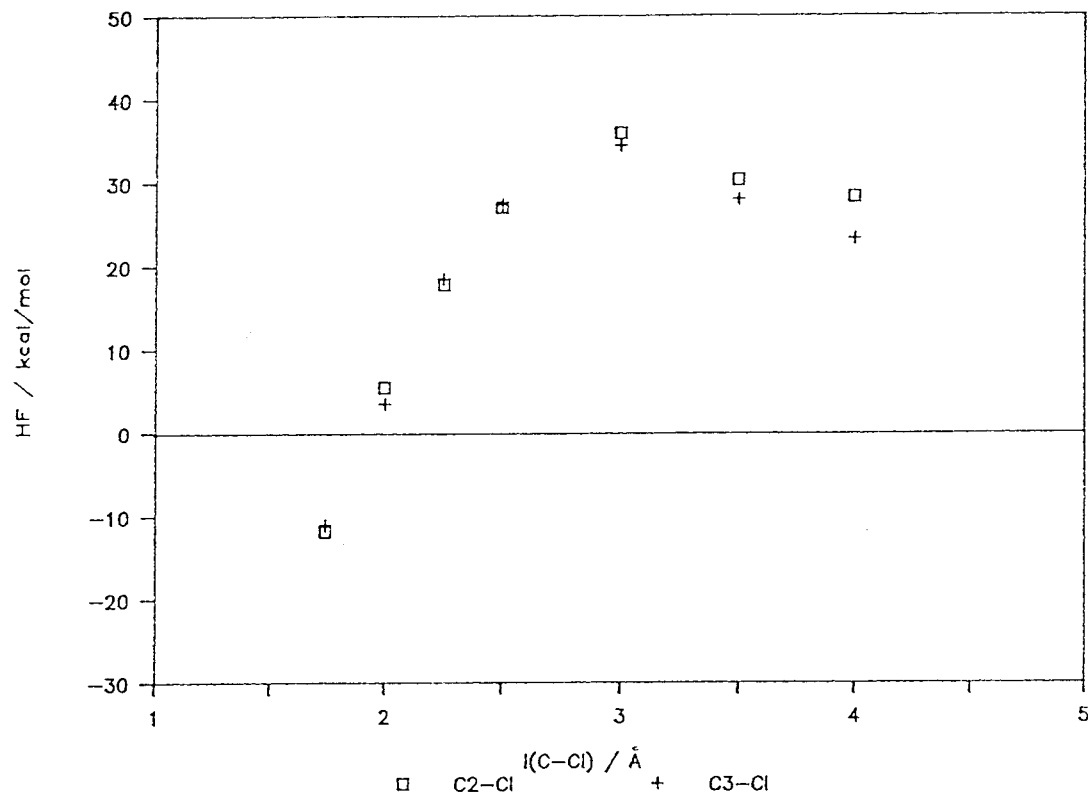


Figure A.4.10. Energy profiles of 2,3-di-CDBF radical anion calculated by AM1 UHF method.

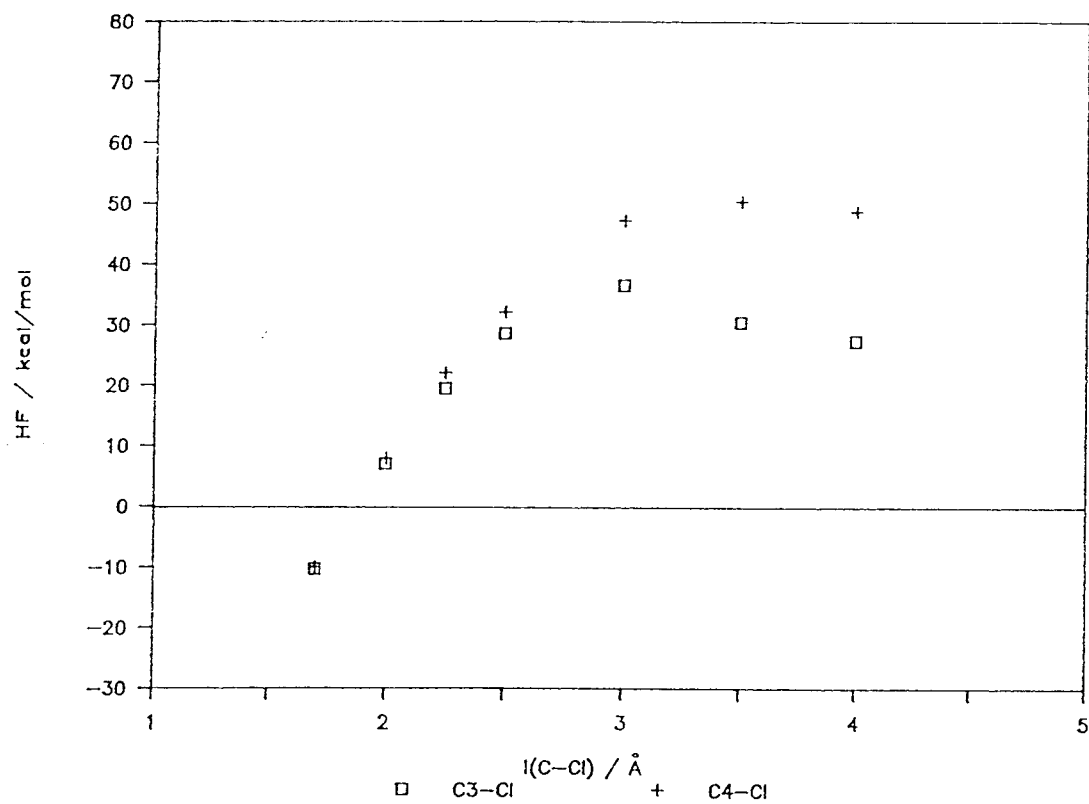


Figure A.4.11. Energy profiles of 3,4-di-CDBF radical anion calculated by AM1 UHF method.

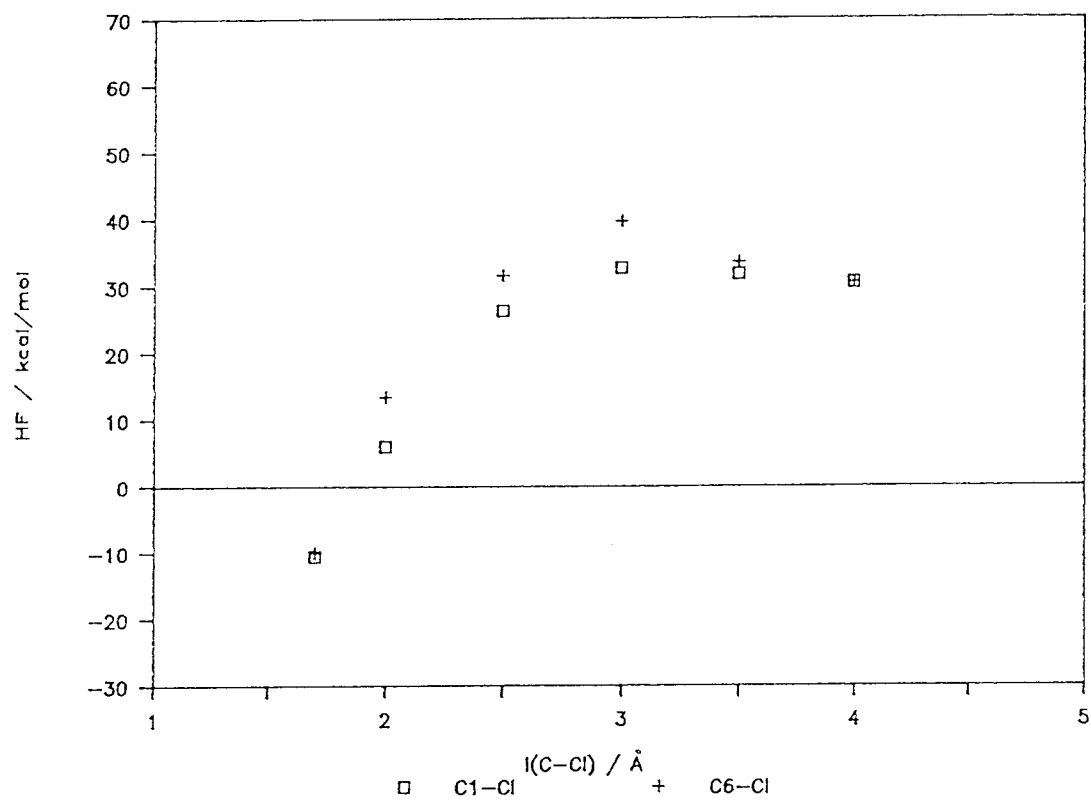


Figure A.4.12. Energy profiles of 1,6-di-CDBF radical anion calculated by AM1 UHF method.

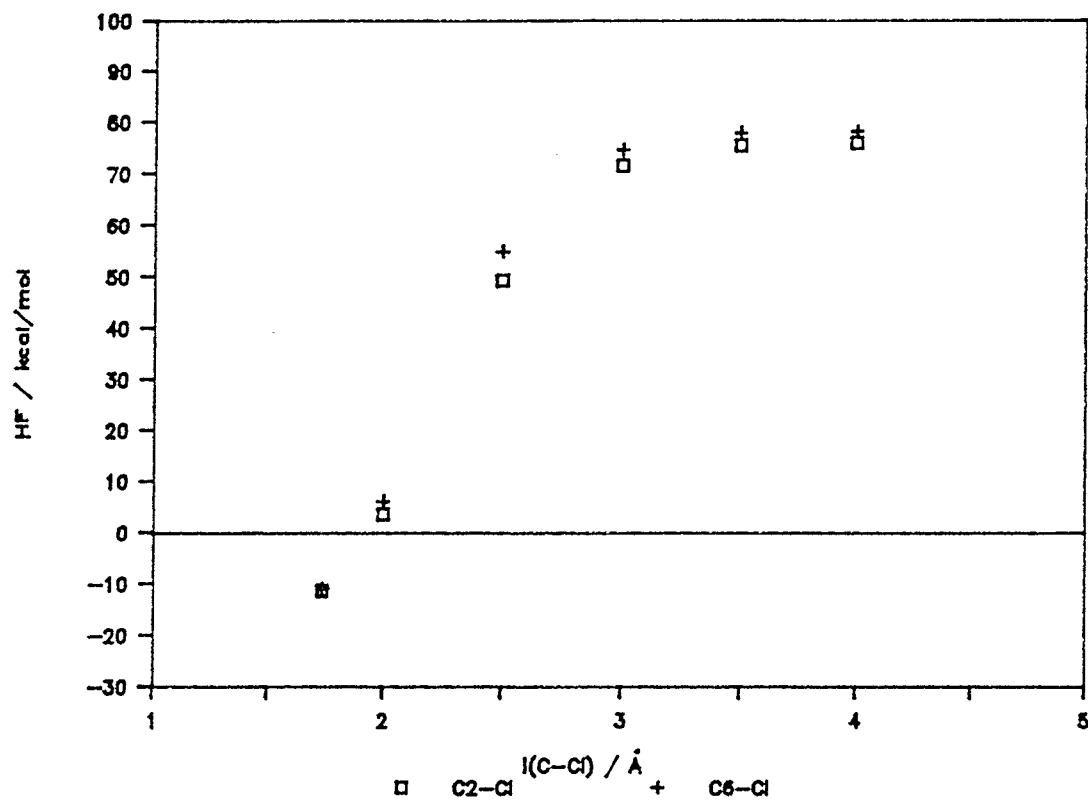


Figure A.4.13. Energy profiles of 2,6-di-CDBF radical anion calculated by AM1 UHF method.

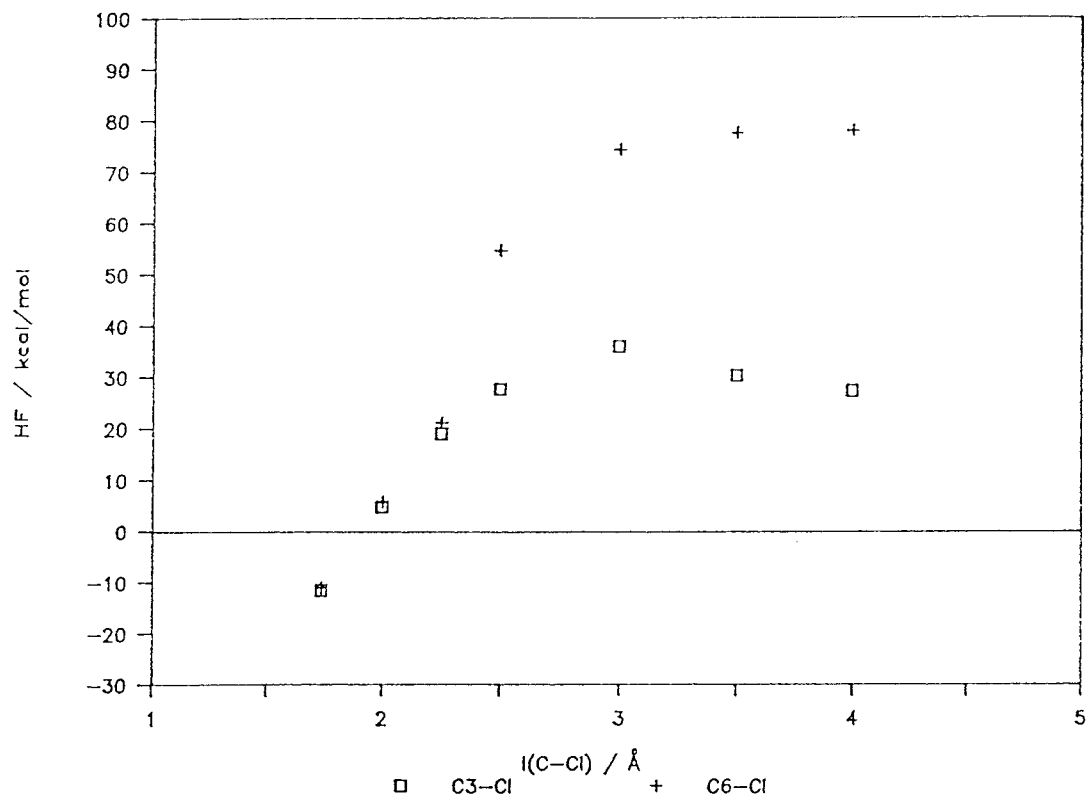


Figure A.4.14. Energy profiles of 3,6-di-CDBF radical anion calculated by AM1 UHF method.

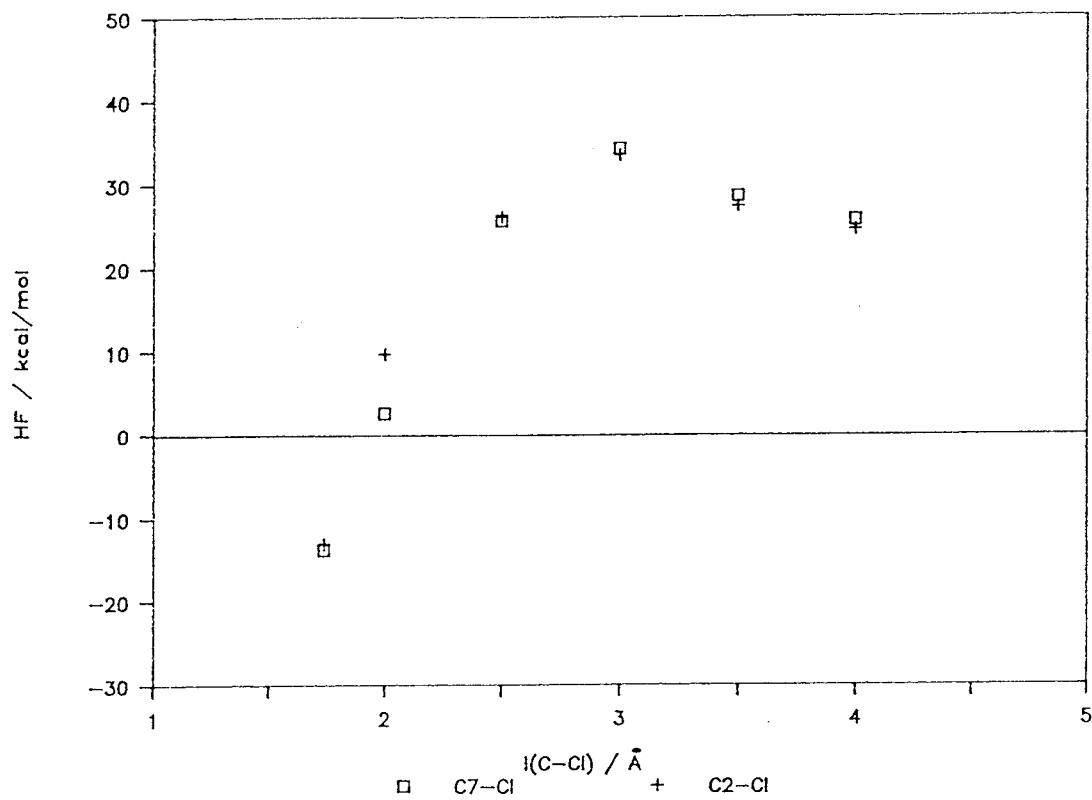


Figure A.4.15. Energy profiles of 2,7-di-CDBF radical anion calculated by AM1 UHF method.

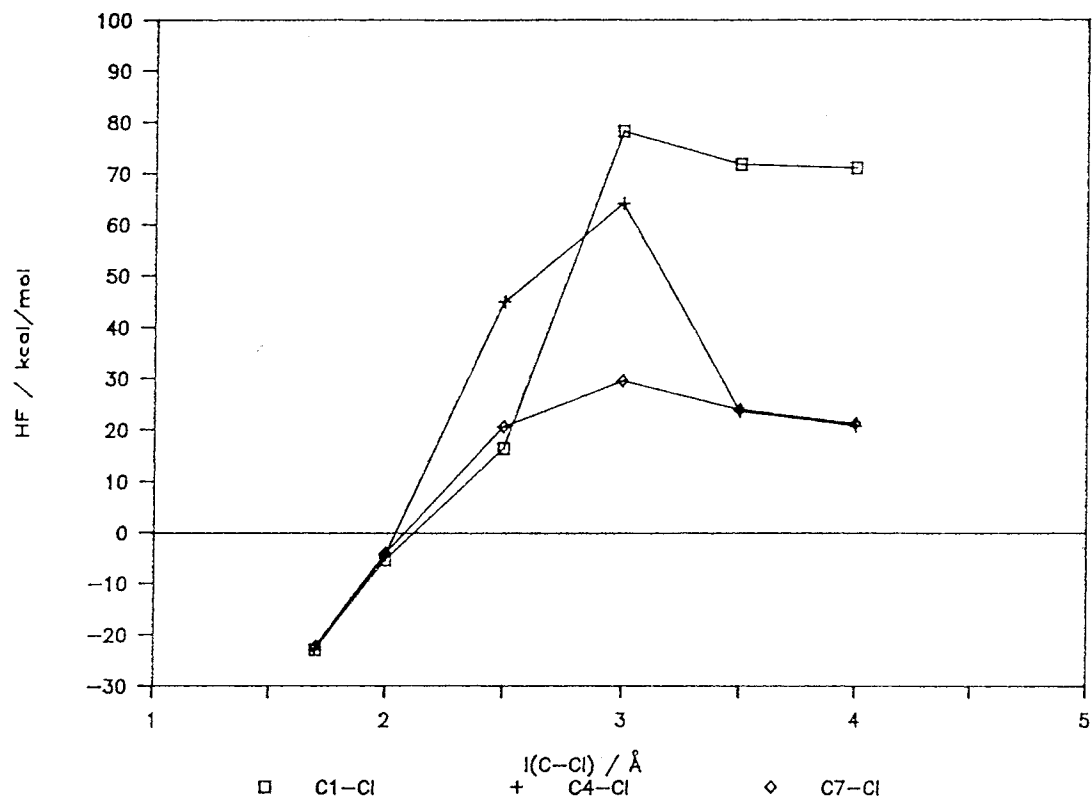


Figure A.4.16. Energy profiles of 1,4,7-tri-CDBF radical anion calculated by AM1 UHF method.

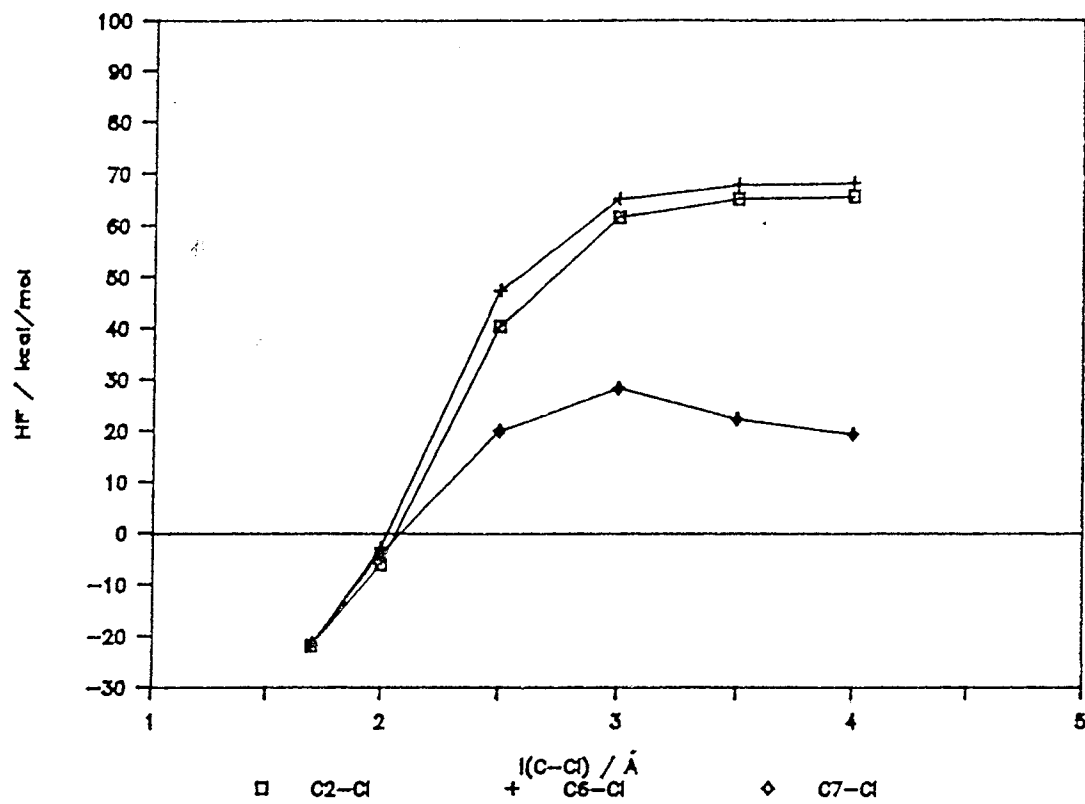


Figure A.4.17. Energy profiles of 2,6,7-tri-CDBF radical anion calculated by AM1 UHF method.

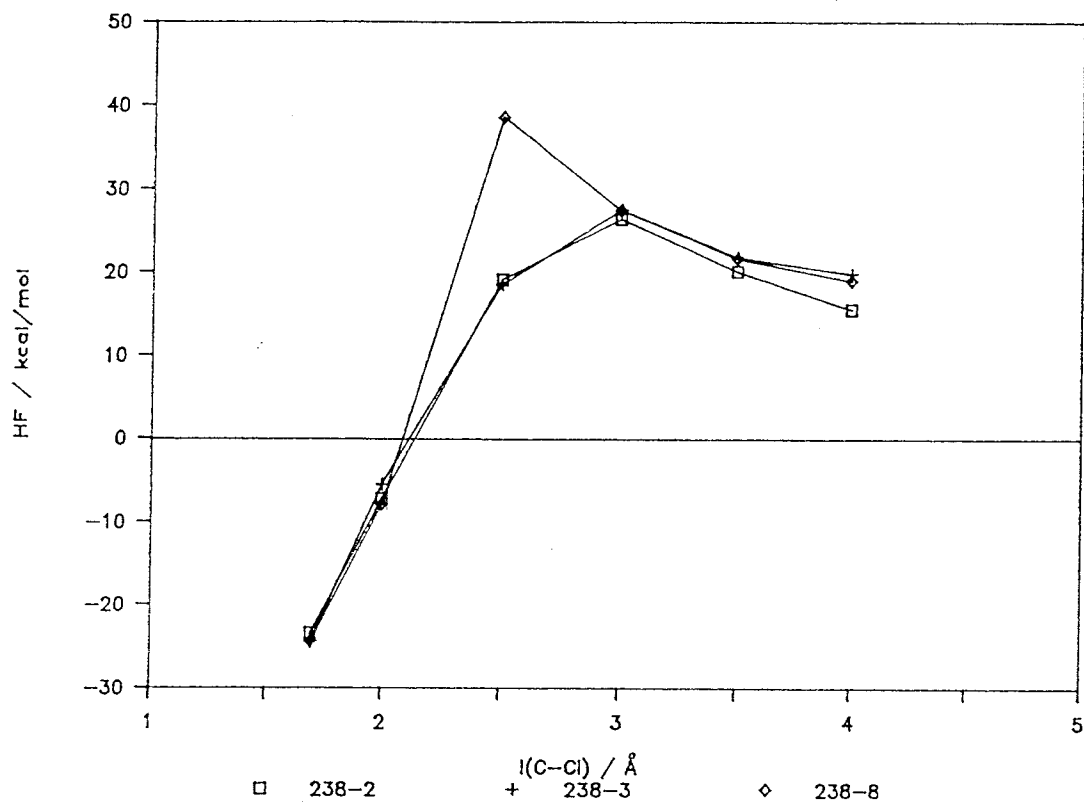


Figure A.4.18. Energy profiles of 2,3,8-tri-CDBF radical anion calculated by AM1 UHF method.

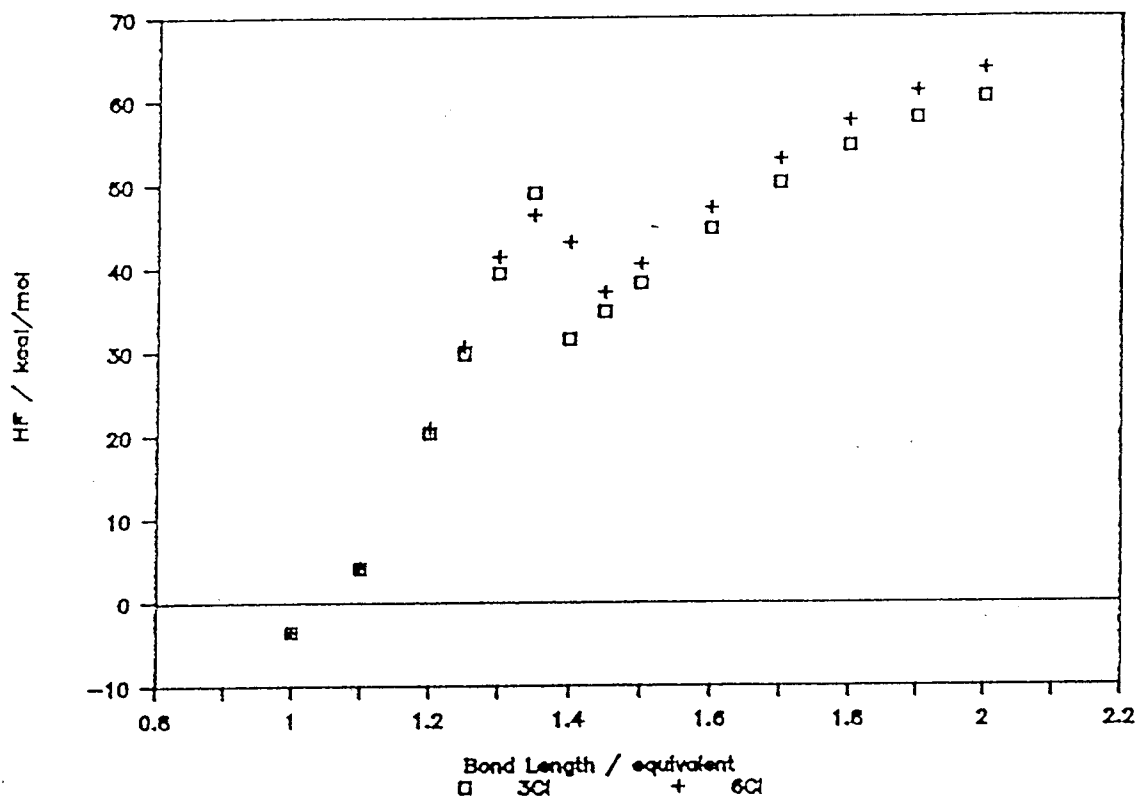


Figure A.4.19. Energy profiles of 3,6-di-CDBF radical anion calculated by AM1 RHF method.

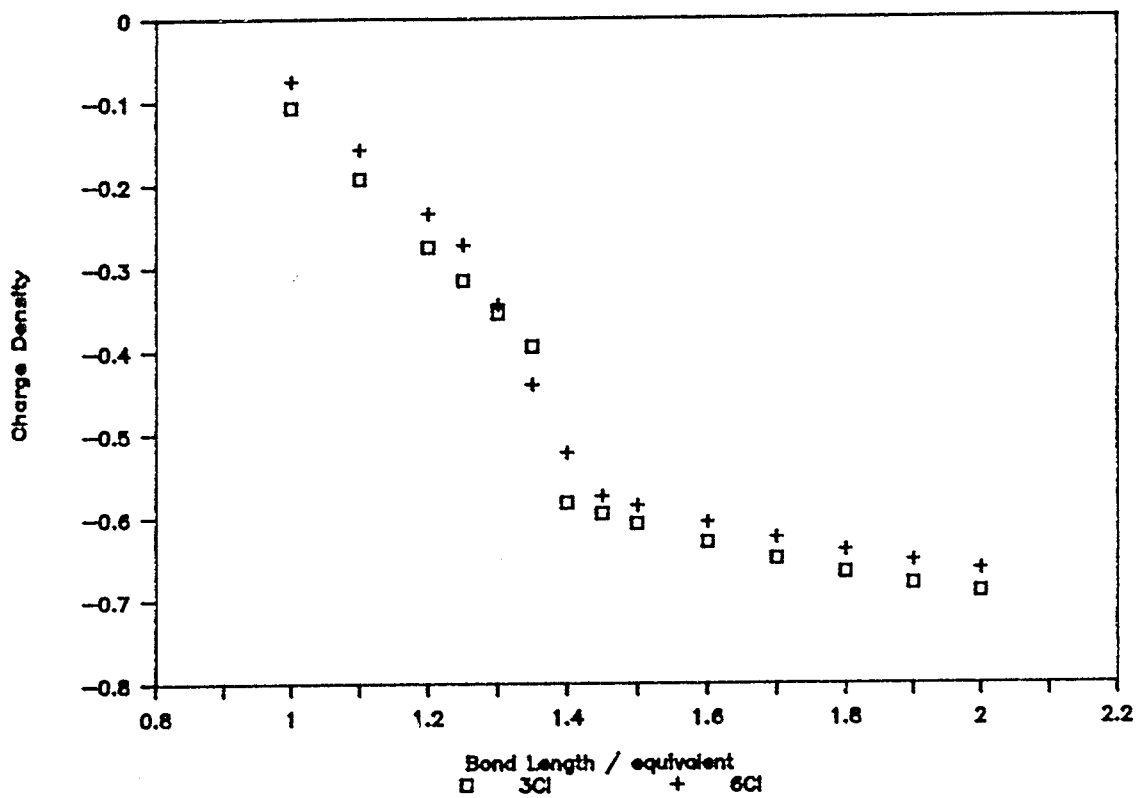


Figure A.4.20. Free electron density changes on the departing chloride ion of 3,6-di-CDBF (AM1 RHF).

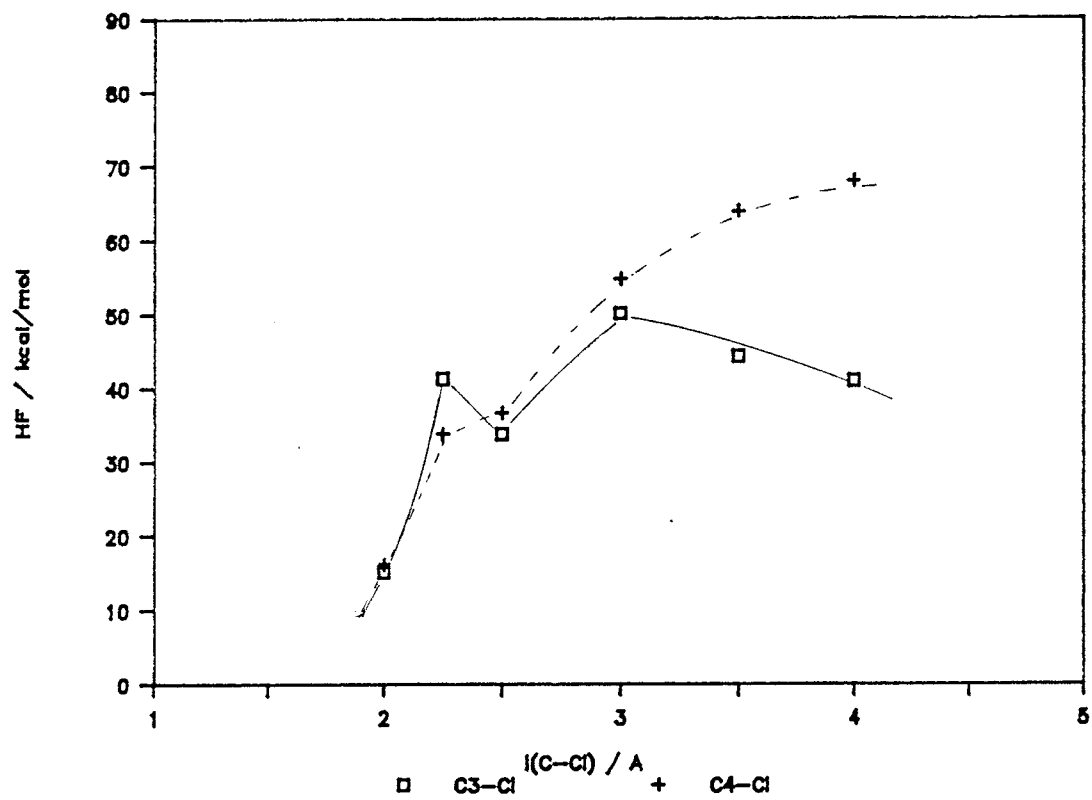


Figure A.4.21. Energy profiles of 3,4-di-CDBF radical anion calculated by AM1 RHF method.